Understanding the Dynamics and Determinants of Survival in a Regionally Iconic Wild Food Resource Following Its Near-Extinction Due To Infectious Disease

A thesis submitted to Cardiff University for the degree of Doctor of Philosophy

By

Nina Frances Daisy White

December 2022

Biotechnology and
Biological Sciences
Research Council

Understanding the Dynamics and Determinants of Survival in a Regionally Iconic Wild Food Resource Following Its Near-Extinction Due To Infectious Disease

Nina White
School of Biosciences, Cardiff University
Institute of Zoology, Zoological Society of London

Supervisory Team:

Dr. Pablo Orozco-terWengel

School of Biosciences, Cardiff University

Prof. Andrew Cunningham

Institute of Zoology, Zoological Society of London

Dr. Michael Hudson

Durrell Wildlife Conservation Trust
Institute of Zoology, Zoological Society of London

Prof. Michael Bruford

School of Biosciences, Cardiff University

Prof. Mark Beaumont

School of Biological Sciences, University of Bristol

Summary

The Mountain Chicken Frog (*Leptodactylus fallax,* MCF) is a giant amphibian, endemic to the Lesser Antilles. Once an abundant wild food resource on its home islands of Dominica and Montserrat, the MCF became Critically Endangered and illegal to harvest in the 2000's following an outbreak of the infectious disease chytridiomycosis. Chytridiomycosis is caused by a fungal pathogen, *Batrachochytrium dendrobatidis* (Bd). Bd has driven population declines in over 500 amphibian species and is a major threat to amphibian biodiversity and the MCF's survival. Susceptibility to Bd infection can vary within amphibian host species, across habitats, and through time. Indeed, a small MCF population recovery was observed in 2014, with some MCFs even able to survive or clear Bd infection. The mechanisms enabling the survival of this population and its apparent tolerance to Bd infection are unclear, but also crucial to understand in order to conserve the MCF and aid wider amphibian conservation efforts. Changes in infectious disease dynamics occur with changes in one or more of: the host, the pathogen, and their environment. This thesis presents a series of investigations into potential host- and pathogen-related determinants of the MCF's susceptibility to or survival from the Bd epizootic, complementing existing studies which focus on environmental determinants.

The first two host-related studies in this thesis involve a reconstruction of the demographic history of the MCF and a characterisation of key immune loci in the major histocompatibility complex (MHC). Historic MCF population reductions, identified by the demographic models, probably led to the depleted MHC diversity identified by the immunogenetic study. Low MHC diversity potentially explains the susceptibility of most MCFs to lethal Bd infection. Meanwhile, three MHC-I alleles were identified at an increased in frequency in Bd-tolerant MCFs, linking MHC-I diversity to Bd-tolerance for the first time. The increased frequency of these alleles in Dominica also explains why more MCFs survived there than in Montserrat. This thesis then carried out a novel characterisation of the MCF's skin microbiome, a key innate immune system component. This study revealed that the skin microbiome of surviving wild MCFs has potentially Bd-protective features, but these features were not explicitly tested against Bd infection. Replenishing microbiome diversity in Bd-naïve MCFs did not protect them from Bd infection, raising doubts around the utility of the skin microbiome in determining MCF survival from Bd infection. The last host-related study quantified remaining genetic diversity in captive MCFs and produced breeding recommendations which will influence future population recovery dynamics in the MCF. A final study into pathogen changes across the Bd epizootic revealed that the same, hypervirulent Bd lineage was implicated in the MCF's decline. As such, determinants of MCF survival or susceptibility to Bd infection are likely host- rather than pathogen-related.

Following these studies, new avenues for research have been opened which will improve our understanding of amphibian chytridiomycosis. Conservation strategy is now more fully informed and better able to work towards mitigating Bd in the wild, a fundamental step in recovering the MCF.

Acknowledgements

The best thing about undertaking this thesis was the chance to work with a vast and varied team of brilliant people, whom I would like to thank for their help in bringing this work to be.

To my supervisory team: My ultimate thanks go to Pablo, for championing me since the Rere days and for supporting me to go for the PhD in the beginning. Your belief in my abilities was vital. To Andrew, thank you for your thorough scrutiny and encouragement. To Mike Hudson, thanks for introducing me to Durrell and for joining some epic climbs in search of mountain chickens. To Mike Bruford, thank you for emboldening me to shout a bit more loudly about my work. Mark, thank you for your insights to genetic simulation and your reassurance throughout.

To the various branches of the Mountain Chicken Recovery Project: To the team in Dominica – Jeanelle, Machel, Manix, Tifani, Jelani, Walter, Damian, Ricardo – without your help I would have never gotten far. Thank you for all that you taught and shared with me, be it mountain chicken wrangling, the sounds of Farmer Nappy, or the unforgettable taste of bush rum. I am indebted to Jeanelle Brisbane and her dedication to conservation for any success in the field: thanks for your warmth and expertise. I owe all of the microbiome chapter data to the team in Montserrat. To Luke Jones and Luke Brannon, thank you for coordinating sampling, swab deliveries, and answering my frequent questions. I am also most grateful to everyone in Montserrat who took part in the microbiome sampling. To all the mountain chicken keepers at Bristol, Chester, Durrell, Norden's Ark, and ZSL – in particular, Ben Tapley, Gerardo Garcia, Kristofer Försäter, and Matt Goetz – thank you for giving me access to frogs, samples, and your in-depth knowledge of mountain chicken biology.

To the Molecular Ecology lab, Cardiff University: I know I was very lucky to land in a lab as supportive and kind as ours. Being able to share in the various successes and many failures of lab work was a big comfort. Special thanks go to Kat Mullin, for sharing those highs and lows particularly closely as we journeyed through the land of swabs and buffers. To those who helped me as a new starter in the lab: Nia, Ewan, Isa Pais, Iain, Isa-Rita, Mafalda – your kindness was greatly appreciated. To Dan Pitt, for masterfully guiding me through the treacherous waters of ABCtoolbox. To all those who helped out with the arduous task of planning MID-tags – Alex, Becca, Jenny, and Ewan, thanks for your generosity and time. To all of the above, plus Max, Jordan, Sarah D, Anya, Sarah DP, Luke, Christina, Ali, Sophie, Josie, Manon, thank you for the laughs, the lunches, and your friendship. To Frank and Bill, I'm most grateful for your thoughtfulness and guidance throughout my time in the lab.

To the Cardiff Genomics Hub and Biocomputing Hub staff: The completion of this thesis depended hugely on your help. To the Genomics Hub team, I know that Covid placed an enormous amount of work in your lap and I am so grateful for the work you did on my behalf. I'm especially thankful to Angela Marchbank for always making time to offer useful and extensive advice. To Ian Merrick, thank you for your patient help and for always being a Teams call away for bioinformatic issues.

To collaborators outside of Cardiff: Thanks to Erica Bree Rosenblum and Allison Byrne for generously sharing Fluidigm primers. Thanks also to Charles Mein and the Blizard Institute team for all your work to run the Fluidigm assay.

To those who exist in the world beyond the PhD: To all my friends, thanks for providing an ample measure of life to balance out the work: for always asking "How are the frogs?", but moving swiftly on. To Joe WR, thanks for your reminders that doing a PhD is a cool opportunity, for reliable comic relief, and for being my best mate.

She's not going to thank the cat is she…? To Glen the cat, your contributions to the thesis during your keyboard naps were enjoyed, if not kept. Thanks for being a good boy.

To Jake, this marks the end of another academic journey embarked upon together. Time to pay some council tax, at long last. While taxes may eventually be for certain in life, love and laughter are not. Thank you for always providing the latter – through B.Sc. and PhD.

Finally, to my family: Mum, Dad, Will. Any of my achievements, including the completion of this thesis, were built on the foundations that you laid of love, encouragement, and support. Thank you.

Statement of Contributions

This thesis was supported by funding from the Biotechnology and Biological Sciences Research Council (BBSRC) South West Biosciences Doctoral Training Partnership [grant code: BB/M009122/1], the Durrell Wildlife Conservation Trust, and the Institute of Zoology at the Zoological Society of London.

Access to carry out research was generously granted by the government of the Commonwealth of Dominica and the government of Montserrat.

All members of my supervisory team contributed to the overall project conception and all provided feedback on chapter drafts.

The specific contributions of others besides myself to the work presented in this thesis are detailed as follows:

Chapter Two: Samples and eight microsatellite markers used in this study were previously collected for the study by Hudson et al. (2016a).

Chapter Three: All but eight mountain chicken frog samples used in this study were collected by Mountain Chicken Recovery Program teams in Dominica and Montserrat, and by teams at Bristol, Chester, Durrell, Norden's Ark, and ZSL London zoos. Some DNA extractions were performed by Josephine D'Urban Jackson, Owen Wright, and Ellie Thomas. Library preparation and sequencing was performed by staff at the Genomics Hub, Cardiff University.

Chapter Four: Microbiome sampling of Montserratian mountain chicken frogs was carried out by the Mountain Chicken Project team in Montserrat. Library preparation and sequencing was performed by the Genomics Hub, Cardiff University.

Chapter Five: DNA of *Batrachochytrium dendrobatidis* samples was collected by Mountain Chicken Recovery Program teams in Dominica and Montserrat. DNA extraction was carried out by researchers at the Institute of Zoology, Zoological Society of London. Library preparation and sequencing was performed by staff at the Blizard Institute, Queen Mary University, London. Fluidigm primers were selected and pooled by Allison Q. Byrne.

Chapter Six: Buccal sampling of captive frogs was performed by keepers at Bristol, Chester, Durrell, Norden's Ark, and ZSL London zoos. DNA extraction was performed by Ellie Thomas.

Publications

Publications arising from this thesis:

- White et al. (2021). The complete mitogenome of the Mountain chicken frog, *Leptodactylus fallax. Mitochondrial DNA B Resources* **6**(4): 1372–1373. **1st Author.**

- White et al. (In Prep.) Ten Years of Captive Breeding for a Critically Endangered Amphibian: Successful Maintenance of Wild Diversity and Conservation Recommendations. *Endangered Species Research*. **1st Author.**

- White et al. (In Prep.) Novel Characterisation of MHC class I and II molecules in the Critically Endangered Mountain Chicken Frog. *Immunogenetics*. **1st Author.**

- White et al. (In Prep.) MHC Class IA Variants Associate with Batrachochytrium Dendrobatidis Tolerance in the Mountain Chicken Frog (*Leptodactylus fallax*). *Molecular Ecology*. **1st Author.**

Publications authored alongside this thesis:

- White et al. (2022). A population genetic analysis of the Critically Endangered Madagascar big-headed turtle, *Erymnochelys madagascariensis* across captive and wild populations. *Scientific Reports* **12**:8740. **1st Author.**

- Mullin et al. (2021). The complete mitochondrial genome of rare and Critically Endangered *Anilany helenae* (*Microhylidae*) of Madagascar. *Mitochondrial DNA B Resources* **7**(1): 153-155. **3rd Author.**

- Hudson et al. (2021). First Detection of the Amphibian Chytrid Fungus *Batrachochytrium dendrobatidis* in Guadeloupe: Implications for Conservation. *Herpetological Review* **52**(4):765-768. **6th Author.**

Table of Contents

List of Figures

List of Tables

Chapter One

General Introduction

“The giant mountain chicken frog,

Bigger than a normal frog,

The little mountain chicken frog (mountain chicken frog)

As big as a tiny dog,

It comes from Dominica,

Which is an island,

The water is warm there,

It’s in the Caribbean,

It’s dying from a fungus,

A fungus among us,

A humongous fungus, is trying to take away,

The giant mountain chicken frog.”

“Mountain Chicken Frog” from the album Organic Gangster, by Spencer the Gardener.

Chytridiomycosis: Epidemiology, Pathogenesis, and Impacts

Earth's biodiversity has waxed and waned throughout history (Barnosky et al. 2011). The planet has experienced five mass extinctions that arose from natural, stochastic geological or atmospheric changes (Barnosky et al. 2011). Our current epoch is unofficially termed the Anthropocene, as human activity becomes the driver of massive planetary disruption and the loss of biodiversity and ecosystem functioning (Crutzen 2006; Barnosky et al. 2011). Human activity, predominantly in the global north and predominantly following industrialisation, has rapidly accelerated the production of greenhouse gases and subsequent climate warming (Crutzen 2006; Cowie et al. 2022). In our quest to consume ever more, humans disrupt and destroy habitat, overexploit fauna and flora, and spread invasive species and pathogens (Barnosky et al. 2011; Dirzo et al. 2014). As a result of our actions, we are now in the sixth mass extinction (Cowie et al. 2022). Mass extinction is characterised by losses in a wide range of taxa. Extirpation of species and population declines have been recorded across plants, vertebrates and invertebrates (Dirzo et al. 2014). A recent estimation put the current level of species extinctions at 100 – 1,000 times greater than the expected background level of 0.1 - 1 extinctions per million species-years (Cowie et al. 2022). Among the >16,000 species listed as threatened with extinction by the Red List of the International Union for Conservation of Nature (IUCN), amphibians are experiencing particularly pronounced declines (Wake and Vredenburg 2008; IUCN 2021). Of the amphibian species assessed by the IUCN Red List, 41% are threatened with extinction (IUCN 2021).

Excessive losses in amphibian populations were noted in the 1980's, where between ten and 50 species were experiencing declines each year (Scheele et al. 2019a). Further studies of diminishing populations in South America and Australia in the late 90's attributed the declines to an infectious fungal disease, chytridiomycosis (Berger et al. 1998). Chytridiomycosis is caused by a fungus of the phylum chytridiomycota, named *Batrachochytrium dendrobatidis* and abbreviated to Bd (Longcore et al. 1999). Since the identification of Bd, another *Batrachochytrium* species, *B. salamandrivorans* (Bsal), was discovered to also cause chytridiomycosis after declines were noticed in European fire salamander (*Salamandra salamandra*) populations (Martel et al. 2013). The link between chytridiomycosis and amphibian declines prompted the World Organisation for Animal Health to list chytridiomycosis as a globally notifiable disease (Schloegel et al. 2010). Infection with either of the two chytrid species, Bd or Bsal, occurs in all six continents where amphibians are found, but amphibian declines have been most pronounced in Australia and South and Mesoamerica (Scheele et al. 2019a). Chytridiomycosis has driven declines in 6.5% of all amphibians, which is over 500 species, and is implicated in the extinction of at least 90 species (Scheele et al. 2019a). Of the two Batrachochytrids, Bd is responsible for >90% of severe amphibian declines because it causes chytridiomycosis in anurans as well as urodeles, whereas Bsal appears to predominantly lead to disease in urodeles – a smaller taxonomic group – although Bsal infections have been recorded in anurans (Nguyen et al. 2017; Stegen et al. 2017; Scheele et al. 2019a). The chytridiomycosis panzootic represents the greatest recorded loss of biodiversity attributable to an infectious disease (Scheele et al. 2019a).

Like several other infectious disease epizootics of the Anthropocene (Daszak et al. 2000), the devastating impacts of chytridiomycosis are likely to have arisen due to the human-mediated introduction of a pathogen outside of its enzootic range (O'Hanlon et al. 2018). Bd is thought to

originate from the Korean peninsula, based on genomic analyses by O'Hanlon et al. (2018) which revealed the highest genomic diversity in Bd from this area. No Bd-associated amphibian declines have been reported in Asia (Scheele et al. 2019a) and Asian amphibians may be resistant to the pathogenic effects of Bd after a longer history of host-pathogen coevolution (approximately 50 million years) than amphibians elsewhere in the world (Martel et al. 2014). From an ancestral Bd lineage in Asia, a global panzootic lineage, BdGPL, has been exported around the world and introduced to Bd-naïve amphibian populations (O'Hanlon et al. 2018). BdGPL (or its ancestor) is estimated to have originated at some time between 1898 and 1962 and is responsible for almost all recorded amphibian population declines due to chytridiomycosis (O'Hanlon et al. 2018; Scheele et al. 2019a). The worldwide spread of BdGPL was facilitated by the globalised nature of human activity, be it the harvesting of Asian amphibians for the international pet trade, for use in scientific experiments in international laboratories, or simply the transport of infected substrate from endemic areas to areas in which the amphibian community is Bd-naïve (O'Hanlon et al. 2018). Amphibian species traded commonly for these uses, e.g. *Xenopus laevis* and *Lithobates catesbeianus*, have been shown to be resistant to chytridiomycosis and thus act as transcontinental carriers for the disease (Fisher and Garner 2007). There may be strain-dependent variations in chytridiomycosis resistance, however, as demonstrated for *L. catesbeianus* (Gervasi et al. 2013).

Bd is one of ~1,000 species belonging to the basal group of fungi Chytridiomycota (James et al. 2006). Chytridiomycota occupy a range of substrates and climatic zones, from tropical estuaries to arid soils (James et al. 2006). Bd is an aquatic fungus which relies on moisture for survival and can be found in fresh water and moist soils (Johnson et al. 2003). Bd is also limited by thermal conditions, able to grow and reproduce between 4 - 25°C but having optimal growth between 17 - 25 °C (Piotrowski et al. 2004). Death has been recorded after exposure to temperatures >30°C (Voyles et al. 2009). At optimal temperature and pH, the life cycle of Bd takes approximately four days. Many chytridiomycota are parasitic, but Bd is the only member of the phylum to parasitise vertebrates. Characteristic of the phylum, Bd incorporates motile, infectious zoospores within its life cycle that conduct the initial colonisation of a substrate (Figure 1.1, Rosenblum et al. 2010). The substrates in which Bd can survive are varied in vitro — including sugars such as lactose and glucose, yeast extract, sterile snakeskin, and feathers (Voyles et al. 2009). In vivo, Bd usually infects the ventral abdomen (namely the 'pelvic' or 'drink' patch) and feet and toes of adult anurans, while in larval stages it infects the mouthparts (Van Rooij et al. 2015). Here, Bd completes its life cycle in synchrony with developing cells of the amphibian epidermis (Berger et al. 2005). Bd initially invades deeper levels of the host epidermis and propagates in the presence of prekeratin, before completing later stages of its life cycle in time with the epidermal cell's maturation and keratinisation in more superficial layers of the epidermis (Berger et al. 2005). Purified mucin from amphibian skin mucus has can trigger the encystation of Bd in amphibian skin, a process required for the switch to a reproductive mode in the fungus (Robinson et al. 2022). On completion of its life cycle, Bd releases new zoospores onto the host's skin surface, meaning that new Bd infections in amphibians occur through direct contact (e.g. amplexus) or through contaminated water or soil (e.g. congregation in water bodies) (Rosenblum et al. 2010). Bd has been recorded as infecting zebrafish, crayfish, geese toenails, and nematodes, which alongside amphibians have the

potential to spread Bd zoospores in the environment (Garmyn et al. 2012; Shapard et al. 2012; Brannelly et al. 2015; Liew et al. 2017).

While many parasitic chytrids exist, it is unusual that a fungal infection of the skin can cause mass mortality without any other predisposing factors such as co-infection (Voyles et al. 2009). Amphibian skin, however, is a particularly sensitive site for infection, responsible for the maintenance of osmotic balance and exchange of gases in the host (Voyles et al. 2007). A typical symptom of chytridiomycosis is the thickening of the epidermis by two to five times its original thickness (Longcore et al. 1999). This thickening disrupts normal epidermal functioning — Bd-infected green tree frogs (*Litoria caerulea*) were observed to have >50% of normal electrolyte transport disrupted, with plasma sodium and potassium subsequently reduced by ~20% and 50%, respectively (Voyles et al. 2009). The reduction or lack of key ions is thought to lead to osmotic shock, ultimately leading to host death by cardiac arrest (Voyles et al. 2009). Prior to death, clinical signs of chytridiomycosis in metamorphosed adult amphibians include, but aren't limited to: lethargy, a red ventral surface, excess skin sloughing, abnormal posture and loss of righting reflex (Pessier 2008). Clinical signs in larval amphibians are more limited, but can include the depigmentation of mouthparts (Berger et al. 1998).

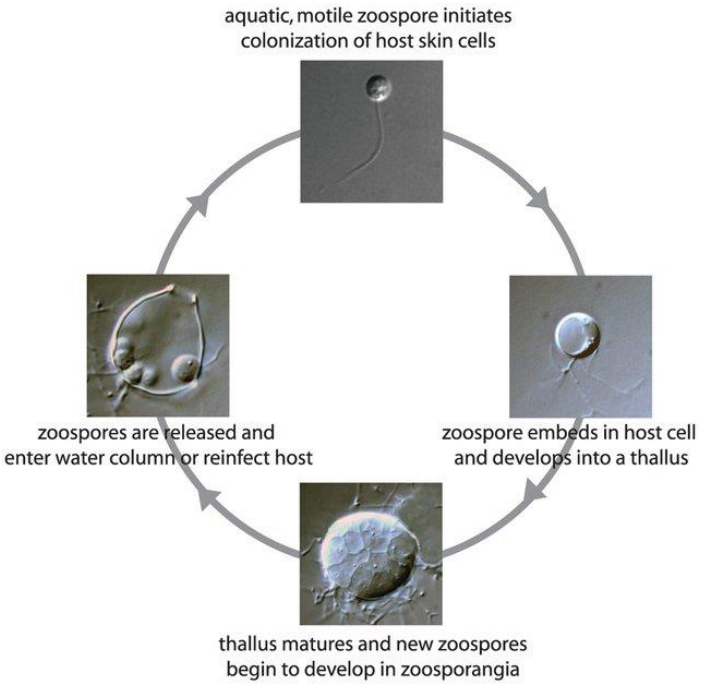

Figure 1.1: Image and caption from (Rosenblum et al. 2010). Life cycle of the pathogenic chytrid fungus *Batrachochytrium dendrobatidis*. Images were taken of Bd in pure culture grown in 1% tryptone media.

A Spectrum of Responses to Bd Infection

Chytrid infection is devastating for many amphibian populations, but not all (Scheele et al. 2017). The number of amphibian populations with recorded Bd infections is higher than the number of populations that experience a decline in size (Scheele et al. 2019a). While Bd may infect hundreds of amphibian species, chytridiomycosis does not develop in every individual infected with the fungus. A spectrum of amphibian host responses exists, from resistant (the host is able to limit or prevent Bd infection and avoids disease or reduced fitness), tolerant (Bd persists on the host skin but disease and fitness impacts are limited or non-lethal), and susceptible (Bd colonising the host skin causes lethal chytridiomycosis) (Eskew et al. 2018; Brannelly et al. 2021). One Bd-resistant species is *Agalychnis callidryas*, while *L. catesbeianus* and *Litoria ewingii* are Bd-tolerant (Brannelly et al. 2021). Recorded, severe declines due to Bd appear to be in concentrated susceptible species from Neotropical genera such as *Atelopus*, *Craugastor*, and *Telmatobius* (Scheele et al. 2019a).

Susceptibility to Bd is varied through time and space as well as host species. Bd-susceptible species that initially decline with Bd can eventually reach an equilibrium with the fungus, persisting into an enzootic phase where Bd infection prevalence is low and/or infection intensity lower relative to the initial epizootic (Scheele et al. 2017; Voyles et al. 2018). Briggs et al. (2010) observed persistence of *Rana sierrae* in pockets of Yosemite National Park following an unobserved Bd epizootic, while other populations were extirpated. These populations were characterised by low mean Bd loads of 200 zoospore equivalents, compared to 10,000 – 100,000 in populations of *R. sierrae* experiencing epizootic dynamics (Briggs et al. 2010; Vredenburg et al. 2010). In this instance, population density, habitat structure, and the number of survivors of an initial infection were determined to predict population persistence (Briggs et al. 2010). In the Bd-susceptible Harlequin toad *Atelopus cruciger*, a high compensatory recruitment enabled this transition despite the detrimental impact of Bd on individual survival (Lampo et al. 2017). Sometimes, these populations can go further than equilibrium, and tip the balance back in favour of host population size recovery (Scheele et al. 2017). For example, populations of the tropical Andean frog *Pristimantis toftae* are growing in number ten years after a Bd epizootic despite being susceptible to Bd infection in laboratory trials (Catenazzi et al. 2017). Almost forty years after the recorded peak in Bd-driven declines, 39% of declining populations have continued their downward population trend, while 12% have experienced a population recovery (Scheele et al. 2019a).

Determinants of Bd Infection and Chytridiomycosis are Context-Dependent and Multifaceted

We know that amphibian hosts can vary in Bd infection outcome, but we do not yet fully understand why. Research into variations in host responses to Bd has been ongoing for almost 20 years and has taken place on several continents (Rollins-Smith et al. 2005; Woodhams and Alford 2005; Fisher and Garner 2020). Despite this considerable global effort, there is still no clear or consistent mechanism that explains what determines Bd infection outcome in amphibians (reviewed in Brannelly et al. 2021).

Even in well studied species, such as *Litoria verreauxii alpina* or the *R. sierrae/muscosa* species complex, the combination and relative contribution of different factors determining Bd infection outcome can be uncertain (Brannelly et al. 2021). For example, it is understood that adult *R. sierrae* from sites with known Bd presence are more resistant to Bd infection, but the exact reason why is yet to be elucidated (Knapp et al. 2016). Within the same species complex, studies of pathogen virulence, environmental factors, community composition and density have not revealed any strong contenders for determinants of population persistence, and some factors such as behaviour remain unstudied (Brannelly et al. 2021). As chytridiomycosis research accumulates, we are made more aware of the highly context-dependent and multi-faceted nature of the disease (Fisher and Garner 2020; Brannelly et al. 2021).

Understanding the determinants of Bd infection outcome is complex and challenging, but also a crucial task. The scale and severity of the chytridiomycosis panzootic mean that the persistence of hundreds of amphibian species relies on the development of effective mitigations against Bd – which in turn rely on a fuller comprehension of the determinants of Bd infection outcome (Scheele et al. 2019a; Scheele et al. 2019b). As these determinants vary between host species, mitigation strategies also need to be specific to each amphibian host species that we wish to conserve (Brannelly et al. 2021). To begin to understand what factors allow chytridiomycosis to occur, the disease triangle theory of infectious disease may be used (McNew 1960). The disease triangle was originally conceptualised by McNew (1960) in the field of plant pathology. McNew (1960) stated that a disease epidemic is dependent on variations in three factors: host susceptibility, pathogen virulence, and a conducive environment for infection proliferation (Figure 1.2). This framework is widely applicable to infectious disease and has been used to frame epidemics such as potato late blight, malaria, and the chytridiomycosis panzootic (Scholthof 2006; Brannelly et al. 2021). To have the best chance of developing Bd mitigation strategies, research must focus on accumulating a suite of studies relating to host, pathogen, and environmental determinants of Bd infection outcome in as many amphibian species as possible (Brannelly et al. 2021).

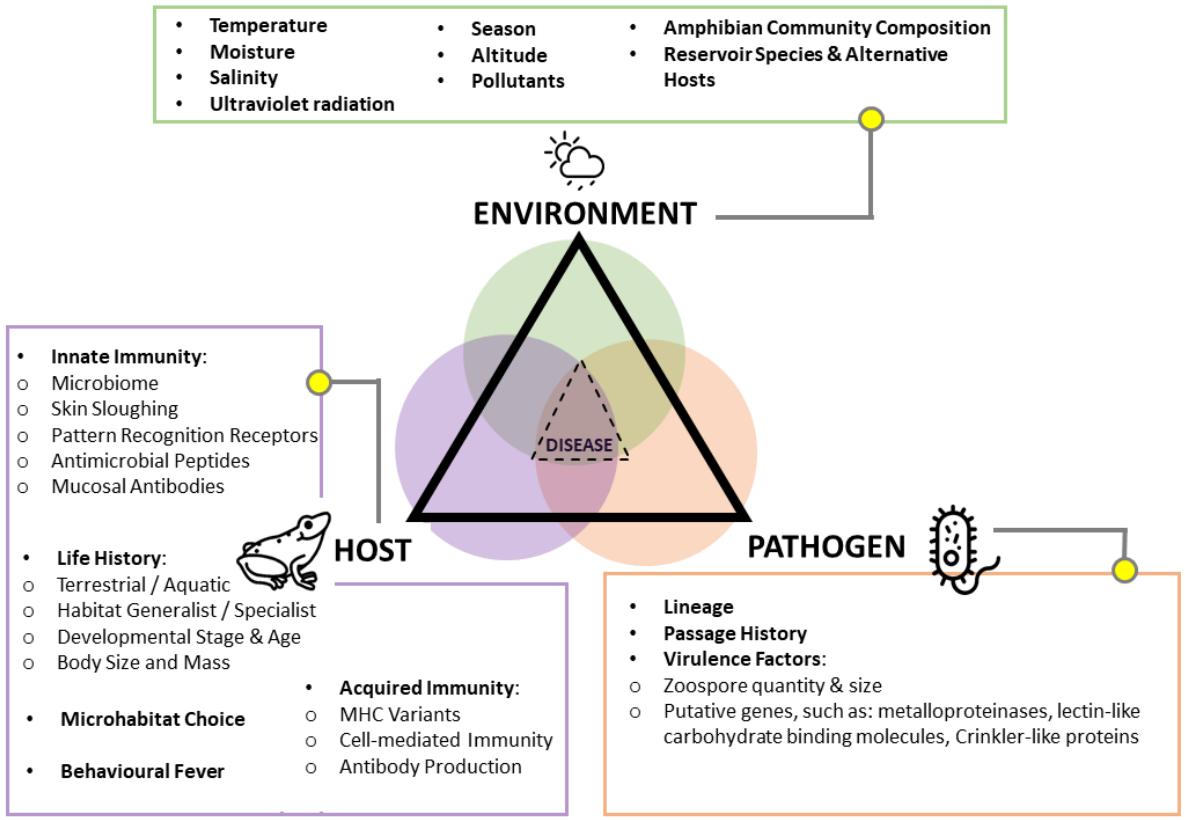

Figure 1.2: An outline of the disease triangle theory of infectious disease applied to amphibian chytridiomycosis. Determinants of chytridiomycosis occurrence and severity in amphibian hosts are related to host susceptibility, pathogen virulence, and environmental conduciveness to infection proliferation. Examples of host, pathogen, and environmentally-related determinants that potentially alter the occurrence and/or intensity of chytridiomycosis are listed here.

The Mountain Chicken Frog as a Case Study for Determinants of Bd Infection Survival or Susceptibility

Critically Endangered amphibian species that have been negatively impacted by Bd infection are in most urgent need of effective mitigation strategies for chytridiomycosis. Unfortunately, these highly vulnerable species are often the least well studied (Brannelly et al. 2021). One such Critically Endangered amphibian is the mountain chicken frog (*Leptodactylus fallax Müller, 1926*), hereafter abbreviated to MCF. The MCF represents one of the most devastating incidences of Bd-driven amphibian population crashes (Hudson et al. 2016a). The massive population crash in most of the species, and the survival of some MCFs, presents an opportunity to target determinants of both Bd-susceptibility and Bd infection survival in a highly vulnerable species in dire need of mitigations for Bd.

The MCF is one of 84 species in the Neotropical genus *Leptodactylus* (Frost et al. 2021). While the genus is predominantly located in Central and South America, the MCF is one of four species endemic to the Caribbean (Hedges and Heinicke 2007). The MCF itself is endemic to the Lesser Antilles, in the east Caribbean. The home range of the MCF has been restricted to the islands of Dominica and Montserrat since approximately the 1900's, though it is thought to have previously been found on

neighbouring St. Kitts and Nevis, Martinique, St. Lucia, Antigua, and Guadeloupe (Daltry 2002; King and Ashmore 2014). *Leptodactylus* frogs tend to be medium to large in size, but the MCF is the largest of the genus (Rosa et al. 2012; Couto et al. 2018). The MCF is in fact one of the world's largest amphibians, with the biggest individuals reaching in excess of 1 kg in weight and 20 cm snout-vent length (SVL) (Rosa et al. 2012). This large size, coupled with a voracious appetite, places the MCF as the native apex predator on both islands where native mammalian predators are absent (Adams et al. 2014). The MCF's key role in the ecosystem food chain and in invertebrate crop pest control was demonstrated via reports of an increase in centipede, millipede, and cricket abundance followed the decimation of the MCF population in Dominica (Adams et al. 2014). The giant MCF was an attractive food source in both Dominica and Montserrat (Adams et al. 2014). Until recently, mountain chicken was the unofficial national dish of Dominica and widely eaten on Montserrat – up to 36,000 MCFs were harvested annually on Dominica alone prior to their population collapse (Daltry 2002; McIntyre 2003). The cultural importance of the MCF is demonstrated via its appearance on Dominica's coat of arms and inclusion in traditional jokes, proverbs, and calypso songs on both islands (Adams et al. 2014).

Following the eruption of the Soufrière Hills volcano on Montserrat in 1995, 10% of MCF habitat was destroyed (Daltry and Gray 1999). This habitat loss, coupled with high levels of harvesting, began to cause concern for the persistence of the MCF in the wild, and monitoring of the population was initiated in 1998 in Montserrat and Dominica in 2002 (Daltry 2002)**.** The threats of habitat destruction and harvesting were, however, dwarfed by the impacts of Bd's arrival to the MCF's home range (Hudson et al. 2016a). An epizootic wave of chytridiomycosis occurred from 2002 in Dominica and 2009 in Montserrat, resulting in the fastest ever recorded decline of a species due to infectious disease (Hudson et al. 2016a). In 2002 it was recommended that the MCF be classified as Endangered, and the IUCN officially listed the MCF as Critically Endangered in 2004 (Daltry 2002; Fa et al. 2008). On Dominica, an estimated 85% of the MCF population died from chytridiomycosis in 18 months, while just four MCFs were detected during surveys after 2009 on Montserrat (Hudson et al. 2016a). All wild Montserratian MCFs are presumed to have died since their last sighting in 2016, although their descendants exist in a captive biosecure safety net population, founded from 50 individuals evacuated ahead of the epizootic wave in Montserrat in 2009 (Adams et al. 2014; Hudson et al. 2016a). As of 2019, there are estimated to be fewer than 50 MCFs remaining in the wild in Dominica (*Author's unpublished data* 2019). Once a ubiquitous element of the soundscape on both islands, the call of the MCF is now preserved only in small fragments of Dominica and in the memory of people old enough to remember (Daltry 2002).

The majority of MCFs were highly Bd-susceptible, succumbing rapidly to Bd infection and fatal chytridiomycosis (Hudson et al. 2016a). A small number of MCFs were Bd-resistant or Bd-tolerant, surviving the epizootic in Dominica between 2002 and 2006 (Hudson et al. 2016a). The number of surviving MCFs in Dominica was so few that the population was undetectable between 2006 and 2014 (Hudson et al. 2016a). Following surveys in 2014, where 44 MCFs were detected, it was evident that Dominican MCFs had experienced a small population recovery (Hudson et al. 2016a). This last population of MCF persists in the wild today (*Author's unpublished data* 2019) and is presumed to be

Bd-tolerant because infection has been recorded in individuals that have continued to survive and clear infection (A. Cunningham, *pers. comm*.). However, following the devastating impacts of tropical storm Erika and Hurricane Maria on the MCF's Dominican habitat, recovery in the MCF has stalled - fewer than 50 surviving MCFs are now thought to co-exist with Bd on Dominica (*Author's unpublished data* 2019). This co-existence likely represents a shift from an epizootic to an enzootic disease state, which will be mediated by increased host tolerance and/or reduced pathogen virulence according to host-pathogen coevolution theory (De Castro and Bolker 2005). According to the disease triangle theory, the environmental situation will also influence whether chytridiomycosis occurs in the MCF or not (McNew 1960).

Population monitoring was initiated prior to the arrival of Bd to Dominica and Montserrat (Daltry 2002). Data, in the form of host and pathogen genetic samples and environmental measures, have been routinely collected throughout the transition from epizootic to enzootic disease in the MCF (Hudson et al. 2016a; Hudson et al. 2019). These types of data – from before, during, and after a population's decline due to infectious disease – are relatively rare in the case of chytridiomycosis and infectious disease in general (Lloyd-Smith et al. 2005). For example, just 23 of the 501 species listed as having declined due to Bd by Scheele et al. (2019a) were listed as having "robust before-after decline sampling", including the MCF. With the information collected from Bd-susceptible and surviving MCFs, across both time and space, there is an opportunity to learn more about how, when, and where the 'winners' and 'losers' of Bd infection arose in the MCF. This thesis will seek to understand the dynamics and determinants of susceptibility to or survival of the chytridiomycosis incursion that all but wiped out the MCF. Prior to outlining how this will be achieved, the following section will review our current knowledge (or lack of) for each element of the disease triangle and how it relates to Bd infection and/or chytridiomycosis risk in the MCF.

Determinants of Chytridiomycosis Risk in the MCF

Host-Related Factors

Life History

A larger amphibian body size has been linked to higher Bd infection intensity and associated mortality, possibly due to the increased abundance of keratinised tissue in which Bd can proliferate (Lips et al. 2003; Gervasi et al. 2017; Scheele et al. 2019a). However, body size showed the opposite trend in a study of *Bufo bufo*, with larger individuals better able to resist Bd-induced mortality (Smith et al. 2022). As the MCF is a very large amphibian, it was possibly at increased risk of high Bd infection intensity relative to other species (Gervasi et al. 2017; Scheele et al. 2019a). To support this hypothesis, the worst impacts of chytridiomycosis on population size were seen in Montserrat, where the largest of the MCFs lived (Daltry 2002; Hudson et al. 2016a). MCFs are thought to reach a maximum age of seven years in the wild, which is moderate longevity for tropical amphibians of a similar size (Guarino et al. 2014). Increased age has been linked to increased Bd infection risk several amphibian species (Bradley et al. 2019; Rumschlag and Boone 2020). Again, the number of surviving MCFs was fewest on Montserrat, where a relatively older population of MCFs than Dominica was present (Daltry 2002).

Behaviour

The MCF is a specialised breeder (Gibson and Buley 2004). Like other *Leptodactylus* species, the MCF builds foam nests within terrestrial burrows, into which eggs are laid and tadpoles develop, although obligatory oophagy and a high degree of maternal care make the MCF unique within its genus (Gibson and Buley 2004). The terrestrial reproductive mode may offer some protection from Bd transmission through avoidance of shared water bodies for breeding (Bancroft et al. 2011). The foam nest itself may confer protection from fungal infection as its outer layer hardens into a 'skin' within 24 hrs, though this has not been formally tested (Adams et al. 2014). MCFs lay clutches of ~15-45 eggs, a fairly small amount compared to other amphibians which may lay many thousands (Bohenek and Resetarits Jr 2017). Bielby et al. (2008) noted that species with smaller brood sizes were more at risk of rapid decline due to Bd and other threats, and this could be a contributing factor in the MCF's susceptibility to Bd. Compensatory recruitment, which could be through increased breeding rates or clutch sizes, has been identified as a mechanism of host persistence with Bd in species such as *L. v. alpina* (Brannelly et al. 2016). Skin sloughing is a clinical sign of chytridiomycosis (Van Rooij et al. 2015), but may help to clear infection and can count as a first-line defence against Bd (Grogan et al. 2018b). Excess skin sloughing has been documented as a clinical sign of chytridiomycosis in the MCF, but no information has been collected on whether this lessens Bd infection intensity or reduces mortality (Adams et al. 2014).

Behavioural fever describes the tendency for ectothermic hosts to seek out microhabitats with elevated temperatures in order to clear infections (Rakus et al. 2017). Behavioural fever could help to clear Bd infection if host temperature is raised above the thermal optimum for Bd growth of 17-25°C (Woodhams et al. 2008). At higher temperatures, amphibian immune system functionality is also improved (Rollins-Smith et al. 2011). Behavioural fever has been suggested as a possible means for lessening Bd infection intensity in the MCF (M. Hudson*, pers. comm.*). Both Montserrat and Dominica are volcanic islands, with areas of MCF habitat containing water bodies that are geothermally heated above 30°C, the thermal maximum for Bd (Daltry 2002; Piotrowski et al. 2004). Bathing in these hot springs could help to clear MCFs of infection, and one of the last strongholds of wild MCFs is located in a geothermally active area (*Author's unpublished data* 2019). Studies are ongoing within a semi-wild enclosure in Montserrat, containing artificially heated pools, to assess whether MCFs use behavioural fever to clear Bd infection (Jameson et al. 2019a). In other amphibian species, there have not been many examples that decidedly link behavioural fever to Bd resistance or tolerance, although it has been demonstrated to reduce Ranavirus infection (Sauer et al. 2018; Sauer et al. 2019). MCFs are mainly nocturnal and show increased activity on cool, humid nights, which again may render them more vulnerable to Bd infection if they are encountering one another more often and doing so in cool, moist conditions best suited to Bd proliferation (Piotrowski et al. 2004; Adams et al. 2014).

Neutral Genetic Diversity

Neutral genetic diversity (NGD) is not under the influence of natural selection (Holderegger et al. 2006). As NGD is a product of mutation, migration, drift, and mating, it provides an insight into a population's effective size, growth, and inbreeding levels (Holderegger et al. 2006). For this reason, high levels of NGD are commonly linked to higher population fitness, because they are typically

generated from a historically large effective population size and random mating (García-Dorado and Caballero 2021). Greater genomic diversity may lend an individual or population adaptive capacity or 'plasticity' in the face of threats such as disease (Keller and Waller 2002). As such, multiple investigations into amphibian host NGD and Bd responses have been carried out (Savage et al. 2015; Horner et al. 2017; Christie and Searle 2018; Smith et al. 2022). Savage et al. (2015) used microsatellites to quantify NGD in populations of *Lithobates yavapaiensis* over three years. They found higher heterozygosity and allelic richness in Bd-tolerant populations compared to Bd-susceptible or uninfected ones (Savage et al. 2015). However, the opposite relationship has been observed in other studies (Horner et al. 2017; Smith et al. 2022). Horner et al. (2017) revealed that reduced microsatellite heterozygosity was correlated with reduced Bd prevalence in *Pseudacris ornata.* This was proposed to be due to historical selection for Bd-tolerant genotypes, which resulted in lower heterozygosity (Horner et al. 2017). These conflicting findings demonstrate that the relationship between NGD and Bd prevalence may vary with the host's unique demographic and evolutionary history.

Prior to the arrival of Bd, Montserratian and Dominican MCFs did not differ significantly in expected heterozygosity or allelic richness, although Dominica did have more alleles (Hudson et al. 2016a). The similarity in NGD between islands may mean that the determinants of survival from Bd infection in the MCF are linked to functional, rather than neutral, diversity. Heterozygosity and allelic richness declined in Dominica after the arrival of Bd, showing that NGD is still a useful tool to study the dynamics of survival in the MCF (Hudson et al. 2016a). For any study of genetic diversity as a determinant of Bd outbreak survival in the MCF, NGD can provide important demographic context to findings (García-Dorado and Caballero 2021). NGD can help to distinguish selection imposed by chytridiomycosis from other demographic processes (Trujillo et al. 2021). For example, *L. yavapaiensis* had been subject to ancient population expansion before the last glacial maximum, but also following more recent Bd outbreaks, and it was microsatellite data that enabled the two to be distinguished (Savage et al. 2015). Similarly, Bd-induced selection in a functional immune gene was identified using a comparison with NGD (Kosch et al. 2016). Furthermore, quantifying remaining levels of NGD in current MCF populations, such as those surviving in the wild and those being held in captivity, will enable us to devise conservation and breeding management plans that have the best chances of success by maximising NGD (García-Dorado and Caballero 2021).

Innate or Acquired Immunity

The innate and acquired branches of the amphibian immune system have demonstrable involvement in responding to Bd infection (reviewed by Grogan et al. 2018b; Grogan et al. 2020). The innate immune system is always present in a host, regardless of prior infections, and the response is generalised across pathogens (Flajnik and Du Pasquier 2004). In amphibians, innate immunity is made from constitutive defences (present regardless of an infection), and inducible innate components (activated upon detection of a pathogen) (Grogan et al. 2018b). Acquired immunity is developed through exposure to pathogens, with each exposure triggering a pathogen-specific response. Activation of the acquired immune system should provide an immunological memory for the pathogen against which it was activated, providing a faster and more effective defence against the pathogen if it is ever reencountered (Grogan et al. 2018b).

Amphibian skin and its mucus act as the first constitutive barriers to Bd infection (Grogan et al. 2018b). Mucosal defences against Bd could include antimicrobial peptides, defensive enzymes such as lysozyme, and mucosal antibodies (Rollins-Smith 2009; Rosenblum et al. 2009; Grogan et al. 2018b). However, very few studies have tested the efficacy of lysozyme or mucosal antibodies against Bd (Grogan et al. 2018b). Antimicrobial peptides have received more attention (Rollins-Smith 2009), including in the MCF (Rollins-Smith et al. 2005). Rollins-Smith et al. (2005) characterised an antimicrobial peptide, named Fallaxin, from two Dominican MCFs. Fallaxin has antimicrobial activity against several Gram-negative bacteria (Rollins-Smith et al. 2005), and may halt the growth of Bd at a minimum inhibitory concentration of 100 μM, which is deemed to be of low potency (Rollins-Smith 2009). The role of antimicrobial peptides such as Fallaxin in determining Bd-tolerance in the MCF are unclear, as the presence of such constitutive defences have not been compared between Bd-susceptible and surviving MCFs. The final form of constitutive defence is that offered by the community of commensal microbiota on an amphibian's skin (Grogan et al. 2018b)**.** This community, termed the microbiome, has been linked to lower Bd infection intensity or prevalence in some amphibians (Woodhams et al. 2007). Higher microbiome diversity (Ellison et al. 2019), and the presence of bacteria which produce antifungal metabolites (Harris et al. 2009) have both been linked to reduced Bd infection or mortality risk. No microbiome research exists for the MCF, despite promising links to reduced Bd infection prevalence or intensity in the literature for other amphibian species. If constitutive defences fail to prevent Bd encystation within the amphibian skin, the next line of defences against the fungus are components of the induced innate immune response (Grogan et al. 2018b). The role of induced innate defences in limiting Bd infection have not been as widely or thoroughly studied as constitutive innate defences. Some examples of inducible innate defences are pathogen recognition receptors (PRRs), the alternative complement cascade, cytokine upregulation, and innate leukocyte recruitment (reviewed more extensively in Grogan et al. 2018b). Induced innate defences tend to trigger an inflammatory response involving the recruitment of immune cells to tackle invading pathogens via phagocytosis, cytotoxicity, and apoptosis (Grogan et al. 2018b). No studies have been completed in the MCF relating to induced innate immune system components.

Adaptive immunity in amphibians is reliant on the innate immune system for initial activation (Grogan et al. 2018b). When PRRs are successfully activated by pathogen antigens, the pathogen is endocytosed during the innate response and antigens are bound to and presented by proteins of the major histocompatibility complex (MHC) on cell surfaces (Grogan et al. 2018b). The presentation of pathogen antigens by MHC molecules enables the B and T cells of the adaptive immune system to recognise the pathogen antigen, mount a targeted response, and form an immunological memory. MHC proteins are, therefore, a crucial interface between innate and adaptive immunity, and MHC genetic diversity determines the diversity of pathogens that the adaptive immune system can respond to (Piertney and Oliver 2006). For this reason, the MHC has been a target of several studies into determinants of Bd infection survival. MHC allelic diversity and selection for particular MHC alleles has been linked to Bd resistance in several amphibian species (Savage and Zamudio 2011; Bataille et al. 2015; Kosch et al. 2016; Savage and Zamudio 2016). As with most aspects of innate immunity, there have been no studies into the adaptive immune system and its role in determining survival in the MCF

following chytridiomycosis. As there is a strong precedent for MHC involvement in determining Bd resistance/tolerance, it would be a sensible first target for immunological studies in the MCF.

Environmental Factors

Seasonal Infection Dynamics

The MCF is endemic to the Lesser Antilles, and amphibians in Mesoamerica have been amongst the worst hit by Bd (Scheele et al. 2019a). Both Dominica and Montserrat have two seasons: a warm and wet season between June and November and a cool, dry season that runs from December to May (Daltry 2002; Hudson et al. 2019). Seasonal fluctuations in temperature and moisture influence the prevalence of Bd infection amongst amphibians in Dominica and Montserrat (Hudson et al. 2019). One might predict that drier conditions would reduce Bd infection prevalence or intensity, given that Bd relies on moisture for growth and transmission (Johnson et al. 2003), but the opposite was found in Montserrat (Hudson et al. 2019). A study of the *Eleutherodactylus* species on the island revealed higher Bd infection prevalence and intensity in cool, dry months – although correlated with temperature rather than rainfall (Hudson et al. 2019). With less rainfall, the number of water bodies declines during the cool, dry season. MCFs and sympatric amphibians congregate around the remaining water sources in larger numbers than the warm, wet season (Adams et al. 2014). Congregation in large groups could lead to increased infection prevalence via both density and frequency-dependent transmission (Adams et al. 2014). This observation has enabled strategies for potential future reintroductions to be developed, through planning to release captive bred MCFs in the wet season when Bd infection risk is lowest (Adams et al. 2014). Bd was first detected in Dominica in December (Hudson et al. 2016a), and Montserrat during February (Adams et al. 2014). Both detections were during the cool, dry season associated with higher infection prevalence and intensity, which may have aided the rapid spread of Bd throughout both islands.

Habitat Preference

Association with aquatic habitat is a risk factor for Bd infection (Bancroft et al. 2011; Gervasi et al. 2017). As Bd relies on moisture for survival and Bd zoospores are readily transmitted via water bodies, terrestrial species such as the MCF are predicted to have lower Bd infection risk (Johnson et al. 2003; Bancroft et al. 2011). However, as discussed in the prior section, the MCF does seek out areas of water and so is not completely protected from high Bd-risk areas (Adams et al. 2014). The MCF will spend only some of its time near aquatic habitat, which may increase its risk of more intense Bd infection (Gervasi et al. 2017). As water bodies present a risk of exposure to Bd, reducing the frequency of this exposure may lessen the selective pressure on evolved host defences, rendering hosts more susceptible to intense infections when they are exposed (Gervasi et al. 2017). Association with ephemeral aquatic habitat increased the intensity of Bd infection in an analysis of 20 North American amphibian species (Gervasi et al. 2017). Habitat specialisation, such as having a restricted elevation range (Lips et al. 2003), can increase Bd infection risk. Generalists are more likely to inhabit areas with unsuitable Bd habitat and therefore have lower infection risk (Scheele et al. 2019a). The MCF is not an extreme habitat specialist, although there were differences between the habitat use between island populations (Adams et al. 2014). Montserratian MCFs were found at all elevations in Montserrat, from 0 – 1,000 m above sea level (Daltry 1999; Adams et al. 2014), whereas Dominican MCFs are found

below 330 m above sea level (McIntyre 2003). More restricted elevation ranges can be associated with increased Bd infection risk and/or mortality, because the host has fewer options for retreat into unsuitable Bd habitat (Lips et al. 2003). This was evidently not the case for the MCF, which did not survive in the wild in Montserrat despite a full spread across elevations. Dominican MCFs occupied a range of habitats in gardens, plantations, and mesic and wet forests, whereas Montserratian MCFs were found in forests only (Daltry 2002; Adams et al. 2014). This may have increased the chances of some Dominican MCFs existing in habitat less suitable for Bd growth.

Reservoir Species

Sympatric amphibian species, capable of acting as a reservoir for Bd, exist on both Dominica and Montserrat (Hudson et al. 2019). The MCF shares Dominica with the *Eleutherodactylus* species *E. martinicensis* and *E. amplinympha*. In Dominica, there are also unconfirmed reports of *E. johnstonei*, and the confirmed presence of invasive species Cuban tree frog (*Osteopilus septentrionalis*), the Venezuelan snouted treefrog (*Scinax x-signatus*), and *E. lentus* (van den Burg et al. 2020; *Author's unpublished data* 2019). On Montserrat, *E. johnstonei* and the invasive cane toad (*Rhinella marina*) are also found. Infections recorded in *Eleutherodactylus* species without concurrent population crashes indicate they are Bd-resistant or tolerant reservoir species (Hudson et al. 2019). The existence of the MCF within a community made up of a majority of reservoir species ensures a supply of Bd even when susceptible host MCFs crash in number (Scheele et al. 2017).

Pathogen Factors

Several pathogen-linked factors have been suggested as mechanisms underlying the variable ability of Bd to cause disease (reviewed in Fisher and Garner 2020). Putative virulence factors, that could explain inter- or intra- lineage virulence variation, have been identified via genomic and gene expression studies (Fisher et al. 2009a; Farrer et al. 2017; Fisher and Garner 2020). These include metalloproteinases which facilitate in host invasion (Farrer et al. 2017), carbohydrate-binding modules that could aid in host recognition and adhesion (Abramyan and Stajich 2012), and crinkler-and-necrosis-like genes expressed during the early stages of infection but with unclear function in virulence (Farrer et al. 2017). Additional work is needed to robustly link these genes to virulence (Fisher and Garner 2020). Similar whole-genome studies for the Bd implicated in the decline of the MCF would require high quality isolates taken from multiple time points during the epizootics of 2002 and 2009, and unfortunately these do not exist (Farrer et al. 2017).

Bd samples can differ in virulence traits such as zoospore size and quantity, and these traits can vary both within and between lineages (Fisher et al. 2009a; Greener et al. 2020). Lineage is a key predictor of virulence in Bd: the hypervirulent BdGPL has caused most amphibian declines, whereas endemic Bd strains in Asia have not caused disease in co-evolved local hosts (O'Hanlon et al. 2018). A recent study demonstrated that virulence can also differ within Bd lineages, with BdGPL isolates from some northern European amphibians exhibiting lower zoosporangia production and size (Greener et al. 2020). Very little is known about the pathogen that contributed to the near-extinction of the MCF. Aside from identifying the species, Bd, we have almost no finer-scale analyses of the pathogen. One Bd isolate cultured from a MCF in Montserrat in 2009 was attributed to BdGPL (Byrne et al. 2019). The presence of this hypervirulent lineage in Montserrat may explain why the wild population was

extirpated from that island, but it does not provide evidence for the situation in Dominica. Identifying the lineage(s) of the Bd implicated in the decline of the MCF across its full range would enable us to understand whether lineage-related variation in virulence, as has been demonstrated by Becker et al. (2017a) and Greenspan et al. (2018), contributed to the difference in Bd infection outcome between MCFs.

Thesis Overview and Aims

The mountain chicken frog is Critically Endangered and in urgent need of effective conservation measures to mitigate the harmful impacts of Bd infection for Bd-susceptible individuals. As factors determining Bd infection outcome vary between amphibian host species (Brannelly et al. 2021), developing relevant mitigation strategies for Bd in the MCF relies on an understanding of host, pathogen, and environmental factors specific to the MCF. Following the work of Daltry (2002) and Hudson et al. (2016c), we have an understanding of host ecology and several environmental determinants of Bd infection in the MCF: reservoir species and seasonal Bd infection dynamics (Hudson et al. 2019). Work is also ongoing to uncover the relationship between environmental manipulation and Bd infection in Montserrat (Jameson et al. 2019a). Aside from an evidenced decline in neutral genetic diversity following the epizootic in Dominica (Hudson et al. 2016a), we have not focused on any host genetic or pathogen factors that may associate with Bd infection survival in the MCF. The overarching objective of this thesis is to fill some of the knowledge gaps around host- and pathogen-related determinants of the Bd epizootic survival in the MCF. This objective will be fulfilled over five data chapters, which will cover assessments of demographic history, adaptive immunity, constitutive innate immunity, pathogen genotype, and remaining neutral genetic diversity in the MCF. With all three corners of the disease triangle better understood, it is hoped that we will have a more accurate story of chytridiomycosis susceptibility and/or survival in the MCF. This information will provide the means to develop more specific and effective measures with which to conserve the MCF, in addition to being of relevance to the wider field of amphibian chytridiomycosis research. The specific aims of each data chapter are outlined in the following section:

Outline of Thesis Data Chapters

Chapter 2 Back and Forth: Integrating Backwards and Forwards Genetic Simulation to Reconstruct the Demography of the Mountain Chicken Frog

This chapter provides context for the rest of the thesis, as well as the first assessment of the MCF's historic demography. In this chapter I develop a novel framework in which backwards coalescent simulations, implemented in ABCtoolbox, are used in tandem with forwards genetic simulations, run in SLiM. The purpose of this approach is to 1) provide a method of model validation by checking replicability between simulators, and 2) to benefit from the ability to explore parameter distributions in ABCtoolbox while also being able to generate more complex models with SLiM. With this back-and-forth framework, I aim to estimate the timing and magnitude of demographic events, such as population divergence, bottlenecks, and migration for both island populations of MCFs. Establishing the demographic history of the MCF will aid interpretation of the findings in subsequent chapters

relating to host genetic diversity and help to properly explain differences in Bd-susceptibility between islands.

Chapter 3 Not A Lot, But Maybe Enough: Low MHC Diversity in the Mountain Chicken Frog Still Holds Variants Linked to Bd-tolerance

In Chapter Three, I address the first knowledge gap surrounding determinants of survival following chytridiomycosis in the MCF: adaptive immune factors. MHC class I and class II molecules will be characterised, as they have been linked to Bd-tolerance or Bd-susceptibility in other species (Bataille et al. 2015; Kosch et al. 2017). I design new, multi-locus DNA primers with which exon 2 of MHC class I and II can be amplified in the MCF. These regions were chosen as highly polymorphic sites coding for the peptide binding regions in each MHC class. With these primers, I genotype ~250 MCFs from across the Bd epizootic in space and time for both MHC classes. This is the first concurrent study of both MHC class I and II in an amphibian-Bd system. In this study I am to provide 1) genetic resources for the continued genetic monitoring of functional genetic diversity in the MCF and 2) insight into the importance of MHC variants in determining Bd infection outcome in the MCF. Any genetic link to Bd infection survival in the MCF may be exploited in conservation management through directed breeding of captive individuals or of supplementation of individuals with protective genotypes into vulnerable populations.

Chapter 4 Guardian Commensals or Inconsequential? The Skin Microbiome of the Mountain Chicken Frog and its Interaction with the Pathogen *Batrachochytrium dendrobatidis*

In Chapter Four, I continue to investigate host-associated determinants of chytridiomycosis survival in the MCF by looking at a constitutive innate immune component: the skin microbiome. Using 16S metabarcoding, I describe the diversity, composition, and predicted functional capacity of MCF skin bacterial communities. Through the study of microbiome structure and function in the last surviving wild MCFs, I aim to gain an insight to microbiome features which potentially enable this population to persist in the wild. With repeated microbiome measurements in a cohort of Bd-naïve MCFs through their first Bd infection in the wild, I aim to study 1) the impact of release to the wild and 2) the impact of Bd infection and antifungal treatment on the MCF skin microbiome. Understanding more about the characteristics of different MCF microbiomes, and also the impact of disturbances on the microbiome could provide a foundation for conservation measures such as probiotic supplementation (Kueneman et al. 2016).

Chapter 5 Know Your Enemy: A Genetic Assessment of *Batrachochytrium dendrobatidis* Implicated in the Decline of the Mountain Chicken Frog

Chapter Five addresses knowledge gaps surrounding pathogen-related determinants of survival from Bd infection. With the knowledge that six lineages of Bd exist, and that they all vary in their ability to cause disease, it is important to establish which were involved in the decline of the MCF. Using a newly developed genotyping assay that enables the use of swab-collected Bd DNA, I aim to assign Bd samples

collected from across the epizootic to lineage level. Using the single nucleotide polymorphisms (SNPs) detected during the multi-locus genotyping assay, I aim to complete a population genetic analysis of the Bd genetic structure and diversity across different facets of the epizootic: location, time, and amphibian host species. The results from this chapter will help to discern the relative importance of pathogen genotype to Bd infection survival, compared to host- or environmentally-associated determinants.

Chapter 6 Looking Ahead: A Genetic Assessment and Recommendations for Future Management of the Biosecure Mountain Chicken Frog Captive Population

Upon the first detection of Bd in Montserrat in 2009, conservationists evacuated a safety net population of 50 MCFs to biosecure, captive facilities in Europe. This population has been bred in captivity since 2009 across five different institutions with the aim of providing stock for experimental releases and reintroductions of MCFs to the wild. One genetic assessment of eleven of the population's founders was undertaken in 2009, but no further genetic analysis has been done. As captive breeding can diminish or change genetic structure and diversity over generations, it is important to assess the impact of ten years of captive management. In this chapter I aim to provide an up-to-date assessment of remaining genetic diversity in the biosecure population and make recommendations for its future management in relation to maximising neutral genetic diversity. Understanding how management has impacted the representativeness of the population to its wild source population will enable current practices to be reviewed and if necessary, improved, to ensure a genetically viable population for future reintroductions of the MCF. This final chapter provides us with a view to the future of MCF conservation strategy.

Chapter Two

Back and Forth: Integrating Backwards and Forwards Genetic Simulation to Reconstruct the Demography of the Mountain Chicken Frog

Abstract

The mountain chicken frog is a Critically Endangered amphibian with a long-standing, close connection to human culture. Beyond its large population decline that has been documented over the past two decades, little is known about the past demography of the mountain chicken. Before further study into potential genetic determinants of the species' decline, it is important to have demographic context with which to interpret future findings. In this study, both backwards and forwards genetic simulators were used to reconstruct the most likely timings, magnitudes, and patterns of demographic processes that have shaped the current genetic variation of the mountain chicken frog. Among the models tested, the most probable scenario involved a very large population bottleneck (>99% reduction in effective population size) within the past millennium, followed by a recent divergence into current populations in the last 500 years. It was also estimated that these populations have sustained a small level of connection through gene flow after their divergence. This demographic scenario, coupled with a slight male biased sex ratio, provides an explanation as to how the mountain chicken frog has diverged in nuclear DNA, but maintained homogenous mitochondrial DNA across its two island populations. This study also proposes that a close connection to human activity has potentially shaped the demography of the mountain chicken, as timings of major population changes in the MCF coincide with timings of major societal disruption in the Caribbean.

Introduction

Frogs of the genus *Leptodactylus* are distributed throughout mainland South America and the Caribbean, purportedly dispersing from the continent to the Caribbean some 20 - 30 million years ago (Hedges and Heinicke 2007). The mountain chicken frog (*Leptodactylus fallax*, MCF) is endemic to the esser Antillean islands of Dominica and Montserrat. The MCF was a popular meal in both Dominica and Montserrat, prized for its large, muscular legs. Alongside forming part of the national cuisine, the distinct whooping calls of the MCF formed a conspicuous feature of the soundscape on both islands. Consequently, a strong bond between human culture and this charismatic frog exists — proverbs, calypso music, carnival, and cuisine have all been influenced by the MCF (Adams et al. 2014). The MCF is Critically Endangered following habitat loss due to volcanic activity in Montserrat, high levels of harvesting, and an outbreak of chytridiomycosis (McIntyre 2003; Hudson et al. 2016a; IUCN SSC Amphibian Specialist Group 2017). Chytridiomycosis, caused by the fungus *Batrachochytrium dendrobatidis* (Bd), spread rapidly throughout Dominica from 2002, and reached Montserrat in 2009 (Hudson et al. 2016a). Today, wild MCF remain only in a few small patches in Dominica, equalling ~5% of their former range (Hudson et al. 2016a).

The once ubiquitous call of the MCF is now absent from much of Dominica and Montserrat, and efforts to maintain the memory of this iconic species are integral to current conservation practice (Adams et al. 2014). Successful conservation relies on positive engagement with communities, and on having an effective story to tell (Foster 2000). One aspect of the MCF's ecological history that is still unknown is how it arrived and dispersed throughout the Lesser Antilles. Being able to explain how the MCF came to exist on Dominica and Montserrat could add important detail to the history of the species as a regional endemic, creating a persuasive narrative that works to ensure public commitments to the conservation of the MCF. Aside from community engagement, a better understanding of a species' demographic past is helpful for conservation practice. For example, do particular environmental changes coincide with population size change? How connected were current populations in the past, and what factors affected this? Uncovering this information has guided conservation of several species (Orozco-terWengel et al. 2013; Nater et al. 2015), and will provide context for planned genetic analyses of immune gene variation in the MCF in subsequent chapters of this thesis (García-Dorado and Caballero 2021). There is an unusual pattern in the genetic diversity of the two extant populations of the MCF. Analysis of DNA using microsatellite markers revealed an F_{ST} of 0.2 between Dominica and Montserrat – indicating that the two populations are significantly genetically diverged from one another (Hudson et al. 2016a). However, analysis of four different mitochondrial gene fragments (12S, 16S, cytochrome b, and cytochrome oxidase I) revealed identical haplotypes throughout both populations (Hedges and Heinicke 2007; Hudson et al. 2016a). Subpopulations which are genetically diverged in their nuclear DNA but homogenous in their mitochondrial DNA are uncommon, and the underlying demographic processes warrant investigation. Little evidence exists that could help to uncover the history of the MCF in the Lesser Antilles. Archaeological records are scant, and a few historical records exist as museum specimens or as recorded sightings in the literature (King and Ashmore 2014). Furthermore, inconsistent historic nomenclature for the species, missing specimens, and mistranslations from French records all reduce the reliability of these historic artefacts. Genetic

simulators can aid in the reconstruction of demographic pasts using genetic data and statistical models that describe how DNA evolves through time under certain population processes.

Four major types of genetic simulators exist (Ritchie and Bush 2010; Yuan et al. 2012): resampling, probabilistic simulators, forwards time, and backwards time. This study will focus on using forwards and backwards simulators. Backwards time, or coalescent, simulators attempt to reconstruct the genealogy of populations by starting from present-day genetic data and working backwards in time, merging lineages in coalescent events until the most recent common ancestor of the sample (MRCA) is found (Kingman 1982). A common framework in which backwards simulation is implemented is approximate Bayesian computation (ABC). ABC uses backwards simulation to build millions of genealogies under different models of demography, called prior assumptions. The observed data from the present population and the many genealogies of each of the models are summarised with a set of statistics (Bertorelle et al. 2010). These summary statistics are used to identify models that can generate summary statistics most similar to the observed data, based on an acceptance threshold. Models that generate summary statistics closest to observed data are used to estimate demographic parameters of interest, e.g. effective population sizes or times of divergence. This is based on the assumption that if the model's simulations resemble the observed data, it is because the demographic parameters used to generate the simulated data are the same or close to the parameters that explain the observed data. Backwards simulators within an ABC framework have been implemented to reconstruct the demographic history of wild and domestic populations (Almathen et al. 2016; Pitt et al. 2019). Forwards time simulators begin with an ancestral population, in which individuals mate to produce the next generation, until the desired number of generations have been simulated. Mutations and other demographic processes are implemented during the simulation (Yuan et al. 2012). Forwards simulation has been applied to genetic disease modelling and to the history of introgression between humans and Neanderthals (Peng et al. 2007; Harris and Nielsen 2016).

Both forwards and backwards simulators are applicable to a wide range of organisms and genetic markers (Liu et al. 2008). Coalescent simulators are often less computationally expensive, because they focus only on the genealogy leading to the MRCA, meaning individuals existing in the history of the population that were not linked in the genealogy do not need to be considered. Coalescent simulators are also disadvantaged by relative inflexibility, e.g. one cannot incorporate sex ratio variation into any currently available coalescent simulator (Yuan et al. 2012). Backwards simulators within an ABC framework are suited to initial model design, as a range of parameter space can be explored through the definition of prior and hyperprior ranges from which parameter values are drawn – especially useful when aspects of demography are unknown, as is commonly the case (Bertorelle et al. 2010). Taking these advantages and disadvantages of backwards/coalescent simulators in hand, the advantages and disadvantages of forwards simulators appear to complement them. For instances when backwards simulators are less flexible, forwards simulators can model almost any demographic scenario, while including all individuals in the population. Where forwards simulators can only be parameterised with single values for parameters, the parameter ranges explored by ABC-coalescent simulations can provide best estimates for the likely values after exploring

a wide range of other values. In their review of genetic simulators, Yuan et al. (2012) call for the integration of these two methods due to their complementary nature.

The demographic history of the MCF is largely unknown. Using an ABC approach with backwards time simulation could generate likely estimates for key demographic parameters. These values could then be used to build a well-informed forwards simulation, which could also incorporate complex population features such as sex ratio skew, to explore questions surrounding the mismatched nuclear and mitochondrial divergence in the MCF. This backwards and forwards approach also has the advantage of thoroughly testing models for their ability to be replicable and realistic in relation to real data. To outline the approach: based on real data and working backwards, what demographic parameters are most likely? Then, given the values for these parameters, can a similar set of summary statistics be produced working forwards? Using a back and forth approach to characterise the past demography of the MCF is valuable from an evolutionary and historical standpoint. Furthermore, understanding the demographic context for present day patterns of genetic diversity and the mechanisms that drove fluctuations in demography is highly useful for conservation genetic studies of the MCF. The aim of this study is to model demographic scenarios of the MCF in the Lesser Antilles that could have led to two divergent populations which share the same mitochondrial DNA. This study also aims to evaluate these models for their replicability across simulators and plausibility within the known history of the region and biology of the species. These aims will be fulfilled by first calculating best estimates for demographic parameters using coalescent simulations in ABCtoolbox. These best estimates will be used to build forward simulations which incorporate sex ratio skews to test the hypothesis that female-biased sex ratios can explain shared mtDNA between MCF populations. Finally, model outputs will be compared between simulators and to data from other population genetics softwares, in order to conclude the most probable demographic history of the MCF.

Methods

Backwards Simulation: Approximate Bayesian Computation

Coalescent simulations within an ABC framework were implemented within ABCtoolbox (Wegmann et al. 2010). Eleven microsatellite loci, previously developed by Hudson et al. (2016a) and for this thesis (*Author's unpublished data* 2018 – see supplementary Table S6.1) were used to genotype MCF samples. Eighteen Dominican samples taken from before the Bd-induced decline (to prevent confounding results due to the strong population decline from the early 2000s), and 23 from Montserrat, were used to produce a set of observed summary statistics with Arlequin 3.5 (Excoffier and Lischer 2010). An important step in the creation of models in ABCtoolbox is the selection of relevant summary statistics (Wegmann et al. 2010). An optimal set of summary statistics will provide the maximum amount of information relevant to the model in question, with the fewest summary statistics possible. Selecting too many summary statistics increases the chances that the model may become uninformative due to the large amount of statistical 'noise' created. To determine an optimal number of summary statistics, a partial least squares (PLS) transformation was run, as recommended by Wegmann et al. (2009). The number of comparisons was set to 35, as this was the maximum number of potential useful summary statistics identified in Arlequin, while a matrix of parameters from the first 10,000 simulations produced in a preliminary round of simulations was produced. The optimal number of summary statistics was determined from viewing the outputted root mean squared error plots and identifying the smallest number of summary statistics that carried the largest reduction in parameter prediction error rate across all parameters (Wegmann et al. 2009).

Eighteen scenarios were created to model patterns of divergence and migration between current MCF populations (Table 2.1, supplementary Figure S2.1 and Table S2.1). The demographic parameters used include effective population sizes and times of divergence, among others (a complete list is shown in Table S2.1). The microsatellite mutational prior distributions included the microsatellite mutation rate (gamma distribution) following a strict stepwise mutation model (SMM) (Ohta and Kimura 1973). The SMM was chosen to match the underlying mutation model of the forwards simulations and Msvar also used in this chapter. Additionally, no information existed on the probability of mutations of >1 repeat unit for the microsatellites used, which was required to specify a generalised mutation model. ABCsampler was used to draw a value from these demographic and mutational prior distributions. This value was passed to the coalescent simulator fastsimcoal2 v.2.6 (Excoffier et al. 2013) to generate a single the backward simulation and a total of 1×10^6 simulations per scenario were produced in this manner. For each simulation, arlsumstat v.3.5.2.2 (Excoffier and Lischer 2010) was used to generate the simulation's summary statistics.

Table 2.1: Descriptions of demographic scenarios and their marginal density (MD) and posterior p-value (PPV). Anc = Ancestral Population. Mon = Montserrat. Dom = Dominica.

Scenario	MD	PPV	Description
1	0.003	0.032	Divergence from Anc then no migration
2	0.014	0.066	Divergence from Anc then single migration event Mon to Dom
3	0.012	0.072	Divergence from Anc then single migration event Dom to Mon
4	0.078	0.314	Divergence from Anc then single bidirectional migration event
5	0.002	0.041	Divergence from Anc then single, modern bidirectional migration event
6	0.000	0.000	Divergence from Anc then single, ancient bidirectional migration event
7	0.079	0.322	Divergence from Anc then a Dom to Mon migration event before Mon to Dom migration event
8	0.082	0.396	Divergence from Anc then a Mon to Dom migration event before Dom to Mon migration event
9	0.377	0.069	Divergence from Anc then an equal migration matrix
10	1.350	0.133	Divergence from Anc then a migration matrix – < 10% from Mon, < 5% from Dom
11	0.319	0.082	Divergence from Anc then a migration matrix – < 10% from Dom, < 5% from Mon
12	1.11e-12	0.002	Divergence from Anc then 1 ancient & 1 modern migration event
13	0.003	0.024	Mon founded by Dom (no ancestral pop)
14	0.383	0.113	Mon founded by Dom (ancestral pop)
15	0.002	0.041	Mon founded by Dom, then one, equal bidirectional migration event
16	0.039	0.040	Dom founded by Mon (ancestral pop)
17	0.627	0.427	Divergence from Anc to Dom and an intermediate population. Admixture of Dom and intermediate forms Mon
18	6.79e-23	0.000	Divergence from Anc then three bidirectional migration events

A Spearman's rank correlation test between pairs of statistics was run using a random subset of 20,000 simulations (2% of total) to identify and remove highly correlated summary statistics (Almathen et al. 2016). Summary statistics identified as highly correlated across models were removed from further analyses. To verify that observed summary statistic values occurred within the range of simulated values, plots of their relative distributions plus 2.5% and 97.5% confidence intervals were created (Wegmann et al. 2010; Almathen et al. 2016). Plots of posterior and prior density distributions were created using the 1,000 simulations closest to the observed data to check that posterior distributions

were not biased by priors (i.e. if posterior distributions were skewed to one end of the prior distribution). Finally, models were re-run through ABCtoolbox, using the posterior mode values estimated for prior parameters, to check that similar summary statistics could still be obtained. A principal components analysis (PCA) was plotted to check that the observed data were still within the reach of the 20,000 best simulations in multivariate space. To evaluate model fit to the observed data, an ABC-general linear model (ABC-GLM) was used to generate a value for the marginal density (MD) and a posterior probability p-value for the model based on the 20,000 (2%) simulations that produced the most similar summary statistics to the observed statistics (Wegmann et al. 2010). Pairwise Bayes factors were calculated as the quotient of MD between two models, and a model selected over another if the resulting Bayes factor was >3 – equivalent to three orders of magnitude more likely (Wegmann et al. 2010). A posterior probability p-value was also generated to indicate how well the observed data fit the ABC-GLM produced for a given model.

SLiM Forwards Simulations

To check the results of ABCtoolbox, the forward simulator SLiM v.3 (Haller and Messer 2019) was used to recreate the models (Figure 2.1). SLiM simulations were parameterised using the mode value from the posterior density distribution of parameters simulated in ABCtoolbox. As well as model scrutiny for standard 1:1 sex ratio models, forward simulations were used to replicate favoured demographic scenarios, but with skewed sex ratios to investigate possible demographic factors that might explain the shared mitochondrial haplotype, such as a large male: female skew in the population of MCFs (Figure 2.1, supplementary Table S2.2). SLiM was initiated using amended code from Jullien et al. (2019). Two haploid genomes per individual were simulated from an empty genomic state, firstly accumulating mutations for 12N generations to generate a mutation drift equilibrium before beginning the data collection phase of the simulations (Haller and Messer 2019). Each genome was comprised of 11 neutrally evolving loci, representing the same number of microsatellites used in ABCtoolbox. To ensure that microsatellites were completely unlinked, a recombination rate of 0.5 was defined between loci. Each scenario was run once with a default sex ratio of 0.5 (equal numbers of males and females), and then again with a sex ratio of 0.7 (2.3 males to each female), 0.9 (9 males to each female), and 0.99 (99 males to every female). One-hundred independent replicates of each scenario and sex ratio variation were run.

Twenty individuals from each population were randomly sampled following completion of the simulation. Only one number could be selected for population sampling in the SLiM scripts, and 20 most closely reflected the number of MCFs sampled for ABCtoolbox analysis. SLiM simulation output files were read into R using custom scripts (R Development Core Team 2008; Jullien et al. 2019), converted to microsatellite alleles, then diploid genotypes. More information on this process can be found in Jullien et al. (2019). The same summary statistics retained in ABCtoolbox simulations were calculated for SLiM simulations using arlsumstat v.3.5.2.2 (Excoffier and Lischer 2010). An additional 6 summary statistics were computed for SLiM scenarios to aid in the power to evaluate model accuracy, i.e. how closely could SLiM replicate real observed values for summary statistics, when parameterised with ABC posterior values? The summary statistics analysed were the observed heterozygosity for both populations (Ho_1 and _2), expected heterozygosity for both populations

(Hs_1 and _2), and the inbreeding coefficient for both populations (F_{IS}_1 and _2), generated for both populations using SLiM and observed datasets in the R package hierfstat (Goudet 2005).

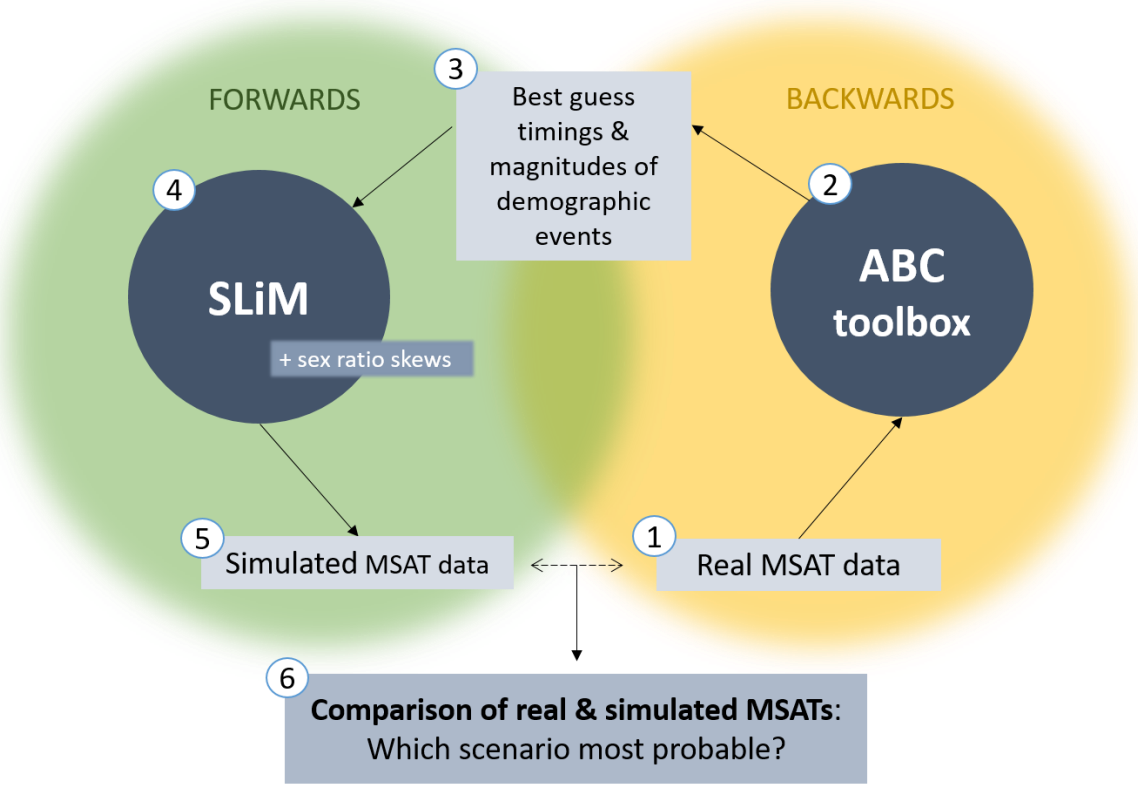

Figure 2.1: Illustration of the backwards-forwards simulation approach used in this study. Real data (1) from microsatellites (MSATs) are used in a backwards simulator, ABCtoolbox (2), to produce best estimates for demographic parameters (3). These values then guide the parameterisation of forwards simulations in SLiM (4), with the advantage of also being able to change sex ratio. In theory, the most robust estimate of demography will be replicable between simulators and able to produce data close to what is observed in real life (5 & 6).

Other Estimates of Demography and Migration

To aid in the evaluation of models from ABCtoolbox and SLiM, additional analyses of past demography were carried out on the same 41 individuals used to build ABC models. Msvar v.1.3. (Beaumont 1999) was used to analyse both populations for three scenarios: a stable population, a population expansion, and a population bottleneck. The MCF generation time was set as three years (IUCN SSC Amphibian Specialist Group 2017) and a standard vertebrate microsatellite mutation rate of 10^{-6} to 10^{-2} was used as no specific data exist for the MCF (Bulut et al. 2009). Each model was run 4 X10^{9} times and the first 20% of iterations discarded as burn-in of the Markov Chain Monte Carlo (MCMC) algorithm. Gelman and Rubin's test (Brooks and Gelman 1998), implemented using the CODA R package (Plummer and Murrell 2006), was used to determine convergence of the MCMC algorithms, with values < 1.2 selected as optimal. This score was used to select the best models, which were plotted in R.

The proportion of migrants between the two islands was estimated using the private allele method in Genepop, and also using F_{ST} values with the equation $Nm = \frac{1-FST}{4FST}$. The software 2mod (Ciofi et al. 1999) was used to test whether observed differences/similarities in allele frequencies between populations were more likely to be due to a drift-immigration equilibrium or to genetic drift alone. 1 x 10^6 iterations were run and the proportion of results in favour of model 0 (drift model) or 1 (gene flow model) were calculated as a probability. Both models assume negligible effects of microsatellite mutations relative to migration rate (gene flow model) or divergence time (drift model) (Ciofi et al. 1999). The first 10% of iterations of the MCMC algorithm were discarded as burn-in. The analysis was repeated three times to ensure convergence of the MCMC algorithm. A Bayes factor for each model was calculated as the probability of one model over the other. To further understand the influence of drift and immigration acting within each population, density distributions of F (the inbreeding coefficient) and the number of migrants per generation (M) were calculated from F using $M = \frac{1-F}{4F}$ as per Ciofi et al. (1999). The 90% highest posterior density intervals were calculated using the R package HDinterval (Meredith and Kruschke 2018).

Comparison of Backwards and Forwards Simulations

ABC vs. SLiM

To identify how closely SLiM simulations could replicate the 13 summary statistic values outputted by ABCtoolbox, distributions of the summary statistics gained from the 100 best ABCtoolbox and SLiM simulations were plotted to visualise the agreement of both simulators. Ranges between the 5% and 95% quartiles of each data distribution were calculated, and the extent to which these ranges overlapped or were separated between ABC and SLiM were calculated. To enable comparison between summary statistics, values were rescaled to compensate for the larger scales on which certain statistics exist (e.g. F_{ST} is limited to 0-1 while K ranged from 0 - 7). The rescaled values were calculated using:

$$y = \left(\frac{X-Xmin}{Xrange}\right) n.$$

ANOVAs (or Kruskal-Wallis for non-normal data) tests were run to identify differences in overlap amounts between scenarios.

SLiM vs. Observed Data

For each of SLiM's simulations, the absolute difference (or Euclidean distance in one-dimensional space) was calculated between each simulated summary statistic and the corresponding summary statistic value estimated from the real genetic data. Absolute differences were plotted in order to represent model closeness to observed data. A one sample t-test, (or Wilcoxon tests for non-normally distributed data) were used to test whether the mean of SLiM-generated summary statistics were significantly different from the observed data point estimates.

Results

ABCtoolbox

PLS analysis identified the optimal number of summary statistics as 14 (supplementary Figure S2.2). After removal of highly correlated or poorly-estimated statistics, a number close to this was still achieved - 13 summary statistics were retained for final models (Table 2.2). K (mean number of alleles across loci) and H (mean genetic diversity across loci) were selected as standard estimates of genetic diversity within populations. Pairwise F_{ST} was selected as a measure of genetic differentiation between the island populations. The genetic distance Delta Mu Square (DMUSQ) was selected as a measure of divergence between populations designed specifically for microsatellites under SMM. Spearman's correlations identified H_1, H_2, and mean_K as consistently highly correlated across models, and therefore these summary statistics were removed from the final analyses (supplementary Figure S2.3). The observed values for GW_1, GW_2, GWsd_1, GWsd_ 2, mean_GW, and tot_GW were seen to lie outside of the 2.5% or the 97.5% confidence intervals estimated from the simulated data, and therefore these statistics were also removed from the analysis (supplementary Figure S2.4).

Table 2.2: Retained summary statistics and observed values produced from eleven microsatellites and 21 mountain chicken frogs.

Summary Statistic	Observed Value
K_1	4.91
K_2	3.55
Ksd_1	1.64
Ksd_2	1.04
sd_K	0.96
tot_K	5.45
Hsd_1	0.20
Hsd_2	0.16
mean_H	0.57
sd_H	0.03
tot_H	0.63
FST_2_1	0.17
DMUSQ_2_1	5.00

Analysis of the MD and posterior probability p-value (PPV) values indicated that scenarios 10 and 17 were the optimal models (Table 2.1). Model 10 had a MD equal to 1.35, which resulted in a Bayes factor at least three times larger than other scenarios, except for 17, which had a MD of 0.627 (Table 2.1). Other scenarios had a MD in the range of 6.79×10^{-23} – 0.383 (Table 2.1). Pairwise MD and Bayes factor comparisons are shown for all scenarios in supplementary Table S2.3. Scenario 17 had a greater PPV than scenario 10, meaning the ABC-GLM predicted for scenario 17 was a better fit to the observed data. Both scenarios were considered in further analyses as Bayes factors could not choose one over the other.

Scenario 10 involved the divergence of an ancestral population into current day populations, Dominica and Montserrat (Figure 2.2). After the time of divergence, migration was modelled every generation

at a rate of 0 - 0.1 from Montserrat into Dominica, and 0 - 0.05 in the other direction. The mode of the posterior density for the time of divergence was 149.93 generations ago, with the 50% highest posterior density interval (50 % HPD) at 16.93 - 2,423.26 generations ago. With the generation time of MCFs estimated at three years, this equates to a time of divergence 449.79 years ago (50% HPD = 50 – 7,269 years ago). The estimated effective population size of the ancestral population before divergence was 78,426 (50% HPD = 8,703 - 396,251). The effective population size on Dominica was estimated at 295 (50% HPD = 99 - 928). The effective population size on Montserrat was estimated at 53 (50% HPD = 22 - 135). This indicates a large bottleneck occurring in both islands after divergence. The mode value for the migration rate from Montserrat to Dominica was 0.07, equating to 3.71 migrants per generation based on the Ne, and 0.005 in the other direction, equating to 1.48 migrants per generation.

Scenario 17 modelled the divergence of an ancestral population at time t_div giving rise to the Dominican population (sampled) and an intermediate population (unsampled), which at a later time (t_adm) hybridised with Dominica, giving rise to Montserrat (sampled; Figure 2.3). Dominica and the intermediate population were simulated to admix at time t_adm, forming the Montserratian population, in which a varied proportion (0 - 1) of genes were sourced from Dominica. This model aimed to take into account the geography of the region, where other islands neighbour Dominica and Montserrat, and are likely to have hosted intermediate populations in the movement of MCFs between Dominica and Montserrat. The mode for time of divergence between Dominica and the intermediate population was 6,997.78 generations ago (50% HPD = 2,760.46 – 71,877). This puts the time of divergence, taking into account generation time, at 20,993.34 years ago (50% HPD = 8,281.38 – 215,631 years ago). The ancestral population's effective population size was 227 (50% HPD = 42 - 2899). The mode estimate of effective population size for the other populations were 1,645 (Dominica, 50% HPD = 581 – 4,908), 327 (Intermediate, 50% HPD = 116 – 11,291), and 295 (Montserrat, 50% HPD = 94 - 977). The time of admixture to form Montserrat's current population was estimated at 21 generations ago, equating to 63 years ago (50% HPD = 10 - 45 generations). The proportion of genes from Dominica moved to Montserrat at this admixture was estimated at 0.9 (50% HPD = 0.76 - 0.99).

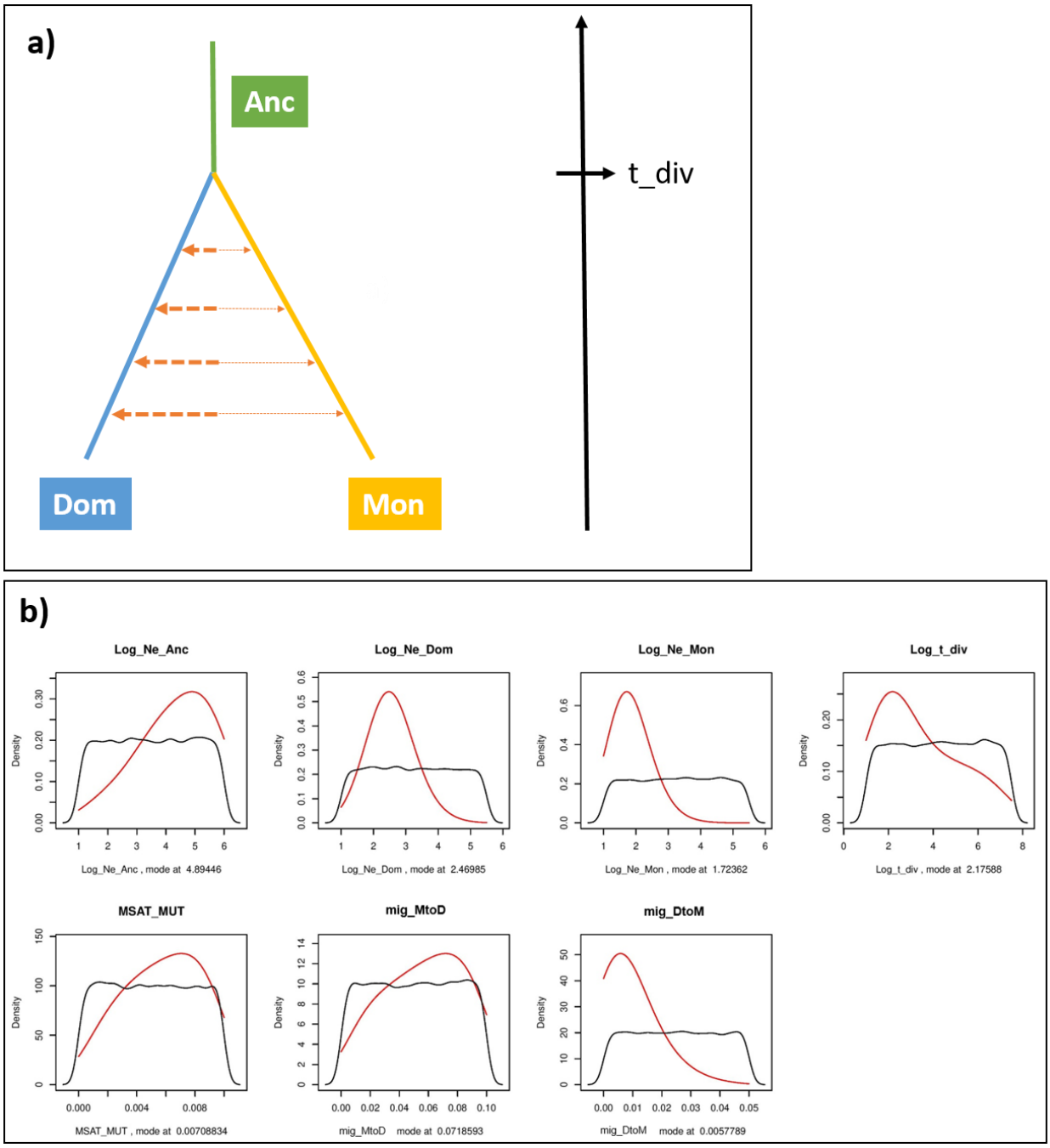

Figure 2.2: ABC Scenario 10. A) Illustration of the scenario, backwards in time. Anc = ancestral population, Dom = Dominica, Mon = Montserrat, t_div = time of divergence. Orange horizontal arrows indicate migration direction and magnitude. B) Distribution of priors (black) and posteriors (red) for model parameters. Log_Ne_(Anc/Dom/Mon) = Log of the effective population size, t_div = time of divergence, MSAT_MUT = microsatellite mutation rate, mig_DtoM = migration rate into Montserrat, mig_MtoD = migration rate into Dominica.

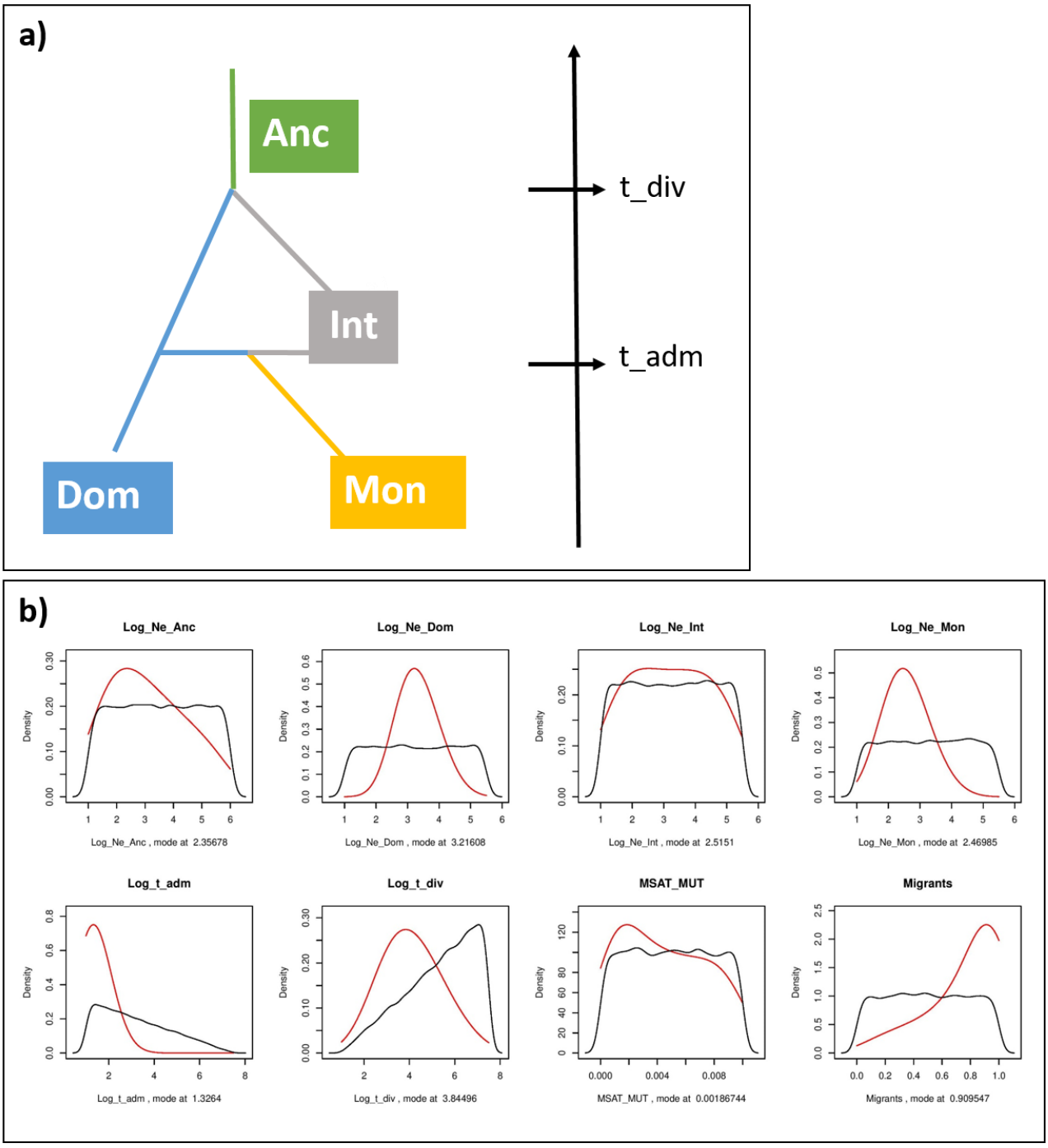

Figure 2.3: ABC Scenario 17. A) Illustration of the scenario, backwards in time. Anc = ancestral population, Dom = Dominica, Int = intermediate population, Mon = Montserrat, t_div = time of divergence, t_adm = time of admixture. B) Distribution of priors (black) and posteriors (red) for model parameters. Log_Ne_(Anc/Dom/Int/Mon) = Log of the effective population size, t_div = time of divergence, t_adm = time of admixture, MSAT_MUT = microsatellite mutation rate, Migrants = proportion of migrants from Dominica admixed with an intermediate island to form Montserrat.

SLiM

Variants of the two best ABCtoolbox scenarios (10 and 17) with different sex ratios were generated with SLiM. Scenarios with an equal sex ratio are suffixed with 'A', with sex ratio 0.9: 'B', with sex ratio 0.99: 'C', and with sex ratio 0.7: 'D'. SLiM scenarios 10A, 10B, 10C, and 10D were compared to ABC scenario 10. SLiM scenarios 17A, 17B, 17C and 17D were compared to ABC scenario 17. For scenario 10, an ancestral population of size N = 8,700 was run for 12N generations to generate a mutation drift equilibrium (Haller and Messer 2019). Taking the mode 50% HPD value (Ne = 78,425) was too computationally expensive to run for 12N generations with available time and processing power, so the lower 50% HPD estimate from ABCtoolbox for the ancestral population was used (N = 8,700). After 12N generations, the ancestral population size was expanded to 78,425 and run for two generations to distribute mutations across the simulated lineages. The mutation rate was set at 0.007 per generation and per locus. At generation 104,402 a divergence was simulated, creating Dominica (Ne = 295) and Montserrat (Ne = 53), and the ancestral population was removed. Between generations 104,402 and 104,552 (reflecting the most probable time in generations ago that the divergence of the ancestral population occurred, according to ABCtoolbox estimates) a migration matrix was established, with the proportion of migrants moving to Dominica at 0.07 and to Montserrat at 0.005.

For scenario 17, an ancestral effective population size of 227 was initiated and left to progress until generation 2,725 (allowing 12N generations for burn-in). The mutation rate was set at 0.001 per generation and per locus. At this point, two new subpopulations, representing Dominica and an intermediate island were created from the ancestral population. Dominica had an effective population size of 1,645 and intermediate population a population size of 327. The ancestral population was removed from the simulation at generation 2,726. At generation 9,723, a new subpopulation representing Montserrat, of size 295, was formed from the admixture of individuals in Dominica and the intermediate population – 90% being from Dominica and 10% from the intermediate. This reflected the mode time of admixture determined by ABCtoolbox of 21 generations ago. The intermediate population was removed at generation 9,724 and the simulation finished at generation 9,744.

Comparison of Simulated and Observed Data

SLiM vs. ABC Simulations

Concerning just the basic models with equal sex ratio, SLiM scenario 10A better replicated ABC simulation outputs than SLiM scenario 17A – having a higher degree of net overlap in the rescaled summary statistic units (RSU) (Figure 2.4, supplementary Figure S2.5). The average net overlap of ABC and SLiM outputs was thrice as large for scenario 10A (185 RSU) than 17A (60 RSU). Across all sex ratio variations, scenario 10 better replicated ABC simulations than scenario 17 (Figure 2.4). The SLiM scenario that overlapped most with its corresponding ABC simulation was 10D (scenario 10 with a sex ratio of 0.7). No significant difference was found in the overlap amount between scenarios (ANOVA $F_{7, 88} = 1.762$, p-value = 0.105, Figure 2.4A) or in the size of the average gap between SLiM and ABC outputs (Kruskal-Wallis $\chi^2_{(7)} = 13.7$, p-value = 0.056, Figure 2.4B). When the total gap was subtracted from the total overlap for each scenario, scenario 10D was the simulation with a distribution most closely matched to the ABC simulation (Figure 2.4). A one-way ANOVA found a significant difference

between the net overlaps of all scenarios ($F_{7, 88}$ = 2.239, p-value = 0.038, Figure 2.4C). However, no significant pairwise differences were identified with a Tukey HSD post-hoc test. SLiM scenarios 10C and 17C performed the worst in terms of reproducing data from ABC, with the smallest overlaps and largest gaps of all the scenarios (Figure 2.4). This indicates that an extreme sex ratio of 99 males to one female is, unsurprisingly, unlikely to occur in the MCF. In terms of the summed net overlaps, the closeness of SLiM scenarios to their corresponding ABC scenarios, nearest to farthest, was: 10D, 17B, 10A, 10B, 17D, 17A, 17C, 10C.

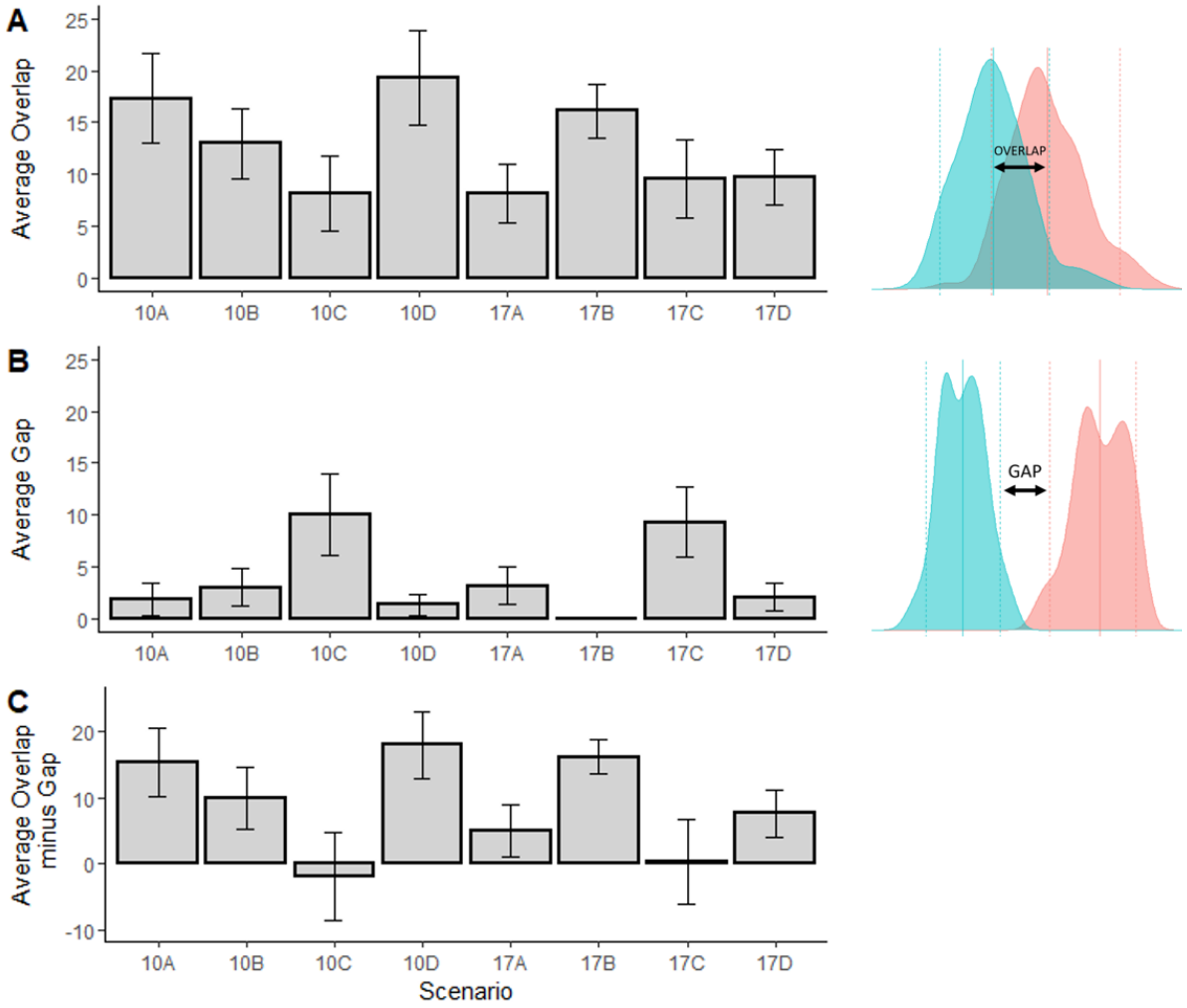

Figure 2.4: Amount of range overlap between the central 90% quantiles of ABCtoolbox and SLiM summary statistic distributions. Distributions were rescaled to enable comparison between all summary statistics. A) Average overlap, B) Average gap, C) Average overlap minus the average gap. Error bars = standard error of the mean.

ABC vs. Observed Data

From running ABCtoolbox with the mode values gained from scenario 10 and 17, scenario 10 produced summary statistics closest to the observed data (Figure 2.5A). The summed Euclidean distance over all summary statistics for scenario 10 was 110, and for scenario 17 was 351. The PCA of the 20,000 best simulations from these scenarios is shown in Figure 2.5B.

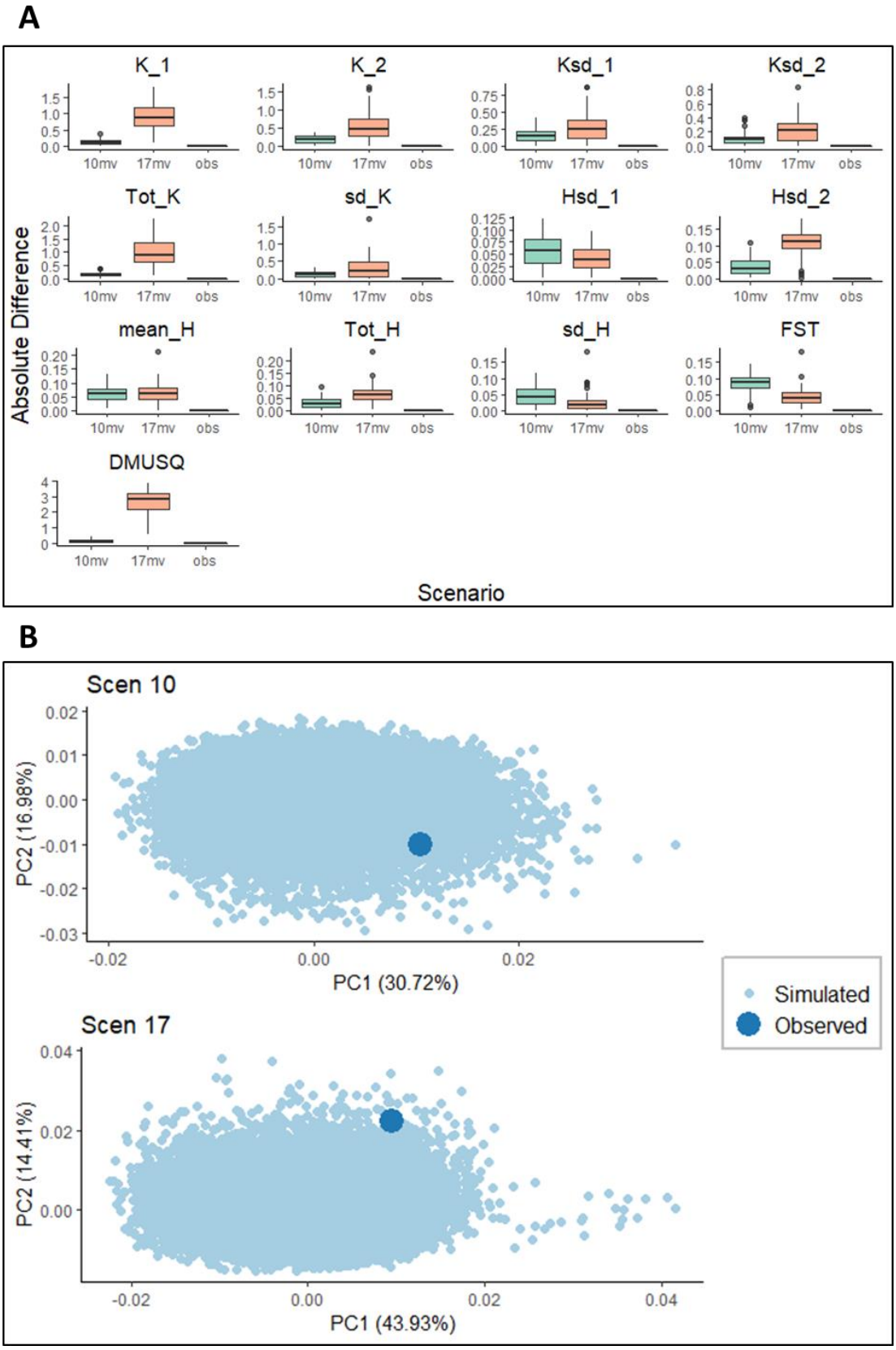

Figure 2.5: A) Absolute difference between summary statistics and observed data (obs), generated when re-parameterising ABCtoolbox with mode value estimates for scenario 10 (10mv), and scenario 17 (17mv). B) PCA of the 2% of simulations closest to the observed data for both favoured models from ABCtoolbox analysis.

SLiM vs. Observed Data

The average absolute distances between each simulated summary statistic and the observed data were calculated for each of the 100 SLiM replicates. The scenario which produced a Euclidian distance (across summary statistics and replicates) nearest to the observed data was recorded in each instance. From the comparison of models with equal sex ratio, scenario 10A had a lower Euclidean distance over all summary statistics than 17A (902 vs. 1,138) and was closer to observed data for 12/18 summary statistics (Figure 2.6). Taking all sex ratio variations together, scenario 10 matched the observed data more closely than 17, having an overall Euclidean distance of 3,674 vs. 4,243 for scenario 17 and an average distance of 918 vs. 1,061. Looking at individual sex ratio variations, scenario 17B had the most summary statistics nearest to observed data (5/18) and the smallest overall summed difference (645). The largest difference was found in scenario 17C (1,441), followed by 10C (1,313). This trend was mirrored in the average differences. The vast majority of simulations were significantly different from the observed data (p-value < 0.05). There were nine instances where the value of a simulated summary statistic was not significantly different from the observed data, and these instances are listed in Table 2.3.

Table 2.3: Summary statistics not significantly different from observed data, based on either a one sample t-test or one-sample Wilcoxon Signed Rank test. D.f. = degrees of freedom.

SLiM scenario	Test	Summary Statistic	t-value	p-value	D.f.	V
10A	Wilcoxon	Sd_K		0.404		2011
10A	t	Hsd_2	-0.16	0.869	99	
10B	t	Tot_K	-0.05	0.960	99	
10C	t	Hsd_1	-0.11	0.912	99	
10C	Wilcoxon	Hsd_2		0.404		2768
10D	t	Mean_H	-0.36	0.721	99	
17A	t	F_{ST}	0.66	0.514	99	
17B	t	Ksd_2	1.28	0.203	99	
17C	t	Hsd_1	0.14	0.889	99	

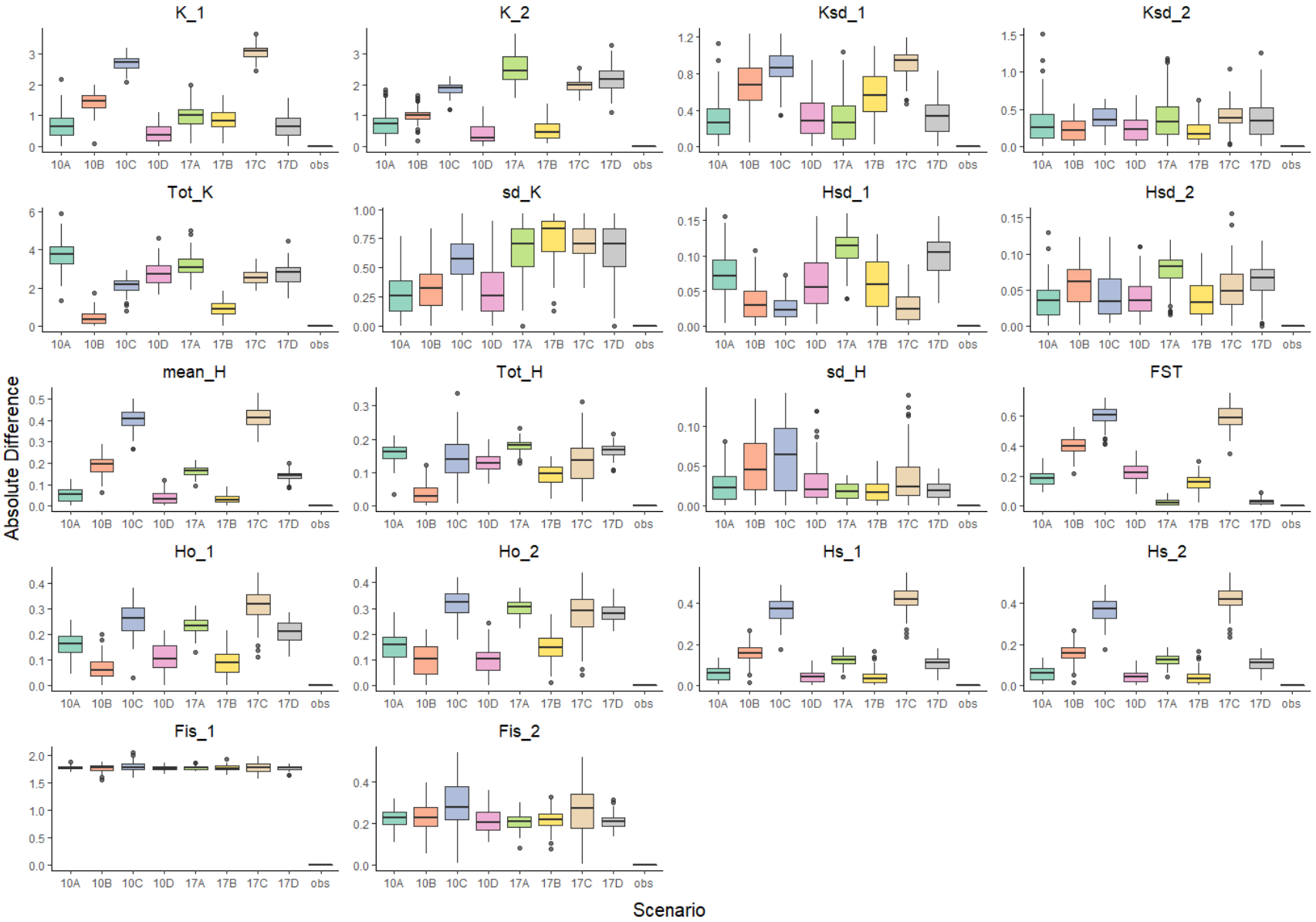

Figure 2.6: Absolute difference for each SLiM scenario between each summary statistic and the observed data (obs).

Additional Estimators of Demography

The optimal combinations of Msvar priors (Gelman & Rubin score < 1.2) were selected across populations. All populations showed a signal of a bottleneck, with the ratio of current to ancestral population size being < 1 in all cases. The single population based analysis of Montserrat showed a bottleneck from Ne = ~92,000 (90% HPD 11,000 - 632,000) to ~192 (90% HPD 10 – 1,300) at ~11,000 years ago (90% HPD 700 - 77,300). The Dominica pre-decline population showed an identical ancestral Ne of 92,000 that declined to ~200, but with a more recent bottleneck ~6,800 years ago (90% HPD 832 - 65,800). Combining the Dominica pre-decline and Montserrat samples resulted in a bottleneck reducing Ne from 92,600 (90% HPD 11,000 - 596,000) to 230 individuals (90% HPD 20 – 1,800) ~8,700 generations ago (90% HPD 760 - 71,400). This best reflects scenario 10, which also features a large population decline. Scenario 17 estimated a population expansion from the ancestral population. Msvar was initiated with a wide parameter range for the mutation rate, mu (10^{-6} - 10^{-2}) which is lower than mutation rates used in ABCtoolbox (mu = 10^{-5} - 10^{-2}). Mutation rates have been demonstrated by Girod et al. (2011) to be inversely correlated with estimates of current effective population size (N0), which in turn is positively correlated with the timing of events, t. With a lower mutation rate than ABCtoolbox, Msvar may have overestimated the current population size, and in doing so, the time since the bottleneck. To attempt to account for mutation rate variation between programs, the current effective population size (N0) was rescaled based on the quotient of mu between ABCtoolbox scenario 10 and Msvar. The time (t) was then re-estimated using t/(2*N0) – indicated to improve the estimation of these parameters by Girod et al. (2011). This resulted in rescaled mode estimates for time of bottleneck in Msvar of 1,341 years ago for Montserrat (50% HPD 1,285 - 1,534), and 599 years ago for Dominica (50% HPD 598 - 684), Figure 2.7.

The F_{ST} value between the two islands was relatively large and significant (F_{ST} = 0.183, p-value = 0.0001). Using Nm to calculate F_{ST} estimated 1.12 migrants per generation. The Nm proportion of migrants calculated via the private allele method after sample size correction was 0.9, with the mean frequency of private alleles = 0.086. All three iterations of 2MOD converged on a posterior probability between 0.83 - 0.84 and a Bayes factor of 5 - 5.4 in favour of a gene flow model. From the favoured gene flow model, it was found that Dominica showed a lower influence of inbreeding (F) relative to migration than Montserrat. Dominica pre-decline F = 0.091 (HPD 0.00002 - 0.076) and M = 2.483 (HPD 1.159 - 29.44). Montserrat exhibited an opposite effect, with higher levels of inbreeding relative to migration. Montserrat F = 0.290 (HPD 0.188 - 0.351) and M = 0.611 (HPD 0.417 - 1.003). Again, this best reflected the demography described by scenario 10, where gene flow to Dominica was higher from Montserrat. Scenario 17 estimated a larger gene flow from Dominica into Montserrat.

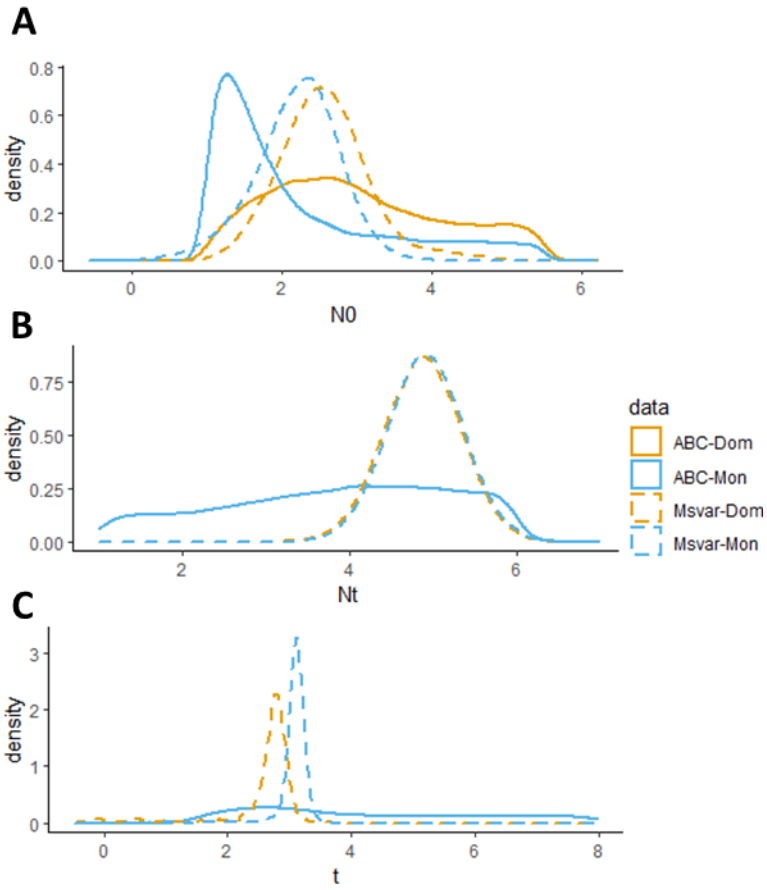

Figure 2.7: Comparison of estimates for the A) current effective population size (N0), B) ancestral effective population size (Nt), and C) time of event given by ABCtoolbox and Msvar. Values for Msvar have been rescaled based on the discrepancy in mode mutation rate between the softwares. Values for N0, Nt, and t are given as Log10(value). Solid lines represent ABC estimates, dashed lines represent Msvar estimates.

Discussion

This study aimed to answer how the MCF dispersed and diverged in the Lesser Antilles into today's extant populations on Dominica and Montserrat, which are significantly genetically diverged based on nuclear genetic markers, but have monomorphic mitochondrial DNA. A 'back and forth' approach was taken, using both backwards-time coalescent simulations and forwards-time simulations, to interrogate different models of demography. Backwards-time simulations from ABCtoolbox highlighted two scenarios as being of equal likelihood, 10 and 17. Values for demographic parameters estimated in these favoured scenarios were used to build forwards-time models in SLiM. Simulated and observed summary statistics were compared between SLiM and ABCtoolbox. Similarity between outputs was used as a measure of which demographic scenario was best able to be reproduced between simulators and to reproduce observed data. Overall, scenario 10 (a divergence and subsequent bidirectional gene flow matrix) produced more similar summary statistics between ABC and SLiM than scenario 17 (admixture with intermediate population). Scenario 10 also produced summary statistics that were closer to observed data than scenario 17. Various skews in sex ratio were implemented in forwards simulations, a feature not available with coalescent backwards simulators. These scenarios were used to attempt to explain the lack of mitochondrial diversity through a male-biased skew in populations of the MCF. Of scenario 10's sex ratio variants, scenario 10D, with a sex ratio of 2.3 males per female was best able to replicate ABC and observed data.

Divergence

Scenario 10 was a stronger model than scenario 17, given the closer replication of ABC-simulated and observed summary statistics, the agreement with signals of a large bottleneck and gene flow detected in other population genetics softwares, and higher marginal density value. Therefore, the most likely estimation of the MCF's demography, using the ABC-estimated values, is that Dominica and Montserrat became genetically diverged from a large ancestral population ~450 years ago (1570 CE), and underwent a very large bottleneck in the process. Since divergence, the two populations continued to experience a small level of gene flow, with more gene flow into Dominica from Montserrat. Scenario 17 gave an estimation of population expansion in both populations, a trend not detected by any other software, and an estimate for the production of the Montserratian population which is too recent: ~60 years ago. At this point in time, a population was already known to exist on Montserrat, with 12 museum specimens dated from 1962 collected in Montserrat cited by King and Ashmore (2014). The only factor indicating that scenario 17 was superior to scenario 10 was the posterior p-value gained from the ABC-GLM. Both marginal density and posterior p-value are estimates of the likelihood of a model, but there is little information in the literature as to which should be given more weight to decide model selection. However well the GLM generated for scenario 17 fit to the observed data, the posterior parameter estimates appear unlikely given what is known about the historical distribution of the MCF and the contrast to demographic processes detected by other software.

Scenario 10 estimated that Dominica and Montserrat diverged into two distinct populations fairly recently, for an evolutionary timescale. Divergence was estimated within the last 7,000 years, most likely ~450 years ago. Divergence was coupled with a large reduction in both populations. Msvar

supported this signal of a large bottleneck, with the magnitude of effective population decline for Dominica 99.6% in ABC and 99.7% in Msvar, and for Montserrat 99.9% in ABC and 99.8% in Msvar – so differing only by 0.1% in both cases. Msvar estimated that the bottleneck occurred ~6,000 years earlier than the mode value from ABCtoolbox, which is still within the 50% HPD interval estimated by ABC, supporting a population decline in the last 7,000 years. When the time of bottleneck was rescaled in Msvar due to the originally unequal mutation rate parameters, it moved forwards to more closely coincide with the timing of the divergence from ABCtoolbox, being 520 years earlier than the divergence event in ABCtoolbox. This rescaling approach has not been applied in other literature, and should be taken only of a rough approximation of how results from ABCtoolbox and Msvar might be made more comparable – though it is based on an established relationship between mutation rate, population size, and timing of population size change, illustrated in Girod et al. (2011). Regardless of rescaling, Msvar and ABC both detect a substantial population bottleneck and indicate that the MCF underwent a very large decline and a subsequent divergence into two genetically distinct populations.

The broadest conclusion that may be drawn based on the estimates for time of divergence is that the MCF declined and diverged as humans arrived in the Caribbean. The Lesser Antilles have been inhabited for ~6,000 years, and the arrival of humans may have prompted a population decline in the MCF through hunting, or the initiation of founding effects if individuals were moved onto new islands (Siegel et al. 2015). The most likely estimate for the time of the divergence and decline, within the past 500 years, coincides with European colonisation of the Caribbean (Hofman et al. 2014). The ancestral population of MCFs was not estimated to diverge prior to this point. How could a frog, not suited to saltwater or the exposure associated with overseas migrations, have sustained a connected population through the Lesser Antilles? Firstly, the MCF lived on an estimated eight islands in the Lesser Antilles, hence populations were in closer proximity to one another than today (King and Ashmore 2014). The distances between the former island populations range from 30 - 70 km, but islands would have been closer during the last glacial maximum (26,000 - 19,000 years ago) as sea levels were ~130 m lower (Kwiecinski et al. 2018). Camargo et al. (2009) estimated that *Leptodactylus validus* was able to disperse in the Lesser Antilles during these periods of low sea level via rafting. However, while rafting could explain some gene flow in the MCF, it is unlikely to have been a frequent enough event to maintain similar allelic frequencies between islands. It has often been proposed that MCFs were transported deliberately by humans, given their well-documented use as a food source throughout the history of the region (King and Ashmore 2014; Kemp et al. 2020). The pre-Columbus Caribbean islands were highly connected, with stretches of sea between islands functioning as 'aquatic motorways' that facilitated trade and travel in canoes carrying up to 60 people between indigenous communities (Hofman et al. 2010; Fitzpatrick 2013; Rosa and Fernandez Loras 2014). Archaeological and written accounts document the movement of flora and fauna by indigenous people in the Caribbean, for cultivation, trade, and sustenance, which were also accompanied by the unintentional movement of stowaway species (Newsom and Wing 2013; Kemp et al. 2020). Camargo et al. (2009) also attribute movement of *L. validus* between St. Vincent and Grenada to human transportation. It is agreed that inter-island travel in the pre-Columbian Caribbean was 'frequent', but no quantitative records exist for the number of journeys made during a given time frame (Fitzpatrick 2013). However, it is reasonable to assume that 'frequent' equates to several journeys made within a 3-4 year period,

the generation time for a MCF (IUCN SSC Amphibian Specialist Group 2017). Given the known association of humans and the MCF, and the human connectedness of the region, it is plausible that one translocation and successful mating of a MCF between islands could have occurred every 3-4 years. This is enough to satisfy the one migrant per generation rule to prevent population divergence established by Wright (1931) and Slatkin (1985).

A divergence time of 450 years ago equates to approximately the mid-16th century, by which point Europeans had begun to colonise the Caribbean (Hofman et al. 2014). The timing of population divergence and bottlenecks detected in the MCF coincides with a point in time when normal aspects of pre-Columbus Amerindian society were halted. Looking specifically at the Lesser Antilles, in the 16th century the enslavement and murder of Kalinago people (indigenous Lesser Antillean) was occurring, and the introduction of diseases from Europe and Africa through the Atlantic trade of enslaved people also caused declines in indigenous human populations (Wilson 1997). The arrival of European colonists to the Caribbean may well have interrupted usual patterns of MCF gene flow that were before maintained by indigenous communities. European colonisation also altered the flora and fauna of the Caribbean. Invasive species such as mongoose, rats, and pigs were introduced and remain a threat to MCF survival today (Adams et al. 2014; Kemp et al. 2020). Natural landscapes were converted to agriculture and forests were logged, all culminating in the extinction of many species in the Lesser Antilles (Steadman et al. 1997; Ricklefs and Bermingham 2008; Brace et al. 2015). The alteration of habitat and introduction of invasive species could have triggered a population decline in the MCF, as evidenced in this study. A smaller MCF population, coupled with disruption to regular patterns of Kalinago trade and transport, could have culminated in there being fewer frogs to find and fewer instances to move them. A once well connected MCF population in the Lesser Antilles may, as a result, have split into two divergent populations on Dominica and Montserrat.

Migration

Scenario 10 estimates that following divergence between the two populations, some level of gene flow was maintained. A higher proportion of Dominican genes were estimated to be of Montserratian origin each generation, than the genes in Montserrat of Dominican origin. This pattern of gene flow is supported by the theory of island biogeography, where larger, more connected, islands are expected to have larger rates of immigration (MacArthur and Wilson 1967). Dominica is both larger than Montserrat and nearer to the nearest continental mainland of South America and to its nearest neighbouring islands (29 km) compared to Montserrat (39 km). Dominica's nearest neighbouring islands of Martinique and Guadeloupe are also larger than the neighbours of Montserrat, too (Guadeloupe, Antigua, St. Kitts). This pattern was also observed in Komodo dragons, where the influence of drift relative to migration was higher on a smaller island (Gili Motang) that was more distantly situated from the nearest large landmass of Rinca or Flores West, which both had a higher influence of migration relative to drift (Ciofi et al. 1999). Montserratian MCFs are typically larger than Dominican MCFs (Daltry 2002), which aligns with the theory of island gigantism (Lomolino 1985). Gigantism in island populations of frogs was demonstrated by Rebouças et al. (2018) and could explain why the more isolated MCFs on Montserrat tended to be larger frogs. Consensus was found among all estimators of gene flow: ABC and 2mod both found higher immigration to Dominica than

Montserrat. Nm averaged between both islands resulted in an estimate of 2.6 based on ABC results, and 1.5 based on 2mod. Estimates of a single Nm for both islands were smaller when based on private alleles and on F_{ST}, with both being close to one migrant per generation (0.9 and 1.12, respectively). The figures given for Nm range from 0.9 – 2.6, while the estimate for F_{ST} is 0.183. This value of F_{ST} is significant as it is the level of population differentiation expected under the one migrant per generation rule in a population in equilibrium, which is also close to the values for Nm calculated in this study (Wang 2004).

Estimates of gene flow seem plausible when considering similar studies; Nm ranged from 3.66 – 19.65 over distances of 60 – 200 km in Bahamian subpopulations of *Anolis* lizards (Calsbeek and Smith 2003). A ground cricket of the Virgin Islands had an Nm 0.8 – 4 after periods of island connectedness and separation over the last 8,000 years (Papadopoulou and Knowles 2015). Looking at amphibian studies of gene flow in island populations, *Rana temporaria* and *Bufo bufo* showed high levels of migration (Nm 3.6 – 83.1) over short (< 10 km) distances between islands in the Tvärminne archipelago, demonstrating that seawater is not a total barrier to gene flow in amphibians (Seppä and Laurila 1999). Nm among coastal and island populations of *Thoropa taophora* in São Paolo was low (0.1 – 0.62) but existent nonetheless over distances of up to 40 km (Duryea et al. 2015). Given that terrestrial species in the Lesser Antilles have similar, or higher levels of gene flow over the same region as the MCF, and that overseas amphibian dispersal is demonstrated, the levels of population connectedness found in this study are reasonable.

The MCF continued its close relationship with humans through pre-colonial, colonial, and modern day times, as evidenced in archaeological records and from its known popularity in the cuisine and culture of modern day Dominica and Montserrat (Adams et al. 2014; Wallman 2018). It is possible that humans continued to transport MCFs between Dominica and Montserrat through history. A consistent history of inter-island connection between Dominica and Montserrat is detailed by Honeychurch (2003). Under threat from colonists in the Greater Antilles, Kalinago people migrated away from the northern islands in the Lesser Antilles through the 1500-1600's, eventually settling on Dominica (Wilson 1997). This would also support the higher proportion of Montserratian genes in Dominica, if the Kalinago carried MCF on their migration. Dominica was eventually colonised in 1763, and from this point until the independence of Dominica from Britain, both islands were both under British rule, meaning free movement of ships between islands considered effectively the same country. Trade in enslaved people and the eventual free movement of people between the two islands is documented (Honeychurch 2003). While the connectedness of human populations on Dominica and Montserrat is proven, this does not explicitly address whether MCFs were too. However, the transport of live animals for trade and sustenance is documented in the colonial Caribbean (Shapiro 2015; Hart 2016). Trade has facilitated the spread of other amphibian species, for example *Eleutherodactylus coqui* and *E. johnstonei* throughout the Caribbean and further afield (Kaiser 1997; Marr et al. 2008). Being relatively small and tree-dwelling, they are easily caught up in botanical shipments. The MCF is larger and perhaps harder to accidentally transport, however this has not been a barrier to the similarly sized cane toad *Rhinella marina*, which has spread inadvertently in overseas shipments (Heinsohn 2006; White and Shine 2009; Moro et al. 2018).

Sex Ratio and mtDNA

The scenario most closely resembling its corresponding ABC scenario was scenario 10D, meaning that the demographic model including a migration matrix was best replicated when a sex ratio of 2.3 males to 1 female was present. As hypothesised, having fewer females than males in a population could contribute to a lack of mitochondrial diversity without impacting nuclear diversity as much, as mitochondria are maternally inherited and their diversity is linked to female effective population size (Perlman et al. 2015). No information exists on the sex ratio in natural populations of the MCF. For most populations of organisms, sex ratio is close to 1:1 (Alho et al. 2008). In captivity, MCF breeding is encouraged by creating a male:female sex ratio of 2:1 within enclosures (Jameson et al. 2019a). Males are territorial and will engage in competition for females through calls and wrestling with one another. This indicates that females are the limited resource, and a male skewed operational sex ratio is predicted in this case (Kvarnemo and Ahnesjö 1996; Grayson et al. 2012). Gazoni et al. (2018) recorded a very high number of sex chromosomes in *Leptodactylus pentadactylus*, the MCFs close relative, stating this can arise through heterogametic sex advantage, in this case being males. However it should be noted that there is no evidence, other than the XY/XX system in other species of the genus Leptodactylus (Gazoni et al. 2018), for the XY/XX system being used in the MCF. Other studies of *Leptodactylus* frogs have recorded male biased sex ratios (Reading and Jofre 2003; Ferreira et al. 2007; Lucas et al. 2008), but these findings should be viewed with caution as they may be subject to biases in the detectability of either sex.

Despite some evidence to suggest a male biased sex ratio, there are probably additional and interacting demographic factors that have all culminated in identical mitochondrial DNA amongst all MCFs. A male-biased sex ratio could enhance the impact of processes such as founder events or selection. The impact of a founder effect in house finches was exacerbated by the artificially male-biased sex ratio of the imported population (10:1 male:female) (Hawley et al. 2008). Identical mtDNA supports the model of recent divergence between Dominica and Montserrat, as a relatively small amount of evolutionary time has passed where mutations could accrue. Monomorphic mtDNA (a 722 bp fragment of the 12S gene) was found in all but one population of UK Adonis blue butterflies (Harper et al. 2008). This haplotype differed from a French haplotype by one nucleotide and indicated a strong recent bottleneck or founder effect (Harper et al. 2008). No nuclear DNA information was given to indicate whether a similar pattern to the MCF was present in this case. Analysis of bottlenose dolphins with a single mtDNA haplotype (based on 750 bp from the control region) and moderate nuclear heterozygosity also suggested recent colonisation by a common ancestor (Barragán-Barrera et al. 2017). The time since divergence between Dominican and Montserratian populations is 450 years, which may not have been long enough for mutations to arise. Based on a mitochondrial mutation rate at the ND2 gene in *Eleutherodactylus* frogs of 14.8 – 24.5 $x10^{-9}$ substitutions per site per year (Crawford 2003), this would equal 0.12 – 0.19 mutations over 450 years, assuming a mitogenome size of 17,500 bp. A recent divergence from an identical haplotype, coupled with the evident gene flow, could prevent divergence, and be further enhanced if the male biased sex ratio skew is true. Mitochondrial and nuclear incongruence could be due to adaptive processes (Allio et al. 2017). MtDNA is not neutral, and it is possible that selection could also be occurring. The mitogenome can be subject to positive selection if there is an adaptive advantage to a particular haplotype and as mtDNA typically

doesn't recombine, the impact of selection on a particular gene can reach throughout the mitogenome (Bazin et al. 2006; Perlman et al. 2015; Allio et al. 2017). MtDNA diversity can reflect the time since the last event of selective sweep, rather than population history and demography (Bazin et al. 2006).

To further investigate processes shaping the contrasting mitochondrial and nuclear diversity in the MCF, several investigations can be done. Firstly, it would be important to establish the sex ratio in the wild by undertaking a sufficiently large capture-mark-recapture study, but this will be difficult given the very small remaining wild population (Alho et al. 2008). Secondly, whole mitogenome sequencing could offer a full insight into the diversity of the mitogenome and allow extensive tests of selection to be performed to check for any selective sweeps that may have fixed one haplotype throughout the population. Until then, this study provides evidence that a recent divergence of the two populations, coupled with a slight skew in the sex ratio towards males, could allow for the same haplotype to be distributed through all individuals.

Conclusion

The advantage of using a back and forth approach comes in having a double validation of findings, and in being able to account for limitations of either approach. Given the high flexibility of forward simulators, the fact that SLiM could replicate distributions for summary statistics given by ABCtoolbox, allows one to more confidently support the mode parameter values from ABCtoolbox. However, the estimates of timing and magnitudes of demographic change given in this study should not be taken as exact figures, as models are not able to truly replicate the intricacies of population dynamics over time. This study has shown that MCF populations on Dominica and Montserrat have likely recently diverged into two genetically distinct populations, and that some small level of connection has probably persisted in following generations. Aligning the demography of the MCF with the timeline of human activity in the Lesser Antilles reveals the coincidence of anthropogenic disturbance and population decline and separation in the MCF. Through this, we can see how humans have impacted on the historical demography of the MCF and it also allows us to believe that we can be impactful in influencing its future. This message is key to the conservation of the MCF. This study revealed that there is possibly a slight skew in the sex ratio of MCFs towards males. Further investigation of this male-biased skew is needed, as it is a key part of MCF biology that would be integral to ongoing captive breeding and reintroduction efforts. It is also important that signatures of selection in the MCF mitogenome be investigated further, as identifying selective pressures or adaptive processes in the mitogenome could also be important to consider for successful MCF population recovery in the wild.

Chapter Three

Not A Lot, But Maybe Enough: Low MHC Diversity in the Mountain Chicken Frog Still Holds Variants Linked to Bd-tolerance

Abstract

Almost all wild mountain chicken frogs (*Leptodactylus fallax*, MCF) died in the years 2002 – 2009 with an infection of the fungal pathogen *Batrachochytrium dendrobatidis* (Bd). A small number of MCFs survived the initial epizootic, including animals known to survive Bd infection, but the determinants of their survival are unclear. The determinants of Bd infection resistance, tolerance, or elimination in amphibians are likely to encompass a variety of host, pathogen, and environmental factors. One host factor that has been shown to be associated with increased tolerance or susceptibility to Bd infection is the major histocompatibility complex (MHC). Variation at the MHC is influenced by pathogen-mediated selection, but the MHC in the MCF remains uncharacterised. To address this, this study designed new, multi-locus primers and high-throughput deep sequencing with which to study two key exons of the MHC in the MCF. It also provides the first concurrent assessment of both MHC class I and class II classes in relation to amphibian survival from a Bd outbreak, covering the entire range of the MCF as it experienced a transition from epizootic to enzootic Bd prevalence. Characterising the MHC in 250 MCFs revealed a pronounced lack of allelic diversity relative to other amphibians, with seven MHC-I and two MHC-II variants found. MHC diversity has likely been depleted by several prior population bottlenecks. The MHC-II was almost monomorphic across individuals and showed no link to survival following the Bd epizootic. In contrast, between one and three MHC-I variants repeatedly showed significant increases in frequency in surviving MCF populations and in MCFs known to clear Bd infection. Positive selection was identified in MHC-I variants associated with this survival. These results, for the first time, highlight the importance of studying the MHC-I in relation to the intracellular pathogen Bd. This is a crucial new insight into the determinants of the wild MCF population's ability to persist despite the presence of Bd and provides new information with which to inform conservation management of this Critically Endangered species.

Introduction

The mountain chicken frog (*Leptodactylus fallax*, MCF), like hundreds of other amphibian species, has suffered population declines due to infection with the fungal pathogen *Batrachochytrium dendrobatidis* (Bd) (Hudson et al. 2016a; Scheele et al. 2019a). The MCF suffered the fastest ever recorded decline of a species due to infectious disease, becoming Critically Endangered after Bd reached its home range in Dominica in 2002, and Montserrat in 2009 (Hudson et al. 2016a). MCFs now exist in a few, fragmented populations in Dominica, where individuals persist with exposure to enzootic levels of Bd (*Author's unpublished data* 2019). Some of these MCFs have been observed to clear detectable Bd infection, indicating that at least some of the population are Bd-tolerant. Recovery strategies for the MCF focus on protecting existing wild populations, and replenishing lost populations from captive-bred stock (Adams et al. 2014). To ensure that these approaches have the best chance of success, it is crucial to understand the determinants of survival of Bd infection, i.e. why did some frogs in Dominica survive, while most of the species did not? Since the devastating impacts of Bd on amphibian populations have been identified, much work has been done to uncover the possible determinants of Bd infection outcome (Fisher and Garner 2020). A considerable amount of research has focused on immunogenetics, given that Bd is a pathogen that should, in principle, elicit some form of immune response (Fu and Waldman 2017; Grogan et al. 2020). A key component of an amphibian's immunological response to pathogens, including Bd, is the major histocompatibility complex (MHC).

The MHC is a multi-gene complex that encodes many proteins involved in both innate and adaptive immunity (Flajnik 2018). The MHC is a feature of the immune systems of jawed vertebrates and is divided into several subclasses of genes, based on the structure and function of the proteins they encode. Classes I and II are responsible for displaying pathogen molecules to host immune cells. MHC class I proteins can be found in all nucleated cells and are therefore more widespread than MHC class II proteins, which are found only on dendritic cells exposed to external environments (Wieczorek et al. 2017). Class I proteins bind to intracellular antigens which are then displayed on cell surfaces for recognition by cytotoxic CD8+ T cells (Acevedo-Whitehouse and Cunningham 2006). Class II proteins bind to extracellular antigens and activate helper CD4+ T cells. The MHC gene complex can span millions of bases as a whole (Janeway et al. 2001), but studies often focus on key, functionally important regions. These regions are determined by the peptide binding region (PBR) of each class and are often only 100 - 300 bases long (Kiemnec-Tyburczy et al. 2012; Bataille et al. 2015). The MHC class I protein is formed from a single α chain (Janeway et al. 2001). This α chain forms the transmembrane anchor (domain α3) and the PBR (domains α1 and α2). Domains α1 and α2 are translated from the genetic sequence of class I exons 2 and 3, respectively. The MHC class II protein is a heterodimer, consisting of an α and β chain (Janeway et al. 2001). Within each chain there is a transmembrane domain (α2 and β2) and the PBR is formed by domains α1 and β1. The β1 domain is encoded by exon 2 of the Class II gene. Genetic variation within genes encoding PBRs determine which peptides or antigens can be displayed to immune cells (Radwan et al. 2020). With a larger range of pathogen peptides that can be bound to an MHC protein comes an increased capacity to respond to a range of diseases. Consequently, the MHC contains the most variable functional genes described in

vertebrates (Piertney and Oliver 2006), with tens to hundreds of variants at MHC loci within the same population (Radwan et al. 2020).

Parasites or pathogens can drive evolution in the MHC. Having enough MHC diversity to respond to a diverse pathogen community can be advantageous (Spurgin and Richardson 2010). When a particularly virulent pathogen is present within the population, a rare allele that confers resistance to this pathogen is often more beneficial than a wide range of allelic variation (Spurgin and Richardson 2010). It is most widely accepted that these two forces, heterozygote advantage (higher diversity) and negative frequency dependent selection (rare allele advantage), act on the MHC and result in balancing selection – maintaining multiple alleles at high frequencies in the population (Radwan et al. 2020). The forces vary through time and space with varying pathogen exposure (Spurgin and Richardson 2010). Evidence of large selection coefficients measured over a short time period, alongside high non-synonymous to synonymous base substitutions within the PBR, indicate that rapid adaptive evolution can take place in the MHC in the face of a disease threat (Radwan et al. 2020).

The MHC has been an obvious target for studies looking to uncover immunogenetic and evolutionary dynamics of amphibian survival or decline with Bd. Involvement of the MHC has been demonstrated by transcriptomic studies, which have revealed that both MHC-I and MHC-II expression can be upregulated in the skin of infected and susceptible frog species (Rosenblum et al. 2012; Ellison et al. 2014), while the downregulation of both classes was observed in spleen tissue (Rosenblum et al. 2012). As well as changes in their expression, genetic variation of both class I and II loci has been studied, with most literature focusing on class II loci in the β1 domain (Savage and Zamudio 2011; Bataille et al. 2015; Kosch et al. 2016; Savage and Zamudio 2016; Trujillo et al. 2021). Kosch et al. (2019) chose to study the MHC-I α1 domain with the reasoning that Bd is an intracellular pathogen. Across multiple continents and species, in both laboratory and field settings, an association between particular MHC alleles or supertypes (functionally similar alleles) with Bd infection survival or susceptibility has been found (Savage and Zamudio 2011; Bataille et al. 2015; Kosch et al. 2016; Savage and Zamudio 2016; Kosch et al. 2019; Trujillo et al. 2021). Often, directional or positive selection is implicated through MHC-II variants in surviving or Bd-resistant amphibians (Savage and Zamudio 2011; Bataille et al. 2015; Kosch et al. 2016; Savage and Zamudio 2016). Savage and Zamudio (2011) identified a particular confirmation of the PBR – 'allele Q' which was under directional selection in both lab and field populations of *Lithobates yavapaiensis* that survived Bd infection. Bataille et al. (2015) recorded similar observations in the Australian tree frog *Litoria verreauxii alpina*, where amino acid substitutions were under selection and associated with Bd outbreak survival in the same region as allele Q, termed pocket P9 in their study. Trujillo et al. (2021) observed protective alleles and supertypes matching the regions or conformations of allele Q and P9 in *Lithobates pipiens*.

To date, studies of amphibian MHC diversity in relation to Bd infection outcomes have constituted a 'snapshot' view of the evolutionary dynamics between host and pathogen, either by sampling just one time point in the host-pathogen interaction, just a fraction of a host population, or by focusing on just one MHC class (Savage and Zamudio 2011; Kosch et al. 2016; Trujillo et al. 2021). Such studies can, however, miss important changes in allele frequencies over time which arise due to spatiotemporal variation in host-parasite coevolution (Radwan et al. 2020), or fail to account for the fact that Bd is an

intracellular pathogen (Berger et al. 2005). The archive of genetic data collected from MCFs spans the entire range of the species in Dominica and Montserrat. Samples exist from across 20 years of host-pathogen coevolution: prior to declines in Dominica, throughout the fastest-ever recorded decline of a species, to samples from the current day, where MCFs survive in the wild with enzootic Bd infection. These samples provide a rare opportunity to study the evolutionary dynamics of the MHC across an entire species from disease emergence through epizootic mortality to post-decline survival. In addition, the establishment of a biosecure captive population provides an opportunity to gain insight into the impacts of this conservation intervention on MHC diversity, enabling an immunogenetic assessment of stock for potential reintroductions, and may provide valuable insights for conservation practitioners. This study will provide the first simultaneous assessment of MHC-I and MHC-II variants in relation to Bd infection survival in a species of amphibian. This approach may highlight whether Bd exerts selective pressure equally on each class, and perhaps identify which class has variants associated with MCF populations that survived a Bd epizootic.

To do this, functionally relevant exons implicated in peptide binding will be studied. No genetic resources to study the MHC currently exist for the MCF, so this study will aim to develop primers with the potential to amplify multiple loci from exon 2 of both MHC-I and MHC-II in the MCF. As a starting point, a 'black box' multi-locus approach will be employed, designing primers to amplify as much variation as possible. These primers will be used to generate the first characterisation of the genetic variation of MHC-I and MHC-II exon 2 in the MCF. Furthermore, MHC variation in the MCF will be studied across space, time, and between groups of MCFs that are susceptible or tolerant to Bd, in order to better understand the evolutionary forces or variants determining survival following Bd infection. It is hypothesised that in line with similar studies, MHC-II will have variants associated with surviving populations. Similarly, MHC-I should also have variants associated with survival as Bd is an intracellular pathogen. It is also expected that signatures of selection will be observed in MHC PBRs.

Methods

Sample Collection

Genomic DNA was sourced from the tissue sample and DNA archive of the MCF project, stored at the Institute of Zoology, London. DNA had previously been isolated from skin, blood, or buccal swab samples using a Qiagen DNEasy Blood & Tissue kit extraction protocol for animal tissue or nucleated blood. A total of 268 MCF samples were included in this study. Samples were collected during post-mortem examinations or as part of routine population monitoring in Dominica, Montserrat, and the biosecure captive population housed across Bristol, Chester, Durrell, Norden's Ark, and ZSL zoos. All sampling occurred from 2002 – 2020.

Primer Design

No published primers exist for the MCF MHC. As the MHC is hypervariable, using pre-existing primers designed for another species risks missing allelic variation in the MCF (Gillingham et al. 2021). To design species-specific primers, more general amphibian MHC primers were first used on MCF DNA, to locate target MHC regions and generate a variety of MCF-specific sequences. Additionally, MCF whole genome sequence data were generated to supplement and guide primer design in identifying where MCF sequences vary from published primer sequences. This method aimed to design MHC primers that were a) targeting the PBR, and b) capturing as much allelic variation present in MCFs as possible by incorporating degeneracy and base changes into the primers.

A MCF sample was submitted to Novogene, Hong Kong for whole genome sequencing (~66.7 million paired-end reads of length 150 bases). These data were used to create an alignment with the most closely related, annotated amphibian genome: *Rhinella marina* (assembly reference GCA_900303285, Edwards et al. 2018). First, MCF reads with phred score < 28 and length below 90 bases were removed using Trimmomatic v.0.39 (Bolger et al. 2014). Remaining reads were then aligned to the *R. marina* genome using BWA mem v.0.7.17 (Li 2013). Due to the likely divergence of the two genomes, mapping parameters were relaxed to allow quality >10 and gaps of up to 1,000 bases. PCR duplicates and unmapped reads were removed using samtools v.1.10. *Rhinella marina* genome regions annotated as MHC were located using Integrative Genome Viewer (Thorvaldsdóttir et al. 2013). To verify these regions as MHC loci, a BLAST search was performed within the *R. marina* genome, using published MHC-I and –II exon 2 sequences from other amphibian species: *Engystomops pustulosus, Litoria verreauxii, Agalychnis callidryas, Smilisca phaeota,* and *Pseudophryne corroboree*. Regions of the *R. marina* genome that consistently matched to published amphibian MHC sequences were selected as the candidate MHC-I and –II exon 2 regions. Aligned MCF reads mapping to these *R. marina* MHC regions were extracted as consensus sequences for MHC- I and II exon 2 using samtools mpileup, allowing ambiguous bases (Li et al. 2009). Tablet genome viewer (Milne et al. 2010) was used to generate a second MCF consensus sequence for each exon, which excluded ambiguities arising from *R. marina* vs. MCF variants. For each MHC class exon, the Tablet-generated consensus sequence was used as a new genomic reference to which MCF reads were re-mapped using BWA mem (Li 2013). This resulted in an increased read coverage for the region of interest, from which a final consensus sequence for primer design was produced.

Published primers for the MHC-I exon 2 region of *R. marina,* Class I_AlphadomF and ClassI_AlphadomR (Lillie et al. 2014), were initially used to generate comparable sequences for the MCF. MCF DNA template was chosen from both Dominica and Montserrat to maximise potential genetic variation captured. PCR reactions consisted of 5 µl 2X QIAGEN multiplex mastermix, 0.5 µl of 5X QIAGEN Q solution, 0.4 µl of 10 µM forward and reverse primer, and 2.7 µl of H_2O. Cycling conditions began with denaturation at 95°C for 10 minutes, then 35 cycles of 94°C for 45 s, 54°C for 1 minute, 72°C for 1 minute, and an elongation for 10 minutes at 72°C. Sanger sequencing of PCR products was performed by Eurofins genomics. Resulting sequences were aligned in Geneious v.6.06, alongside published primers for the same region (Lillie et al. 2014; Kosch et al. 2017), the NGS-generated MCF consensus sequence, and sequences from other amphibian species taken from Genbank. Several primer pairs were designed in conserved regions to capture allelic variation at MHC-I exon 2 but were edited to take into account MCF-specific variants found by NGS sequences and PCR amplicons. Each combination of compatible primer pairs was evaluated for its ability to capture variation and quality sequences. A final, exonic primer pair that captured 257 bp of the exon was generated (Table 3.1). The same process was repeated for class II exon 2 using primers BobomSR and BC6F (May and Beebee 2009) to amplify initial MCF sequences from the MHC class II β1 chain. PCR annealing temperature was 56°C, but all other conditions were the same. A final, exonic primer pair was designed to capture 248 bp of the exon (Table 3.1). The details of all published primers used and initial primers designed can be found in supplementary Tables S3.1 and S3.2. PCR cycles with a reduced cycle number of 28, 30, or 32 were trialled using final primer pairs, as this reduces the number of PCR artefacts that can impede MHC studies (Babik 2010). The lowest number of cycles that produced enough PCR product (as determined by gel band brightness) was 30 cycles.

Table 3.1: Details of the final primer pairs designed to amplify the MHC class I exon 2, and MHC class II exon 2 in *Leptodactylus fallax*.

Primer ID	Direction	Target Region	Sequence (5'-3')	Length	Amplicon Length	Reference
LfMhcIEx2F3	Forward	MHC **Class I** exon 2 (α1 domain)	ACAGTCACTCTCTGCVTTATT	21	220 *257 (with primers)*	Generated for this study
ClassI_Alpha1domR	Reverse		GTTGAAGCGGCTCATC	16	*277 (with MID tags)*	Lillie et al. (2014)
LfMhcIIEx2F2	Forward	MHC **Class II** exon 2 (β1 domain)	CTGCCGTGGATTACATGTTAGAA	23	196 *248 (with primers)*	Generated for this study
Bobom-DEG	Reverse		CCATAGTTGTGTWTACAGWMTSTYTCCAC	29	*268 (with MID tags)*	Edited from May & BeeBee (2009)

Amplicon Barcoding and Illumina Sequencing

Initial sequencing primers (Table 3.1) were amended to include unique multiplex identifier tags (MID-tags) to allow de-multiplexing of samples after Illumina sequencing. MID tags consist of 10 bases and are appended to the 5' end of each primer so that every sample is identifiable from a unique forward and reverse MID tag combination (Binladen et al. 2007). Samples were amplified in final PCR reactions for each MHC class using 10 µl 2X QIAGEN Multiplex Mastermix, 1 µl 5X Q solution, 0.8 µl of 10 µM forward MID-tagged primer, 4 µl of 2 µM reverse MID-tagged primer, 2.2 µl of PCR-grade H_2O, and 2 µl DNA. PCR conditions for each MHC class were as before. Seven samples were included in three separate PCR reactions to assess the consistency of PCR amplification. PCR products were checked for amplicon size and DNA concentration (ng/µl) using a Qiaxcel high sensitivity cartridge. Successfully amplified products were pooled in equimolar quantities within each PCR plate. Initial pools were cleaned using a SPRI bead clean-up method and quantified using a TapeStation and Qubit. Initial pools from each MHC class were combined in equimolar quantities into a pool for sequencing. Paired end Illumina 2x250 sequencing was run on an Illumina MiSeq, allowing for the possibility of ultra-deep sequencing (>5,000x coverage per amplicon) which is thought to overcome the majority of MHC genotyping inconsistencies (Biedrzycka et al. 2017). Sequencing and library preparation were performed at Cardiff School of Biosciences' Genome Hub.

Allele Calling

Calling of alleles from sequencing data was performed by ACACIA (Gillingham et al. 2021). ACACIA was chosen for genotyping due to its basis on a clustering method – deemed robust by Biedrzycka et al. (2017) – and its ability to handle deep sequencing data. Raw data were demultiplexed using cutadapt's combinatorial demultiplexing facility (Martin 2011). One base mismatch per MID tag was allowed, as this was found to be optimal from preliminary analyses (Lorna Drake, *pers. comm.*). Reads without a complete MID tag were discarded from the analysis. Fasta reference lists were compiled using >100 sequences from a Genbank query for: "MHC class [I/II]" OR "MHC class [IA/IIB]" AND "exon 2" AND "amphibia". ACACIA was run for each MHC class to perform read merging, primer trimming, and quality filtering. Only reads containing perfect primers were retained, singletons were removed, and quality thresholds were set to retain reads with at least 90% of bases with a phred score >30. Subsequently, variations of the minimum number of reads supporting an allele within an amplicon (abs_nor) and the minimum proportion of reads representing an allele within an amplicon (low_por) were performed as recommended by Gillingham et al. (2021) to decide the optimal parameter values. Finally, amplicons with < 50 reads in total were removed. Details of the pipeline and final ACACIA settings can be found in supplementary Figure S3.1 and Table S3.3, respectively.

To ensure that amplicons were not the result of contamination or MID tag jumping, the maximum read depth per negative control or unused MID combination was used as a minimum amplicon threshold in each MHC class (supplementary Figure S3.1). Variants were also scrutinised for their credibility against a set of criteria: 1) Differed from next most similar (parent) allele by >2bp, or 2) If not, they must occur at >50% of parent's frequency or be present without the parent across >1 amplicons to be accepted (Razali et al. 2017). Variants failing to satisfy these criteria were regarded as artefacts, and their reads added to parent alleles (supplementary Figure S3.1). To check whether read depth was likely to have an impact on MHC diversity, the number of variants obtained per individual, and the read depth of that individual, were checked for correlation using a Spearman's Rank test of correlation. Variants were named according to Klein et al. (1990), but given the species abbreviation Lepfal, rather than Lefa, to avoid confusion with MHC alleles described for *Lemur fulvus albifons* (Gaur and Nepom 1996). As alleles could not be assigned to loci, they were given a general name to denote the MHC region they belong to: Lepfal-I-a1*, meaning MHC class I α1 domain or Lepfal-II-B, meaning MHC class II β1 domain.

Sequence Analysis

Final variants were translated into amino acids and checked for the presence of stop codons or frameshift mutations using Geneious Prime (Kearse et al. 2012). Putative PBRs were predicted based on the analysis of Lillie et al. (2014) for *R. marina* in class I, and from *Bufo gargarizans* KJ679317.1 for class II (Bataille et al. 2015). Nucleotide diversity was calculated across variants and across their PBR using DNAsp v.6 (Rozas et al. 2017). Amino acid diversity was calculated in MEGA X using a Poisson model. Evolutionary divergence, calculated as the number of substitutions per site, was calculated in MEGA using aligned amino acid sequences.

Function

Functional supertypes were investigated using the R package Peptides (Osorio et al. 2015), which calculates a value for five physiochemical descriptors for the PBR in each MHC allele, z1-z5. A discriminant analysis of principal components (DAPC) was performed on the physiochemical values matrix using the R package adegenet (Jombart 2008). The number of supertypes was inferred from the most likely number of clusters denoted by the lowest Bayesian Information Criterion (BIC) value. Information on each MHC class and their associations with Bd resistance was collected from the literature and compared to the residues found for the MCF MHC. For class I, data relating to MHC conformation and Bd-infection outcome in amphibians were from Kosch et al. (2019). MCF MHC sequences were compared to the three alleles identified by Kosch et al. (2019) to be associated with increased Bd susceptibility in *Pseudophryne corroboree*: Psco-UA*5, 7, and 23. For class II, Bataille et al. (2015) described conformations of four key pockets of the class II PBR that were significantly associated with Bd resistance in 13 amphibian species. An overall percentage identity was calculated between MCF amino acids and the amino acids of the MHC PBRs associated with Bd susceptibility (Class I) or resistance (Class II).

Selection

Tajima's D estimates were produced in DNAsp v.6 (Rozas et al. 2017). Nonsynonymous to synonymous substitution ratios (dN/dS) were calculated using the Z-test of selection implemented in MEGA-X (Kumar et al. 2018). The hypotheses of neutrality, positive selection, and purifying selection were tested across the entire alignment of alleles, across just the PBR codons, and across non-PBR codons. The pairwise-deletion option was selected, and the Nei-Gojobori model was used to estimate dN and dS (Nei and Gojobori 1986). The Nei-Gojobori model was chosen as a simple and commonly applied model for estimating dN/dS proportions (Yang and Nielsen 2000). The Nei-Gojobori method is useful for its simplicity but it has limitations in its ability to accurately deal with instances of multiple substitutions or high levels of divergence between taxa, and does not take into account phylogeny (Kosakovsky Pond and Kosakovsky 2016). In light of this, other methods that use the more refined MG94xREV model of codon evolution were also used to test for evidence of selection (Pond and Muse 2005). These methods were accessed using the Datamonkey Web Server (Weaver et al. 2018), which uses HyPhy (Kosakovsky Pond et al. 2020) to run tests of selection on alignments of at least three sequences. Alignments of MHC alleles were first tested for recombination using the Genetic Algorithm for Recombination Detection (GARD) to identify whether alignments could be analysed as a whole or required splitting into recombining segments. Following this, alignments were tested for evidence of selection. Branch-specific selection was assessed using aBSREL. Gene-wide evidence of selection was tested using BUSTED. Site-specific selection was also tested using FEL (Fixed Effects Likelihood) which can detect pervasive positive or purifying selection and MEME (Mixed Effects Model of Evolution) which can detect episodic selection acting on a proportion of branches. Grantham's distance, which ranges from 5 – 215 (Grantham 1974) was used to calculate the amino acid differentiation (based on composition, polarity, and molecular volume) at sites under positive selection.

Individual and Population Level Diversity

MHC variants, their frequency and diversity, were investigated across five divisions of the dataset. To look at spatial patterns of MHC diversity, variants were compared between Dominica and Montserrat. To understand the levels of MHC diversity in captivity, variants were compared between MCFs from the wild and the captive population. MHC variants were also assessed between MCFs that succumbed to Bd infection (Bd-susceptible), and MCFs that persist in the wild despite the presence of Bd in their environment or population (probable Bd-tolerant). Probable Bd-tolerant MCFs were classed as such because not every MCF had been observed to clear or survive with Bd infection, so it is possible that some survived due to chance avoidance of infection. The choice to include probable Bd-tolerant MCFs was made due to the small sample size of confirmed Bd-tolerant MCFs: nine MCFs have been confirmed to be Bd-tolerant based on repeated Bd infection monitoring. Seven of these MCFs had been recorded to clear Bd infection, five from Dominica (Colihaut = 2, Soufriere = 2, Wallhouse = 1) and two from Montserrat. Two more MCFs from Colihaut in Dominica were observed to survive Bd infection for over one year. These nine confirmed Bd-tolerant individuals were also compared to the Bd-susceptible group. Finally, to look at temporal patterns in MHC diversity either side of the Bd epizootic, Dominican MCFs were studied pre- and post-decline (sampled before 2006 in Dominica are pre-decline, sampled after 2006 in Dominica allocated to post-decline, as in Hudson et al. (2016a)). This comparison also eliminated patterns of MHC diversity associated with different islands.

To test for associations between MHC alleles and sample groups, chi-square tests with Yate's continuity correction were performed. Chi-square tests were performed on all alleles, and between pairs of alleles. In instances where expected values were < 5, a Fisher's exact test was used. All pairwise p-values were corrected for multiple testing using a false discovery rate method (Benjamini and Yekutieli 2001). To determine whether allele frequency changes between group pairs were statistically significant, a bootstrap resampling method was employed, using 10,000 bootstrap replicates to compare allele frequencies in a pairwise manner. For each replicate, the data for one allele being compared were resampled with replacement to include the same number of observations as the other allele being compared. Allele frequency and the allele frequency ratio (AFR) between group pairs was calculated for each replicate and used to plot a histogram. The observed allele ratio difference of one allele was compared to the bootstrap distribution of the other. An observed allele ratio change between group pairs was determined to be statistically significant if it sat outside of the 2.5% or 97.5% confidence intervals, equivalent to an alpha level of 0.05.

Due to the inability of this study to assign alleles to individual loci, statistical tests requiring knowledge of the number of loci could not be used. Instead the total number of unique alleles per population (Ap), the average number of alleles per individual (Ai), and the number of private alleles (Pa) were calculated, as in Kosch et al. (2019). The evolutionary distance between alleles within an individual was calculated using the seqinr package in R (Charif and Lobry 2007). The square root of the pairwise distances was calculated in a pairwise matrix, and an overall mean was computed for each genotype. This was done for nucleotide sequences (DNUC) and for amino acid sequences (DAA). Pairwise population differentiation was calculated using Jost's D (Jost 2008), a measure which does not rely on a priori knowledge of the number of loci behind population alleles. Jost's D was calculated using the

SpadeR web app and 1,000 bootstrap replicates (Chao and Chiu 2016). Unpaired two-sample Wilcoxon tests were used to determine whether Ai, DNUC, or DAA were significantly different between group pairs, as the data were non-normal and could not be transformed to fit the assumptions of a parametric t-test. Samples with data for both class I and class II were retained (n = 244) and alleles were coded as present or absent to enable Principal Component Analysis (PCA) using the R package adegenet (Jombart 2008; R Development Core Team 2008).

Comparison with Neutral Markers

To compare MHC diversity to that of a neutral marker, data from eight microsatellite (MSAT) loci, previously generated by Hudson et al. (2016a) and for Chapter Six of this thesis, were used. Only samples containing genotype information for microsatellites, MHC class I, and MHC class II were retained for this portion of the analysis. Alleles per population (Ap), allelic richness, average number of alleles per locus (ANAPL), private alleles, expected and observed heterozygosity (He, Ho), and the inbreeding coefficient (F_{IS}) were calculated for microsatellite data and for both classes of MHC. Unpaired two-sample t-tests were used to determine whether Ai, DNUC, DAA (for MHC data), or ANAPL, He, or Ho (for MSAT data) were significantly different between group pairs. Data that were non-normal and did not fit the assumptions of a parametric t-test were tested with a Wilcoxon test. Jost's D was calculated for all markers to allow direct comparison of group pair differentiation. A PCA was also calculated for each group pair's MHC and MSAT data, as previously described.

Results

Sequencing Outcome

For class I data, 256 samples (including PCR replicates) were outputted from ACACIA. From 3,473,379 raw reads, 1,456,772 (42%) were retained after merging, primer matching, quality filtering, and removal of singletons and chimeras. The optimal settings for abs_nor and low_por were 15 and 0.03, respectively, meaning that only alleles with >15 reads and present at >3% of all reads within an amplicon were retained. This value had 93% repeatability amongst replicates. Unused MID tag combinations contributed 9,617 reads, equating to 0.75% of the total pool from an initial input of 15% of total samples, showing a low level of tag jumping. Twelve negative PCR controls accounted for 0.4% of the final reads while representing 4.5% of the total input to the sample pool (supplementary Figure S3.2). After contaminant cleaning, 1,260,390 reads across 251 samples were retained with read depth of 1,503 - 16,648 (mean = 5,021, s.d. ± 2,497). Seven variants were detected, with a range of 2 - 5 variants per individual and an average of 2.49 (s.d. ± 0.69), indicating at least three MHC class I loci. After merging of replicated samples, the final number of individuals with a Class I genotype was 239. For class II data, 286 samples (including PCR replicates) were outputted from ACACIA with 86.6% (2,803,036) of raw reads remaining. Retaining alleles with >15 reads and present at >2.5% of all reads had 100% repeatability amongst replicates. Unused MID combinations totalled 1.3% of the final pool, from an input of 16% of total samples. PCR controls accounted for 0.7% of the final reads while representing 4% of the total sample pool – showing low levels of contamination or tag jumping (Figure S3.2). After filtering for unused MID combinations and PCR negatives, 2,257,047 reads were retained across 268 samples. Amplicon read depth was 3,408 – 42,464 (mean = 8,462, s.d. ± 3,970). Four variants were detected with a range of 1 - 4 variants per individual, and average of two (s.d. ± 0.24). Variants Lepfal-II-B*03 and Lepfal-II-B*04 failed to satisfy the criteria set for accepting true alleles. Both only varied by 1bp from either of the two major alleles and could have been chimeric sequences formed from the two major alleles. In addition, variants *03 and *04 were never present without a parent allele and were never present at >50% of the read count of the more common parent variant. Thus, both variants were considered artefacts and removed from the analysis. This resulted in 1-2 variants remaining per individual. The final number of individuals with a class II genotype was 256. Read depth and number of variants were not correlated for MHC class I (Spearman's rank correlation s = 2720204, p-value = 0.61, rho = -0.03), or for MHC class II (Spearman's rank correlation s = 3325755, p-value = 0.55, rho = -0.04).

MHC Sequence Overview

No stop codons or frameshift insertions or deletions were detected in any alignment, meaning that all sequences are potentially functional (Figure 3.1). Class I alleles ranged from 69 – 73 codons in length and incorporated 14 of 15 PBR residues predicted by (Lillie et al. 2014). Alleles Lepfal-I-a1*01, *02, *04 each had 70 codons, with an insertion of three amino acids at codon positions 45 – 47 in alleles Lepfal-I-a1*03,*05 and *07 (Figure 3.1). This insertion did not cause a frame-shift mutation, and deletions have been observed between MHC class I alleles in the α1 domain before (Kiemnec-Tyburczy et al. 2012). Allele Lepfal-I-a1*06 was one codon shorter at the start of the sequence when compared with all other class I alleles. The most diverged class I alleles were Lepfal-I-a1*01 and *06 (average

pairwise base substitutions per site = 0.217 and 0.218, respectively) and the least diverged were Lepfal-I-a1*03 and *05, each with a Grantham's distance of 0.166. Both class II alleles were 64 codons in length and captured 14 PBR residues. Alleles Lepfal-II-B-*01 and *02 differed at three amino acid sites and at four nucleotide positions, all present in a PBR residue (Figure 3.1). The number of substitutions per site between the alleles was 0.02. The variation amongst MHC class I alleles was greater than class II, with ~34% of nucleotide sites polymorphic, compared with just 2% of nucleotide sites between the two class II alleles (Table 3.2). In both MHC classes, amino acid diversity was larger than nucleotide diversity. The nucleotide and amino acid diversity of the PBRs was greater than that of the overall alignment in both classes, with 66% of sites variable in the class I PBR and 10% in class II. Amino acid diversity was three times greater for class I and five times so for class II (Table 3.2).

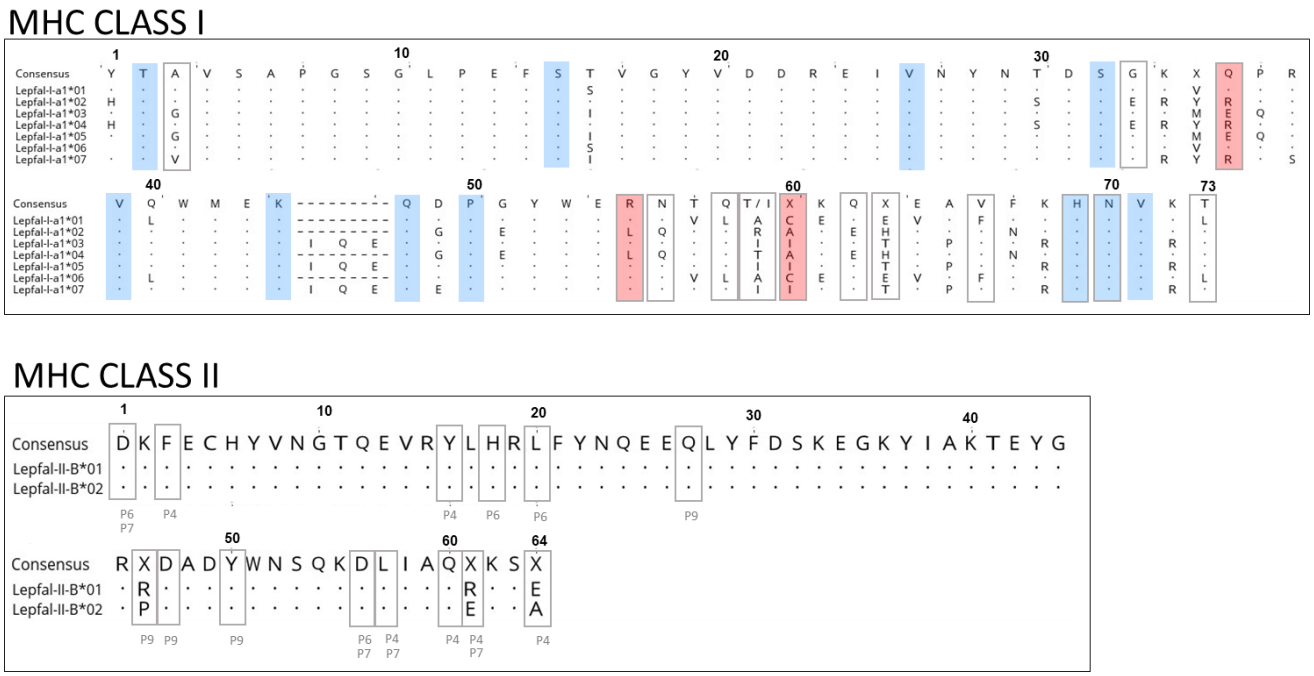

Figure 3.1: Alignments of amino acid sequences of exon 2 in the MHC class I and II in the mountain chicken frog. Dots (vertically) in the alignments indicate agreements with the consensus sequence (majority consensus of all alleles). Putative peptide binding regions (PBRs) are marked with an open, grey rectangle. PBRs are inferred from Lillie et al. 2014 for MHC class I, and Bataille et al. 2015 for class II. Site-specific signatures of selection were calculated only for class I, due to a lack of data in class II. Sites under positive selection are highlighted in red, sites under purifying selection are shown in blue, both at a p-value threshold of 0.1. Pocket identification is noted for class II by grey IDs underneath PBR sites.

Table 3.2: Diversity of MHC class I and class II alleles in the mountain chicken frog. PBR = peptide binding region.

	Whole Alignment Diversity		PBR Diversity	
Class	**Nucleotide**	**Amino Acid**	**Nucleotide**	**Amino Acid**
I	0.165 (s.d. ± 0.023)	0.27	0.366 (s.d. ± 0.06)	0.83
II	0.021 (s.d. ± 0.01)	0.05	0.095 (s.d. ± 0.05)	0.24

MHC Functional Analysis

Using DAPC analysis, two allele supertypes were detected in MHC-I. Alleles Lepfal-I-a1*01, *03, *05, *06, and *07 were grouped into supertype 1, while Lepfal-I-a1*02 and *04 were assigned to supertype 2. Each individual held at least one allele of each supertype. This analysis could not be performed for class II as too few PCAs were generated (n = 1) from a matrix with only two alleles. Overall, there was a 64.7% pairwise identity with MCF MHC-I alleles and alleles associated with Bd-susceptibility in *P. corroborree* (Table 3.3). Comparing just the PBR amino acids identified by Kosch et al. (2019) with the same positions in the MCF alleles showed that the MCF shared the fewest identical PBR residues with Psco-UA*5 (35%), between 23 – 54% with Psco-UA*23, and the most with Psco-UA*7 (46%) (Table 3.3). The MCF alleles with the lowest overall similarity to the susceptibility-associated alleles were the functionally identical Lepfal-I-a1*01 and *06 (Table 3.3). The most similar alleles were Lepfal-I-a1*03, *05, and *07 (Table 3.3). Comparison of the two class II alleles with three pocket conformations associated with Bd resistance in several amphibian species (Bataille et al. 2015) showed that both alleles had the same level of similarity with pocket 4 and 6, while Lepfal-II-B*02 shared one more amino acid with the pocket 9 conformation of resistant species (Table 3.3). Lepfal-II-B*01 had 50% of residues matching the overall profile of Bd-resistant species while Lepfal-II-B*02 had 57%. MCF class II alleles were least similar to pocket 6; Lepfal-II-B*01 more closely resembled pocket 4, while Lepfal-II-B*02 was closer to pocket 9 (Table 3.3).

Table 3.3: Top half shows percentage identity of MHC class I alleles with three alleles associated with *Batrachochytrium dendrobatidis* (Bd) susceptibility in *Pseudophryne corroboree* (Kosch et al. 2019). Bottom half shows percentage identity of MHC class II alleles with three different peptide binding region conformations associated with Bd resistance in 13 species of anuran amphibians (Bataille et al. 2015).

MHC class	**% Identity**	**Lepfal-I-a1***							
		01	**02**	**03**	**04**	**05**	**06**	**07**	***Overall Average***
Class I	**Psco-UA*5**	23	46	38	38	38	23	38	35
	Psco-UA*7	31	38	62	38	62	31	62	46
	Psco-UA*23	23	46	54	46	54	23	54	43
	Overall Average	26	44	51	41	51	26	51	
	% Identity	**Lepfal-II-B*01**				**Lepfal-II-B*02**			***Overall Average***
Class II	**Pocket 4**	66				66			66
	Pocket 6	25				25			25
	Pocket 9	50				75			62.5
	Overall Average	50				57			53.5

Evidence of Selection

At the whole-alignment level of class I alleles, evidence of positive selection was detected using the z-test for selection (dN/dS = 1.81, p-value = 0.04). No evidence of selection was detected in the MHC-I PBR or non-PBR regions (p-value > 0.05). Tajima's D estimates indicated a signal of balancing selection (D = 1.07) but this was not significant (p-value > 0.10). Positive selection for the MHC-II alleles was detected in the whole alignment (dN/dS = 1.84, p-value = 0.03) and the PBR (dN/dS = 1.83, p-value = 0.04). No evidence of selection was detected in the non-PBR. Tajima's D could not be calculated for MHC-II data due to too few sequences. Only data from the MHC-I alignment could be analysed in the datamonkey web server, because the class II alignment had less than three sequences. GARD found no evidence of recombination, so further analyses were carried out on one partition. BUSTED analysis of all 73 sites found evidence of diversifying selection (p-value = 0.001). Diversifying selection on three of nine branches was detected by aBSREL. These were Node 5 leading to the alleles Lepfal-I-a1*02 and *04 (p-value = 0.0002), Node 2 leading to the alleles Lepfal-I-a1*01 and *06 (p-value = 0.0364), and the branch of Lepfal-I-a1*03 (p-value = 0.001). At the α-level of 0.05, MEME detected positive selection at codon 55 (supplementary Table S3.4). FEL detected nine sites under purifying selection with p-value < 0.05 (Table S3.4). With seven sequences, the power to detect moderate site-specific selection is low with MEME and FEL (S. Pond, *pers. comm*.). To account for the stringency of these tests on a small alignment, the results at an α-level of 0.1 are also reported, which is the default on the datamonkey web server. At this level, FEL found sites 36 and 60 under diversifying selection, and purifying selection at eleven sites (Figure 3.1, Table S3.4). MEME detected codons 36 and 55 to be under positive selection (Figure 3.1, Table S3.4). All three sites putatively under positive selection were in the PBR (Figure 3.1). Amino acids at codon 36 (Q, E, R) held a mean Grantham's distance of 42, while amino acids at site 60 (C, A, I) were more differentiated based on Grantham's distance, which had an average of 162. Codon 55 represented a change to leucine in Lepfal-I-a1*02 and *04 from arginine in all other alleles, which has a Grantham's distance of 102.

MHC Diversity across Individuals and Populations

Of the 239 individuals successfully genotyped for MHC-I, 14 unique genotypes were found. The most common genotype was Lepfal-I-a1*01,02 which was present in 64% of individuals. Genotypes with five alleles or with allele Lepfal-I-a1*07 were the rarest, each accounting for < 0.8% of all individuals (n = 6). For MHC-II, there were three unique genotypes among 256 individuals (Figure S3.3). The region was almost entirely monomorphic, with 98% of individuals possessing the genotype Lepfal-II-B*01,02. Four individuals had the single allele Lepfal-II-B*01 and two individuals had just Lepfal-II-B*02. Little to no variation between population groups was found for MHC class II due to the low number of alleles and majority of shared genotypes. Subsequently, there were no significant differences between any population pair for MHC-II Ai, DNUC or DAA (Wilcoxon test p-value > 0.05). This result contrasts with the microsatellite data, which did show differing patterns of diversity between population pairs (Table 3.4). There was no association between the number of MHC alleles (Class I or II) and the number of microsatellite alleles per individual, or per individual per locus (Pearson correlation coefficient ranged from -0.03 to -0.13 and p-value > 0.05), indicating that the MHC may be shaped by forces other than neutral demography.

Dominica vs. Montserrat

Mountain chicken frogs from Dominica and Montserrat shared the same number of MHC-I alleles, albeit with one private allele each: Lepfal-I-a1*04 was found only in frogs from Dominica and Lepfal-I-a1*06 was found only in frogs from Montserrat (Table 3.4, Figure 3.2). Individual allelic diversity (Ai) was significantly higher in Dominica (Wilcoxon test w = 7294.5, p-value = 0.02), but the genetic distance between the MHC-I alleles of Dominican and Montserratian frogs was not significantly different (DNUC and DAA p-values > 0.05, Table 3.4). The most common MHC-I genotype was Lepfal-I-a1*01,02 at 54% in Dominica and 69% in Montserrat (supplementary Figure S3.3). Frogs from both islands had four genotypes in common, six were found only in Dominica, and four were found only in Montserrat (Figure S3.3). The subset of samples with both microsatellite and MHC data revealed that Dominican frogs also had significantly higher neutral diversity in Montserrat, measured as ANAPL (Wilcoxon test w = 1772, p-value = 0.003, Table 3.4). An overall chi-squared test found a significant association between country and allele (χ^2 = 53.039, df = 6, p-value < 0.0001), mainly due to Lepfal-I-a1*04 which contributed 81% to the test statistic. Also, Lepfal-I-a1*04 was found to be significantly associated with frogs from Dominica when compared with all alleles in pairwise chi-squared tests, except Lepfal-I-a1*07 (supplementary Table S3.5).

Captive vs. Wild

The restriction of Lepfal-I-a1*04 to Dominica meant that captive MCFs, bred from Montserratian stock, lacked this allele (Figure 3.2). The overall chi-square test was significantly large due to this (χ^2 = 16.128, df = 6, p-value = 0.01, contribution of Lepfal-I-a1*04 = 85%). Captive MCFs presented higher MHC-I diversity in terms of Ai, DNUC and DAA than wild MCFs, but only Ai being significantly higher (Wilcoxon test w = 5545.5, p-value = 0.01, Table 3.4). Comparing just wild Montserratian MCFs with the captive-bred frogs, five of seven MHC-I genotypes were shared between them (Figure S3.3). The allele Lepfal-I-a1*07 was found in the captive population, but not in the wild Montserratian frogs. In contrast to MHC data, microsatellites showed significantly higher allelic diversity in the wild population (ANAPL: W = 4740, p-value = 0.04, Table 3.4), which had 17 private microsatellite alleles compared to just two in the captive population (Table 3.4). Observed microsatellite heterozygosity was highest of all population pairs in the wild group (0.664), which was 25% higher than expected (Table 3.4). The captive population had lower than expected microsatellite heterozygosity and subsequently a significant F_{IS} of 0.251 (Table 3.4).

Pre- vs. Post Decline in Dominica

Pre-decline MCFs had lower values for MHC-I Ai, DNUC, and DAA than post-decline (Table 3.4). Only values for Ai were significantly lower, however (Wilcoxon test w = 826.5, p-value = 0.007). There was a five-fold increase in the frequency of the MHC-I genotype Lepfal-I-a1*01,02,04 post-decline, from 5% to 25%. The most common genotype, Lepfal-I-a1*01,02, reduced from 81% pre-decline to 45% post-decline (Figure S3.3). Through the Bd epizootic, alleles Lepfal-I-a1*01 and*02 had a frequency of 1 (Figure 3.2). Rarer alleles Lepfal-I-a1*03, Lepfal-I-a1*04, Lepfal-I-a1*05 increased in frequency by between three and four-fold post-decline (Figure 3.2). Lepfal-I-a1*07, the rarest allele, was reduced by four times its original frequency to almost zero after 2006 (Figure 3.2). No significant association was found between alleles and pre- or post-decline groups based on chi-squared tests (Table S3.5).

However, the bootstrap analysis revealed a significantly large increase in the frequency of Lepfal-I-a1*04 from pre- to post-decline compared to all other MHC-I alleles (supplementary Table S3.6). The increases in Lepfal-I-a1*03 and *05 post-decline were also significant compared to all other alleles except Lepfal-I-a1*04 in the bootstrap analysis (Table S3.6). MHC data showed higher diversity post-decline, but MSAT data showed that neutral diversity (ANAPL, Ar) was lowest of all in the post-decline group, which also had the strongest signal of inbreeding (Table 3.4). Pre-decline animals had significantly more microsatellite alleles (41) than post-decline (28) (ANAPL, t.test t = -3.9793, df = 33, p-value = 0.0004, Table 3.4). Values for MHC statistics calculated from the MHC-MSAT comparison subset can be found in supplementary Table S3.7.

Of the eight MCFs sampled in Dominica in 2019, six possessed Lepfal-I-a1*04, and only one individual did not have any of Lepfal-I-a1*03, *04, or *05. Lepfal-I-a1*04 was identified in both of the two remaining strongholds in Colihaut and Soufriere, while Lepfal-I-a1*05 was found only in Soufriere and Lepfal-I-a1*03 only in Colihaut. Only a small number of wild frogs could be sampled in 2019 because the population had declined to probably fewer than 50 individuals (*Author's unpublished data* 2019). Therefore it is possible that other alleles, such as *03 and *05, also continue to exist in extant MCFs on Dominica in unsampled individuals.

Bd-tolerant vs. Bd-susceptible

Probable Bd-tolerant MCFs had a significantly higher number of MHC-I alleles than Bd-susceptible MCFs (Wilcoxon test w = 2862.5, p-value = 0.005). DNUC and DAA were similar between the two groups (Table 3.4). Bd-tolerant frogs did not have Lepfal-I-a1*06, but almost all Bd-tolerant individuals come from Dominica, where this allele was not found (Figure 3.2). The most common genotype was Lepfal-I-a1*01,02 at 65% in Bd-susceptible frogs, and a lower 44% in the probable Bd-tolerant group (Figure S3.3). The genotype Lepfal-I-a1*01,02,04 was 2nd most common (23%) in the probable Bd-tolerant group, while present at just 1% in Bd-susceptible frogs. Allele *04 was present in 34% of probable Bd-tolerant individuals, compared to 1% of Bd-susceptible. This was a highly significant change when compared to all other allele frequency group differences according to the bootstrap analysis (supplementary Table S3.6). Allele *05 more than tripled in frequency from 4% in Bd-susceptible frogs to 15% in probable Bd-tolerant MCFs. An overall chi-squared test found a significant association between Bd-status and all alleles (χ^2 = 40.67, df = 6, p-value < 0.0001), with Lepfal-I-a1*04 contributing 75% to the test statistic. Lepfal-I-a1*04 was found to be significantly associated with Bd-tolerance when compared with all alleles except *05 and *07 (supplementary Table S3.5). The groups had five genotypes in common (Figure S3.3). Four genotypes were only found in Bd-susceptible frogs, while three were unique to the probable Bd-tolerant group – these being Lepfal-I-a1*01,02,03,04, Lepfal-I-a1*01,02,03,07 and Lepfal-I-a1*01,02,04,05. Again, neutral diversity patterns contrasted to those found in the MHC data. Microsatellites showed that probable Bd-tolerant individuals had fewer alleles than susceptible ones in terms of Ap, Ar, and ANAPL (Table 3.4). Only ANAPL was significantly lower (Wilcoxon test w = 2451, p-value = 0.00003). Both Bd-tolerant and Bd-susceptible MCFs were significantly inbred (Table 3.4).

Eight of the nine confirmed Bd-tolerant MCFs produced an MHC-I genotype. The same patterns of diversity as seen in the probable Bd-tolerant group relative to Bd-susceptible MCFs were observed in

the confirmed Bd-tolerant group. MHC-I diversity was larger in the confirmed Bd-tolerant MCFs than Bd-susceptible MCFs (Table 3.4). MCFs which cleared Bd-infection in Dominica had genotypes containing alleles Lepfal-I-a1*03, *04, or *05 (supplementary Figure S3.3). In Montserratian Bd-tolerant MCFs (n = 2) the genotypes were Lepfal-I-a1*01,02,03,05 and Lepfal-I-a1*01,02,03. The two Dominican individuals with a Lepfal-I-a1*01,02 genotype were those which remained alive with Bd infection for >1 year but were not recorded as clearing Bd infection. Within the eight Bd-tolerant MCFs, Lepfal-I-a1*03 held the highest frequency at 50% while being present in 23% of Bd-susceptible frogs (Figure 3.2). Lepfal-I-a1*04 followed at 38%, which was the largest difference in relation to its frequency in Bd-susceptible MCFs, where Lepfal-I-a1*04 was present at 2% (Figure 3.2). Only Fisher's tests were possible due to the small sample sizes; an overall test revealed a significant association of Bd-status and allele (p-value = 0.01), but no pairwise tests were significant (supplementary Table S3.5). Again, bootstrap tests showed that Lepfal-I-a1*04 had a highly significant increase in frequency in Bd-tolerant frogs (supplementary Table S3.6). Lepfal-I-a1*05's increase in Bd-tolerant MCFs was larger than *01 and *02, and within that expected of Lepfal-I-a1*03 and *04. Lepfal-I-a1*03's increase in Bd-tolerant MCFs was larger than *01 and *02, equivalent to *05, but smaller than *04's expected difference (supplementary Table S3.6). The contrast between MHC-I and neutral diversity remained the same as for the larger, probable Bd-tolerant group and Bd-susceptible groups. Neutral diversity was lower in confirmed Bd-tolerant MCFs compared with Bd-susceptible frogs, but MHC-I diversity was higher (Table 3.4, supplementary Table S3.7).

Table 3.4: Population diversity statistics. N = number of individuals, Ap = unique alleles within population, Ai = average number of alleles per individual, Pa = private alleles, DNUC = average square root pairwise distance between allele nucleotides within individuals, DAA = average square root pairwise distance between allele amino acids within individuals. Ar = allelic richness corrected for sample size, ANAPL = average number of alleles per locus, He = expected heterozygosity, Ho = observed heterozygosity, F_{IS} = inbreeding coefficient – bold values indicating significance, Jost's D value is the pairwise differentiation between two populations. * indicates significantly different means between the population pair as determined by a two-sample Wilcoxon Test (p-value < 0.05). P = probable, C = confirmed Bd-tolerant.

MHC Class I

Population	N	Ap	Ai	Pa	DNUC	DAA	Jost's D
Dominica	79	6	2.59*	1	0.259	0.305	0.017
Montserrat	160	6	2.39*	1	0.259	0.302	
(P) Bd-Tolerant	61	6	2.72*	0	0.262	0.309	0.023
Bd-Susceptible	121	7	2.43*	1	0.259	0.302	
(C) Bd-Tolerant	8	5	3.12*	0	0.279	0.329	0.023
Bd-Susceptible	121	7	2.43*	2	0.259	0.302	
Pre-decline	21	6	2.29*	0	0.254	0.298	0.008
Post-decline	58	6	2.71*	0	0.261	0.308	
Wild Bred	143	7	2.27*	1	0.253	0.296	0.003
Captive Bred	93	6	2.71*	0	0.266	0.309	

MHC Class II

Population	N	Ap	Ai	Pa	DNUC	DAA	Jost's D
Dominica	91	2	1.97	0	0.070	0.104	0
Montserrat	165	2	1.98	0	0.071	0.106	
(P) Bd-Tolerant	69	2	1.99	0	0.071	0.106	0
Bd-Susceptible	124	2	1.97	0	0.070	0.105	
(C) Bd-Tolerant	8	2	1.88	0	0.063	0.095	0
Bd-Susceptible	124	2	1.97	0	0.070	0.105	
Pre-decline	25	2	1.92	0	0.066	0.099	0
Post-decline	66	2	1.98	0	0.071	0.106	
Wild Bred	154	2	1.99	0	0.071	0.107	0
Captive Bred	99	2	1.99	0	0.072	0.107	

Microsatellites (a subset of n = 183)

Population	N	Ap	Ar	ANAPL	Pa	He	Ho	F_{IS}	Jost's D
Dominica	35	42	5.25	4.67*	12	0.529	0.393	**0.261**	0.391
Montserrat	148	39	4.06	4.33*	8	0.528	0.481	**0.088**	
(P) Bd-Tolerant	19	31	3.88	3.88*	1	0.508	0.359	**0.298**	0.350
Bd-Susceptible	112	49	4.46	6.13*	19	0.635	0.531	**0.164**	
(C) Bd-Tolerant	6	36	2.63	2.63*	0	0.441	0.333	0.263	0.38
Bd-Susceptible	112	49	4.46	6.13*	28	0.635	0.531	**0.164**	
Pre-decline	17	41	5.12	4.56*	14	0.57	0.478	**0.166**	0.082
Post-decline	18	28	3.48	3.11*	1	0.442	0.312	**0.300**	
Wild	94	49	6.13	6.13*	17	0.498	0.664	0.051	0.105
Captive	86	34	4.25	4.25*	2	0.579	0.549	**0.251**	

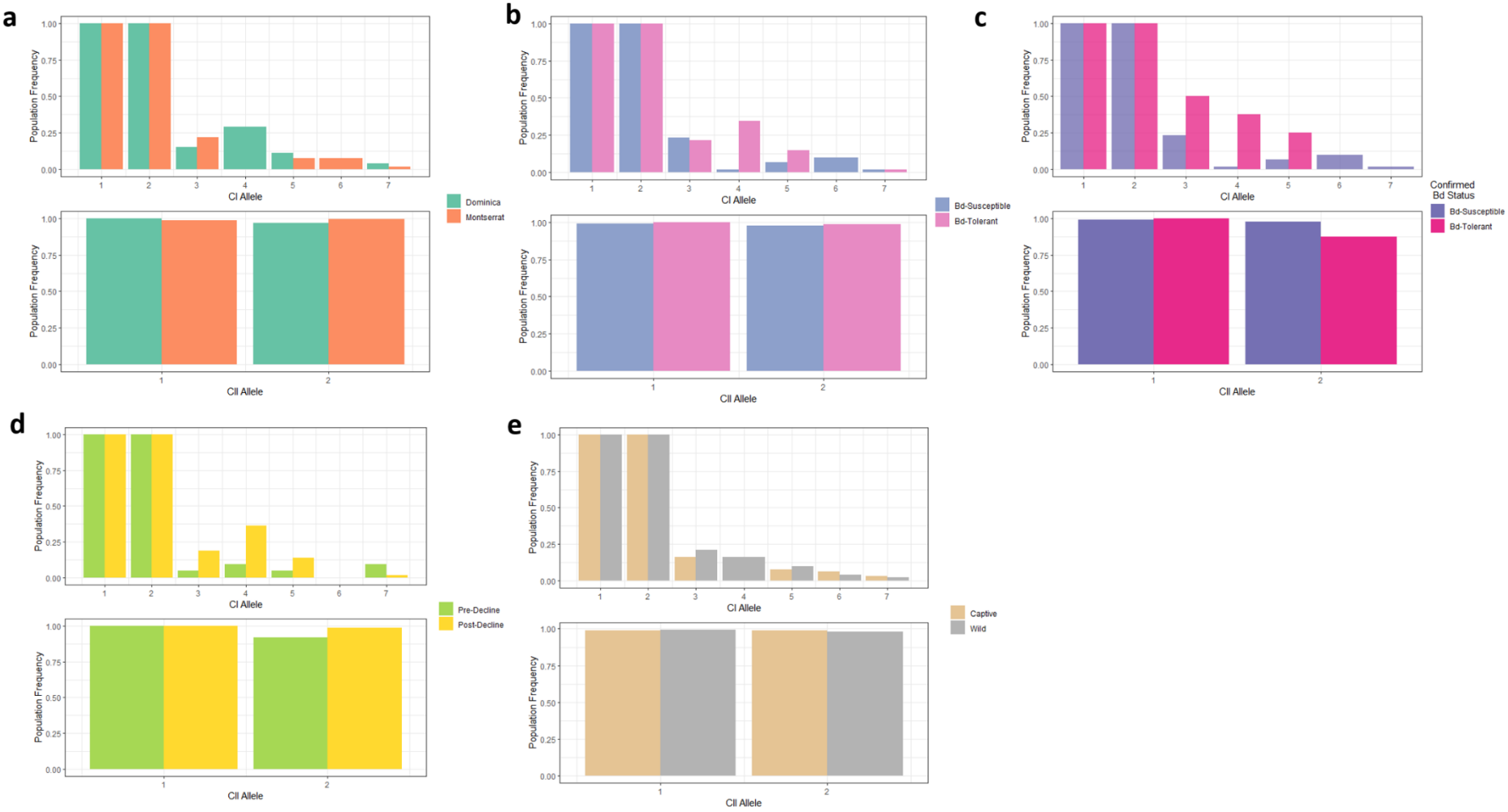

Figure 3.2: MHC class I and II allele frequencies in four different population groupings of the mountain chicken frog dataset. A) Dominica and Montserrat, B) Bd-susceptible or probable Bd-tolerant, C) Bd-susceptible or confirmed Bd-tolerant, D) Pre-decline or Post-decline, E) captive or wild.

Population Structure

Values for Jost's D based on the full MHC-I dataset ranged from 0.003 - 0.023 (Table 3.4) and from 0 - 0.02 in the microsatellite comparison subset (supplementary Table S3.7). The largest differentiation in both MHC-I datasets occurred between probable Bd-tolerant and Bd-susceptible individuals, and the smallest between wild and captive bred frogs. Jost's D detected no population differentiation using MHC-II data. PCA plots based on the full MHC dataset showed that no population pair had complete separation along the two first principal components (Figure 3.3). Any distinctions between individuals appeared to be driven most notably by MHC-I alleles Lepfal-I-a1*04 and *03. Microsatellites consistently resulted in higher population differentiations when compared with MHC data (MSAT D_{EST} range 0.082 - 0.391, Table 3.4). Jost's D calculated with microsatellites revealed the most differentiation between Dominica and Montserrat, with a D_{EST} = 0.391, similar to that between Bd-tolerant and Bd-susceptible individuals (probable Bd-tolerant D_{EST} = 0.35, confirmed Bd-tolerant D_{EST} = 0.38, Table 3.4). Jost's D based on MHC data for these population pairs was 15 - 40 times lower for class I and zero for class II (Table 3.4). Pre- and post-decline populations were most similar based on microsatellite data, but wild vs. captive individuals were most similar based on MHC class I data. In keeping with Jost's D estimates, the PCAs generated from MHC allele occurrence did not show extensive separation between populations (Figures 3.3, 3.4, and supplementary Figure S3.4). Two - four groups of points were identified by the MHC PCA plots, but it was unclear what factor united either of the groups (Figures 3.3 & 3.4). PCA plots based on microsatellite data did not show clear divisions between individuals belonging to pre- and post-decline groups, or between wild and captive MCFs (supplementary Figure S3.4). However, in contrast to MHC data, MSATs did show a clearer separation between frogs from Dominica and Montserrat, and between probable/confirmed Bd-tolerant and Bd-susceptible individuals (Figure 3.4).

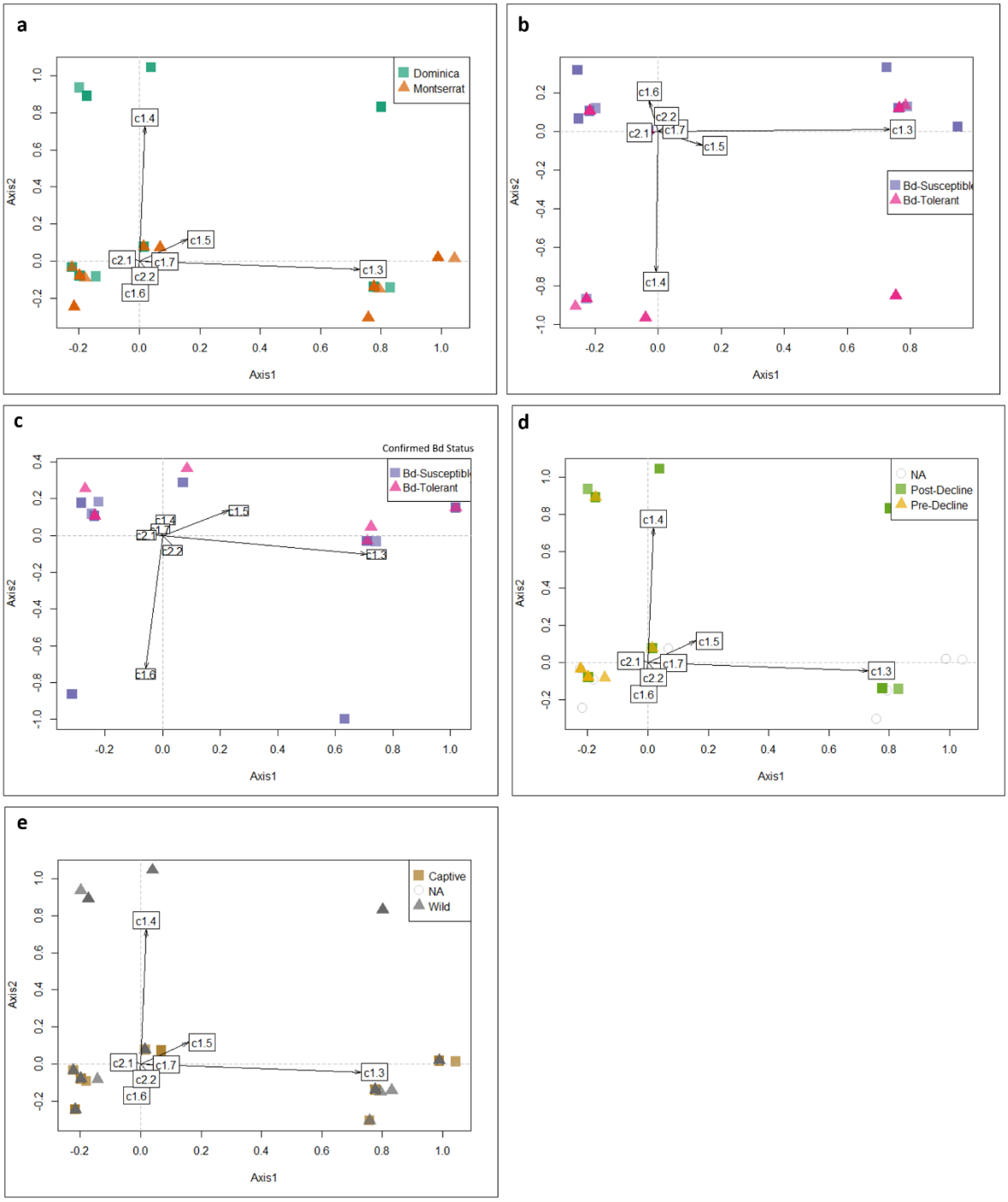

Figure 3.3: Principal components analysis (PCA) of collated MHC class I and II allele occurrence. Alleles Lepfal-I-a1*01 and *02 were not included in the analysis as no difference in occurrence was present amongst individuals. MHC class and allele number are denoted by "C(1 or 2).(allele number)" – i.e. Lepfal-I-a1*04 = C1.4. A) Dominica and Montserrat, B) Bd-susceptible or Bd-tolerant, C) Bd-susceptible or CONFIRMED Bd-tolerant, D) Pre-decline or Post-decline, E) captive or wild.

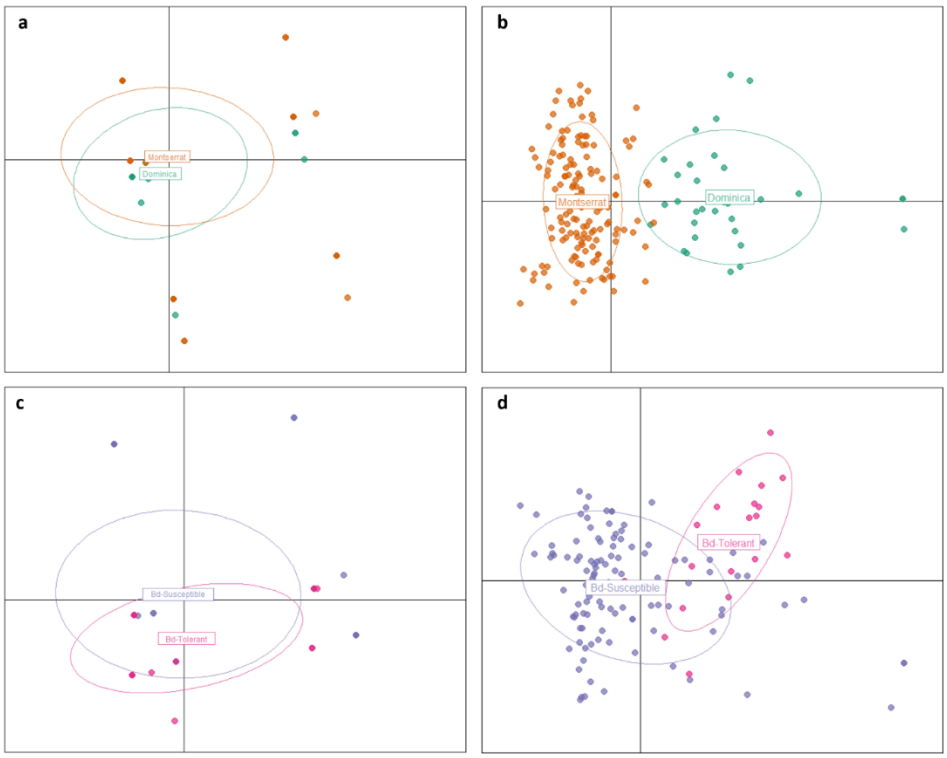

Figure 3.4: Principal components analysis (PCA) comparing collated MHC- I and II allele occurrence with microsatellite allele frequencies across a subset of 183 samples with data for all three marker types. a) MHC: Dominica and Montserrat, b) Microsatellite: Dominica and Montserrat, c) MHC: Bd-susceptible or probable Bd-tolerant, d) Microsatellite: Bd-susceptible or probable Bd-tolerant. Confirmed Bd-tolerant plots not shown due to similarity with panels c) and d).

Discussion

The purpose of this study was to characterise key, peptide-binding fragments of the MHC in the MCF, due to their reported involvement in Bd-resistance or Bd-susceptibility in other amphibian species. Newly designed, potentially multi-locus primers were used to amplify exon 2 of both class I and class II loci. Successful primer design enabled multiple loci to be co-amplified and sequenced for analysis, providing new genetic resources with which to study the Critically Endangered MCF, and potentially other species in the genus *Leptodactylus*. To investigate the potential forces shaping MHC diversity in the MCF, MHC diversity was examined across space, time, and tolerance to Bd.

Bottlenecks and Selection Shape MHC Diversity

The MCF has relatively low MHC diversity when compared with other amphibian species. While at least three class I loci are present, they comprise just seven alleles. This is equivalent to the findings of Zhao et al. (2013) where seven alleles and three MHC class IA loci were found in *Polypedates megacephalus*, although only eleven individuals were sampled, compared to ~250 in this study. Four class I loci were found in *P. corroboree* and *R. marina* (Lillie et al. 2014; Kosch et al. 2017), while just one is known in *Xenopus laevis* (Shum et al. 1993). Numbers of MHC-I alleles in the α1 domain (exon 2) tend to be higher than seven, ranging from nine to 20, based on studies of anuran amphibians (Kiemnec-Tyburczy et al. 2012; Zhao et al. 2013). In birds, ancestral lineages have fewer MHC-I and II loci than more-recently evolved taxa (Minias et al. 2019b). The family of the MCF, Leptodactylidae, is a more-recently diverged anuran lineage of the superfamily hyloidea, having arisen during the Cretaceous–Tertiary boundary 45 – 54 MYA (Roelants et al. 2007) and thus low allelic diversity is not attributable to Leptodactylidae being an ancient lineage.

While MHC-I allelic diversity in the MCF is low, it is still higher than observed MHC-II diversity, where only two alleles were found. If these two alleles were shared in one locus, this would approach the highest possible level of heterozygosity in a population (0.5), based on the Hardy-Weinberg theorem. There may instead be two monomorphic loci for MHC class II. Two MHC-II loci have been observed in the Túngara frog (*Engystomops pustulosus*) which is in the same family as the MCF (Kosch et al. 2016). Other studies of MHC-II in amphibians generally reveal higher polymorphism than detected in the MCF. The Túngara frog had 48 MHC class IIB alleles across 63 individuals (Kosch et al. 2016). The number of class IIB alleles detected in other amphibians ranges from 15 in *Espadarana prosoblepon* (Kiemnec-Tyburczy and Zamudio 2013), 20 in *Odorrana tormota* (Shu et al. 2013), 33 – 84 in *Lithobates yavapaiensis* (Savage and Zamudio 2011), to 263 alleles across two newt species (Dudek et al. 2019). Comparable MHC-II diversity to that in the MCF is observed in *Thoropa taophora*, where small, island populations were found to hold just one or two MHC class IIB alleles (Belasen et al. 2019). Reduced MHC diversity compared to mainland populations in *T. taophora* was attributed to genetic drift in a small island population, amplified by the impact of divergent selection (Belasen et al. 2019). The axolotl, *Ambystoma mexicanum,* has a monomorphic MHC class II locus with just one allele (Laurens et al. 2001). The axolotl MHC is thought to have reached monomorphism after a strong population bottleneck and its existence in a single Mexican lake without incoming gene flow (Laurens et al. 2001).

Low MHC diversity is frequently attributed to a demographic bottleneck, which is often more powerful than the strength of selection for diversity (Amills et al. 2004; Miller et al. 2011; Lillie et al. 2014; Minias et al. 2019a). The MCF has experienced a declining population since the 1990's, and monomorphism has been observed in its mitochondrial DNA (Hedges and Heinicke 2007). The pressure from high levels of harvesting, loss of habitat after the 1995 eruption of the Soufrière Hills volcano on Montserrat, and most significantly, the arrival of chytridiomycosis, reduced the wild population to 15% of its former size (Adams et al. 2014; Hudson et al. 2016a). The effects of this population reduction are present in the reduced microsatellite genetic diversity seen post-decline and significant levels of inbreeding in Dominica and Montserrat shown in this study. Additionally, the MCF is thought to have once been distributed across seven islands in the Lesser Antilles (King and Ashmore 2014). A reduction of this range to just two islands points to the likelihood that the species has undergone a more historic bottleneck than that of the 1990's – 2000's. Additionally, Chapter Two of this thesis presents evidence of a large genetic bottleneck having occurred ~500 years ago, reducing the MCF's effective population size by ~99%. It is also possible that before the bottlenecks in the past 500 years, the first MCFs reached the Lesser Antilles in a series of migrations and founder events from the continental mainland across the islands of the southern Caribbean (Hedges and Heinicke 2007). As seen in *T. taophora,* island populations can have severely reduced MHC repertoires (Belasen et al. 2019). Founder events also have a demonstrable impact on MHC diversity (Lillie et al. 2014). Therefore it is likely that a series of genetic bottlenecks are responsible for the low MHC diversity observed in the MCF.

Loss of MHC diversity after a bottleneck does not necessarily mean that selection in these populations is weak or non-existent. Ejsmond and Radwan (2011) showed that the effects of selection within a bottlenecked population were not large enough to counteract genetic drift, resulting in reduced MHC polymorphism. In the axolotl, monomorphism is observed at the MHC-II, while a diverse suite of MHC-I alleles (19 - 21 per individual) also exists, indicating that forces besides the genetic bottleneck have once acted or are still acting on MHC-I (Shum et al. 1993; Laurens et al. 2001). While genetic bottlenecks may have reduced MCF MHC diversity, selection may still have acted upon its limited variation. Comparison of neutral microsatellites and MHC alleles from Dominica and Montserrat show that the populations have diverged at neutral loci due to reproductive isolation and genetic drift. MHC divergence, however, remained very low between islands, indicating that drift may have been counteracted by balancing selection across the MCF population, as observed in Túngara frog populations challenged with Bd (Kosch et al. 2016). Selection and population bottlenecks have not uniformly reduced or maintained diversity in the MCF MHC, as MHC-I diversity was higher than MHC-II. Contrasting patterns of diversity between class I and II alleles can occur due to a variation in the presence of endogenous or exogenous pathogens and the selective pressures they exert (Sallaberry-Pincheira et al. 2016). For example, over five times as many PBRs were under diversifying selection in MHC-II than in MHC-I in five species of prairie grouse and this was proposed to be due to higher exposure to extracellular pathogens (Minias et al. 2016). Without being able to run aBSREL, BUSTED, or site-specific tests of selection for class II alleles, the strength or pervasiveness of selection between the two MHC classes cannot be compared for the MCF. A z-test was run on both classes and showed evidence of positive selection in both. No evidence of purifying selection was detected in MHC-II variants, which might otherwise explain its lack of diversity.

Higher MHC-I than MHC-II diversity could be because MCFs have been exposed to more (or more virulent) intracellular pathogens than extracellular pathogens. Studies of intracellular pathogens infecting the MCF are limited, but until 2002 in Dominica and 2009 in Montserrat, mountain chickens were not known to have been infected with the intracellular pathogens Bd or Ranavirus (Garcia et al. 2007; Hudson et al. 2016a). Other studies show endemic infection of the MCF with several extracellular pathogens or parasites, so a lack of extracellular challenges is unlikely to have limited the diversification of the MHC-II. A review of post mortem examinations conducted on captive MCFs showed a range of nematode species infecting 35% of wild-born MCFs, although it is not certain if these worms were wild-sourced (Ashpole et al. 2021). The MCF has a varied diet in the wild (Jameson et al. 2019b), and it is reasonable to assume it is exposed to a range of extracellular parasites in this way. Ticks (*Amblyomma rotundatum*) were transferred from the invasive *R. marina* to infected wild MCFs in Montserrat (Jameson et al. 2019a). Other invasive amphibian species in Dominica or Montserrat known to harbour parasites, such as the Cuban tree frog (*Osteopilus septentrionalis*) could add to the pathogen community challenging the mountain chicken (Ortega et al. 2015). It is unlikely that the two very similar MHC-II variants from this study are sufficient to recognise all extracellular pathogens, which in some cases can explain low MHC diversity in healthy populations (Radwan et al. 2010). Strong innate defences against extracellular pathogens could compensate for low class II diversity. Rollins-Smith et al. (2005) detected an antimicrobial peptide, fallaxin, secreted by the MCF. Fallaxin was tested by Rollins-Smith and Conlon (2005) against Bd zoospores, against which it inhibited growth at a minimal inhibitory concentration (MIC) of 100 µM. The MIC of fallaxin against four Gram-negative bacteria was deemed to be of 'relatively low potency' when compared with other species' antimicrobial defences. Fallaxin was present in very high amounts in the skin secretions so that, despite its relatively low potency, its concentration may exceed the MIC value for many pathogens which the MCF may encounter in the wild, though evidently not for Bd.

MHC and Survival Following Bd Infection

Comparisons made between the PBR of MCF variants, and PBR conformations associated with Bd-susceptibility in *P. corroboree* did not reveal striking similarities or differences. All genotyped MCFs possessed Lepfal-I-a1*01 and *02, which had 26% and 44% similarity to MHC-I conformations associated with Bd-susceptibility and no allele had more than 51% similarity. Individual *P. corroboree* frogs were challenged with an Australian strain of Bd and MHC-I conformations conferring susceptibility to this strain may be different to conformations determining susceptibility to the strain infecting MCFs many thousands of miles away in the Caribbean. Both strains are likely to be BdGPL (Byrne et al. 2019), however BdGPL can develop genetic differences especially across large distances or timeframes (Rothstein et al. 2021). Similarly, the two MCF MHC-II alleles did not show strong differences or similarities to MHC conformations conferring Bd-resistance in other species (Bataille et al. 2015). Most MCFs that were genotyped also possessed both MHC-II alleles, so it was not possible to see any trends in Bd infection or epizootic survival using MHC-II variants.

Comparing MHC-I variants between populations did reveal clear patterns of association with populations that have persisted beyond the Bd epizootic. MHC-II diversity was unchanged through the Bd outbreak in both islands and no variants were singled out for their association with populations

persisting with enzootic Bd levels, which differs from much of the current literature (Bataille et al. 2015; Savage and Zamudio 2016; Trujillo et al. 2021). The difference between the current study and previous studies that identified a link between MHC-II and Bd outbreak/infection survival in other species might be due to the very low MHC-II diversity in MCFs (Kosch et al. 2016). The MHC-II could have been so depleted due to prior genetic bottlenecks that there was little scope for selection within this locus (Ejsmond and Radwan 2011). Alternatively, selection favouring these alleles within the declining populations could have lead them to fixation much faster than expected under neutral scenarios (Ejsmond and Radwan 2011). The current study provides evidence that the intracellular nature of Bd infection (Berger et al. 2005) makes MHC-I diversity more important than MHC-II diversity for Bd infection survival in the MCF, as proposed by Kosch et al. (2019). Individual-level MHC-I diversity was significantly greater in post-decline, probable, and confirmed Bd-tolerant frogs. Microsatellites, in contrast, showed higher allelic diversity and heterozygosity in Bd-susceptible or pre-decline individuals, even when corrected for sample size. The contrast between neutral and MHC-I diversity points to the action of diversifying selection. This selection could have maintained immunogenetic diversity in populations that have lost neutral diversity due to a bottleneck – see Aguilar et al. (2004) for a similar, albeit more extreme, observation. Higher MHC-I diversity in surviving MCFs may have conferred a more effective immune response to Bd, and/or to co-occurring pathogens, rendering these frogs more robust to the stress of Bd infection. Jost's D showed that MHC-I allele frequencies have remained more similar between population pairs than microsatellite alleles. The discordant patterns between MHC and neutral marker frequencies also indicate the action of selection. Contrasting patterns of neutral and MHC divergence were found in a study of *Lithobates pipiens* infected with Bd (Trujillo et al. 2021), although the opposite trend was observed. Balancing selection, or homogenising directional selection, could have acted in a relatively constant manner across MCF populations to maintain similar MHC profiles, while neutral markers have diverged under demographic processes such as drift (Piertney and Oliver 2006; Evans et al. 2010). PCA plots indicate that this difference was most striking in the country or Bd-susceptibility comparisons where, despite MHC diversification in groups that fared better with Bd, the extent of diversification was far lower than observed in microsatellites, suggesting that selection has counteracted some divergence.

Comparing MHC-I variant frequency between populations revealed key associations of variants with Bd infection outcome. The most striking observation in populations that fared better against Bd (Dominica, Bd-tolerant, and post-decline) was that all had significantly higher frequencies of the allele Lepfal-I-a1*04 than their Bd-susceptible counterparts. The former groups are largely formed of the same individuals – e.g. most Bd-tolerant individuals were from Dominica – but the replication of the analysis serves to depict how Lepfal-I-a1*04 is at increased frequency whether Bd-tolerance is ascribed to a group geographically, temporally, or phenotypically. Furthermore, when only confirmed Bd-tolerant MCFs were assessed, Lepfal-I-a1*04 was still the most dramatically increased allele. Lepfal-I-a1*04 formed a distinct functional supertype with Lepfal-I-a1*02. The strongest branch-specific example of positive selection was found at the node leading to these two alleles, and the strongest example of site-specific positive selection (detected by MEME at codon 55) distinguished these alleles from others. Despite evidence of selection on both, only Lepfal-I-a1*04 was associated with surviving populations, while Lepfal-I-a1*02 was fixed in all populations. These two alleles differed

only at one codon (59), with a moderate physiochemical difference between the arginine in Lepfal-I-a1*02 and threonine in *04. This change occurs in the PBR, so could translate to a functional difference that could confer better protection against Bd infection. However, no evidence of selection was found at codon 59. The alleles Lepfal-I-a1*03 and *05 were also increased in Bd-tolerant and post-decline groups relative to Bd-susceptible groups, although not to the same extent as *04. Lepfal-I-a1*03 was also most commonly found in confirmed Bd-tolerant MCFs. Evidence of significant positive selection was found at the branch and two codons distinguishing Lepfal-I-a1*03 and *05. Functionally, these alleles are identical so should have equal ability to protect from Bd. Rarer alleles Lepfal-I-a1*06 and *07 were associated negatively with Bd-surviving groups in chi-square analyses. Lepfal-I-a1*06 was absent from any group associated with survival, and Lepfal-I-a1*07 declined in frequency after the Bd epizootic and was less frequent in Bd-tolerant vs Bd-susceptible frogs. Two MCFs which survived for one to two years while Bd-infected had the simplest MHC-I genotype, Lepfal-I-a1*01,02. It is possible that other alleles were missed due to low sequencing depth (both samples had below average read depth) but this may indicate that for some individuals, other factors than MHC-I can aid Bd-tolerance. Individual MHC-IA alleles have been singled out for their association with Bd susceptibility during laboratory challenge assays (Kosch et al. 2019), but the current study presents the first evidence of specific MHC-I alleles being associated with persistence with Bd in wild populations. MHC-I diversity may explain why only a relatively small proportion of MCFs, almost entirely within Dominica, were able to survive the Bd epizootic, as the alleles most associated with Bd epizootic survival were relatively rare across the pre-decline dataset, and were found more commonly in Dominica.

Implications

This study provides a possible explanation for how some MCFs survive Bd infection and why a greater proportion of the population survived the epizootic in Dominica than in Montserrat. This new information is critical for shaping future actions to conserve the MCF. The descendants of the Montserratian MCFs, rescued before they were infected with Bd, exist in a biosecure population, protected from novel pathogens (Jameson et al. 2019a). It is the hope of the MCF recovery programme that this captive population will provide stock for reintroductions to the wild (Adams et al. 2014). Unfortunately, the comparison of captive and wild MCFs has revealed that the MHC-I variant most convincingly linked to Bd-tolerance, Lepfal-I-a1*04, is not held within the captive population. The captive population does, however, possess some alleles still associated with clearing Bd infection: Lepfal-I-a1*03 and *05. Wild MCFs in Dominica must be protected due to their possession of Lepfal-I-a1*04, which appears to be important for the species' persistence in the wild. Ideally, Lepfal-I-a1*04 would also be incorporated into the captive population via breeding to provide the population with a full suite of potentially protective MHC-I variants. This may be challenging to achieve, because the only known source of Lepfal-I-a1*04 is in wild Dominican MCFs, a highly endangered population which ideally should not have individuals removed to captivity. It is unlikely that there are additional sources of Lepfal-I-a1*04 in non-biosecure collections, as the last Dominican-bred captive MCFs died in 2015 (Jameson et al. 2019a). This leaves making recommendations for conservation difficult: to boost the chances of survival of a potential wild MCF population, one would have to reduce the chances of survival in an existing wild MCF population by removing individuals. Is a bird (or mountain chicken) in

the hand worth two in the bush? Or, at what point does removing Dominican individuals for the sake of introducing Lepfal-I-a1*04 to the captive population become viable?

To best inform future interventions, the captive population beyond the biosecure one included in this study should be genotyped at MHC-I exon 2. Although it is unlikely that Lepfal-I-a1*04 will be present, it is worth confirming either way. Additionally, Bd-challenge assays should be carried out on captive individuals with and without Lepfal-I-a1*03 and *05. If a link between these alleles and Bd infection survival can be established, then the need to incorporate Dominican individuals with Lepfal-I-a1*04 is negated. In doing this, these individuals would no longer be biosecure. However, the establishment of a semi-wild enclosure in Montserrat – build for the purpose of experimental releases of biosecure MCFs – provides an ideal setting for these experiments without introducing pathogens into the biosecure captive populations in Europe. If it is confirmed that Lepfal-I-a1*04 is not present outside of the Dominican population, and that Lepfal-I-a1*03 and *05 cannot protect against lethal chytridiomycosis, then incorporating Dominican individuals to the captive population should be considered. The number of individuals to incorporate should be guided by an up to date population viability assessment for Dominica, as the last population size estimation of < 50 individuals is from 2019 (*Author's unpublished data* 2019). If Lepfal-I-a1*03 and *05 can be confirmed to protect against Bd, management of the biosecure captive population should aim to increase the frequency of these alleles in the population. Of the 57 captive individuals with MHC-I data, alleles Lepfal-I-a1*03 or *05 were identified in only nine individuals and these were distributed across Bristol (n = 1), Durrell (n = 4), ZSL (n = 2), and Norden's Ark (n = 2) zoos. The pair at ZSL are no longer part of the biosecure population after either dying or being released to Montserrat (G. Garcia, *pers. comm*.). Durrell contains two males and two females, Norden's Ark also has one of each sex, and the Bristol MCF is a male. As Lepfal-I-a1*03 or *05 are rare alleles, it would be best, if possible, to move the individuals into a single collection to maximise chances of these alleles being passed on to the next generation of that collection. In the meantime, aiming for the general preservation of genomic diversity through minimising inbreeding is the best way to promote population fitness for future releases, and has been shown to often increase MHC diversity too (Radwan et al. 2010).

Limitations and Future Work

This study was able to co-amplify multiple loci but was not able to assign variants to loci. More statistical analyses could be carried out if the exact number of loci were known. For example, calculating heterozygosity and F-statistics, which would enable a fuller comparison with neutral markers and insight into selection (Babik 2010; Kosch et al. 2016). Assigning variants to loci would also enable the designation of true genotypes, which could illuminate whether Lepfal-I-a1*04 is maintained in surviving populations due to hetero- or homozygous advantage (Spurgin and Richardson 2010). To establish exactly how many MHC loci exist for each class, an assembled MCF reference genome would be required for use in read mapping (He et al. 2021). To establish whether the four homozygous MHC-II genotypes are genuine, Sanger sequencing should be performed for these individuals, using the primers developed in this study. If both MHC-II alleles (Lepfal-II-B*01 and *02) can be found in an individual that appeared homozygous in this study, it would establish that the homozygous genotypes were a result of sequencing or laboratory error.

In order to increase the chances of capturing expressed allele variants in the MCF, the primers used in this study were based on those that amplify expressed loci in other amphibian species (May and Beebee 2009; Lillie et al. 2014; Kosch et al. 2016). However, this does not guarantee that all variants identified are expressed in all MCFs. This study did not extend to studying expression profiles, which would require RNA to be extracted from samples (Lillie et al. 2014). Most samples from this study were prepared as DNA extracts, which is likely to have low amounts of RNA due to the presence of RNases in the sample which are not removed during DNA extraction. Procuring RNA from live, wild MCFs in 2019 would have required taking a tissue sample in which both MHC classes are expressed, which at the very least would be a skin sample (Grogan et al. 2018b). This level of invasiveness was deemed inappropriate for a Critically Endangered species. However, understanding MHC expression would make the conclusions drawn from this study about Bd-protective variants more robust, and help to better direct conservation actions. If future work could extract sufficient RNA from historical tissue or blood samples, or future post-mortem tissues, then it would be very valuable to determine which variants are expressed, and by which MCF populations. Time and finances required that just one exon in two MHC classes was studied, however, the MHC consists of other exons that are functionally important (Flajnik 2018). The third exon of MHC-I is also involved in peptide binding, and is the focus of many studies, especially in birds (Minias et al. 2018). Further study of other MHC exons could add resolution to the results from this study.

Conclusion

This study provides the first insight into the immunogenetic basis for Bd-tolerance in the MCF. From an assessment of exon 2 in both MHC-I and II, the MCF has low diversity relative to other amphibian species. Diversity is higher in the MHC-I, while the MHC-II is approaching monomorphism. The lack of diversity is probably largely due to a sustained history of population bottlenecks in the species and highlights how population reduction can limit the fitness of populations – if the low MHC diversity did render the MCF vulnerable to chytridiomycosis. Evidence of selection, however, was still detected within the small range of MHC-I diversity, which was associated with surviving populations of MCFs. Specific MHC-I variants were at increased frequency in populations that are Bd-tolerant or have survived despite enzootic disease dynamics. This information will help to direct future efforts for the conservation of the MCF, allowing populations and individuals with protective genotypes to be prioritised for conservation action.

Chapter Four

Guardian Commensals or Inconsequential? The Skin Microbiome of the Mountain Chicken Frog and its Interaction with the Pathogen *Batrachochytrium dendrobatidis*

Abstract

Populations of the mountain chicken frog (*Leptodactylus fallax*, MCF) were differentially impacted by infection with the fungal pathogen *Batrachochytrium dendrobatidis* (Bd) in the 2000's. Most MCFs died, while a small number survived and still exist in the wild today, twenty years later. The determinants of this discrepancy in survival are uncertain, but studies of other amphibian species have linked skin microbiome diversity and structure to Bd infection survival. To investigate this theory in the MCF, this study used 16S metabarcoding to study the skin microbiome structure and function in MCFs that survive in the wild, captive bred MCFs that were Bd-naïve, and captive bred MCFs following their release to the wild and first infection with Bd. The surviving wild MCFs harboured diverse skin bacterial communities and potentially protective functional profiles that may limit Bd infection. The Bd-inhibitory capacity of these eight wild MCFs appeared to be low, however, with only 10% of their microbiome made up of Bd-inhibitory taxa. This was hypothesised to potentially be attributable to a reduced need for Bd protection in a Bd-enzootic phase. This study also revealed the dysbiosis induced by Bd infection and itraconazole treatment in 27 previously Bd-naïve MCFs, with a 40%-60% reduction in alpha diversity measures and a significant reduction in beta dispersion. Microbiome functional profiles were mostly maintained through this dysbiosis, however. Releasing captive bred MCFs to the wild in Montserrat replenished their skin bacterial diversity to levels of wild surviving MCFs in Dominica. However, this did not lead to protection from chytridiomycosis, indicating that protecting reintroduced MCFs from Bd may rely on factors other than the skin microbiome, such as host genetics or environmental manipulation.

Introduction

The mountain chicken frog (*Leptodactylus fallax*, MCF) has suffered massive population declines due to the fungal disease chytridiomycosis (Hudson et al. 2016a). Chytridiomycosis, caused by the fungus *Batrachochytrium dendrobatidis* (Bd), wiped out almost all wild MCFs within two years of its arrival to the Caribbean islands of Dominica and Montserrat (Hudson et al. 2016a). To ensure the species' survival, 50 Montserratian MCFs were removed to biosecure breeding facilities in Europe before they could become infected with Bd (Jameson et al. 2019a). These frogs now provide stock for experimental releases to the wild (Adams et al. 2014). Despite the extreme susceptibility of many MCFs to chytridiomycosis, some individuals in the wild were able to survive the initial epizootic. In Dominica, a small population has persisted for 20 years since the first detection of Bd on the island, with fewer than 50 individuals remaining when surveyed in 2019 (McIntyre 2003, *Author's unpublished data* 2019). A spectrum of susceptibility to Bd infection exists in amphibians (Brannelly et al. 2021). Some are Bd-resistant, meaning they can prevent or limit the fungus colonising their skin (Eskew et al. 2018). Some are Bd-tolerant, able to coexist with Bd while limiting the detrimental impacts on their health (Reeder et al. 2012). Most MCFs alive prior to the Bd epizootic in Dominica and Montserrat were Bd-susceptible, exhibiting clinical signs of and dying from chytridiomycosis (Hudson et al. 2016a). The remaining wild MCFs on Dominica persist in an environment where levels of Bd are sustained in the environment by sympatric amphibian species (Hudson et al. 2019) and several Bd-tolerant Dominican MCFs have been confirmed to be able to survive detectable Bd infection on Dominica since 2014 (A. Cunningham, *pers. comm*.). The determinants of Bd-resistance, tolerance, or susceptibility are likely to be a combination of host, pathogen, and environmental factors – a classic disease triangle (Scholthof 2006; Brannelly et al. 2021). Bernardo-Cravo et al. (2020) suggest that the disease triangle is oversimplified, neglecting a crucial extension of both the host and environment – microbiomes. The incorporation of the microbiome into our understanding of amphibian-Bd interactions may contribute to better disease mitigation (Bernardo-Cravo et al. 2020). In this instance, the skin microbiome is of particular interest, being the site of Bd infection in amphibians (Piotrowski et al. 2004).

The microbiome is a term used to describe the community of microorganisms that live on and in another organism (Bahrndorff et al. 2016). Most animals have a microbiome and microbiomes are usually distinct between different body areas, such as the skin or gut (Hammer et al. 2019). Microbiomes include bacteria, fungi, protozoa, and viruses – although most microbiome studies to date have been limited to describing the bacterial community due to the availability of barcoding genes for this kingdom, namely the 16S ribosomal RNA gene (Caporaso et al. 2011). With recent, rapid advances in sequencing and 'omics technologies, the ways in which the microbiome is intertwined with host physiology and fitness are increasingly brought to our attention (reviewed in Bahrndorff et al. 2016). The composition of a microbiome can impact host metabolism, immune function, and behaviour (Scharschmidt et al. 2015; Marchesi et al. 2016; Vuong et al. 2017; McLaren and Callahan 2020). In turn, the microbiome is sensitive to changes in its host and their joint environment, for example due to host genetics or environmental temperature, pollution, or habitat type (Fouladi et al. 2020; Belasen et al. 2021). Host, microbiome, and environment are constantly interacting, with varied outcomes for hosts and their associated microbes (Bernardo-Cravo et al. 2020).

The microbiome has been an area of research in the field of amphibian-Bd interactions since 2006, when it was revealed that the skin microbiomes of *Plethodon cinereus* and *Hemidactylium scutatum* harboured bacteria with the ability to inhibit Bd in culture (Harris et al. 2006). Since this time there have been many more such studies, recently reviewed by Rebollar et al. (2020). In some instances, particular members of the microbiome may offer protection from Bd infection through the production of antifungal metabolites. A bacterial species that has gained a great deal of attention for its anti-Bd activity is *Janthinobacterium lividum*, which produces antifungal compounds violacein, 2,4-diacetylphloroglucinol, and indol-3-carboxaldehyde (Brucker et al. 2008). Such compounds are of interest for their potential in probiotic mitigation of chytridiomycosis (Rebollar et al. 2020). The addition of Bd-inhibitory bacteria to the skin microbiome has increased Bd infection survival in some species (Kueneman et al. 2016), but not in others (Becker et al. 2011). The structure of the microbiome has also been associated with lower Bd infection intensities (Becker et al. 2015; Walke et al. 2015). Mitigation of Bd infection through skin microbiome structure is proposed to be mediated by more effective microbiome function or by host immunogenetics that promote microbial diversity in the first place (Walke et al. 2015). Additionally, more diverse microbiomes may be more resilient to the disturbance induced by Bd infection (Jani and Briggs 2014).

In the case of the MCF, an ideal investigation into the role of the microbiome as a determinant of survival following Bd infection would characterise the skin microbiome of frogs that suffered lethal Bd infection against those that survived Bd infection (Hudson et al. 2016a). Unfortunately, no microbiome samples were taken during the initial epizootic waves in either Dominica or Montserrat, which occurred when culture-independent studies of microbiomes were in their infancy (Berg et al. 2020). Because samples were not taken at the time of Bd incursion, an exact assessment of the host-pathogen-microbiome dynamics during the chytridiomycosis epizootic implicated in the decline of the MCF is not possible. There are, however, existing MCF populations which may still provide useful insights into the MCF skin microbiome and how it differs with Bd infection history and environment. The first population is in Dominica, where MCFs survived the epizootic of 2002 and have persisted despite the continued presence of Bd (M. Hudson, *Unpublished data* 2014 – 2017). These frogs provide an insight to a wild population that survives without interventions to treat Bd infections. The second population is a cohort of captive bred MCFs that were released to Montserrat in 2019, having never been exposed to Bd and which experienced a widespread Bd outbreak within eight months of their release. These MCFs required intervention with antifungal drugs to ensure survival. This population can provide an insight to the Bd-naïve microbiome, and the changes induced following release to the wild, Bd infection, antifungal treatment, and seasonal change in the same individuals.

Aims

This study will use 16S metabarcoding to present the first insight into the skin bacterial community of MCFs, an important component of amphibian host constitutive immunity. The structure and function of skin microbiota will be compared between groups of MCFs with different Bd infection histories. Understanding the changes in microbiome structure and/or function between these groups may aid the conservation of the MCF through directing conservation management towards practices that encourage Bd-protective microbiome characteristics, if any are found (Kueneman et al. 2016).

Observing any changes associated with MCF reintroduction to the wild, a long term goal of the MCF recovery plan, will also inform on how this intervention will impact a key constitutive immune defence in the MCF.

The first aim of the study is to compare the skin microbiomes of surviving wild MCFs in Dominica to the microbiomes of captive bred MCFs that were released to Montserrat. It is hypothesised that Dominican frogs will hold higher microbial diversity and Bd-inhibitory function in their microbiome than captive bred Montserratian MCFs, enabling them to persist in the wild. Secondly, the study aims to assess the impact of Bd infection and antifungal treatment on Montserratian MCF skin microbiomes. Microbiomes were compared at time points before and after Bd infection and itraconazole treatment in the release of captive bred frogs to Montserrat. It is hypothesised that microbiome community composition and function will be altered by Bd infection and treatment, but the potential direction of change is uncertain. The final aim is to assess the impact of reintroduction to the wild on microbiome structure and function, to provide more information to guide future MCF reintroductions. It is hypothesised that the skin microbiome would become more diverse upon release to a more complex and less sanitised environment.

Methods

Sample Collection

Skin microbiome samples were collected from 35 MCFs across Dominica and Montserrat (Figure 4.1). Of these, eight samples correspond to surviving MCFs in Dominica in 2019. Dominican samples were collected from three sites, Colihaut (n = 2), Soufriere (n = 5), and a wild-collected frog held in a facility in Roseau (n = 1). The presence of Bd has previously been recorded in all three locations (M. Hudson, *Unpublished data* 2014 - 2017; Figure 4.1). None of these eight MCFs had detectable Bd infection in 2019 (*Author's unpublished data* 2019), thus, it is unconfirmed whether they can survive Bd infection. It is possible to say that all have survived despite the confirmed presence of Bd in their population during their lifetime, however (M. Hudson, *Unpublished data* 2014 - 2017). MCFs from Colihaut and Soufriere were over three years of age in 2019, and Bd was been recorded in both locations from within three years prior to 2019 (M. Hudson, *Unpublished data* 2014 - 2017). Age was determined as over three years due to all MCFs having a snout-vent length >13 cm and all males having black spurs - which develop upon sexual maturity at three years of age (Daltry 2002). The Roseau facility is also known to have experienced Bd outbreaks since it was founded (M. Hudson, *Unpublished data* 2014 - 2017).

Twenty-seven Bd-naïve MCFs, bred and reared in biosecure facilities at ZSL London and Jersey zoos, were moved to a semi-wild enclosure in Montserrat in 2019 as part of another experiment (Jameson et al. 2019a). The enclosure is fenced wild habitat with the addition of heated pools (>30°C) complemented by an equal number of ambient temperature pools (M. Hudson, *pers. comm*.). The heated pools are present to study the occurrence of behavioural fever following Bd infection in MCFs. This population was sampled at five time points across 2019 - 2021, covering their release to the wild and an incident of Bd infection and treatment (Figure 4.1). To provide a comparison of microbiomes in captive and wild environments, the same MCFs were sampled prior to release in July 2019 and a month post-release in August 2019. During these first two time points, MCFs were naïve to Bd infection, having been reared under strict biosecurity regimes to protect from novel pathogens (Jameson et al. 2019a). The release population became infected with Bd during April and May 2020. Infection loads of 2 - 182,379 Bd genomic equivalents and clinical signs of chytridiomycosis were recorded (M. Hudson, *Unpublished data* 2020). As the population was needed for another experiment, all individuals were immediately treated with antifungal baths containing 0.001% itraconazole, a modified version of the protocol listed in Hudson et al. (2016b). To study the impact of Bd infection and itraconazole treatment, MCFs were compared pre- and post-infection. The comparison was made between August 2019 and September 2020, both within the warm, wet season, to minimise changes associated with seasonal transition. Additional time points were originally sampled in January and April 2020, capturing key moments (Bd-naïve microbiomes in the dry season and active Bd infection, respectively). Unfortunately, these samples were not able to be processed due to the shutdown of laboratory facilities during the COVID-19 pandemic. After spending up to a year in storage at 4°C, samples were deemed unreliable due to the probable shift in community composition after this time, and not included in the analysis (Song et al. 2016). The final time points (February and May 2021) provide an insight into the skin microbiome change through a transition from wet to dry seasons, but

only in Bd- and itraconazole-exposed MCFs. Twenty-seven frogs were sampled in July and August 2019, 24 frogs were sampled in September 2020 and February 2021, while 20 were sampled in May 2021 (Figure 4.1). Incomplete sampling was due to deaths or because individuals were nesting and could not be disturbed.

Montserrat and Dominica share a tropical climate with two distinct seasons. Warmer and wetter weather occurs between June and November and a cool, dry season runs from December to May (Daltry 2002; Hudson et al. 2019). Average temperatures in the warm, wet season reach 25-32ºC with 200-280 mm monthly precipitation. In the cool, dry season, temperatures are on average 3-5ºC cooler and rainfall declines to 60-120 mm/month. Dominican samples were taken during the warm, wet season, and Montserratian samples were taken across both seasons. Temperatures during sampling ranged from 26 - 28ºC, but no data were available for September 2020 or February 2021. All skin microbiome samples were collected in the same manner. Each frog was caught using a fresh pair of sterile, nitrile gloves and rinsed with 50 ml of filtered water to remove transient bacteria (Culp et al. 2007). A sterile, rayon tipped swab (TS/17 - Technical Service Consultants Ltd.) was swabbed over the ventral surface 20 times, each hind leg five times, and each hind foot five times (Kueneman et al. 2014). Swab tips were placed into sterile 1.5 ml microcentrifuge tubes alongside a sterile silica capsule. The silica desiccant aimed to inhibit hydrolase enzymes involved in nucleotide degradation and bacterial proliferation, slowing community change and DNA degradation (Johnson et al. 2018). Preliminary work also revealed higher DNA yields using silica preservation over RNAlater (*Author's unpublished data* 2018). A sampling negative – a sterile swab opened at the site and stored in an identical manner – was taken during each sampling episode. Sampling negatives were included to characterise the microbiome inherent to the swab or environment itself and to allow removal of these taxa in downstream bioinformatic analyses (Eisenhofer et al. 2019). All samples were refrigerated below 4ºC until DNA extraction. While these storage conditions are not the 'gold standard' for microbiome studies they were selected as the best option in remote field sites without access to continuous freezing (Song et al. 2016).

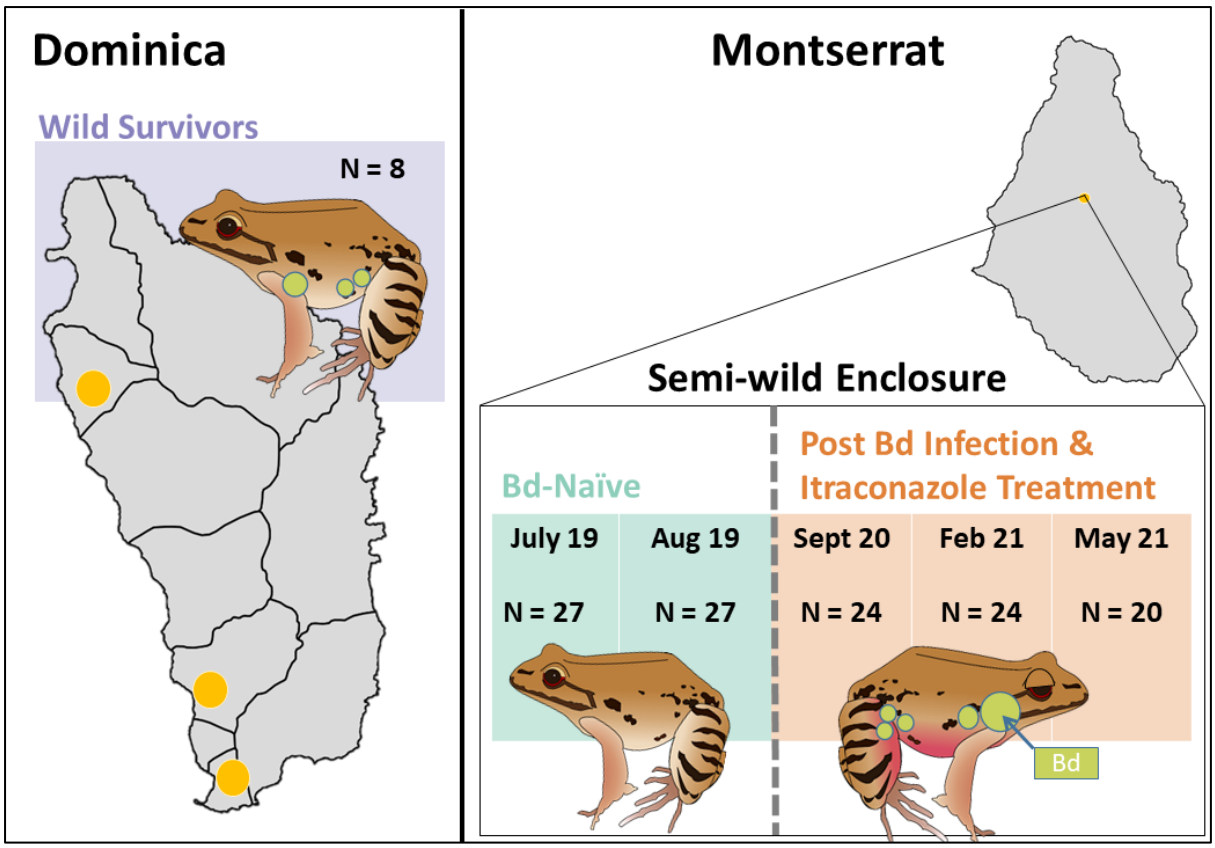

Figure 4.1: Skin microbiome samples were collected from surviving wild mountain chicken frogs in Dominica. Samples were repeatedly collected over two years of an experimental release cohort in Montserrat, where Bd-naïve frogs eventually became infected with *Batrachochytrium dendrobatidis* (Bd) and were treated with itraconazole. Yellow circles represent approximate sampling locations.

DNA Extraction and Sequencing

All samples were extracted using QIAGEN DNeasy PowerSoil extraction kit with two protocol modifications. The swab head was incubated for 10 minutes at 65°C in the powerbead tube with solution C1, as recommended for samples with low biomass (Fierer et al. 2008). A FastPrep homogeniser (MP Biomedicals) was also used in place of a vortex to achieve optimal bacterial cell lysis. Extractions were carried out in a sterile laminar flow hood, using filtered pipette tips and face masks to avoid contamination from external sources and between samples (Eisenhofer et al. 2019). An extraction negative was included for each batch of extractions to identify contaminants within the extraction process. To minimise batch effects, extraction kits were confirmed to hold the same batch ID to minimise effects arising from different 'kitomes' (Salter et al. 2014). An internal control for the effectiveness of DNA extraction was included in the form of a ZymoBIOMICS microbial community standard. This standard was included to identify any biases or errors arising from DNA extraction through to DNA sequencing. An additional mock community was added during sequencing (BEI resources Microbial Mock Community B) to test the accuracy of taxonomic assignment.

PCR amplification, library preparation, and sequencing were performed by the Genomics Hub, Cardiff University. The protocol followed that of Kozich et al. (2013) using dual-indexed primers (515F – 806R) to amplify the V4 region of the 16S rRNA gene (Caporaso et al. 2011). Microbial DNA samples were amplified in triplicate PCRs, consisting of 17 µl of 1.1X Accuprime Pfx Supermix, 1 µl DNA, and 2 µl

indexed primer pairs, each at 10 µM. PCR cycles involved two minutes at 95°C, followed by 30 cycles of 95°C for 20 seconds, 55°C for 15 seconds, and 72°C for five minutes. A final elongation at 72°C for ten minutes finished the PCR. A PCR negative control and microbial mock community were included in each PCR. Triplicate reactions were pooled to accommodate artefacts arising between unique PCR runs. PCR products were visualised using a TapeStation System D1000 and quantified using a Qubit (Life Science Technologies). Successful PCR products were cleaned using SPRI beads, an alternative to gel extraction, where the library was purified and selected for the expected size of the V4 region (240 – 260 bp). Sequencing was performed on an Illumina MiSeq platform using 2x250 chemistry. PhiX (5%) was included to diversify the sequencing library.

Data Processing

Raw data were processed using the DADA2 v.1.22 R package (R Development Core Team 2008; Callahan et al. 2016). Raw reads of 250 bp were trimmed at a length of 240 bases in the forward orientation and 220 in the reverse orientation to remove lower quality ends, after inspection of quality profiles. Reads were truncated at the first instance of a base with a quality score below two, while the maximum expected error rate allowed was also two. Any read containing an 'N' was removed, as these sequences cannot be analysed by DADA2. Reads matching the PhiX genome added during sequencing were removed. Following quality filtering, reads were de-replicated to unique sequences and exact sequence variants (ASVs) were inferred. Forward and reverse reads were merged and any merged read with length outside of the range 240 – 260 bases discarded. Chimeric sequences were removed. Taxonomic classification of ASVs to species level was attempted within DADA2 using a naïve Bayesian classifier algorithm (Wang et al. 2007) with the SILVA training set (version 138.1) (Yilmaz et al. 2014). This training set was chosen as it gave the greatest taxonomic resolution for the dataset, compared to another common choice, RDP classifier (version 18) (Wang et al. 2007). Eighty-two percent of the 100 most common ASVs were assigned to family level with SILVA, but only 66% with RDP.

Contaminants are commonplace in metagenetic studies and in the case of microbiome studies, can arise from sampling equipment, laboratory reagents or surfaces, or sample-sample crossover (Eisenhofer et al. 2019). To identify contaminants that were unlikely to be a true component of the MCF skin microbiome, the decontam R package was used (Davis et al. 2018). A threshold of 0.5, based on prevalence of ASVs in controls (sampling, extraction, PCR) and true samples, was used to identify contaminants. At 0.5, contaminants are identified amongst all sequences as being more prevalent in controls than in true samples. Contaminant ASVs, negative samples, and ASVs identified as chloroplast or mitochondrial (host DNA) were removed from the analysis. Finally, samples with fewer than 100 reads and ASVs with fewer than two reads were discarded. A phylogenetic tree was created from a reference-free alignment of all ASVs in the DECIPHER R package (Wright 2013). Phangorn (Schliep 2011) was used to build an initial neighbour-joining tree, which was used to build a final maximum likelihood tree. The final tree was built assuming a general time-reversible model of nucleotide variation with invariable sites and a gamma rate variation – indicated as optimal for the data using the modeltest function in phangorn. The lowest number of reads in a sample was 111, and the highest 423,810. Commonly, microbiome data are rarefied to the lowest sample read depth to mitigate biases in diversity estimates arising from unequal library sizes. Due to the large range in library size for this

study, a different value than the lowest depth was chosen to avoid underestimating diversity, which can be a pitfall of rarefaction (McMurdie and Holmes 2014). To aid in deciding rarefaction depth, rarefaction curves were produced from the dataset in order to identify the sequencing depth at which all ASVs were captured in all samples (Supplementary Figure S4.1). After inspection of the rarefaction curve, it was evident that at the 9th lowest sample read depth (5,694 reads) 1,000 ASVs could be captured. Only one sample had higher ASV diversity (1,292 ASVs), so this value was deemed appropriate to capture all ASVs in 99% of the data. All samples were rarefied to a read depth of 5,694 via resampling without replacement of ASVs. As a result, eight samples were lost from the analysis as they had fewer than 5,694 reads and 1,993 ASVs were lost because they were no longer present in any sample after random subsampling.

Community Analysis

Alpha Diversity

The Shannon measure of alpha diversity was calculated in the R package phyloseq v.1.38 (McMurdie and Holmes 2013), chosen for its incorporation of both richness and evenness. Faith's PD, a measure of alpha diversity that also considers phylogenetic relatedness, was calculated using the btools R package (Battaglia 2019). To compare alpha diversity between Dominican and Montserratian frogs, a t-test was performed between the Dominican sample group and each of the five time points from the Montserrat release. Pairwise comparisons were chosen, over a mixed model for example, due to the repeated sampling of individuals in Montserrat (non-independent measures), but not in Dominica. In instances where alpha diversity measures could not be transformed to meet the assumptions of normality, a Wilcoxon test was used. A false-discovery rate (FDR) correction for multiple testing was applied to account for the repeated t-tests (Benjamini and Yekutieli 2001).

Linear mixed-effect models (LMM) were used to study alpha diversity through reintroduction and Bd infection in the Montserrat release group, while accounting for repeated sampling of individuals. Shannon diversity and Faith's PD were tested in separate models, which both included month sampled as a fixed factor, and individual frog ID as a random intercept. Model residuals were checked for their agreement with assumptions of normality and homogeneity. Faith's PD was log transformed to meet assumptions of normality in models with this dependent variable. LMMs were run using the R package lme4 (Bates et al. 2015). Fixed effect sizes, standard errors, and t-values most accurately guide interpretation of model outcomes and are included with lme4. Lme4 does not calculate p-values for mixed models, due to uncertainty in the number of degrees of freedom to use, rendering any p-value an approximation (Baayen et al. 2008). Despite this, approximate p-values may aid in the interpretation of model outcomes. For this reason, approximate p-values were calculated using the Kenward-Roger (KR) method implemented in the R package pbkrtest (Halekoh and Højsgaard 2014). The KR method was selected as it performed best at reducing Type I error rates amongst several p-value approximation methods tested by (Luke 2017). The R package Emmeans (Lenth et al. 2022) was used to calculate estimated marginal means (EMMs) and to obtain post-hoc Tukey-adjusted p-values for pairwise group comparisons.

Beta Diversity

To present an overview of the differences in microbiome structure between the six major sampling groups (Dominica and the five time points of the Montserrat release), heat maps of taxa relative abundances were produced using the R packages heatplus (Ploner 2012) and gplots (Warnes et al. 2019). Relative abundance refers to the proportion of reads assigned to a taxon within a sample and ranges from 0 – 1. Taxa with dominant abundances (>3%) were included. Heat maps were paired with hierarchical clustering dendograms of bacterial taxa and sampling groups, based on Bray-Curtis distances between taxa.

Beta diversity was investigated using a compositional data analysis approach (Gloor et al. 2017). Aitchison distance matrices were produced from Centre-Log-Ratio (CLR) transformed, and Phylogenetic Isometric Log-Ratio Transformed (PhILR) data using the R packages phyloseq and PhILR, respectively (McMurdie and Holmes 2013; Silverman et al. 2017). CLR and PhILR are equivalent to the non-compositional beta diversity measures of Bray-Curtis and UniFrac (Gloor et al. 2017; Silverman et al. 2017). Principal components analysis (PCA) ordination was performed on both distance matrices to visualise the similarities between sample groups. To quantitatively assess differences in community composition, permutational multivariate analysis of variance (PERMANOVA) tests were performed using the adonis2 function in the R package vegan (Oksanen et al. 2005). PERMANOVAs were run for CLR and PhILR-transformed data, including all six sample groups and season (wet or dry) as a fixed effect to quantify the extent of differences between Dominican and Montserratian groups. To assess how community composition changed with Bd infection and reintroduction in the same individuals, PERMANOVAs were repeated with just Montserratian sample groups. All PERMANOVAs included frog ID as a random effect to account for repeated measures. Individual-level change in beta diversity was analysed using a PERMANOVA with frog ID as a fixed effect. As PERMANOVA assumes equal dispersion amongst groups, a permdisp test was run using vegan to test differences between group dispersions and in order to contextualise PERMANOVA findings.

To examine differential abundances of taxa between sample groups, an analysis of compositions of microbiomes with bias corrections (ANCOM-BC) was run (Lin and Peddada 2020). ANCOM is a method to measure differential abundance that is suitable for compositional data due to the log ratio transformation it includes (Gloor et al. 2017). ANCOM also has a lower false-discovery rate and higher power than other methods such as DESeq2, especially for sample sizes around n = 20 (Weiss et al. 2017; Lin and Peddada 2020). ANCOM-BC is an ANCOM method that estimates the unknown sampling fraction of a sample (i.e. how much of the real microbial community is represented in the experimental sample), and corrects the bias that arises from differences in this value between samples (Lin and Peddada 2020). Analysis was performed on ASVs with >1% relative abundance, as these are more likely to contribute to overall community functioning than very rare taxa.

Microbiome Function: Functional Overview

To understand the possible functional variation aligned to microbiome compositional changes, picrust2 v.2.3 (Douglas et al. 2020) was run. Picrust2 aligns ASVs within a reference tree of 20,000 bacterial genomes and is able to predict gene family copy numbers based on the ASV placement in the reference tree. Enzyme Commission (EC) gene family copy numbers and ASV abundances are used

to predict the abundance of MetaCyc-classified metabolic pathways (Caspi et al. 2016). Picrust2 was run using default settings, as these were sufficient for the aims of this study (i.e. no per-ASV level of pathway abundance required). Individual pathways were classified into broader classes as defined by the MetaCyc database to enable a higher-level overview of microbiome function. ANCOM-BC was run as specified for bacterial taxa to assess differential abundances in functional pathways between groups. Functional analysis with picrust2 is limited to predictions of functional capacity, and the accuracy of predictions is limited by how related sample microbiota are to sequenced genome references (Langille et al. 2013). A measure of this accuracy is NSTI (Nearest Sequenced Taxon Index), with 'good' NSTI values approximated at 0.03 ±0.2 (Langille et al. 2013). The MCF dataset had a NSTI of 0.05 ±0.05, so is capable of having good accuracy with picrust2.

Microbiome Function: Bd-inhibition Prediction

To link microbiome structure to predicted defensive capability against Bd, the proportion of ASVs matching bacterial isolates with known Bd-inhibitory activity was calculated for each sample. A database of 1,944 bacterial isolates from 37 amphibian host species was used (Woodhams et al. 2015). Each database isolate has been tested for its ability to inhibit Bd growth. A custom BLAST database was created in Geneious Prime, using 16S sequences from isolates marked as inhibitory to Bd growth. Each of the ASVs from the MCF dataset were queried against this Bd-inhibitory database using megablast, to return just the top hit from a query-centric alignment (Muletz-Wolz et al. 2017). ASVs with a 100% match to Bd-inhibitory isolates were deemed to have potential Bd-inhibitory activity. The relative abundance of potentially Bd-inhibitory ASVs within a sample was calculated. Specifically, the number of reads assigned to 'inhibitory' ASVs within a sample was divided by the total reads assigned to that sample. As noted by Muletz-Wolz et al. (2017) a match between ASVs and a Bd-inhibitory isolate does not guarantee that the ASV will inhibit Bd, just that the ASV is a strong candidate to inhibit Bd. Therefore, the proportion of ASVs matching Bd-inhibitory isolates was taken as a prediction of their Bd-inhibitory capacity. The change in proportion of Bd-inhibitory ASVs between sample groups was quantified using a generalised mixed model (GLMM) with a binomial error structure, to account for the dependent variable being proportional. The dispersion of the fitted model was tested using the "dispersion_glmer" test in the R package blmeco (Korner-Nievergelt et al. 2015). Dispersion analysis of the GLMM indicated a slight level of underdispersion in the data (dispersion = 0.67, threshold for normal dispersion = 0.75 – 1.4). Underdispersion is generally not regarded as being as problematic as overdispersion, as it leads to more conservative estimates of model effects (Brooks et al. 2019). Due to this, and the fact that the data were not severely under dispersed, the model was retained. Emmeans (Lenth et al. 2022) was used to obtain post-hoc Tukey-adjusted p-values for pairwise group comparisons.

Results

Of 7,815,141 raw reads input to DADA2, 7,290,426 (93%) of reads were retained after quality and length filtering, ASV assignment, merging, and removal of chimeras. All eight reference 16S sequences from the DNA extraction mock community were represented at a 100% match after extraction, sequencing, and DADA2 processing. This indicates that the extraction protocol was robust for taxonomic detection. Three ASVs in the extraction mock community sample did not match the expected species. This represented just 0.006% of the sample reads, indicating negligible contamination. Sixteen species of the 20 expected in the sequencing mock community were detected as a 100% match to a reference file of 16S sequences. Four species expected to be in the sample were not detected – these were *Enterococcus faecalis, Propionibacterium acnes, Staphylococcus epidermis*, and *Streptococcus pneumonia* – indicating some bias in the ability of the sequencer to capture all taxonomic variation in a sample. Six ASVs assigned to this sample did not match species included in the mock community, but only represented 0.4% of the total sample reads. This points to contamination either of reagents or of sample crossover during sequencing, but only at a low level. Decontam identified 48 ASVs more prevalent in negative controls than true samples and these were removed from the analysis. After removal of negative controls, contaminants, and samples or ASVs with low read depths, 126 samples remained with 11,399 ASVs. After rarefaction, 9,406 ASVs and 118 samples remained: corresponding to 34 phyla, 64 classes, 165 orders, 349 families and 925 genera. Phylum Proteobacteria contributed 58% of reads, followed by Bacteroidota (23%), Actinobacteria (9%) and Firmicutes (3%). Sixteen of the 925 genera held >1% relative abundance: Acinetobacter (17%), Pseudomonas (12%), Sphingobacterium (9%), Klebsiella (7%), Chryseobacterium (7%), Empedobacter (4%), Comamonas (3%), Stenotrophomonas (2%), Sphingomonas (2%), Flavobacterium (2%), Aeromonas (1%), Citrobacter (1%), Massilia (1%), Curtobacterium (1%), Elizabethkingia (1%), and Shewanella (1%).

Alpha Diversity

As predicted, the skin microbiomes of MCFs sampled in Dominica held higher average alpha diversity than any of the Montserratian groups, whether Bd-naïve or post-Bd infection (Figure 4.2). Shannon diversity in Dominica ranged from three to six, while Faith's PD ranged from 31 - 117 (Figure 4.2, Table 4.1). Across the release in Montserrat, Shannon diversity was between 1.5 and 4.9, while Faith's PD ranged from 11 - 53 (Figure 4.2, Table 4.1). Pairwise tests of significance revealed that Shannon diversity was significantly higher in Dominica for all time points except August 2019, one month post release of the captive MCFs to the semi-wild enclosure while the cohort was Bd-naïve (Table 4.1). Faith's PD revealed that when the phylogenetic relationships of microbial species were taken into account, alpha diversity throughout the Montserrat release was significantly lower than surviving wild frogs in Dominica (Table 4.1).

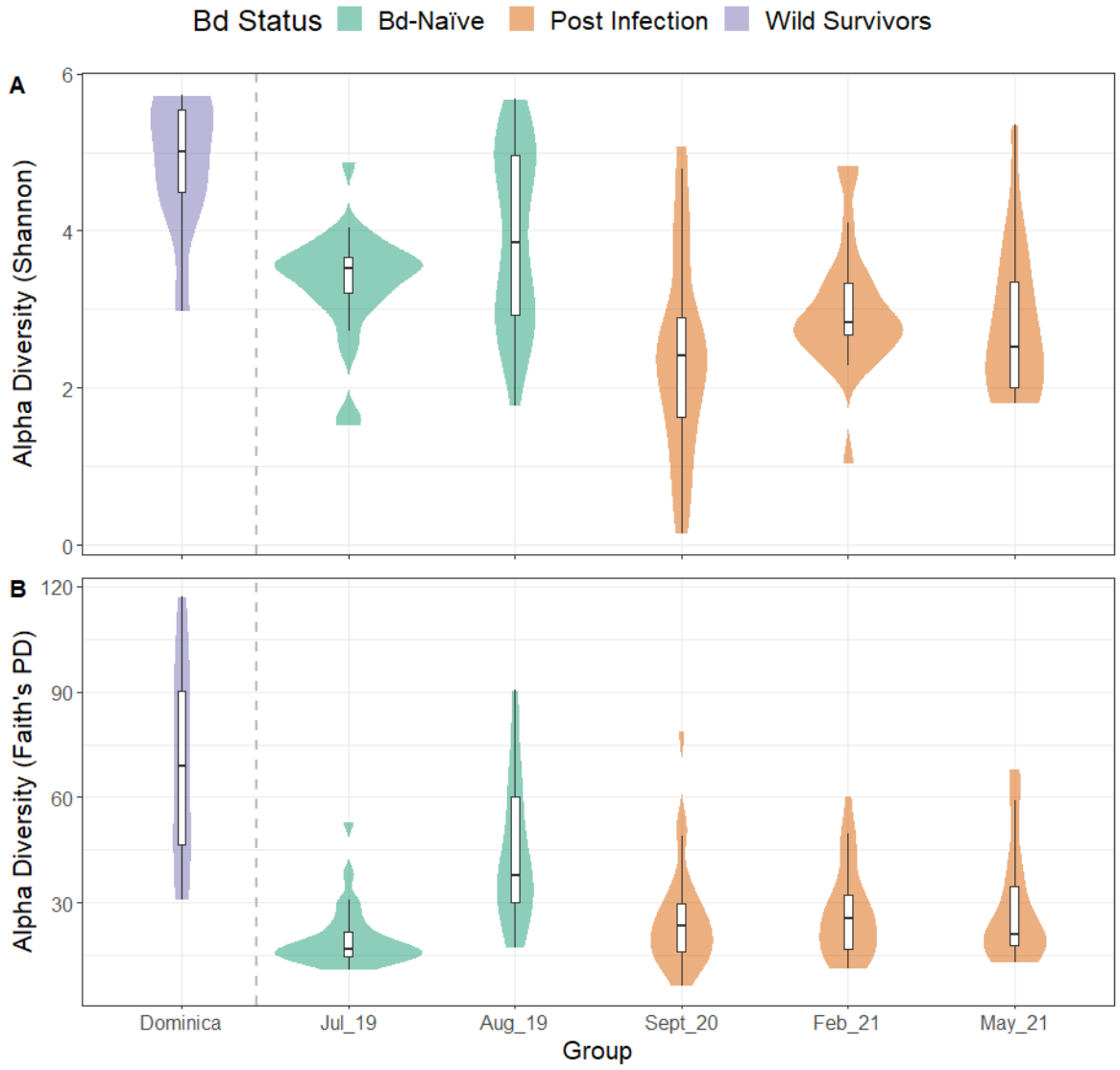

Figure 4.2: Alpha diversity measured as A) Shannon diversity and B) Faith's Phylogenetic Distance. The sample groups on the right of the grey dashed line represent the same 20 – 27 individuals in different months, following release to a semi-wild enclosure in Montserrat.

Table 4.1: Comparison of alpha diversity measures from each time point in the Montserrat release with wild frogs from Dominica. S.d. = standard deviation. P-values are false-discovery rate corrected with a Benjamini and Yekutieli correction: *p-value < .05, **p-value < .01, ***p-value < .001.

Group	N	Bd Status	Country	Mean Shannon (s.d.)	Shannon p-value	Mean PD (s.d.)	PD p-value
Dominica	**8**	**Wild Survivors**	**Dominica**	4.85 (0.93)	-	**69.7 (30.3)**	-
Jul_19	25	Naïve	Montserrat	3.34 (0.70)	0.002**	20.4 (9.34)	< 0.001***
Aug_19	26	Naïve	Montserrat	3.91 (1.15)	0.110	44.4 (20.8)	0.014*
Sept_20	23	Post Infection	Montserrat	2.42 (1.29)	< 0.001***	26.2 (16.3)	0.001**
Feb_21	22	Post Infection	Montserrat	2.99 (0.83)	< 0.001***	27.3 (13.4)	0.002**
May_21	14	Post Infection	Montserrat	2.84 (1.02)	< 0.001***	29.0 (17.1)	< 0.001***

Alpha diversity significantly increased with reintroduction and significantly declined following Bd infection. Release to the semi-wild enclosure coincided with a significant increase in Shannon diversity and Faith's PD between July and August 2019 (Table 4.2). This shows that the diversity gained post-release was in terms of species abundance, number, and phylogenetic distance. Following August 2019, Bd infection and itraconazole treatment (measured in September 2020) associated with a significant decline in Shannon diversity (EMM = 1.5, s.e. = 0.292, t.ratio = 5.123, p-value < 0.0001) and Faith's PD (EMM = 0.242, s.e. = 0.06, t.ratio = 4.266, p-value = 0.0005). Following Bd infection and the transition from wet to dry season, measured in February and May 2021, there was a slight increase in both alpha diversity metrics relative to September 2020, but this was not significant, suggesting that this seasonal shift did not significantly change the number or abundance of bacterial taxa in the MCF microbiome. The significant reduction in both alpha diversity measures relative to August 2019 was sustained in February and May 2021 (Aug-Feb Shannon p-value = 0.021, Aug-Feb Faith's PD p-value = 0.005, Aug-May Shannon p-value = 0.017, Aug-Feb Faith's PD p-value = 0.038). The random effect of individual frog ID contributed a low amount to overall variation (0 - 0.5%) and individual effect sizes ranged from 0.000 - 0.02 in both sets of LMMs (Table 4.2).

Table 4.2: Linear mixed model fixed effect results. The effect of months post release on the alpha diversity of 27 frogs released to a semi-wild enclosure in Montserrat. Individual frog ID was controlled for as a random effect. P-values are approximated with the Kenward-Roger (KR) method: *p-value < .05, **p-value < .01, ***p-value < .001.

Dependent Variable: Shannon, observations = 110
Random Effect: Individual ID, variance = 0.005, s.d. = 0.071

Months Post Release	Group	Estimate	Confidence Intervals	t-value	p-value
Intercept	Intercept	3.340	2.946, 3.734	16.363	0.000***
1	Aug 2019	0.574	0.022, 1.126	2.012	0.047*
14	Sept 2020	-0.922	-1.491, -0.353	-3.133	0.002**
19	Feb 2021	-0.347	-0.922, 0.231	-1.164	0.247
22	May 2021	-0.506	-1.163, 0.154	-1.487	0.140

Dependent Variable: Log_{10}(Faith's PD), observations 110
Random Effect: Individual ID, variance = 0, s.d. = 0

Months Post Release	Group	Estimate	Confidence Intervals	t-value	p-value
Intercept	Intercept	1.300	1.224, 1.377	32.847	0.000***
1	Aug 2019	0.315	0.208, 0.422	5.675	0.000***
14	Sept 2020	0.073	-0.038, 0.183	1.269	0.210
19	Feb 2021	0.109	-0.003, 0.220	1.875	0.066
22	May 2021	0.124	-0.004, 0.251	1.874	0.066

Beta Diversity

Relative bacterial abundances between surviving Dominican frogs and the release group in Montserrat were distinct from each other (Figure 4.3). The most common order in the Dominican samples was Micrococcales (15%), with other orders present between 0.1% - 9% (Figure 4.3). Montserratian samples were dominated by Pseudomonadales (19% - 35%) with the exception of microbiomes sampled in September 2020, three months after Bd infection, which had slightly higher proportions of

Enterobacterales (22%) than Pseudomonadales (20%) (Figure 4.3). August 2019 and September 2020 appeared in distinct dendogram clades (Figure 4.3). July 2019, February and May 2021 clustered in a shared clade. This is in line with the alpha diversity results, where a significant change was found in August 2019 and September 2020 relative to July 2019, but not at other time points. Bd infection and itraconazole treatment appeared to be associated with a community disruption in September 2020. This time point held relatively more Paenibacillales, which was classified as a distinct clade in the cluster dendogram (Figure 4.3). This time point also clustered closest to Dominican samples, though still in a distinct clade.

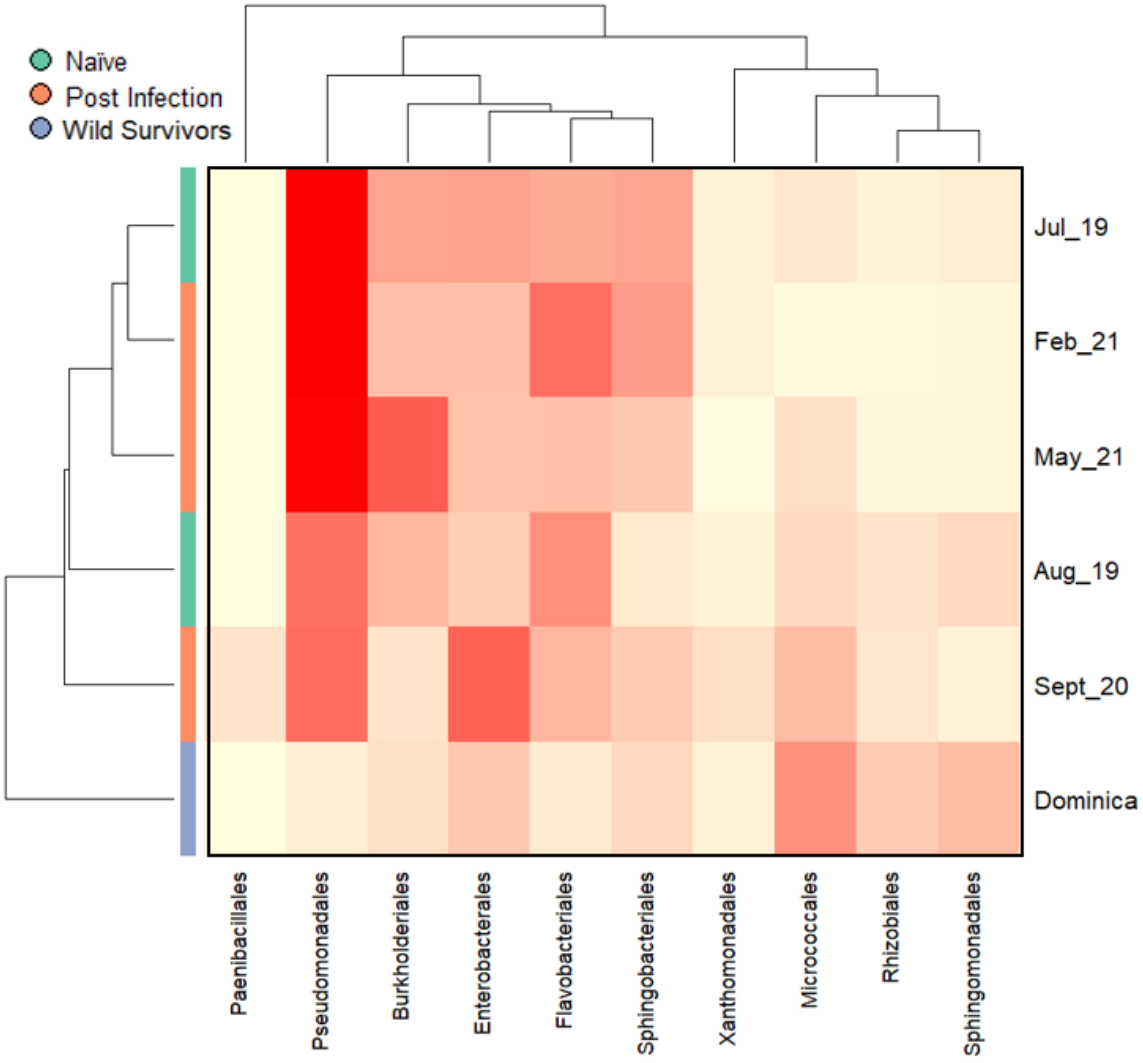

Figure 4.3: Heatmap of bacterial orders per sample group with relative abundance >3%. Darker red denotes higher abundance. Dendograms represent hierarchical clustering of sample group microbiomes (left) and bacterial orders (top). Colour bar on left represents Bd Status. All sample groups besides 'Dominica' represent the same 20 – 27 individuals in different months, following release to a semi-wild enclosure in Montserrat.

When quantified, the beta diversity of skin microbial communities differed significantly between most experimental groups (Figure 4.4). PERMANOVAs with no phylogenetic information (CLR) and with this information (PhILR) revealed similar results: CLR-based: Pseudo-F = 4.29, R^2=0.13, p-value = 0.001, PhILR-based: Pseudo-F = 4.52, R^2=0.14, p-value = 0.001. Post-hoc tests of pairwise differences revealed that most of the variance (13%) was explained by the comparison between Dominica and the pre-release, Bd-naïve frogs from July 2019, for both CLR and PhILR-transformed data (Table 4.3). Samples from July 2019 were also the most distinct from Dominican samples in the PCAs (Figure 4.4). Dominican beta diversity was most similar to August 2019, one month post-release to the semi-wild enclosure and before Bd infection. Both CLR and PhILR post-hoc test p-values were non-significant for this pairwise comparison (Table 4.3). However, PCA plots showed the largest amount of community overlap between post-Bd infection samples from September 2020 and wild MCFs in Dominica (Figure 4.4). Analysis of group dispersion revealed that Dominica had a significantly larger dispersion than other groups, except for August 2019 (Table 4.3, supplementary Figure S4.2). This means that the significant results returned by PERMANOVA analyses cannot be attributed solely to different means of beta diversity but may also be due to the varied dispersion of data points (Anderson and Walsh 2013). The effect of season was also significant, but explained approximately seven times less variation than the experimental group for both CLR and PhILR datasets CLR-based: Pseudo-F = 2.79, R^2=0.02, p-value = 0.001, PhILR-based: Pseudo-F = 3.01, R^2=0.02, p-value = 0.001. Dispersion was also significantly different between the rainy and dry season groups (p-values = 0.002).

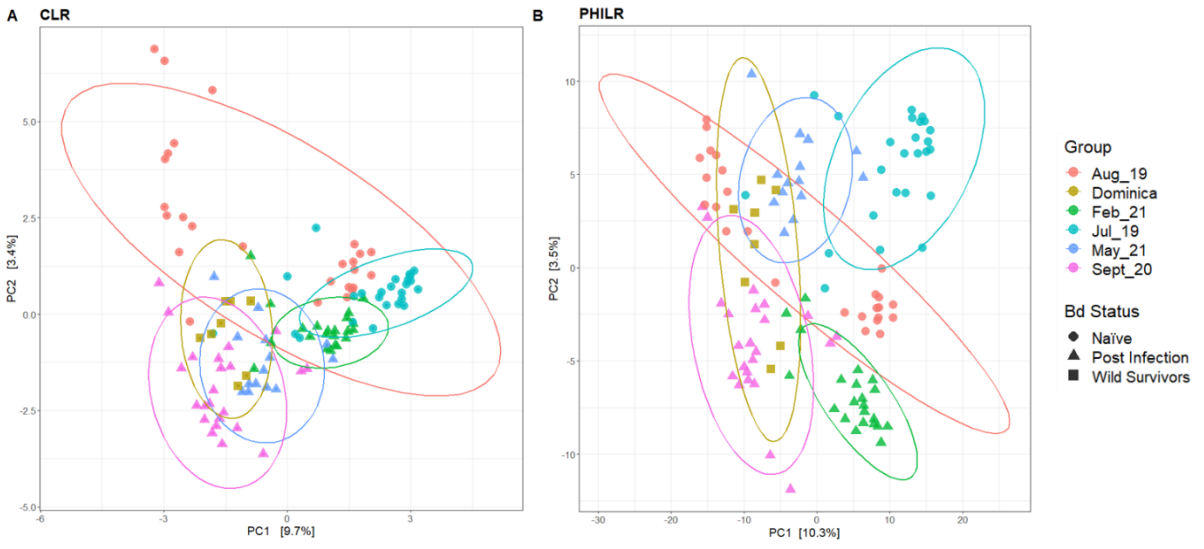

Figure 4.4: Principal components analysis (PCA) of the skin microbiome communities between mountain chicken frogs. Samples are coloured according to their sample group, while the shape of points indicate the Bd status of the sample. PCA plots are based on the Aitchison distance between A) CLR and B) PhILR transformed data matrices.

Table 4.3: Post-hoc pairwise tests between PERMANOVA sample groups and results of the Permdisp test for different dispersion. Significance levels = *p-value < .05, **p-value < .01, ***p-value < .001.

CLR Post-hoc				
Pair	**Pseudo-F**	**R^2**	**p-value (adj.)**	**Permdisp p-value**
Dominica: July 2019	4.494	0.13	0.015*	< 0.0001***
Dominica: August 2019	1.867	0.06	0.030*	0.09
Dominica: September 2020	2.544	0.08	0.015*	< 0.0001***
Dominica: February 2021	3.531	0.11	0.015*	< 0.0001***
Dominica: May 2021	2.219	0.10	0.015*	< 0.001**
PhILR Post-hoc				
Pair	**Pseudo-F**	**R^2**	**p-value (adj.)**	**Permdisp p-value**
Dominica: July 2019	4.693	0.13	0.015*	< 0.0001***
Dominica: August 2019	1.889	0.06	0.015*	0.12
Dominica: September 2020	2.564	0.08	0.015*	< 0.0001***
Dominica: February 2021	3.820	0.12	0.015*	< 0.0001***
Dominica: May 2021	2.316	0.10	0.015*	< 0.001**

To study just the impact of release to the wild and Bd infection within the same individuals, PERMANOVAs were run just on Montserratian samples. PERMANOVAs and post-hoc tests revealed the significant change in microbiome composition between each time point of the Montserrat release: CLR PERMANOVA, Pseudo-F = 5.06, R^2=0.13, p-value = 0.001, PhILR PERMANOVA, Pseudo-F = 5.37, R^2=0.13, p-value = 0.001 (Table 4.4). The change between time points appeared more pronounced for the PhILR-based PCA (Figure 4.4). Release to the wild associated with a significant compositional shift in the cohort, explaining 8 - 9% of the overall PERMANOVA variation (Figure 4.4, Table 4.4). The August 2019 samples were widely dispersed compared with all other time points, showing that individuals gained microbiome compositions differently following release (Figure 4.4). Bd and itraconazole exposure explained less variation for the comparison of August 2019 and September 2020 (6 - 7%, Table 4.4). Most variation in the PERMANOVAs was attributed to the combined impact of release to the wild and Bd infection. The comparison of July 2019 (pre-release and Bd-naïve) and September 2020 (three months post-Bd infection) explained 17-18% of the overall variation (Table 4.4). This large shift in community composition can also be seen in the PCA plots (Figure 4.4). Unlike alpha diversity, there was a significant change in beta diversity through the transition from wet to dry season (Sept 2020: Feb 2021 and May 2021, Table 4.4), and these comparisons explained more variation than release to the wild or Bd infection (R^2 range = 10 - 13%, Table 4.4). Even two months apart within the same dry season, a significant amount of microbiome composition change occurred (Feb:May 2021 R^2 = 13 - 14%, Table 4.4). CLR- and PhILR-based dispersion tests between time points revealed significantly different dispersions between groups (p-value < 0.001, Table 4.4, Figure S4.2). In this case, the largest dispersion was found in the group with most samples (August 2019), which may make PERMANOVA overly conservative (Anderson and Walsh 2013). This is because with more samples that are widely dispersed, the chances of the other samples (which have a smaller dispersion) falling within the dispersion of the larger group are increased and PERMANOVA is more likely to return a non-significant result. Therefore, the significant result from Montserrat-only PERMANOVAs can be

supported. Within the Montserrat dataset, where individuals were repeatedly measured over time, beta diversity did not vary significantly between individual frogs. Both CLR- and PhILR-based PERMANOVAs returned p-values of 1, and dispersion did not significantly differ between individual frogs (p-values > 0.05). Again, season did not explain as much variance as time point in the PERMANOVA: CLR-based: Pseudo-F = 2.98, R^2=0.02, p-value = 0.001, PhILR-based: Pseudo-F = 3.17, R^2=0.03, p-value = 0.001. Dispersion was significantly different between rainy and dry season groups (p-values = 0.016).

Table 4.4: Post-hoc pairwise tests between PERMANOVA sample groups of the Montserrat release and results of the Permdisp test for different dispersion. Significance levels = *p-value < .05, **p-value < .01, ***p-value < .001.

CLR Post-hoc				
Pair	**Pseudo-F**	**R^2**	**p-value (adj.)**	**Permdisp p-value**
Jul_19: Aug_19	4.495	0.08	0.015**	0.001**
Jul_19: Sept_20	9.418	0.17	0.015**	0.001**
Jul_19: Feb_21	5.676	0.11	0.015**	0.001**
Jul_19: May_21	5.723	0.13	0.015**	0.001**
Aug_19: Sept_20	3.164	0.06	0.015**	0.001**
Aug_19: Feb_21	2.937	0.06	0.015**	0.001**
Aug_19: May_21	2.612	0.06	0.015**	0.001**
Sept_20: Feb_21	5.886	0.12	0.015**	0.001**
Sept_20: May_21	3.701	0.10	0.015**	0.001**
Feb_21: May_21	4.904	0.13	0.015**	0.001**
PhILR Post-hoc				
Pair	**Pseudo-F**	**R^2**	**p-value (adj.)**	**Permdisp p-value**
Jul_19: Aug_19	4.686	0.09	0.01*	0.001**
Jul_19: Sept_20	9.759	0.18	0.01*	0.001**
Jul_19: Feb_21	6.034	0.12	0.01*	0.001**
Jul_19: May_21	5.844	0.14	0.01*	0.001**
Aug_19: Sept_20	3.344	0.07	0.01*	0.001**
Aug_19: Feb_21	3.165	0.06	0.01*	0.001**
Aug_19: May_21	2.774	0.07	0.01*	0.001**
Sept_20: Feb_21	6.393	0.13	0.01*	0.001**
Sept_20: May_21	3.989	0.10	0.01*	0.001**
Feb_21: May_21	5.392	0.14	0.01*	0.001**

Differential Abundance of Taxa

ANCOM-BC was run to identify bacterial taxa that underpin the shifts in alpha and beta diversity. The Dominican group was compared with each of the Montserratian time points. Across all five sample group comparisons there were four orders with differential abundances (Figure 4.5). Sphingobacteriales were 3.6 times more abundant in Dominican microbiomes compared with August 2019. Micrococcales were more abundant in Dominica than across the entire Montserrat release, by the largest extent of all comparisons too (13 - 185 times more abundant, Figure 4.5). Enterobacterales were increased in Dominica in all time point comparisons, except August 2019 and September 2020 (Figure 4.5). Flavobacteriales were almost five times more abundant relative to Dominica in August 2019 and September 2020 (Figure 4.5). The months with the most differences (three taxa) to Dominica were August 2019 and February 2021, while September 2020 had the fewest (one taxon).

Differential abundances were also compared between successive time points in the Montserrat release. Following release to the semi-wild enclosure, there was an 8.7 fold increase in Flavobacteriales (p-value < 0.001) and 9.4 fold of Micrococcales (p-value < 0.01) and a reduction of Sphingobacteriales by 2.4 times (p-value < 0.05) (supplementary Figure S4.3). Bd infection and itraconazole treatment were followed by an almost five fold reduction in Burkholderiales (p-value < 0.001) and Flavobacteriales (p-value < 0.01) in September 2020. Moving from wet to dry season saw a 3.8 fold increase in Burkholderiales (p-value < 0.001) and a reduction in Micrococcales by 14 times and Xanthomonadales by five times (p-values < 0.001, supplementary Figure S4.3). There was another shift in the relative abundance of Flavobacteriales and Burkholderiales between February 2021 and May 2021, both by approximately four fold (supplementary Figure S4.3).

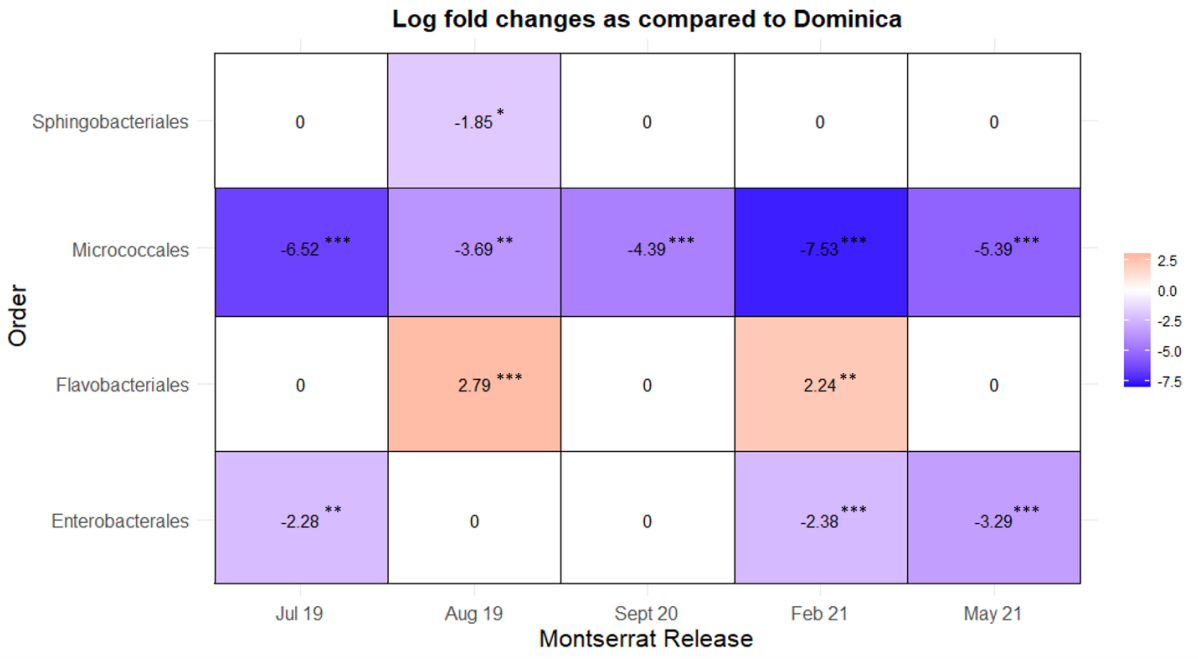

Figure 4.5: Significantly differentially abundant taxa between months of the Montserrat release and Dominican microbiomes from ANCOM-BC analysis. Values represent log fold change in abundance relative to Dominican microbiomes (false discovery rate corrected p-values: *p-value < .05, **p-value < .01, ***p-value < .001).

Functional Analysis: Predicted Metabolic Pathway Abundance

Picrust2 analysis predicted 425 metabolic pathways within the skin microbiome of MCFs. These pathways were most broadly categorised into biosynthesis (56%), degradation (36%), energy metabolism (8%), detoxification (0.4%), and activation-inactivation-interconversion (0.2%). When pathways were categorised at next level of specificity from the MetaCyc database, there were 34 classes found. In the five comparisons between Dominica and the time points of the Montserrat release, eighteen metabolic pathway classes showed a significantly differential abundance at least once (Figure 4.6). Dominican microbiomes were always more enriched for siderophore biosynthesis, except when compared to this pathway's abundance in September 2020 in Montserrat. Alcohol degradation and C1 compound utilisation were also more abundant in Dominican microbiomes in three of five comparisons with Montserrat (Figure 4.6). July 2019, prior to release to the wild, had the largest number of differentially abundant pathways compared to Dominica (14), followed by May 2021 (11) (Figure 4.6). The Montserrat population in August 2019, prior to Bd infection but following exposure to the wild, had the fewest differences with Dominica (4), followed by September 2020 which had five differentially abundant pathways (Figure 4.6). The largest number of differential pathway abundances compared to Dominica was recorded in May 2019, where MCF microbiomes had 4.4 times fewer pathways classed as steroid degradation, and 4.8 times fewer pathways classes as alcohol degradation (Figure 4.6).

Following their release to the wild, Montserratian MCF microbiomes were significantly enriched for the C1 compound utilisation pathway (by 2.7 times, p-value < 0.001), relative to pre-release (supplementary Figure S4.4). Release to the wild also came with a reduction in the relative abundance of five pathway classes by 1.2 – 1.3 times, mainly associated with degradation: metabolic regulation, then the degradation of aromatic compounds, amino acids, and carboxylates (supplementary Figure S4.4). There were fewer metabolic changes following Bd infection and itraconazole treatment than release to the wild (supplementary Figure S4.4). The degradation of secondary metabolites was 1.3 times increased three months following Bd infection (p-value = 0.005). Relative to the last point sampled prior to infection, C1 compounds utilisation and the degradation of alcohols and steroids were all less abundant three months post-infection (supplementary Figure S4.4). Steroid degradation was the most reduced, by 3.7 times (p-value < 0.001). Steroid degradation was almost five times less abundant in February 2021 relative to September 2020, following the onset of the dry season in Montserrat (p-value < 0.001, supplementary Figure S4.4). Despite the lack of disturbances relative to the other pairwise month comparisons, the highest number of differentially abundant pathways (12) was detected between February and May 2021 (supplementary Figure S4.4). The differences were largely of a small magnitude, with nine corresponding to a 1.2 fold change in abundance. Differential abundances larger than this were seen in Microbiomes sampled in May 2021, which had 2.2 times reduced antibiotic resistance pathways, 2.8 reduced aldehyde degradation, and 6.2 times less steroid degradation (supplementary Figure S4.4).

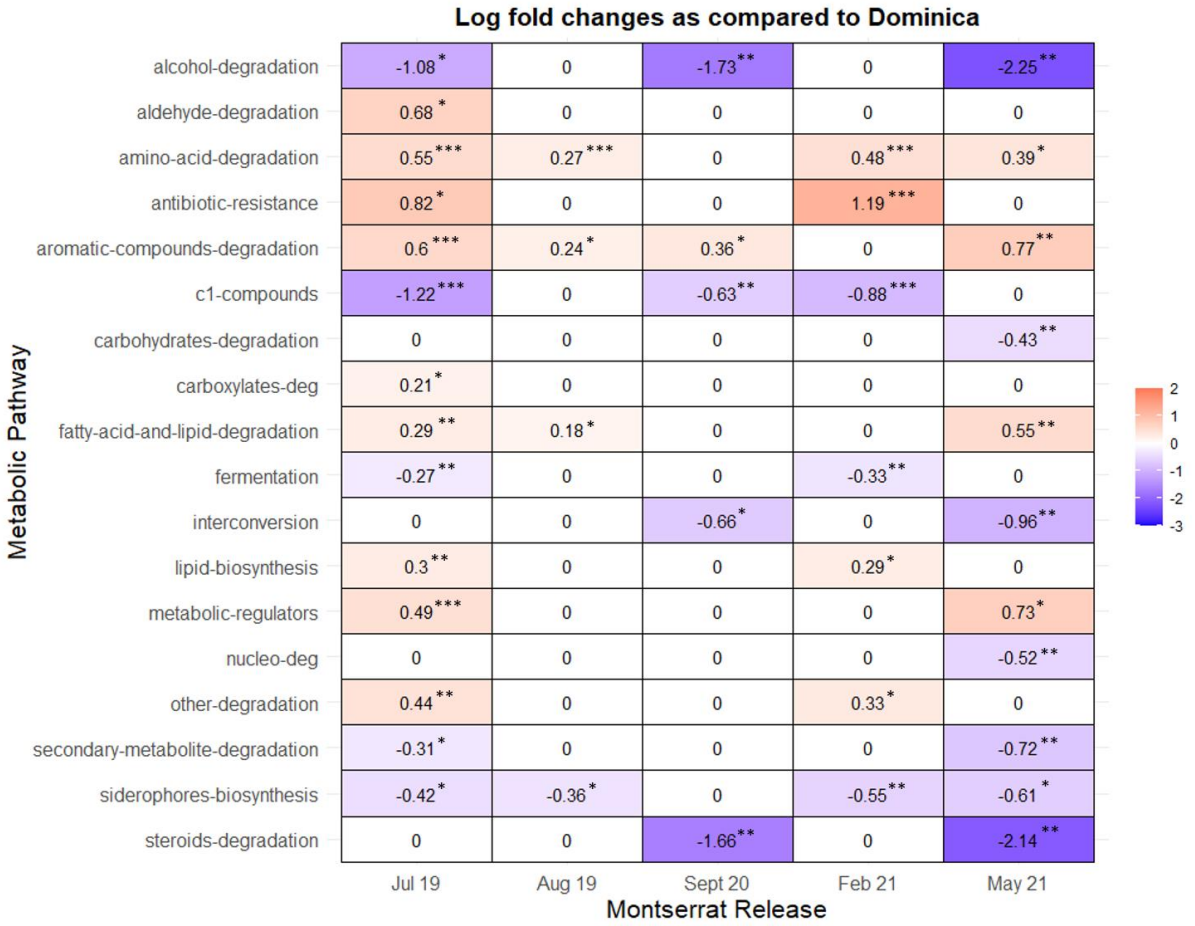

Figure 4.6: Significantly differentially abundant MetaCyc metabolic pathway classes between months of the Montserrat release and Dominican microbiomes from ANCOM-BC analysis. Pathway abundances are predictions from Picrust2. Values represent log fold change in abundance relative to Dominican microbiomes (false discovery rate corrected p-values: *p-value < .05, **p-value < .01, ***p-value < .001).

Functional Analysis: Predicted Bd-inhibitory Capacity

Of 9,406 ASVs, 98 (1%) were a 100% match to sequences listed as having inhibitory activity against Bd (Woodhams et al. 2015). There were 60 Bd-inhibitory ASVs shared between Dominica and the entire Montserrat release cohort, none unique to Dominica, and 38 unique to Montserrat. The shared Bd-inhibitory ASVs between months of the Montserrat release are shown in supplementary Figure S4.5. The proportion of Bd-inhibitory ASVs per sample ranged widely from 1 - 98%. When averaged across sample groups, Dominica had significantly lower Bd-inhibitory proportions than any time point in Montserrat, except for August 2019, one month post-release (Figure 4.7, Table 4.5). In August the spread of data was wide, with ~50% of the data points at a similar level to Dominica and ~50% much higher at >50% (Figure 4.7). The mean proportion of Bd-inhibitory ASVs in August 2019 was still 4.5 times larger than in Dominica (Table 4.5). This is in contrast to the hypothesis that MCFs in Dominica would harbour more Bd-inhibitory bacteria than Bd-naïve or post-Bd infection groups in Montserrat.

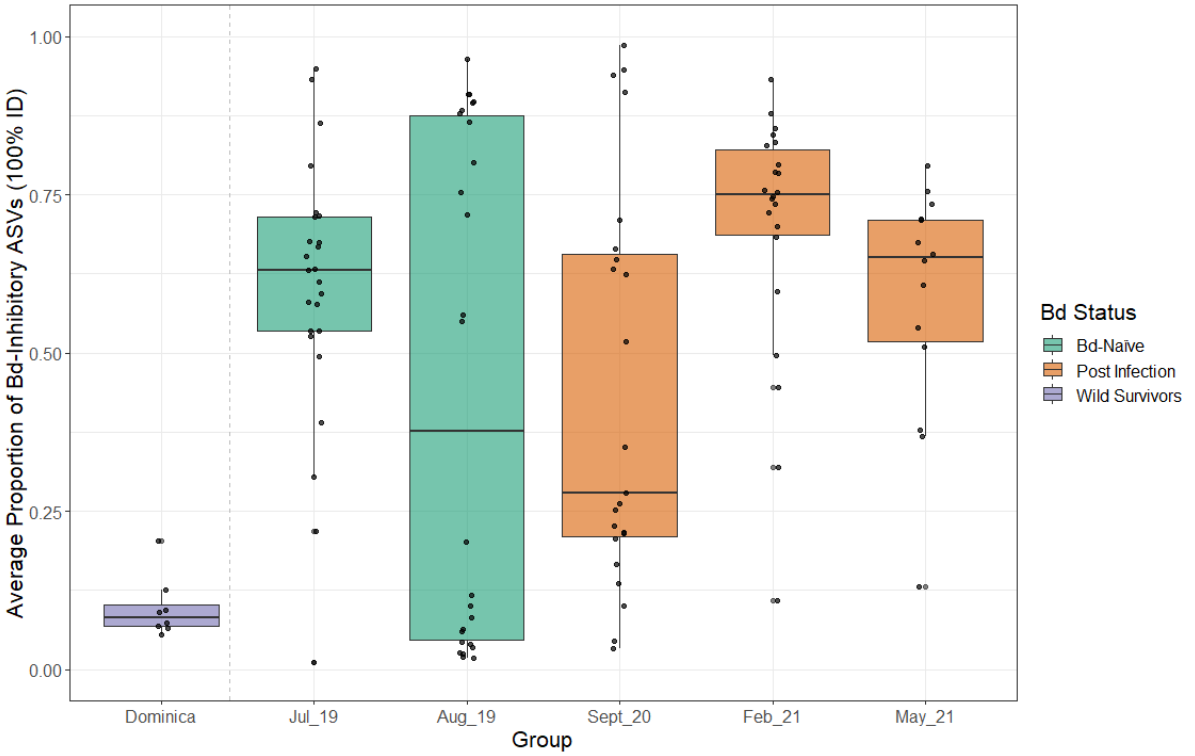

Figure 4.7: Proportions of ASVs with predicted Bd-inhibitory activity within sample microbiomes, averaged across sample groups.

Table 4.5: Comparison of the proportion of ASVs with predicted Bd-inhibitory activity from each time point in the Montserrat release with wild frogs from Dominica. s.d. = standard deviation. P-values are false-discovery rate corrected with a Benjamini and Yekutieli correction: *p-value < .05, **p-value < .01, ***p-value < .001.

Group	N	Bd Status	Country	Mean Proportion of Bd-inhibitory ASVs	s.d.	P-value
Dominica	**8**	**Wild Survivors**	**Dominica**	**0.097**	**0.0483**	**-**
Jul_19	25	Naïve	Montserrat	0.600	0.209	< 0.001***
Aug_19	26	Naïve	Montserrat	0.439	0.395	0.746
Sept_20	23	Post Infection	Montserrat	0.438	0.314	< 0.001***
Feb_21	22	Post Infection	Montserrat	0.697	0.197	< 0.001***
May_21	14	Post Infection	Montserrat	0.587	0.186	< 0.001***

There were significant reductions in the proportion of Bd-inhibitory bacteria relative to the pre-release Montserratian population in August 2019 and September 2020 (Table 4.6). Despite the alpha diversity gained in August 2019, the proportion of Bd-inhibitory bacteria was reduced upon introduction to a non-biosecure environment. However, there was a large spread of Bd-inhibitory proportions across individuals in August 2019 (Figure 4.7) and the post-hoc pairwise test between July 2019 and August 2019 did not find a significant difference in the pair's estimated means (EMM = 1.386, s.e. = 0.653, t.ratio = 2.18, p-value = 0.187). In fact, the post-hoc test did not reveal any pairwise comparisons of Bd-inhibitory capacity to be significantly different. August 2019 and September 2020 held almost exactly the same mean proportions of Bd-inhibitory bacteria (Table 4.5), contradicting the initial

hypothesis that the Bd-inhibitory function would change when microbiomes were disturbed by Bd and an antifungal treatment. The Bd-inhibitory capacity of the microbiome was depleted by release to the wild but levels similar to pre-disturbance were regained over time (Figure 4.7). In dry season months, February and May 2021, the mean proportion of Bd-inhibitory bacteria was similar to the pre-release group in July 2019 (Table 4.5, Figure 4.7). The highest Bd-inhibitory ASV proportion was found in February 2021, showing the fluctuating Bd-inhibitory capacity of the MCF microbiome through seasons. However, as Bd-inhibitory capacity was (non-significantly) reduced in May, the Bd-inhibitory capacity of the Montserratian skin microbiome may also fluctuate within the same season (Figure 4.7). The random effect of PIT tag (individual frog ID) showed no variation, with individual effect sizes all measured as zero.

Table 4.6: Mixed model results. The change in the proportion of ASVs with predicted Bd-inhibitory activity between sampled groups of 27 frogs at different stages following release to a semi-wild enclosure in Montserrat. Individual frog ID was controlled for as a random effect. P-value significance thresholds: *p<0.05; **p<0.01; ***p<0.001.

Dependent Variable: Proportion of Bd-inhibitory ASVs, observations = 110
Random Effect: Individual ID, variance = 0, s.d. = 0

Months Post Release	Group	Estimate	Confidence Intervals	z-value	p-value
Intercept	Intercept	1.386	0.482, 2.487	2.773	0.006**
1	Aug 2019	-1.386	-2.710, -0.185	-2.181	0.029*
14	Sept 2020	-1.649	-3.009, -0.416	-2.523	0.012*
19	Feb 2021	0.118	-1.352, 1.642	0.158	0.874
22	May 2021	-0.087	-1.677, 1.639	-0.106	0.916

Discussion

This study aimed to better understand the skin microbiome of the MCF, an important aspect of amphibian constitutive immunity, and how it varies between some of the last remaining MCF populations. The skin microbiome of Dominican MCFs was explored for characteristics which may have enabled this population to persist despite the presence of Bd. In the absence of microbiome samples from before or during the initial chytridiomycosis epizootic, Bd-naïve individuals were sampled prior to their release to a semi-wild environment and subsequently through the following years and Bd infection. These samples helped to uncover the impact on the skin microbiome introduced via disturbances such as Bd infection, antifungal treatment, release to the wild, and seasonal change.

The Skin Microbiome of Wild, Surviving MCFs

Wild MCFs in Dominica had more diverse skin microbiomes and a larger variation in community composition between individuals than groups from Montserrat did (Bd-naïve or post-infection). Alpha diversity metrics were elevated in the Dominican group, in terms of ASV richness, evenness, and phylogenetic diversity. Community dispersion was wide in Dominican MCF microbiomes, which may have influenced the significant PERMANOVA result between Dominica and time points of the Montserrat release (Anderson and Walsh 2013). MCF Microbiomes in Dominica probably had higher diversity as they were sourced from an environment with more plentiful and/or diverse microbial reservoirs and because they were collected from more than one location (Kueneman et al. 2014; Loudon et al. 2014). As demonstrated by Loudon et al. (2014), wild substrates provide a microbial pool that promotes host skin bacterial diversity and community stability in the face of disturbance. In July 2019, MCFs had not yet been released to the semi-wild enclosure, which is likely to have limited their alpha diversity (Loudon et al. 2014). Faith's PD was significantly higher in Dominican MCFs even after release of Bd-naïve MCFs to Montserrat in August 2019. Montserrat could have substrate that is not as diverse in bacterial taxa as Dominica and it would be useful for future studies to assess the countries' underlying differences in environmental reservoirs such as soil. Microbiomes can vary across locations within the same species (Kueneman et al. 2014). Montserratian samples were restricted to the semi-wild enclosure, while Dominican samples come from sites separated by ~30 km - this wider diversity of locations could have contributed to the higher diversity seen in Dominican microbiomes. Increased richness and evenness of amphibian skin microbiota has been correlated with lower Bd infection intensity, both in vivo and in vitro (Piovia-Scott et al. 2017; Ellison et al. 2019). The mechanisms behind this observation have been suggested to be the dominance of taxa with Bd-inhibitory properties, and/or complementarity amongst the diverse set of taxa (Piovia-Scott et al. 2017). High alpha diversity does not always correlate with lower Bd infection intensity (see Ruthsatz et al. 2020), but in the case of the MCF is associated with the last surviving wild populations following the chytridiomycosis epizootic.

The microbiomes of wild Dominican frogs, relative to the Montserratian frogs, were dominated by Micrococcales, a member of the class Actinobacteria. In another neotropical frog, *Craugastor fitzingeri*, Actinobacteria were enriched in Bd-endemic sites, like those included from Dominica in this study (Rebollar et al. 2018). However, it is not recorded whether these Actinobacteria were

Micrococcales. Members of the order Micrococcales are associated with a wide variety of environments, including marine sediments, soil, amphibian guts, and sloth hair (Kim et al. 2004; Bletz et al. 2016; Rojas-Gätjens et al. 2022). In sloth hair, Micrococcales were observed to have antimicrobial activity, including against fungi of the genus *Cytospora* (Rojas-Gätjens et al. 2022). Flavobacteriales were the only order to show a decrease in abundance in Dominican microbiomes relative to Montserratian microbiomes, in the comparisons with August 2019 and February 2021. Flavobacteriia (the class containing Flavobacteriales) were found in high abundances in two species of Bd-tolerant frogs (*Dendropsophus labialis* and *Rheobates palmatus*) in Colombia (Flechas et al. 2018) and contain species with anti-Bd activity (Shaw et al. 2014). To understand if the Micrococcales enriched in Dominican microbiomes or the Flavobacteriales from Montserrat are conferring antifungal protection, future research should aim to isolate pure cultures of these orders from MCF skin swabs and test isolates (ideally identified at species-level) in vitro for their ability to limit Bd growth, as in Woodhams et al. (2015). If any bacterial species can limit Bd growth, they would be a candidate for probiotic supplementation in Bd-susceptible MCFs (Kueneman et al. 2016).

Functional profiles varied between Dominican and Montserratian groups. MCFs in Dominica had higher abundances of pathways in the class siderophore biosynthesis relative to all Montserratian groups but September 2020. The siderophores being synthesised were aerobactin and enterobactin. It could not be confirmed that sampled Dominican frogs resist or survive Bd infection, as they had no detectable Bd infection at the time of sampling and no previous infection data (*Author's unpublished data* 2019). However, the fact that they exist in Bd-endemic areas and are old enough to have coexisted during documented infections within the local MCF populations leaves open the possibility that they may somehow avoid or limit Bd infection. Siderophore biosynthesis could be a potential mechanism for conferring protection against Bd infection or chytridiomycosis through resource competition for iron. Siderophore production has been documented in all of the differentially abundant orders in Dominican microbiomes (Cabaj and Kosakowska 2009; Tian et al. 2009)**.** Siderophores are molecules produced by bacteria to facilitate the uptake of environmental iron, an essential trace element for the survival of most organisms (Kramer et al. 2020). Siderophores can limit iron availability and in turn reduce the growth of pathogens (Kramer et al. 2020). Chaiharn et al. (2009) observed the antagonistic impact of siderophore-producing bacteria on four strains of pathogenic rice fungi, and proposed iron competition as a mechanism. Notably, the Bd genome has not been found to contain a candidate ferrichrome synthetase gene, responsible for the biosynthesis of siderophores in fungi (Bushley et al. 2008). Fungal species without siderophores may still possess the ability to uptake siderophore-chelated iron produced by other microbiota through the use of siderophore iron transporter (SIT) proteins (Misslinger et al. 2021). However, Bd does not have SIT gene orthologues either (Haas et al. 2008). Bd appears to rely just on reductive iron assimilation – the reduction of Fe^{3+} to Fe^{2+} – to allow iron uptake. This implies that Bd has limited strategies for iron uptake, which may render it vulnerable to being outcompeted within a microbial community rich in siderophore producers, such as that of these Dominican microbiomes. To further support this hypothesis, Longo (2022) found decreased abundance of siderophore production in Bd-infected coqui frogs (*Eleutherodactylus coqui*). Siderophores can also promote bacterial growth through producing chelated iron for non-siderophore producers, which in turn may promote a diverse and resilient

microbiome that is more robust against Bd colonisation (D'Onofrio et al. 2010). Despite this plausible hypothesis, the role of aerobactin and enterobactin siderophores in protection from Bd should be explicitly tested in Bd-growth inhibition assays.

The two next more commonly enriched pathways relative to Montserratian microbiomes were alcohol degradation and C1 compound utilisation pathways. C1 compound pathways include the fixation and oxidation of single-carbon molecules such as CO_2, methane, and methanol and are characteristic of methanotrophic bacteria (Aislabie et al. 2013). Methanotrophs are suited to volcanic soils and geothermally active regions, due to the presence of natural methane and the promotion of methane oxidation within the fine, porous soil (Aislabie et al. 2013). Dominica is a highly volcanic island, and the majority of samples were collected from Soufriere, an area with geothermal activity (Daltry 2002). Dominican microbiomes had relatively lower abundances of pathways in the classes of aromatic compounds and amino acid degradation compared with most Montserratian groups. Aromatic compound degradation related to several phenolic compounds (e.g. gallate, vanillin, protocatechuate) used by plants as a defence (Minatel et al. 2017) and compounds that arise mainly from anthropogenic pollution (nitro/chloroaromatic compounds, toluene and naphthalene) (Ju and Parales 2010). This is possibly linked to the exposure of captive-bred animals to an environment with new plants and a history of anthropogenic activity, demonstrating similar susceptibility of the microbiome to chemicals within the environment as suggested by Hughey et al. (2016).

Unexpectedly, Dominican MCFs held significantly lower proportions of Bd-inhibitory bacteria when compared with all Montserratian groups. This finding is counterintuitive, especially considering that several studies have found increased levels of Bd-inhibitory bacteria within groups that fare better against Bd (Bell et al. 2018; Jiménez et al. 2022). It is possible that this is due to the chance avoidance of infection by these individuals, removing the need for a Bd-inhibitory microbiome. If the Dominican frogs have encountered Bd, then perhaps the selective pressure for Bd-inhibitory capacity in the microbiome is reduced 20 years post-epizootic, when infection levels have been consistently low or negative for several years (M. Hudson, *unpublished data* 2014 - 2017). With at least four MCF generations since the epizootic, genetic adaptations could have arisen that confer protection from Bd infection, lessening the need for a Bd-inhibitory microbiome. Such adaptations could include selection for more potent antimicrobial peptide secretions, as in Voyles et al. (2018), or for adaptive immune factors such as those studied in Chapter Three of this thesis and linked to Bd resistance in other amphibians (Savage and Zamudio 2016). It may also be the case that the skin microbiome is not important for Bd infection survival in the MCF. Aside from biological interpretations of this finding, they might also be attributable to database biases. Just 1% of all the ASVs from this study could be matched to the database of Woodhams et al. (2015). Of the Bd-inhibitory sequences in the database, over 40% are from Panamanian isolates and none are from the Caribbean. If more ASVs from the MCF microbiome could be confirmed to be Bd-inhibitors or not, then the findings of this section would be more robust and the observed trends may well differ. Also, alpha diversity and Bd-inhibition were inversely linked. In a less diverse community, such as Montserrat, more reads are likely to be attributed to the lower number of taxa present due to the compositional nature of microbiome data (Gloor et al. 2017). A similar observation was made by Ellison et al. (2021) where high proportions of

Bd-inhibitory bacteria were associated with low alpha diversity, namely due to the presence of Burkholderiales, the 4th most common order in the database. In the case of the MCF, Montserratian samples had relatively high abundances of Flavobacteriales, the 3rd most common order in the database.

The Impact of Bd Infection and Itraconazole Treatment

A population of Bd-naïve MCFs bred from Montserratian stock were studied through Bd infection and itraconazole treatment to aid our understanding of what might have happened within the MCF skin microbiome during the initial epizootic. Alpha diversity was reduced three months following Bd infection and itraconazole treatment and did not return to levels seen pre-infection throughout the rest of the study. This could constitute a disturbance-induced dysbiosis, as taxa richness, evenness, and/or phylogenetic distances were reduced (Jani and Briggs 2014). Between pre- and post-infection and itraconazole time points, Flavobacteriales and Burkholderiales were reduced, while no taxa increased in relative abundance. These orders could therefore be vulnerable to direct disruption from Bd (Jani and Briggs 2014). They could also be impacted by an indirect effect of itraconazole treatment such as a disruption to the fungal mycobiome with which the bacterial microbiome interacts (Sam et al. 2017). The skin microbiome has been shown to modulate host immunity in mice, through provoking the production of regulatory T-cells (Scharschmidt et al. 2015). Likewise, skin microbiome structure has been noted as an important aspect of innate immunity in amphibians (reviewed in Rebollar et al. 2020). If MCFs infected with Bd during the initial epizootic experienced the same dysbiosis as in this study, then it is possible this contributed to their vulnerability to lethal Bd infection through a loss of innate immunity and possibly a reduced capacity to regulate other aspects of the host adaptive immune system.

The Montserratian MCF microbiomes also appeared susceptible to compositional changes following Bd infection and treatment and microbiomes did not return to the same structure or dispersion as pre-infection, even two years following the disturbance. The MCF microbiome may require longer than two years to recover pre-disturbance levels of structure and dispersion. Between August 2019 (pre-infection) and September 2020 (three months post-infection) the dispersion of communities was reduced following Bd infection and itraconazole exposure. Jani et al. (2021) also demonstrated that following treatment of Bd-infected frogs with itraconazole, skin microbiomes did not return to compositions comparable to control groups and community dispersion was reduced. Jani et al. (2021) hypothesised that the clearance of Bd leaves gaps in the microbiome, which are then filled by a similar set of bacteria with similar niches, leading to reduced dispersion. It is unfortunate that the impacts of Bd infection and itraconazole could not be untangled in this study. Jani et al. (2021) describe itraconazole treatment as a “second disturbance event”, following a Bd infection which has already diminished the resilience of microbiomes to the itraconazole disturbance. If this were found to be true, it would mean that itraconazole could possibly have long term detrimental impacts for hosts if it prevents microbiome recovery following Bd infection. It would be useful for future studies to explicitly test the impact of itraconazole on uninfected and Bd-infected microbiomes, so as to fully understand the impacts of this popular conservation intervention beyond its intended outcome of Bd clearance (Hudson et al. 2016b).

The reduction of Flavobacteriales and Burkholderiales seen between August 2019 and September 2020 coincided with a reduction in steroid and alcohol degradation, and to a lesser extent C1 compound utilisation. There are no details on which steroids or alcohols were available, so it is difficult to hypothesise how this may have affected MCF hosts after they were exposed to Bd and itraconazole. Just one pathway, secondary metabolite degradation, was increased after Bd infection and itraconazole exposure in September 2020. Secondary metabolites are classed as molecules that are not essential for growth but facilitate a bacterium's interaction with its environment (Seyedsayamdost 2019). Bacterial secondary metabolites often facilitate a defensive role, having antimicrobial or cytotoxic properties (Tyc et al. 2017). September 2020 was the only month to have this pathway enriched, indicating that at this point there was likely an increased abundance of secondary metabolites in the MCF microbiome. Without quantification or classification of secondary metabolites during the experiment, it cannot be said for sure to what extent they were increased or what their effect was likely to have been. However, it is possible that there was a defensive response from the MCF microbiome to either or both of Bd and itraconazole exposure via increased production of secondary metabolites or antimicrobial peptides, such as those observed in the microbiomes of other amphibian species (Brucker et al. 2008; Rollins-Smith 2009; Woodhams et al. 2018). Potential anti-Bd capacity was maintained through infection and treatment despite the loss of taxa, with the mean proportion of Bd-inhibitory bacteria being nearly identical in August 2019 and September 2020. As explained from a similar finding in newt skin microbiomes (Bletz et al. 2017), stability of Bd-inhibitory function despite changes in microbiome structure may be due to resilience of some ASVs and functional redundancy of others. As to whether the resilience of function in Montserratian microbiomes could be an adaptive feature, further study is needed. As all individuals were artificially cleared of Bd infection, it is not clear whether the maintenance of microbiome function was associated with increased survival or reduced infection intensity.

Seasonal Shifts in the MCF Microbiome

Season or associated climatic shifts impact the skin microbiome of amphibian species (Ruthsatz et al. 2020; Le Sage et al. 2021). Bacterial richness was negatively correlated with the mean temperature of the wettest quarter and positively correlated with the precipitation of the driest month in 71 species of tree frogs in Brazil's Atlantic forest (Ruthsatz et al. 2020). Similarly, amphibian skin microbiomes have been recorded as being less functionally rich in cool, dry seasons (Longo 2022). In the Montserratian cohort of MCFs, the transition from wet to dry season did not coincide with microbiome changes that were disproportionately large relative to other time point comparisons. The number and evenness of taxa within the Montserratian MCF's microbiomes were unchanged between September 2020 and February 2021, highlighting the larger influences of introduction to the wild or Bd infection compared to the onset of the dry season on alpha diversity. Beta diversity and dispersion were significantly different between September 2020 and February 2021, but this was the case for all pairwise time point comparisons within Montserrat, regardless of season. Season also explained only a small portion of MCF beta diversity variance compared to time point sampled. In keeping with this trend, microbiome predicted function remained relatively constant through the wet to dry season transition in MCFs, with just one differentially abundant pathway and no significant change in the proportion of Bd-inhibitory bacteria. This indicates that MCF microbiome structure and function do

not undergo large changes with the onset of the Montserratian dry season, in relation to what was observed in other months. This is based on the observation of just one year, however, and further samples from several more years would be needed to confirm this.

The stability of the MCF skin microbiome despite seasonal change could be a due to the reasonably similar seasons within a tropical climate compared to other studies in temperate regions (Le Sage et al. 2021). This is unlikely, as significant changes in both microbiome structure and function were observed in *E. coqui* in Puerto Rico, which has similar seasonal shifts to Montserrat (Longo and Zamudio 2017; Longo 2022). The observed stability in the Montserratian MCF's microbiomes could be due to the persistent suppression of microbiome diversity and function following a Bd and itraconazole-induced dysbiosis in the previous year (Jani et al. 2021). However, the apparent limited influence of seasonal change on the MCF microbiome is in contrast to what has been recorded in studies with similar sample sizes and several reviews, making it unlikely that seasonal variables have as little influence on the MCF skin microbiome as suggested by this study (Jiménez and Sommer 2017; Longo and Zamudio 2017; Woodhams et al. 2020; Le Sage et al. 2021; Longo 2022). The seasonal data in this study are based on broad classifications for Montserrat's climate (Hudson et al. 2019) whereas other studies have used more varied and precise climate data (Ruthsatz et al. 2020; Woodhams et al. 2020). Studies using WorldClim or BioClim data have recorded significant associations of microbiome change with climate variables relating to rainfall or temperature on a quarterly, monthly, or daily scale (Ruthsatz et al. 2020; Woodhams et al. 2020). Incorporating finer-scale climate data into this study would reveal how the MCF microbiome shifts with variables such as rainfall and temperature at different temporal scales. This information would help in making more robust conclusions around which microbiome changes are associated to Bd and itraconazole exposure/ release to the wild, and which changes are climate-driven. Finer-scale climate data could also help to explain the large functional shift observed between February and May 2021. Here, the largest number of metabolic pathways differed in abundance but no seasonal change or other (observable) disturbance occurred. May is at the end of the cool, dry season (Hudson et al. 2019) and it is possible that temperature and precipitation had begun to increase in May 2021, which might explain the large functional shift seen relative to February 2021 (Longo 2022).

Fully understanding the influence of weather or seasonality on the MCF microbiome will be important for conservation planning. Bd infection risk in Montserrat is seasonal (Hudson et al. 2019). Other studies of amphibian skin microbiomes have observed increases in the proportion of Bd-inhibitory bacteria (Le Sage et al. 2021) and diversity (Longo et al. 2015) during cooler seasons with higher Bd infection levels or risk. Just as uncovering seasonal patterns in disease risk helps to plan MCF reintroductions (Hudson et al. 2019), information on the seasonal shifts in the MCF microbiome's predicted capacity to be resilient to Bd infection should increase the chances of successful future reintroductions of MCFs to the wild (Adams et al. 2014). The Montserrat enclosure is equipped with climate data loggers which record rainfall and temperature (M. Hudson, *pers. comm*.). Unfortunately, site-specific temperature and precipitation data from these loggers were not available for all months of this experiment, but further study of the population should aim to include the site-specific

precipitation and temperature data. Additionally, BioClim data could be used to equate analyses to that of other amphibian microbiome studies (Ruthsatz et al. 2020).

The Impact of Reintroduction

Finally, the microbiome was studied prior to, and one month following, release to a semi-wild enclosure. This comparison provided an insight into the process of 'microbiome rewilding', additional information which may be of use for conservation managers planning future reintroductions (Adams et al. 2014). One month following release, the microbiome of MCFs increased in diversity. Both alpha diversity metrics were significantly increased, likely due to increased recruitment of bacteria from a more diverse microbial reservoir in the semi-wild enclosure than biosecure enclosures (Loudon et al. 2014). Beta dispersion increased following release, indicating that there was individual-level variance in the recruitment of bacterial taxa to the skin. The beta diversity in August 2019 was comparable to that of wild frogs in Dominica, showing that MCF microbiomes can quickly be rewilded. This is the same finding as Estrada et al. (2022), where skin microbiomes of captive bred *Atelopus limosus* regained diversity comparable to wild populations after a month in a wild environment. The highest number of differentially abundant taxa (22) was also found in the comparison of pre- and post-release groups. This agrees with a review by Kueneman et al. (2022), where 95% of the studies showed an increased dispersion in wild compared with captive population skin microbiomes. Increased skin microbial diversity can be beneficial for the host and bolster defences against Bd (Piovia-Scott et al. 2017; Ellison et al. 2019). Following this evidence, the jump in diversity following release to the semi-wild enclosure should have increased defences against Bd through having a more resilient microbial community and/or higher Bd-inhibitory capacity. However, the increased microbial diversity was not enough to protect the population from chytridiomycosis, which was detected eight months post-release. Increased diversity in August 2019 did not translate into an increased abundance of Bd-inhibitory taxa – which in fact declined significantly relative to pre-release levels. This could be because there was no selective pressure to inhibit Bd in a Bd-naïve population (Bletz et al. 2017). It is also possible that microbiome diversity decreased during the un-sampled period between August 2019 and Bd infection and this led to increased vulnerability to infection (Ellison et al. 2019). Five metabolic pathways were reduced following release, possibly from the disruption to pathways from recruitment of new community members (Argüello et al. 2018). The likely impact of these reductions on the host is unclear. This may also indicate the differing functional requirements for or capacity of the microbiome in the wild and captivity, as demonstrated in a study of 18 amphibian species where functional capacities were altered between wild and captive populations (Kueneman et al. 2022). Just one metabolic pathway was enriched in August 2019: the utilisation/assimilation of C1 compounds. This could be due to reintroduction to the volcanic soils of Montserrat (Daltry 2002; Aislabie et al. 2013).

Reintroductions to the wild replenished the MCFs' skin microbiome, presumably from environmental reservoirs (Loudon et al. 2014). This may be of interest to conservationists interested in micro/holobiome rewilding, especially if increased microbiome diversity can be more definitively linked to fitness in the MCF (Bahrndorff et al. 2016). Crucially, the rewilding of the Montserratian MCFs microbiomes did not protect them from Bd infection and chytridiomycosis, the biggest threat to their

persistence in the wild. This has been observed in captive bred *A. limosus*, which was still susceptible to Bd infection even when its skin bacterial community was replenished to comparable levels to the wild (Estrada et al. 2022). For the Montserratian MCF, these findings imply that factors other than microbiome diversity may be relevant for developing strategies to mitigate chytridiomycosis. These factors could include probiotics using beneficial bacteria from the microbiomes of surviving wild MCFs, if they could be proven to inhibit Bd growth or prevent lethal infection. It is also possible that the skin microbiome is not relevant for Bd infection protection in the Montserratian MCF, and in this case the presence of protective host genotypes in the population or the manipulation of the environment to be unfavourable for Bd may be other useful strategies to implement (Becker et al. 2017b; Jani and Briggs 2018; Basanta et al. 2022). These factors will likely work synergistically in a 'disease pyramid' to determine Bd infection outcome (Bernardo-Cravo et al. 2020).

Conclusion

This study provides the first characterisation of the skin microbiome of the MCF, delivering new insights into the possible dynamics and determinants of Bd infection outcome in the species. Samples collected from wild populations that have persisted despite a Bd epizootic reveal more diverse bacterial skin communities than MCFs released to Montserrat from captivity, both before and after their exposure to Bd. These diverse communities may provide resilience in the face of Bd-induced dysbiosis. Particular taxa, such as Micrococcales, and metabolic pathways such as siderophore biosynthesis could plausibly defend against Bd infection and these microbiome elements warrant further investigations to aid microbiome-centred conservation strategies. The low proportions of bacteria listed as Bd-inhibitory in the Dominican microbiomes may be due to a lack of selective pressure from low or no Bd infections in the remaining Dominican population. Continued Bd monitoring in Dominica is important to better understand the Bd-tolerance levels of the surviving wild population and contextualise any future microbiome studies. Bd-naïve, Montserratian individuals were vulnerable to a dysbiosis in their microbiome following Bd infection and itraconazole treatment. Despite the changes in community composition, predicted antifungal capacity was maintained, indicating that functional redundancy can exist within the Montserratian MCF microbiome. Microbiome dysbiosis could have contributed to the vulnerability of many MCFs to lethal chytridiomycosis during the initial epizootic, while functional redundancy may have protected some individuals, maintaining antifungal function despite alterations in taxa abundances and identities. Season was not found to greatly impact the Montserratian MCF's microbiomes, but more precise climate data are needed to revisit this finding. The long-term goal of the MCF recovery programme is to reintroduce populations to the wild. This study shows that host reintroductions can also achieve the reintroduction of the host skin microbiome, as diversity levels rapidly increased with release to the wild. Microbiome rewilding did not protect MCFs from chytridiomycosis, although whether infections would have been lethal was not possible to determine. Conservation of the Montserratian MCF will therefore most likely require a multifaceted approach, considering aspects beyond microbiome diversity such as probiotic supplementation, host genetics, and the environment.

Chapter Five

Know Your Enemy: A Genetic Assessment of *Batrachochytrium dendrobatidis* Implicated in the Decline of the Mountain Chicken Frog

Abstract

The mountain chicken frog (*Leptodactylus fallax,* MCF) is critically endangered, largely due to mass die-offs from chytridiomycosis caused by the fungal pathogen *Batrachochytrium dendrobatidis* (Bd). Efforts to track the chytridiomycosis epizootic from its beginnings in Dominica in 2002 and Montserrat in 2009, to the present day, have included regular sampling of amphibians on both islands to detect the presence of Bd. Consequently, a genetic archive of Bd DNA exists - spanning the epizootic across space, time, and different amphibian hosts. Recent methodological advances have obviated the need for cultured Bd isolates for genomic studies, and swab-collected Bd DNA held in the existing archive may now be used. Using 191 DNA sequences and their associated polymorphisms in the Bd genome, this study re-examined the decline of the MCF through a pathogen-focused, genetic lens. Analysing 92 Bd samples from across the years 2002 – 2020, from Dominica and Montserrat, and three amphibian host species (including the MCF) showed that a single genetic lineage of Bd drove the decline of the MCF. Phylogenetic analysis revealed this lineage to be the hypervirulent BdGPL. Genetic analysis of the Bd samples detected no population structure, low diversity, and signals of population expansion across the dataset. This genetic pattern points to a continuous, clonal radiation of Bd throughout the amphibian community of Dominica and Montserrat from a possible single point of origin in Dominica. With no change in pathogen lineage, diversity, or genetic structure, it is more likely that surviving MCFs have persisted due to host and/or environmental changes in the disease triangle dynamic - an important revelation for MCF conservationists.

Introduction

Increasing rates of amphibian declines have been recorded globally since the 1970's (Fisher and Garner 2020). A driving factor in many of these declines is the infection of amphibian hosts by the chytrid fungus *Batrachochytrium dendrobatidis* (Bd), often leading to the development of the disease chytridiomycosis. A recent meta-analysis revealed that at least 6.5% of all amphibian species have declined due to chytridiomycosis, with 90 species now presumed extinct after being overwhelmed by the disease (Scheele et al. 2019a). Faced with the task of understanding and mitigating the impacts of chytridiomycosis, research has focused on developing diagnostic and epidemiological tools to track and characterise this panzootic. The most widely used method to establish the presence of Bd is that of Boyle et al. (2004). This method employs qPCR primers that amplify the internal transcribed spacer (ITS) region in Bd's genome and determines infection load, measured in genomic equivalents. This method of qPCR can produce results from environmental, skin swab, or tissue samples relatively easily (Kirshtein et al. 2007). Following global efforts to identify the presence of Bd, it has been found in all continents besides Antarctica (Fisher et al. 2009b). While qPCR has advanced our understanding of the spread of Bd, it cannot distinguish between the different lineages of Bd which exist (Schoch et al. 2012; O'Hanlon et al. 2018). To fully understand the dynamics and spread of the Bd panzootic there is a need to know where Bd exists, but also where the different Bd lineages are.

The most recent and extensive effort to sequence whole Bd genomes sourced hundreds of isolates from around the globe and from all amphibian orders and continents (O'Hanlon et al. 2018). This study revealed five major Bd lineages, named according to the location to which they are endemic (i.e. the location where they commonly occur): BdGPL – Global pandemic/panzootic lineage, BdCAPE – South Africa, BdCH - Switzerland, BdBRAZIL/BdASIA-2 – Brazil and Korea (introduced to Brazil and then back to Korea via trade), and BdASIA-1. A subsequent study by Byrne et al. (2019) revealed the presence of another Asian lineage – BdASIA-3. The most virulent of these lineages is BdGPL, although BdCAPE has also been implicated in amphibian population declines (Ghosh et al. 2020). The current consensus is that multiple Bd lineages emerged from an ancestor in the Korean peninsula. BdGPL is predicted to have spread globally with the expansion of worldwide trade from the ~1900's onwards and is formed of two subclades, BdGPL-1 and BdGPL-2 (Rosenblum et al. 2013). BdGPL-1 is restricted to North and Central America, and BdGPL-2 is more globally distributed (Schloegel et al. 2012; Basanta et al. 2021).

Distinguishing between lineages is important because there are documented differences among lineages in their ability to cause disease in amphibians. For example, lineages that are endemic to a region, such as BdBRAZIL and ASIA-1, are known to co-exist with native amphibians without causing significant population declines (Becker et al. 2017a). Becker et al. (2017a) found that these lineages can differ in virulence, and that lineages besides BdGPL can cause mortality when they are introduced to naïve hosts situated outside of the endemic range of the pathogen. Where lineages co-exist, and co-infect hosts, Bd has the ability to recombine, forming outcrossed variants, which may benefit from the loss of deleterious alleles and increased genetic variation associated with an increased ability to cause disease (Heitman 2010; Fisher and Garner 2020). Co-infection itself, without recombination, may also lead to more severe chytridiomycosis due to competitive interactions between lineages infecting a single host. Thus, the possibility of more virulent recombinants exists wherever more than

one Bd lineage is present, such was the case when BdGPL and BdBRAZIL recombined into a more virulent recombinant (Greenspan et al. 2018).

Until recently, the only reliable way to determine Bd lineage was to perform whole genome sequencing on a high quality sample, sourced from a cultured isolate (Byrne et al. 2016). Culturing Bd is technically difficult, and whole genome sequencing of large numbers of individuals is expensive. Alternative methods involve genotyping Bd samples at ten loci to perform multi-locus sequence typing (Morehouse et al. 2003), but studies have shown that this method underestimates the diversity and divergence of Bd around the world (Farrer et al. 2011; Rosenblum et al. 2013; O'Hanlon et al. 2018). Ghosh et al. (2020) recently developed a lineage-specific qPCR assay based on mitochondrial DNA to detect BdGPL and BdCAPE – the two lineages of Bd most commonly associated with chytridiomycosis in wild populations. However, this test cannot be used to detect any other lineage. Byrne et al. (2017) devised a method for genotyping Bd samples that can determine lineages with comparable efficiency to whole-genome data and is suitable for the low concentrations and qualities of Bd DNA often isolated from swabs. This method is based on a microfluidic amplification of many Bd genomic regions (targets) and multiple samples simultaneously: 191 targets in the Bd genome and one diagnostic target for the related *B. salamandrivorans*.

The mountain chicken frog (*Leptodactylus fallax*, MCF) has been decimated by a chytridiomycosis epizootic. The outbreak was detected first in Dominica from 2002, and in Montserrat from 2009 (Hudson et al. 2016a). Skin swabs from live animals and tissue samples from post-mortem examinations have been routinely collected from MCFs and sympatric amphibian species since the onset of the chytridiomycosis epizootic in Dominica and Montserrat to track Bd infection loads using qPCR (Boyle et al. 2004; Hudson et al. 2019). Bd sampling has also been regularly undertaken as part of a semi-wild release of captive-bred MCFs in Montserrat from 2019. All Bd samples have been archived and may now be repurposed for understanding not only infection load, but also infection genotype with the genotyping method suitable for swab-sourced DNA (Byrne et al. 2017). Genotyping of Bd strains sourced from swab samples has been used to reveal previously unknown distributions of Bd lineages, cryptic diversity, and potential hybridisation between lineages (Byrne et al. 2019; Basanta et al. 2021; Byrne et al. 2022). To date, it has not been applied to an archive such as that of the mountain chicken recovery programme, where an entire, single disease epizootic can be traced through time, geographic location, and host species.

Aims

It is currently believed that the Bd outbreak that decimated the MCF arrived to Montserrat from Dominica (Adams et al. 2014; Hudson et al. 2016a). We also know Bd is maintained by reservoir amphibian hosts on both islands (Hudson et al. 2019). One Bd isolate has been produced from Montserrat and has been determined to be BdGPL (Byrne et al. 2019). Beyond this, we do not know anything about the genetic structure or diversity of the pathogen implicated in the decline of the MCF. Understanding these factors is fundamental to providing a fuller picture of the pathogen-related determinants of survival from Bd infection in the MCF. This study aims to address these knowledge gaps by genotyping Bd samples from across time and space in the epizootic that devastated the MCF. Using the recently developed method of Byrne et al. (2017), this study will aim to assign archived Bd

samples to one of six global Bd lineages and it is hypothesised that at least BdGPL will be present due to the sample already genotyped as such from Montserrat. The polymorphisms within the studied Bd loci will be used to study the genetic diversity and structure of the invading pathogen through geographic location, time, and different amphibian hosts present in Dominica and Montserrat. This new information will hopefully shed light on the dynamics of the pathogen invasion and help to provide evidence for or against the current hypothesis that Bd arrived to Montserrat from Dominica. Currently, only three samples of Bd have been genotyped to lineage level from the Caribbean, and only one of these in the Lesser Antilles (Byrne et al. 2019). This study will provide a greater understanding of Bd in an area greatly in need of more Bd research due to the number of threatened, endemic amphibian species found there (Scheele et al. 2019a).

Methods

Sample Collection and Selection

Archived Bd DNA extracts collected during the mountain chicken recovery program, and stored at the Institute of Zoology, London, were used in this study. Only Bd-positive samples with complete information for location, date, and host species were considered. Samples were selected from this archive subset so as to represent each sampling location and year in the dataset and to maintain as even sampling across groups as possible (Table 5.1). In total, 92 samples remained after selection criteria were applied (Table 5.1). Samples with a Bd load >150 genomic equivalents (GE) were preferentially selected for inclusion as this load yields sufficient coverage for a robust analysis in the Fluidigm assay (Byrne et al. 2017). Five samples with GE < 150 were included to avoid biases associated with only studying high load samples (Byrne et al. 2017). This number of low-load samples (5% of total) was chosen as a compromise between addressing method biases and producing usable data from an expensive assay with irreplaceable samples. Improved coverage from swab-collected Bd DNA has been observed following a DNA concentration and isopropanol precipitation step, but the volumes of Bd DNA remaining in the archive samples (often < 30 µl) were too low to attain the sufficient concentrations required, from 100 µl to 15 µl (A. Byrne, *pers. comm.*). Selected DNA samples had concentrations from 0.2 - 292 ng/µl. All samples were previously extracted from either swabs or tissue samples using the PrepMan Ultra method (Hyatt et al. 2007) with modifications described in (Hudson et al. 2019). GE levels were determined using qPCR (Boyle et al. 2004). Sixteen samples were of Dominican origin and 76 were from Montserrat. Bd samples isolated from MCFs numbered 66, while 26 came from sympatric amphibian species *Rhinella marina* (n = 4) and *Eleutherodactylus johnstonei* (n = 22). A breakdown of samples per year, country, and host species is shown in Table 5.1. A narrower spread of years and species variation was selected for Dominica than Montserrat, because fewer samples had originally been taken, fewer had high enough Bd loads, and some were not found in the archive (Table 5.1). Full details of samples can be found in supplementary Table S5.1.

Table 5.1: Overview of Bd sample sources included in the study. The overall count (N) for each year is listed in bold. Each year total is subdivided into a count of samples per country and per host species.

Year, Country, and Host Species Represented	N
2003	**4**
Dominica	4
Leptodactylus fallax	4
2009	**17**
Montserrat	17
Eleutherodactylus johnstonei	4
Leptodactylus fallax	9
Rhinella marina	4
2011	**14**
Montserrat	14
Eleutherodactylus johnstonei	5
Leptodactylus fallax	9
2012	**5**
Montserrat	5
Eleutherodactylus johnstonei	3
Leptodactylus fallax	2
2013	**8**
Montserrat	8
Eleutherodactylus johnstonei	6
Leptodactylus fallax	2
2014	**22**
Dominica	6
Leptodactylus fallax	6
Montserrat	16
Eleutherodactylus johnstonei	2
Leptodactylus fallax	14
2015	**11**
Dominica	6
Leptodactylus fallax	6
Montserrat	5
Eleutherodactylus johnstonei	2
Leptodactylus fallax	3
2020	**11**
Montserrat	11
Leptodactylus fallax	11
Total	**92**

Target Loci Amplification and Sequencing

Samples were genotyped at 186 loci in the Bd nuclear genome, five loci in the Bd mitochondrial genome, and one locus specific to *B. salamandrivorans* (for primers, pools and genomic targets, see supplementary Table S5.2). The 191 Bd-specific loci are able to distinguish the major lineages of Bd by targeting informative regions located in all chromosomes of the Bd genome (Byrne et al. 2017). Each target locus is between 150-200 bases long and may contain some or no single nucleotide polymorphisms (SNPs) relative to other samples. Two pools of primers were used to perform a pre-amplification step necessary to increase target DNA from the low starting concentrations of DNA present in the samples (0.2-292 ng/µl). Pre-amplification as per Byrne et al. (2017) was carried out at the Genome Centre, Blizard Institute, Queen Mary University London. Genotyping of pre-amplified products was carried out using a Fluidigm Access Array 48.48 system. Target primers with Fluidigm custom sequence (CS) tag prefixes were arranged in 48 pools of four primer pairs and loaded with 48 pre-amplified DNA samples at a time (supplementary Table S5.2). Fluidigm CS-tags enable binding of the primers to sequencing adapters or barcodes, which are added during PCR and enable downstream sample identification. Product sizes and concentrations were checked using a DNA D1000 TapeStation and Qubit before being loaded onto an Illumina MiSeq for a v2 Micro paired-end 150 bp run, using single-indexing barcodes to identify samples.

Data Processing and Consensus Sequence Generation

Reads were demultiplexed according to unique sample Illumina Index at the Blizard Institute Genome Centre. Per-sample forward and reverse reads were then merged using FLASH2 (Magoc and Salzberg 2011) allowing for a maximum overlap of 150 bp, based on the 2x150 bp Illumina cycle and fragment lengths predicted to be between 150 and 200 bp long. Mismatch density was set to 0.3, while all other settings were left as default. Reads were demultiplexed once more, according to the primer sequences of each 192 specific loci, using cutadapt v.3.4 (Martin 2011). Partial primer matches were allowed at the end of reads. An error rate of 3.0 was set to allow for up to three mismatches in primers up to 27 bases long. In this step, primers were removed from the reads and any short reads (< 90 bases) were discarded. To align reads and produce consensus sequences, each set of processed reads produced for each sample and locus were mapped to the relevant reference locus taken from the reference genome of Bd isolate JEL423 (NCBI BioProject reference PRJNA13653). Mapping was performed using BWA-mem (Li 2013) for single end reads. Subsequent bam files were sorted by Bd reference genome coordinate, PCR duplicates were removed, and reads with a mapping quality lower than 20 were discarded. A reference-free consensus sequence for each locus was produced using sam2consensus (https://github.com/edgardomortiz/sam2consensus). Consensus loci including IUPAC ambiguity bases were produced at a threshold of 97%, ensuring variants were present in at least 3% of reads and at a minimum coverage of three. This coverage was selected as the sequencing data were of mixed quality and this threshold maximised the amount of data for analysis while still eliminating rare sequences most likely to be artefacts.

Bd Lineage Representative Locus Generation

To allow assignment of newly sequenced samples to a lineage, it was necessary to generate 191 comparable loci from global Bd lineage representatives. Alongside the existing references from BdGPL

lineage JEL423 (Byrne et al. 2017), 16 isolates were selected, covering BdASIA-1 (n=3), BdASIA-2/Brazil (n=3), BdCAPE (n=3), BdCH (n=1), one hybrid isolate (expected BdGPL/BdCAPE), and isolates from both the recently identified sub-lineages of BdGPL: BdGPL-1 (n=2) and BdGPL-2 (n=2) (Basanta et al. 2021). One isolate had not been identified as either sub-lineage of BdGPL but was included as it was collected from Montserrat and therefore relevant to this study. For details of included lineage representatives see supplementary Table S5.1. Raw SRA files were downloaded from NCBI and converted to fastq format using prefetch and fastqdump (http://ncbi.github.io/sra-tools/SRA Development Team). Raw reads were cleaned of adapters and filtered for phred score quality >20 using seqyclean v.1.10.09 (Zhbannikov et al. 2017), before being aligned to the whole genome of JEL423 using BWA-mem (Li 2013). Reads were sorted and duplicates marked using picard v.2.20.8 (https://github.com/broadinstitute/picard). GATK v.3.8.1 RealignerTargetCreator and IndelRealigner realigned reads around indels (Auwera et al. 2013). Samtools v.1.10 was used to extract all reads mapping to the genomic coordinates of the reference loci, plus 1,500 bp either side (Li et al. 2009). Extended consensus sequences were produced from these reads, in the same way as for the Fluidigm data, using sam2consensus, but this time setting the threshold consensus to 75% and minimum coverage to one, to replicate the methods used by Byrne et al. (2019). Blastn v. 2.10 was used to determine the exact position of the consensus fasta that formed the target locus, and the position coordinates were made into a bed file. The getfasta tool in bedtools v.2.29.1 was used to extract the portion of each extended consensus that corresponded to the target locus.

Lineage Assignment

Species phylogenies were generated from multiple gene tree inputs. Due to the presence of missing data, a gene to species tree method was used as it has a higher tolerance to missing data than species trees created directly from concatenated loci (Xi et al. 2016). For each of the 191 Bd-specific loci, consensus sequences were aligned in Geneious prime using the MUSCLE plugin. A gene tree was produced from each locus alignment using the RAxML plugin for rapid bootstrapping with 100 bootstraps and using a generalised time reversible (GTR) gamma substitution model. The best maximum likelihood tree was produced, as indicated to be the preferable way to generate input gene trees (Mirarab et al. 2016). Tree Collapser v.4 (http://emmahodcroft.com/TreeCollapseCL.html) was used to collapse branches with very low bootstrap support (< 10). Gene trees were inputted to Astral-III (Zhang et al. 2018) to produce a species tree, in which all branches with a local posterior probability of < 0.7 were collapsed using Tree Collapser. Trees were edited using FigTree v.1.4.4 to add clarity to sample and branch labels or support values. Molloy and Warnow (2018) demonstrated that filtering datasets for genes due to missing data has either a neutral or detrimental effect on tree estimation error. This dataset has relatively high levels of missing data (~50%). To assess the impact of missing data on lineage assignment, four species trees were generated with levels of missing data tolerance ranging from strict to relaxed (Table 5.2). The most relaxed tree was created using all data present – any locus was included if its consensus was generated at >3x coverage and its variants present in at least 3% reads, and samples with data for at least one locus were included. Three more trees were created with stricter thresholds for missing data. Here, samples were included if they had at least three loci present, and one of three locus data thresholds applied. These thresholds required loci to have either >33% of sample data present, >50% present, or 66% present. The strictest data inclusion

threshold (>66% of sample data) matches that of Byrne et al. (2019). Xi et al. (2016) concluded that missing data up to 50% had little effect on phylogenetic assessment of data with >25 genes, as long as the missing data were randomly distributed across the genome. As the data from this study are missing in a subset of samples, phylogenetic decisiveness in ~90% of trees may be expected compared with 100% decisiveness in randomly distributed missing data (Xi et al. 2016). Final species trees were made of 184 gene trees (most relaxed constraints), 71 gene trees (>33% sample data per locus), 11 gene trees (>50% sample data per locus), or five gene trees (>66% sample data per locus) (Table 5.2).

Table 5.2: Overview of the data inclusion / missingness thresholds for species tree generation. Species trees range from most relaxed (1) to most stringent (4).

Species Tree No.	Locus Inclusion Threshold	No. Loci Passing Threshold	Sample Data Inclusion Threshold	No. Samples Passing Threshold	Able to Distinguish Bd Lineages?
1	Consensus present at ≥3x coverage and in ≥3% of reads **AND** any % of samples represented	184	At least 1 locus represented	73	Yes
2	Consensus present at ≥3x coverage and in ≥3% of reads **AND** >33% of samples represented	71	At least 3 loci represented	64	Yes
3	Consensus present at ≥3x coverage and in ≥3% of reads **AND** >50% of samples represented	11	At least 3 loci represented	64	Yes
4	Consensus present at ≥3x coverage and in ≥3% of reads **AND** >66% of samples represented	5	At least 3 loci represented	64	No

Analysis of Genetic Structure and Diversity

The polymorphisms from within the 191 loci sequences were also used in an analysis of population genetics. To generate sample level variants for use in this analysis, raw reads were processed in the same way as for the phylogenetic analysis, except for the isolation of individual locus sequence regions. Merged reads were aligned to the reference genome JEL423 using BWA mem, but without being demultiplexed by locus first as done for the sections above. This approach was used to enable the creation of a single VCF file which could be subsetted later, as opposed to dealing with 191 VCF files per individual (i.e. one per Bd genomic target region). Haplotype-based variants were called across all samples and the entire reference genome using FreeBayes (Garrison and Marth 2012). The resulting VCF file was then subsetted using bcftools v.1.10.2 to include only the Bd genomic regions corresponding to the reference loci used in the Fluidigm assay. The presence of missing data was assessed in the dataset and suitable filters were applied to remove low quality variants, and sites or individuals with a high amount of missing data (Rothstein et al. 2021). Variants were filtered using

vcftools v.0.1.16 to retain variants supported by a depth >3, phred quality scores >30, and genotypes with no more than 50% missing data. Individuals with >70% missing data were also removed from the dataset. Due to the positional design of the loci along the Bd genome, some SNPs may be linked (Byrne et al. 2017), which could confound estimations of population structure if linkage is strong (Falush et al. 2003). The extent of linkage disequilibrium in the dataset was assessed, and SNPs were pruned at a stringent level of r^2=0.1 to compare pruned and unpruned data. VCF files containing SNPs were converted for use in ADMIXTURE using Plink v.1.9, where PCA eigenvectors and eigenvalues were also estimated (Purcell et al. 2007). ADMIXTURE (Alexander and Lange 2011) was run for values of K (the number of genetic clusters in the data) from 2-10 and a cross validation level of 20. Results were plotted using the StructuRly web app (Criscuolo and Angelini 2020). Pairwise F_{ST} was calculated using the R package Hierfstat (Goudet 2005) between genetic clusters and groups of samples according to country, year, and host species. Significance of pairwise F_{ST} values was assessed using the "boot.ppfst" function using 1,000 bootstrap replicates to identify whether observed F_{ST} values fell within 2.5% and 97.5% confidence intervals. DNAsp v6 (Rozas et al. 2017) was used to generate divergence and polymorphism statistics. Nucleotide diversity (π), Tajima's D, and Watterson's theta were estimated for groups defined as country, year, or host species. Other tests of neutrality, such as Fu's FS and Ramos-Onsins Rozas's R2, were not investigated as they require phased genotypes – and these are not outputted from FreeBayes (Rozas et al. 2017). Individual levels of nucleotide diversity were assessed alongside mean genomic quantity of Bd per sample using a linear regression in R statistical software.

Results

Lineage Assignment

After read processing and quality filtering, the average number of reads per locus, per sample, was 413 for inclusion in phylogenetic analysis across 92 samples (supplementary Figure S5.1). The indicator locus included for *B. salamandrivorans* returned no reads, as expected. Out of the 191 Bd loci targeted, an average of 71 loci were amplified per sample (coverage $\geq$1), or 41 when coverage was $\geq$3 (supplementary Figure S5.1). Starting quantities of DNA, measured as mean Bd GE from qPCR, appeared to have a non-linear relationship to assay success (measured as either: the total sample reads passing filters, the average number of these reads per locus, or the number of loci amplified above a depth of 3, Figure 5.1, supplementary Figure S5.2). The total amount of Bd appeared to associate with better assay performance from $Log_{10}(0 - 5)$ GE (Figure 5.1). After this point the relationship appeared to begin to plateau or even decline, but the decline appeared to be driven by one sample with a high Bd load but low assay success (supplementary Figure S5.2). There were 18 samples that had a co-occurrence of high Bd load and low assay success and conversely two samples had high assay success with low Bd load (Figure 5.1). Figure 5.1 shows the number of loci passing the quality/coverage threshold against log Bd GE, with the outlier sample removed. A LOESS smoothing curve is fitted to the data using a span of 0.75 and degree of polynomial fit as two.

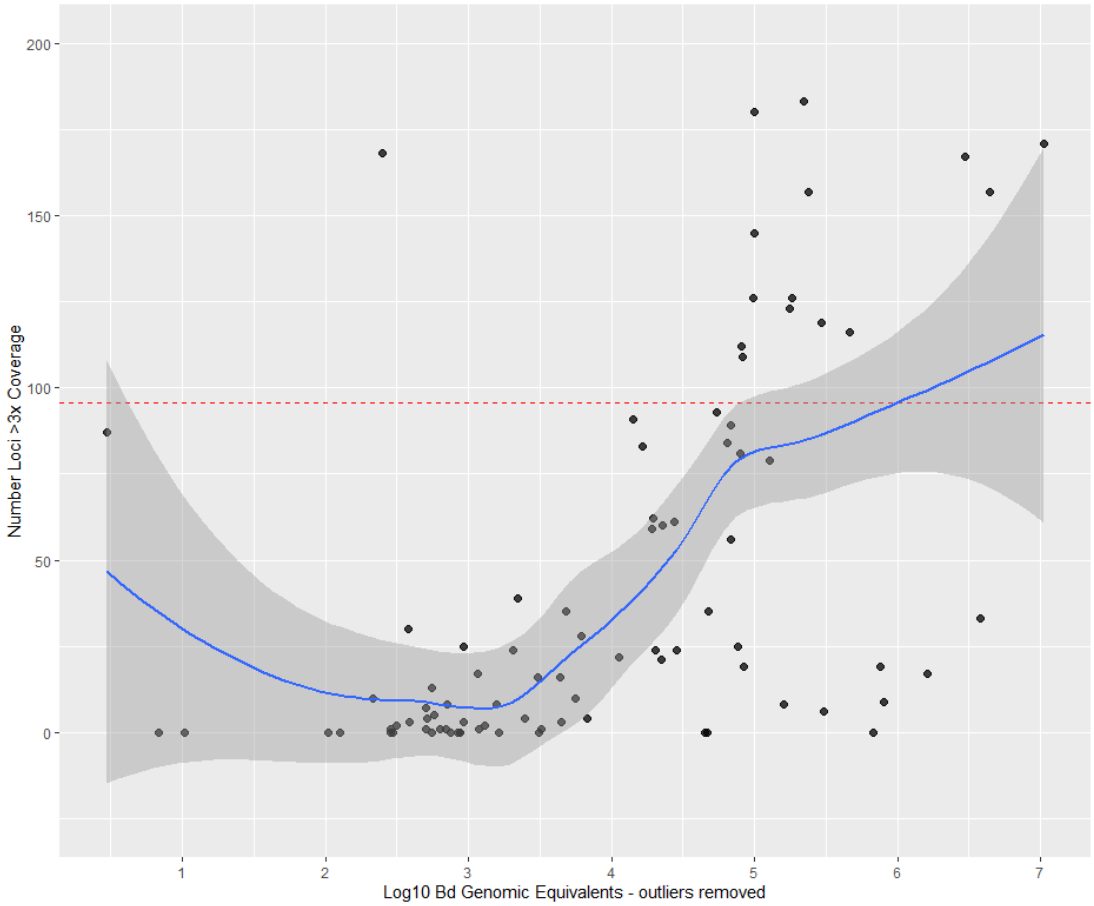

Figure 5.1: Number of Bd loci (of a possible 191) amplified beyond a coverage threshold of 3, and initial log-transformed Bd genomic equivalents measured for each sample. A Loess curve with span 0.75 is fitted. Cut off for a high performing assay is denoted as 95.5 loci (50% loci) shown in red.

Seven gene trees (loci AB77, AB130, AB140, AB145, AB160, AB184, AB185) were discarded from the analysis, as they had zero bootstrap support throughout, leaving 184 gene trees for input to the species trees (Table 5.2). Four species trees were generated with different levels of missingness tolerance, and each tree differed in its ability to delineate Bd samples within the global lineage phylogeny (Table 5.2). Species trees had a normalised quartet score ranging from 0.69 - 0.88, increasing as the number of input gene trees reduced. The normalised quartet score denotes the proportion of input gene quartet trees satisfied by the species tree – a measure of discordance between gene and species trees, with higher numbers meaning less discordance.

The most relaxed species tree (Figure 5.2) included all samples and loci that passed the consensus sequence threshold: 73 Fluidigm-generated samples from Dominica and Montserrat, 16 whole-genome extracted samples from all global lineages, and 184 gene trees (Table 5.2). This tree, species tree 1, could distinguish between major Bd lineages, with each lineage forming its own clade (Figure 5.2). Furthermore, a division was evident between the subclades of BdGPL-1 and -2. All Bd samples taken for this study were grouped in the BdGPL-2 clade, according to species tree 1 (Figure 5.2). Species tree 2 applied additional thresholds to samples and loci, stating that each sample must represent at least three loci and that each locus must represent at least 33% of sample data (Table 5.2). As a result, this tree only included 64 samples and 71 loci. This reduction in data did not change the major conclusions drawn (Figure 5.3). Again, global lineages were separated into clades, the division of BdGPL subclades was evident, and Bd samples from this study were assigned to BdGPL-2 (Figure 5.3).

The resolution of the species tree was reduced when only loci representing 50% of sample data (n = 11) were included for species tree 3 (Table 5.2, Figure 5.4). While species tree 3 could separate global lineages, the BdGPL-1 and -2 division was not observed (Figure 5.4). Species tree 3 also could not distinguish the hybrid Bd lineage from BdGPL. Similarly to species trees 1 and 2, Bd samples from Dominica and Montserrat grouped together, this time in a clade with the entire BdGPL lineage (Figure 5.4). In species tree 3, where the number of input gene trees were drastically reduced in favour of fewer missing data (n = 11), known members of GPL-1, GPL-2, and a hybrid lineage formed a single clade with the Dominican and Montserratian samples. In the strictest tree (Figure 5.5), formed only of 5 gene trees (Table 5.2), global Bd lineages were not clearly distinguishable from one another, except for BdASIA-2/BRAZIL (Figure 5.5).

Further clustering within the BdGPL clade was seen in all trees except tree 4 (Figures 5.2 - 5.5). Source country, year, host species, or genetic diversity did not explain why certain samples appeared divergent from the main GPL clade. Additionally, different numbers of samples split from the main clade across trees, with the number of sub-clades increasing as the number of input gene trees decreased. Samples M14-0436 and M15-0744 formed a clade in trees 1 and 2, but not in tree 3. The same was observed for samples M12-0976 and M09-994. All of these samples had relatively high amplification success (89 – 171 loci), however many samples with lower amplification success also formed subclades. It appears that the apparent divergence of samples across trees may be due to how many, and which loci, have been included in the species tree. As noted by Huang and Knowles (2016), some loci are more phylogenetically informative than others. There was no evidence in any tree of a

separation of samples from Dominica or Montserrat, or between these samples that had been taken in different years of the chytridiomycosis epizootic in either country (Figures 5.2 - 5.5). Based on the results from trees which could distinguish global lineages from one another, species trees 1 – 3, it is most probable that the Bd lineage responsible for the outbreak in Dominica and Montserrat is BdGPL, specifically BdGPL-2.

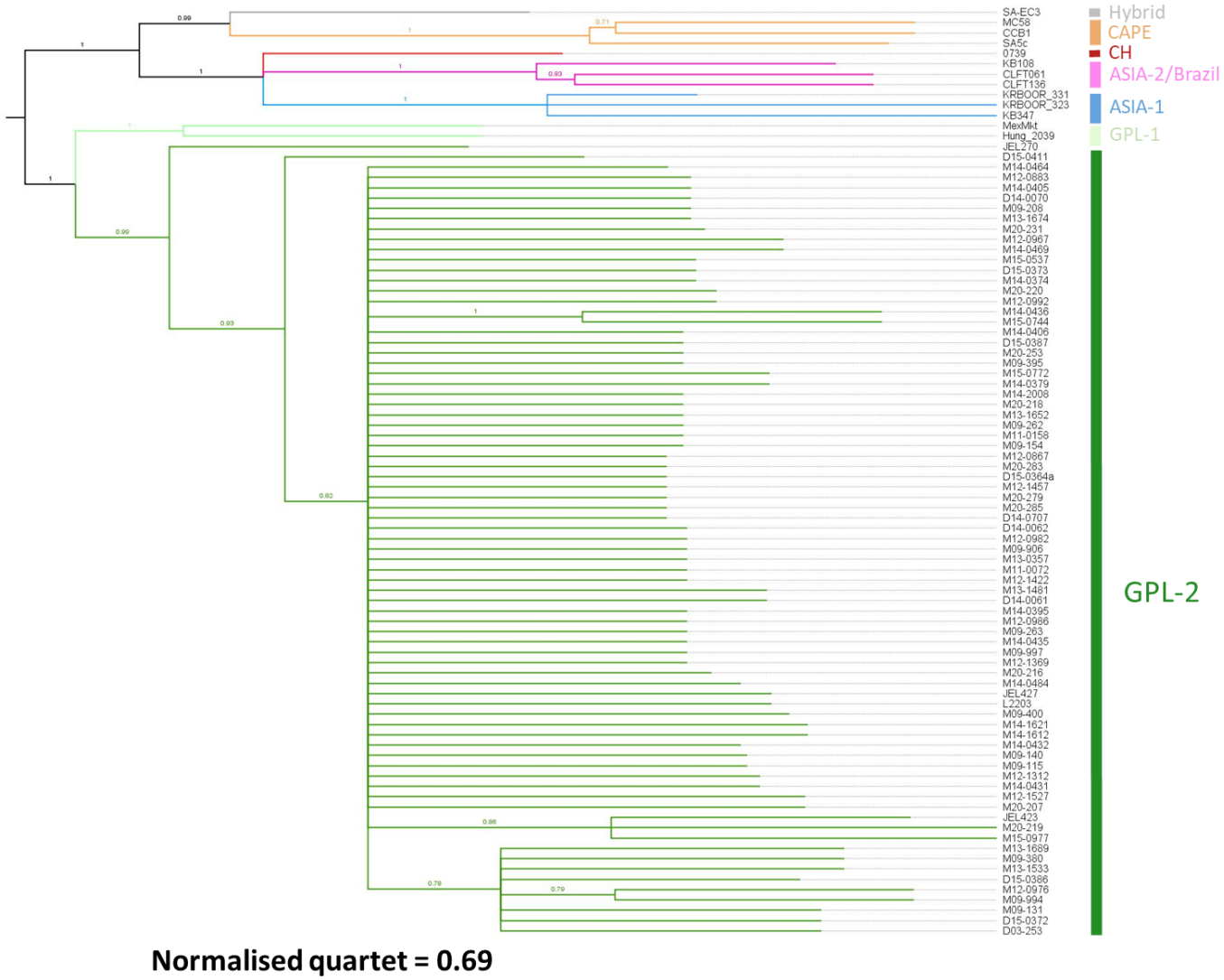

Figure 5.2: Species tree 1 for 73 Dominican & Montserratian Bd samples, plus 16 Bd lineage representatives. Per-locus sample representation threshold = none. Number of gene trees = 184. Tree is midpoint rooted and branches with < 0.7 local posterior probability are collapsed. Normalised quartet = the proportion of input gene quartet trees satisfied by the species tree.

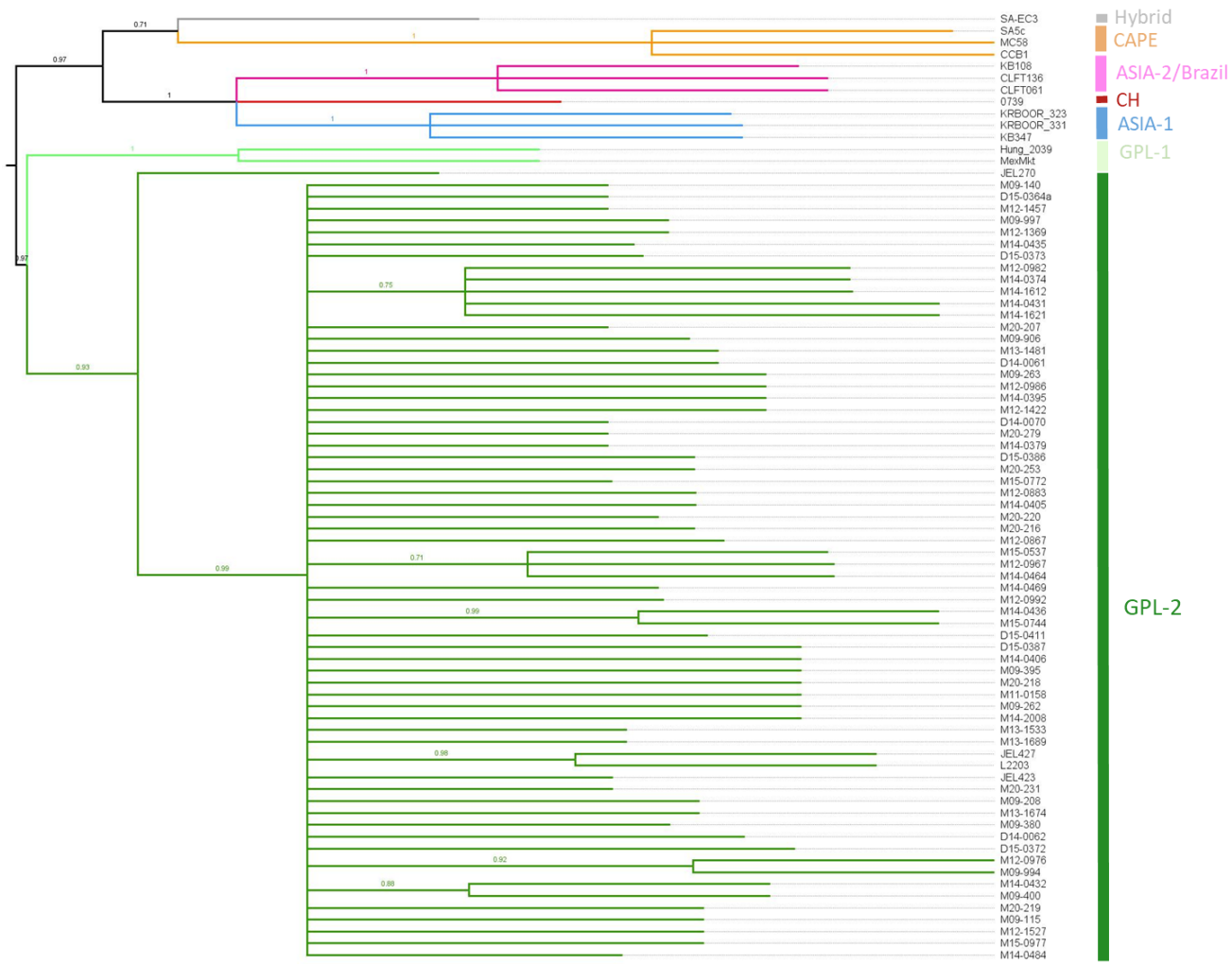

Normalised quartet = 0.71

Figure 5.3: Species tree 2 for 64 Dominican & Montserratian Bd samples with >3 loci, plus 16 Bd lineage representatives. Per-locus sample representation threshold = >33%. Number of gene trees = 71. Tree is midpoint rooted and branches with < 0.7 local posterior probability are collapsed. Normalised quartet = the proportion of input gene quartet trees satisfied by the species tree.

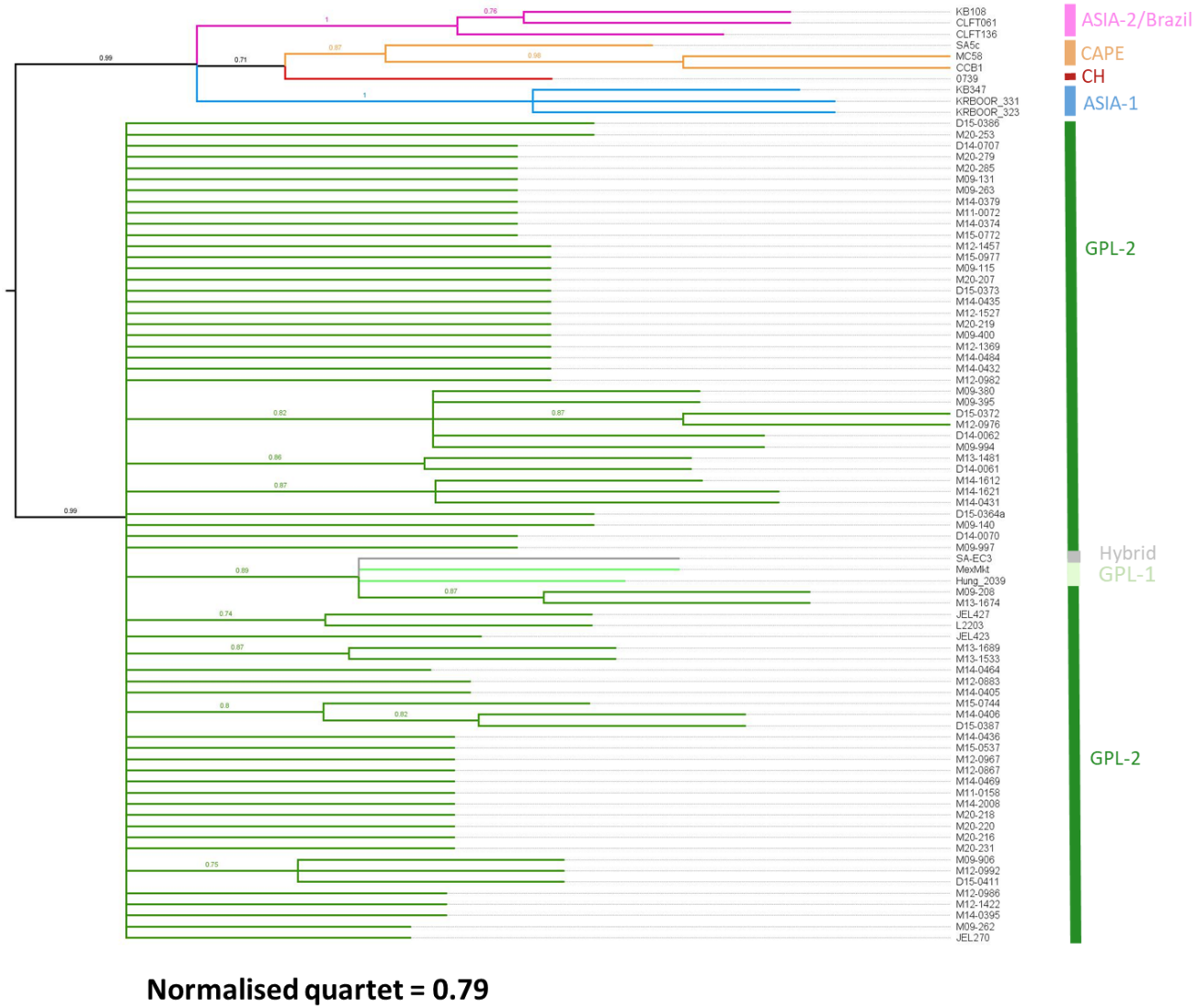

Figure 5.4: Species tree 3 for 64 Dominican & Montserratian Bd samples with >3 loci, plus 16 Bd lineage representatives. Per-locus sample representation threshold = >50%. Number of gene trees = 11. Tree is midpoint rooted and branches with < 0.7 local posterior probability are collapsed. Normalised quartet = the proportion of input gene quartet trees satisfied by the species tree.

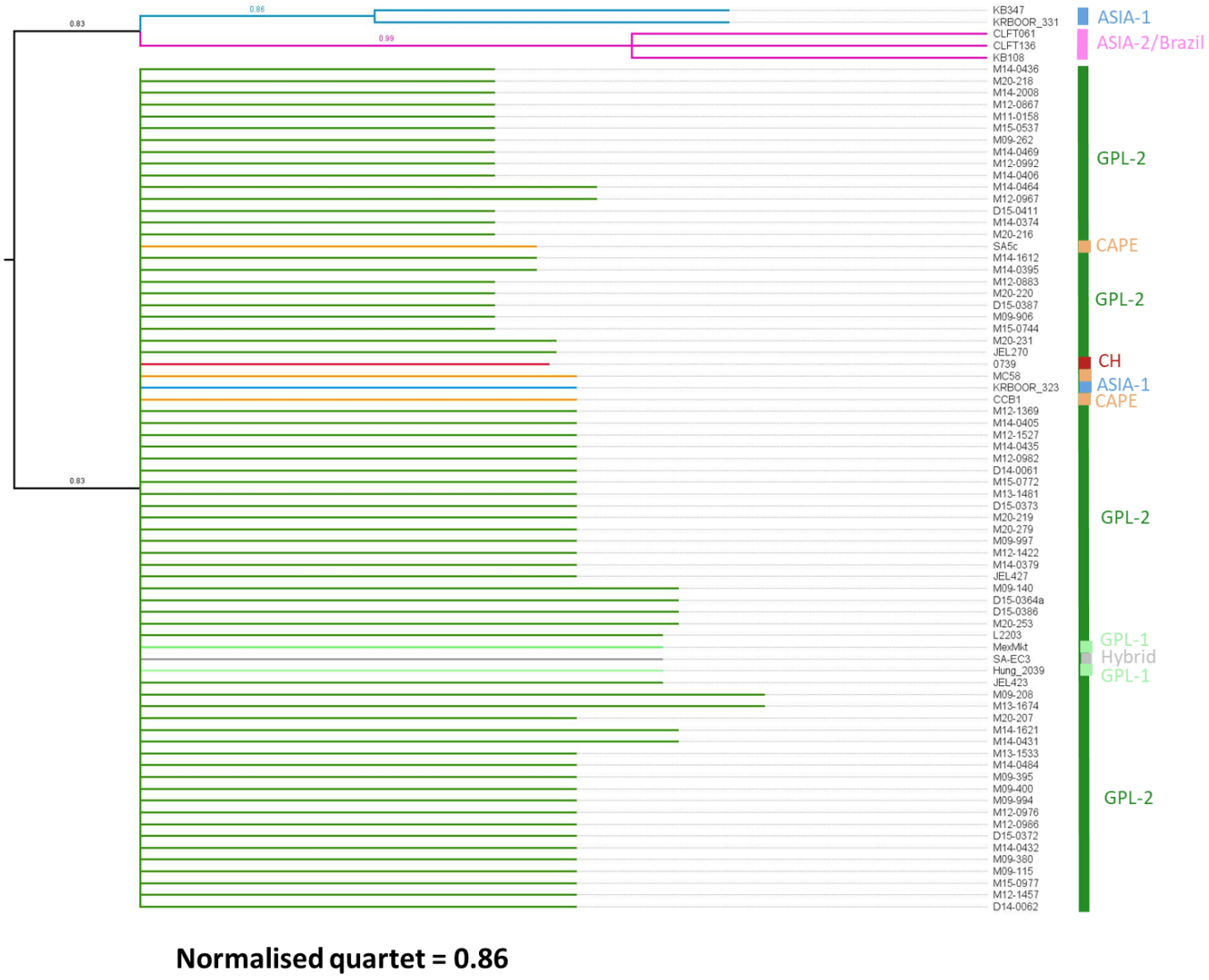

Figure 5.5: Species tree 4 for 64 Dominican & Montserratian Bd samples with >3 loci, plus 16 Bd lineage representatives. Per-locus sample representation threshold = >66%. Number of gene trees = 5. Tree is midpoint rooted and branches with < 0.7 local posterior probability are collapsed. Normalised quartet = the proportion of input gene quartet trees satisfied by the species tree.

Genetic Diversity and Structure

After variant calling, 2,880 variants were found across 92 individuals and 191 loci (Bd genomic regions). Due to a large number of low-quality variants, the final, filtered VCF file contained 187 variants found across 85 samples (seven samples were discarded due to having >70% missing data). There were 167 bi-allelic SNPs contained in this dataset (Table 5.3). This equated to an average rate of SNPs per locus of 2.06, with a range of 1-6 SNPs per locus (Table 5.3). Pruning linked variants at r^2 = 0.1 removed 15% of variants but did not change PCA clustering, estimation of K, or ADMIXTURE findings compared to unpruned data (supplementary Figure S5.3). Due to the low number of variants to begin with, the dataset for subsequent analyses was not pruned for linked variants.

Table 5.3: An overview of single nucleotide polymorphisms (SNPs) contained within the 191 target locus sequences (each 150 – 200bp) of the Bd genome.

Chromosome	No. Locus Sequences	No. SNPs	Average SNP rate per locus
1	45	48	1.07
2	16	9	0.56
3	14	9	0.64
4	11	9	0.82
5	20	10	0.50
6	21	20	0.95
7	5	5	1.00
8	6	5	0.83
9	6	4	0.67
10	5	6	1.20
11	6	5	0.83
12	12	4	0.33
13	2	2	1.00
14	5	4	0.80
15	6	5	0.83
16	6	5	0.83
Mitochondrion	5	17	3.40

Nucleotide diversity was low in all cases (< 0.005), with an average across the whole dataset of 0.002. Equivalent nucleotide diversity was detected in Montserrat and Dominica, but Tajima's D was slightly higher in Montserrat (Table 5.4). Across the timeline of the epizootic, nucleotide diversity ranged from 0.0026 - 0.0041. Nucleotide diversity fluctuated across years, being lowest in 2013, and highest in 2015 (Table 5.4). Nucleotide diversity was the same between MCF and *E. johnstonei* host species and highest in samples sourced from *R. marina*, but this group contained only four samples (Table 5.4). None of the differences in nucleotide diversity, Watterson's theta, or Tajima's D within groups were significant (measured using a Wilcoxon rank sum test between locations, and a Kruskal-Wallis test between years and host species, as the data for these variables were non-normally distributed according to a Shapiro-Wilk normality test p-value < 0.05). In all instances, Watterson's theta exceeded nucleotide diversity, meaning that the number of pairwise differences were fewer than the number of segregating sites. This indicates an excess of rare alleles, which is observed as just 187 polymorphisms were detected in 191 loci – this could be due to either a selective sweep or a

population expansion. This signal was further supported by Tajima's D, which was negative in all cases (Table 5.4). Based on the number of multi-sequence alignments used in the calculation of Tajima's D by DNAsp (47), the values of D observed in this study are not significant at the 95% confidence level (-1.801 - 2.041) set out by (Tajima 1989). No significant association between a sample's nucleotide diversity (square root transformed) and Bd load (Log10 transformed) was detected from a linear regression (Adj R^2= -0.0066, $F_{1, 86}$ = 0.428, Intercept = 0.04, Slope = 0.0018, p-value = 0.51).

Table 5.4: Mean genetic diversity and indicators of neutrality in Bd samples, across all individuals, and across samples grouped by country, year, and host species. π = nucleotide diversity, Θw = Watterson's theta.

Group	**N**	π	**Θ_W**	**Tajima's D**
All	85	0.002	0.120	-0.569
Dominica	16	0.002	0.142	-0.610
Montserrat	69	0.002	0.124	-0.631
2003	4	0.003	0.205	-0.748
2009	15	0.004	0.230	-0.812
2011	4	0.003	0.184	-0.471
2012	17	0.003	0.156	-0.738
2013	7	0.003	0.152	-0.768
2014	21	0.004	0.168	-0.797
2015	9	0.004	0.169	-0.560
2020	8	0.003	0.126	-0.637
Leptodactylus fallax	60	0.003	0.145	-0.643
Eleutherodactylus johnstonei	21	0.003	0.138	-0.714
Rhinella marina	4	0.003	0.184	-0.366

A value of K = 3 had the lowest cross validation error (supplementary Figure S5.3). K = 3 was plotted, grouping the dataset by country, year, and host species. The Bd population did not appear to be structured according to any of the specified population groupings, as all three genetic clusters were apparent in all subpopulations (Figure 5.6). The lack of division between groups was also apparent when the principal components were plotted (Figure 5.7). The extent of missing data was also used to group individuals, and no evidence was found that individual missing data generated the different clusters. When the extent of population genetic difference was quantified using F_{ST} for K = 3, the mean difference between genetic clusters was 0.04, and none of the pairwise comparisons between clusters returned significant values. These small levels of differentiation between the supposed levels of genetic structure in the population suggest that the population is panmictic, and the true value of K is likely to be one. Similarly, low mean F_{ST} was found between countries (0), year (0), and host species (0.02). All of the pairwise F_{ST} comparisons fell within the 2.5% and 97.5% confidence intervals calculated from bootstrap replicates of the data, and therefore were not significantly lower or larger than expected.

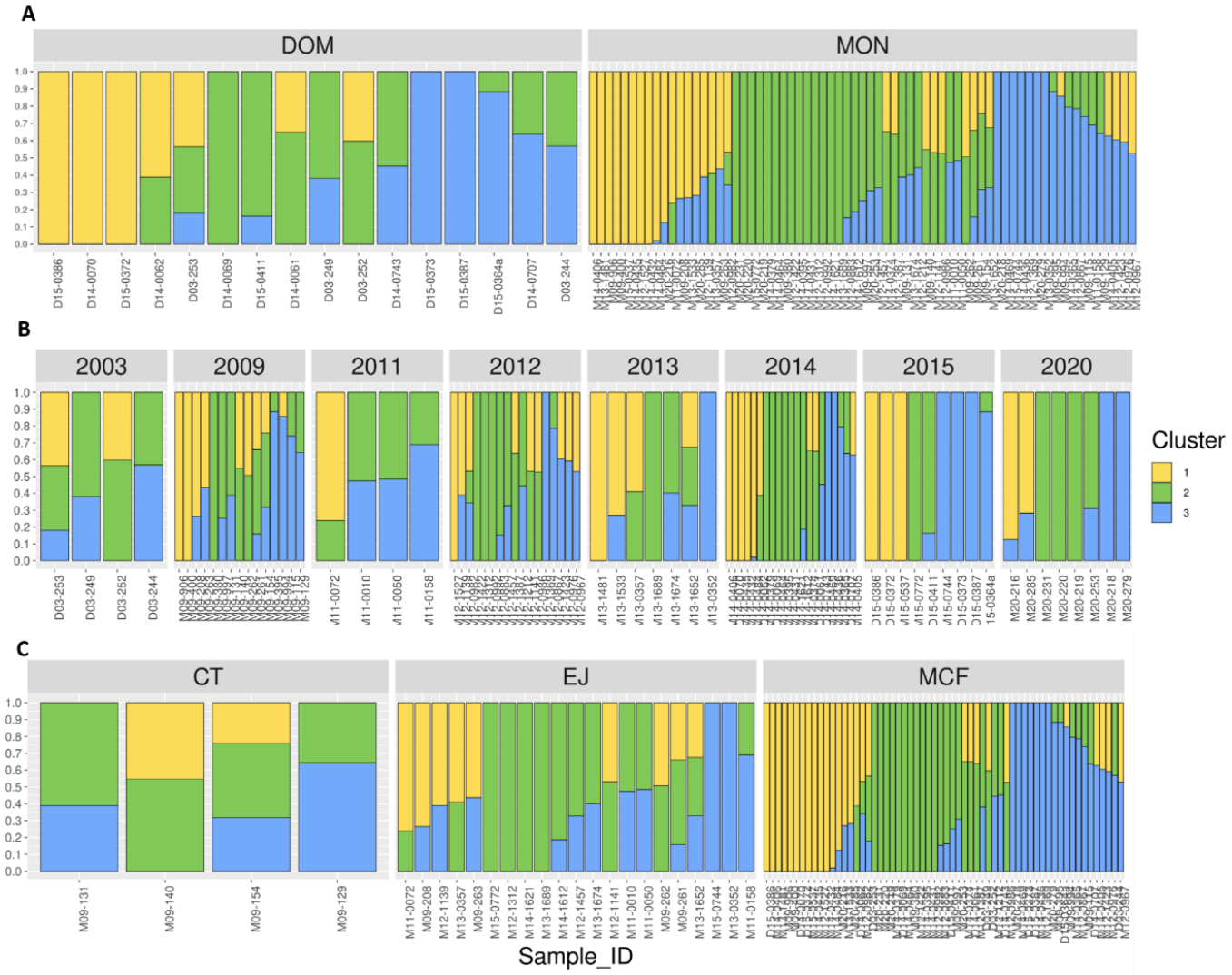

Figure 5.6: ADMIXTURE analysis of population genetic structure at K = 3. Each vertical bar represents an individual, and is coloured according to the proportion of the individual's assignment to a genetic cluster. A) Grouped by sampling location country, B) by year, C) by host species (MCF = *Leptodactylus fallax*, EJ = *Eleutherodactylus johnstonei*, CT = *Rhinella marina*).

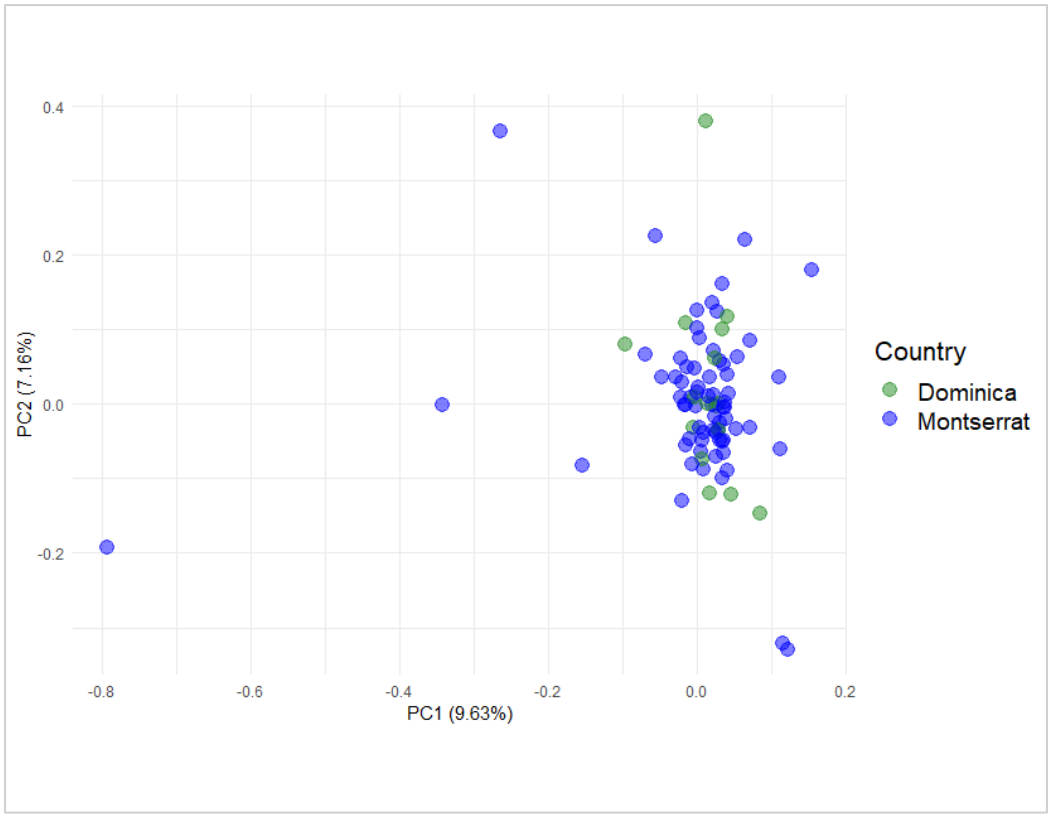

Figure 5.7: Principal components analysis of the two components explaining the highest proportion of the variance between Dominican and Montserratian Bd samples.

Discussion

This study aimed to extend the current understanding of the chytridiomycosis epizootic that led to the near extinction of the mountain chicken frog in Dominica and Montserrat between 2002 and 2010. Using recently developed methods that enable the genotyping of swab-collected Bd samples to lineage level, phylogenetic analysis sought to uncover the lineage, or lineages, of Bd responsible for the incursion of chytridiomycosis across the range of the MCF. The genetic structure and diversity of the Bd population was assessed using samples from across a span of 18 years, two countries, and three amphibian hosts. Results suggest that that one single, genetically homogenous, population of Bd from the lineage BdGPL caused declines in both Dominica and Montserrat.

The Most Virulent Bd Lineage Caused Declines in the MCF

Chytridiomycosis took just 18 months to reduce the MCF population in Dominica to less than 15% of its former size, and a year to all but wipe out the population in Montserrat (Hudson et al. 2016a). This study reveals that the most virulent lineage of Bd, BdGPL, can be attributed to the decline of the MCF, which has been described as the fastest ever recorded decline of a species due to infectious disease (Hudson et al. 2016a). Using 191 sequences from the Bd genome, Bd samples were compared with global lineage representatives to determine their place in the global Bd phylogeny. Phylogenetic reconstructions testing the effect of varying levels of missing data were able to distinguish global lineages from one another and produced trees comparable to regional phylogenies of Bd in the Americas in Byrne et al. (2019) and Basanta et al. (2021). The normalised quartet scores of these trees estimated that there was a low level of discordance between gene quartets and the final species tree, which gives confidence to these estimates of the phylogeny.

Trees used to assign Dominican and Montserratian samples to BdGPL included higher levels of missing data than in previous studies using the Fluidigm assay (Byrne et al. 2019; Basanta et al. 2021). Each of these studies were able to retain both high numbers of loci and high thresholds for missing data (< 33%). In this study, larger quantities of missing data reflect the poor amplification of many loci using the archived samples. When the same data inclusion threshold as in existing literature was used, only five gene trees remained to use in the species tree estimation and the resulting species tree could not clearly separate Bd lineages. Both Huang and Knowles (2016) and Streicher et al. (2016) caution against excluding too many loci or genes due to missing data. Based on simulated RADseq data, Huang and Knowles (2016) found that avoiding missing data also disproportionately omits more variable and thus informative loci. Streicher et al. (2016) found that including loci with up to 50% missing data increased branch support in gene-to-species trees when the number of taxa were low. Furthermore, levels of missing data up to 50% have been shown to have negligible impacts on species tree resolution, as long as missing data are randomly distributed (Xi et al. 2016). For the tree with 50% missing data (tree 3, input of 11 gene trees), the two subclades of BdGPL could not be distinguished from each other, or from a hybrid lineage of BdGPL and BdCAPE (O'Hanlon et al. 2018). However, with 50% missing data, the Bd from Dominica and Montserrat can be determined as BdGPL. Trees 1 and 2 allowed more than 50% missing data per locus, and estimated the phylogeny on 184 and 71 genes, respectively. It is likely that the increased number of genes used here enabled the sub-clades of Bd to

be distinguished, and to diagnose Bd from Dominica and Montserrat as BdGPL-2. However, missing data above 50% may not increase the reliability of the tree. Additional data would allow the lineage assignment of samples in this study to the BdGPL-2 clade to be more robustly assessed (i.e. by achieving >71 loci with < 50% missing data).

The first suspected cases of Bd in MCFs were detected in Dominica in 2002, and confirmed shortly after in early 2003 (McIntyre 2003). The clustering of all Dominican samples with representatives from BdGPL indicates that this lineage of Bd was responsible for the beginning the outbreak in Dominica. BdGPL has been implicated in the majority of Bd-driven population declines in amphibians (Fisher and Garner 2020). This finding extends the known range of BdGPL to Dominica. Of the four samples from Dominica in 2003 used in this study, only one could only be included in the most relaxed phylogeny (tree 1) due to high levels of missing data. Tree 1 placed the earliest Bd sample in a clade with known members of the BdGPL-2 subclade. This finding would be strengthened by including all samples from 2003 and by increasing the number of loci returned by these samples. However, given that that all other samples taken from Dominica in following years were assigned to the same clade as BdGPL-2 or BdGPL, in all trees, it is likely that samples from 2003 are also BdGPL/BdGPL-2. In all phylogenetic trees that could distinguish lineages (trees 1-3), Montserratian samples grouped with Dominican samples as either BdGPL or more specifically, BdGPL-2. The finding that all newly genotyped samples of Bd from Dominica and Montserrat are BdGPL-2 is in keeping with what is known about the distribution of this lineage. The whole genome sample isolated from Montserrat in 2009 was known to be BdGPL, and this study reveals it is probably BdGPL-2. BdGPL has a global distribution and is dominant in the Americas: from 91 swabs collected by Byrne et al. (2019) across North, Central and South America, 95% were BdGPL. BdGPL-2 is more commonly found in South and Central America than BdGPL-1 (James et al. 2015; Marshall et al. 2018; Basanta et al. 2021). No other Bd sample from the Caribbean has been genotyped beyond BdGPL, and this study provides the first insight into BdGPL subclade distribution in the region.

It is believed that the chytridiomycosis outbreak in Montserrat was seeded from Dominica through exports carrying infected reservoir hosts, such as *E. martinicensis* (Hudson et al. 2016a). A single origin of Bd through Dominica and into Montserrat is highly plausible given that the same lineage was detected in both countries, as well as the proximity of the two islands and their established trade and tourism links (Adams et al. 2014). However, it is also plausible that BdGPL-2 could be more widespread across the Lesser Antilles. In this case, the outbreak in Montserrat could have been seeded from another nearby island, if it was seeded from nearby at all. As BdGPL is predominantly clonal, the results from this study could arise with a single introduction of BdGPL from Dominica, or from introduction(s) from elsewhere. For example, reports of Bd exist from Trinidad and Tobago at around the same time as Bd's arrival to Dominica (Alemu I et al. 2008). From data available at: https://wits.worldbank.org/CountryProfile/en/Country/MSR/Year/2009/Summary it is evident that Trinidad and Tobago had a 6% share of total imports to Montserrat in 2009, compared to just 0.5% from Dominica. With this information, and until further genotyping of Bd samples throughout the Lesser Antilles has been completed, it cannot be concluded that there was a single introduction of Bd

to Montserrat from Dominica or multiple / alternative introductions from wider set of islands in the region.

Lack of Genetic Structure and Diversity Points to a Recent, Clonal Expansion of Bd

No genetic structure was detected in any facet of the epizootic; location, year, or host species. ADMIXTURE determined three genetic clusters to be the most likely division of genetic diversity, but this value of K carries little biological or environmental significance based on the low levels of F_{ST} (0.04) found between these clusters. In a simulation of diploid populations with varying rates of clonal reproduction, Balloux et al. (2003) estimated F_{ST} levels of < 0.06 in populations with rates of clonal reproduction close to one. This indicates that the Bd samples from this study are likely to be part of a population with very low or no recombination. A mixture of clusters was found in every group division within country, year, and host species. This finding is supported by Basanta et al. (2021) and Rothstein et al. (2021), who did not detect geographic or temporal patterns of genetic division between populations of BdGPL-2 in Mexico and Panama. Basanta et al. (2021) detected structure in GPL-1, which could be due to the fact that approximately six times more SNPs were used (Morin et al. 2009). However, the study did not report F_{ST} values between groups assigned to each cluster, so it is not clear to what extent the genetic clusters found within GPL-1 differ. Jenkinson et al. (2016) also found limited BdGPL genetic structure in Brazil. Spatially-linked genetic structure has been detected in BdGPL, and was attributed to the time BdGPL has existed within an area (Rothstein et al. 2021). For example, spatial structure was detected between BdGPL samples from the Sierra Nevada, California, where Bd has been present for many more years than in Panama, where no spatial structure was detected between samples (Rothstein et al. 2021). The rapid spread and relatively recent introduction of BdGPL into Dominica and Montserrat has probably obviated the development of population substructure across time or space. Studies of the life history of Bd have revealed a mode of reproduction common to pathogenic fungi, such as *Candida albicans*, which is a predominantly clonal but is a mitotically recombining diploid (Tibayrenc 2010). While often generalised as diploid, Bd can exhibit chromosomal copy number variation, with ploidy varying from haploid to tetraploid (Farrer et al. 2013; Rosenblum et al. 2013; Sumpter 2018). The presence of multiple chromosomes allows for the recombination of segments in mitosis, when chromosomes are in close proximity during metaphase (Symington et al. 2014). Inter-lineage comparisons of Bd have revealed the relatively low rate at which BdGPL recombines (James et al. 2009; Farrer et al. 2013), and that BdGPL has had a predominantly clonal mode of reproduction through its global expansion. Consequently, BdGPL tends to exhibit 'extremely similar' genetic profiles when compared with other Bd lineages which have not undergone such a widespread, clonal expansion (Sumpter 2018). This study supports the description of BdGPL as a predominantly clonal lineage, which does not readily develop population sub-structure as it spreads quickly through time and space.

Unfortunately, it was not possible to assess how Bd spread through the sympatric population of amphibian species in Dominica – which includes *E. martinicensis, E. amplinympha,* and possibly *E. johnstonei* (Hudson et al. 2019) – as no associated samples had a high enough Bd load. Based on the established similarity of Bd between Dominica and Montserrat, and then the lack of structure between host species in Montserrat, it is expected that no structure would be found across amphibian species

in Dominica. However, this cannot be ruled out, and would still merit investigation especially as at least two new species of invasive amphibian have been introduced to Dominica in recent years (van den Burg et al. 2020).

A sustained signal of population expansion was detected in all sample groups. In all cases, numbers of mean segregating sites were larger than mean pairwise differences among samples. Negative values were therefore produced for Tajima's D, which is estimated using the number of segregating sites and pairwise nucleotide differences (Tajima 1989). Tajima's D values were not significant, possibly due to low power from the relatively low number of SNPs used with respect to the number of samples analysed. The negative trend indicates that rare alleles are abundant, which can arise from a recent selective sweep or population expansion. Negative values of Tajima's D have also been detected in populations of *Candida auris*, another pathogenic fungus which has undergone a rapid global expansion (Chow et al. 2020). Tajima's D has been found to vary across the BdGPL genome from -2.6 - 6.2, encompassing the values detected in this study (O'Hanlon et al. 2018). This variation arises as a result of a series of host and spatial radiations around the world, where population growth fluctuates (O'Hanlon et al. 2018). Mean values of Tajima's D were not significantly different within groups of the dataset: location, year, or host species. This indicates that the population growth of Bd was not slowed by any geographical, temporal, or biological factor during its spread through Dominica and Montserrat. Whether this signal of population expansion is residual from BdGPL's global spread, or newly arisen through the epizootic in Montserrat and Dominica, is not clear. The lack of Tajima's D significance found in this study could indicate that the signal of growth is residual, but realistically, BdGPL has spread rapidly both globally and locally, so signals from both types of population expansion may co-exist or mask one another. Bd was able to continue its radiation through the islands and years, even as MCFs declined, thanks to reservoir species, in which the signal of population expansion is maintained, supporting the findings of Hudson et al. (2019).

In concordance with a clonal expansion of BdGPL, low nucleotide diversity was found across the 167 SNPs studied. Whole genome comparisons of Bd lineages by O'Hanlon et al. (2018) detected the lowest average genome wide nucleotide diversity in BdGPL when compared with ASIA-1, ASIA-2/BRAZIL, and CAPE. O'Hanlon et al.'s estimate of genome-wide nucleotide diversity for BdGPL was 0.0009, based on 127,770 SNPs. This value is ~45% of the diversity found in this study, but the number of SNPs used in this study were also far lower, which may not have accurately captured nucleotide diversity due to sampling bias (Moragues et al. 2010). Again, no significant difference was observed between experimental groups for nucleotide diversity. The small variations observed are probably an artefact of varied sample size, rather than any real change in diversity between location, year, or host species. If BdGPL is a predominantly clonal lineage with low levels of mitotic recombination, the lack of differences in nucleotide diversity is expected (Farrer et al. 2013; Sumpter 2018). No association was found between nucleotide diversity and initial Bd load. Evidence suggests that Bd spread clonally in Dominica and Montserrat, and significant differences in diversity were not detected between samples and therefore cannot be linked with the observed variation in Bd load. Other factors behind varied Bd load could include temperature, pH, and moisture levels (Piotrowski et al. 2004). Bd load

may also vary due to host genetic factors, sample storage, or laboratory methods (Van Sluys et al. 2008; Bletz et al. 2015; Dang et al. 2017).

Current and Future Implications for the MCF

Mountain chicken frogs are thought to number fewer than 50 individuals in the wild, and it is unlikely that any wild population remains on Montserrat (*Author's unpublished data* 2019). One potential mitigation for the decline of the MCF in the wild is the reintroduction of individuals to either Dominica or Montserrat from a biosecure, captive population (Adams et al. 2014). Reintroduction successes rely on the reduction of risks in the intended reintroduction site (Viggers et al. 1993; Robinson et al. 2020). Experimental releases of MCFs in Montserrat between 2011 and 2013 found chytridiomycosis driving declines in three out of four cohorts released (Hudson et al. 2016c). Mountain chickens were released into a semi-wild enclosure in Montserrat in 2019 and the continued presence of Bd in Montserrat was confirmed in 2020 when these individuals began to exhibit clinical signs of chytridiomycosis (L. Jones, *pers. comm*.). No differences in lineage, genetic structure, or nucleotide diversity were observed between the Bd from 2020 in Montserrat and the Bd that was involved in the epizootic that killed most of the wild population. The eleven samples from 2020 also appeared to be from an expanding population, based on Tajima's D value. Bd can survive in the environment (Kolby et al. 2015) and it has been established that sympatric amphibian species act as reservoirs of Bd in Dominica and Montserrat (Hudson et al. 2019). The presence of reservoir species has likely maintained a growing population of Bd and enacted little to no selective pressure on its virulence. Continued signals of Bd's population expansion into 2020, and genetic similarity to 2009, indicate that Bd in Montserrat may still be as deadly to MCFs as it was during the initial epizootic. While the ability to rapidly expand is key to a pathogen's ability to cause disease (Voyles et al. 2014), it is important to note that this study did not explicitly examine pathogen virulence. It is likely, being Neotropical BdGPL, that the Bd lineage from this study is more virulent than other lineages or even from less virulent BdGPL strains found in Europe (Greener et al. 2020). However, without characterising zoospore size, quantity, or the expression of putative virulence factors from the samples in this study, it is not possible to definitively say whether Bd virulence differed through the epizootic (Farrer et al. 2017; Voyles et al. 2018). Unfortunately such studies will never be possible for the MCF as not enough Bd isolates exists to cover the same spatial and temporal spread as this study, and no RNA samples exist either.

No Bd infection has been detected in Dominica since 2017, however samples from 2018 and 2020 could not be taken due to the effects of Hurricane Maria and Covid-19. Remaining Dominican MCFs are descended from survivors of the epizootic, and their ability to survive or evade Bd infection is not yet understood. Dominican Bd samples from 2014 and 2015 appeared to be part of the same genetically homogenous population as the rest of the epizootic, suggesting that the ability to survive Bd infection in Dominican MCFs may be more likely to be driven by host factors, as the pathogen appears identical in terms of genotype, structure, and diversity. Research in Panama found that changes in host responses to Bd, rather than attenuation in the virulence of Bd, enabled population recoveries following decline due to chytridiomycosis (Voyles et al. 2018).

These findings have implications for the reintroduction of captive-bred, Bd-naïve individuals to either Montserrat or Dominica. The Bd samples most recently studied in Montserrat (2020), and Dominica

(2015), appear to be part of a clonally expanding lineage, indistinguishable across years of the epizootic. Based on the devastating consequences of exposure of naïve individuals to this Bd population, reintroductions of their captive bred descendants would not be recommended until further mitigation can be implemented to prevent Bd infection or reduce its harmful impact. However, no other lineages of Bd were detected, reducing the chance that novel recombinants, or co-infections could arise in MCFs, as long as they are not introduced in the future (Greenspan et al. 2018). These findings can focus mitigation efforts towards BdGPL specifically and should any of the worldwide, extensive efforts to mitigate BdGPL be successful, the MCF is likely to benefit.

Limitations and Future Recommendations

This study was able to access an archive of Bd samples that spanned all relevant temporal, spatial, and host species diversity. However, due to the requirement of relatively high-load Bd samples for the Fluidigm method, many samples could not be included and therefore there are gaps in the years and species studied. As noted in Byrne et al. (2017), the Fluidigm assay is biased towards high load samples, which could lead to only collecting data on more virulent samples (likely to be BdGPL). Five low-load samples < 150 GE were included in this study; one was assigned to BdGPL, while the others did not produce enough data for inclusion in the trees. Samples all had varied amplification success, which in turn led to relaxed levels of missing data inclusion ($\geq$50%) in phylogenetic and diversity analyses. Association of input levels of Bd appeared to associate with the number of reads and/or loci amplified, until a threshold of ~$\log_{10}(5)$ GEs. Due to the very low volumes of samples available, a concentration and precipitation step was not performed, but this could have improved the levels of loci dropout for several samples (Byrne et al. 2017). If future Bd genotyping were to be done, eluting at least 100 µl of Bd DNA after extraction will allow concentration and precipitation to be performed, hopefully increasing the amount of available data to perform genotyping and diversity analysis.

Conclusion

This study greatly increases the number of genotyped Bd samples from the Caribbean and provides the first genotyping of Bd in Dominica. The known range of BdGPL is now extended throughout Dominica and Montserrat. Phylogenetic analysis was able to further describe the distribution of the BdGPL-2 subclade in the Americas, extending it from South and Central America to the Caribbean. From the first detection of Bd in Dominica, a rapid radiation is detected through Dominican MCFs and in Montserratian amphibians from 2009 onwards. The lack of genetic structure and low levels of diversity indicate that the expansion of BdGPL was predominantly clonal, which is expected for the lineage. The precipitous decline of the MCF, paired with the sustained signal of population expansion in all Bd sampled for this study, suggest that the MCF populations' collapse was driven by a single Bd lineage radiation. This radiation may have arrived to Montserrat from Dominica, or from other locations where the same, clonal Bd strain was circulating. These findings present implications for the direction of future conservation of the MCF, as it appears that the pathogen population is genetically indistinguishable from that of the beginning of the epizootic on each island in 2003 or 2009. The finding of homogeneity of Bd in Dominica and Montserrat establishes that host or environmental factors, rather than pathogen factors, may be of more importance in determining recovery in the MCF.

Chapter Six

Looking Ahead: A Genetic Assessment and Recommendations for Future Management of the Biosecure Mountain Chicken Frog Captive Population

Abstract

The mountain chicken frog (*Leptodactylus fallax*, MCF) is Critically Endangered, due to a multitude of pressures that threaten its existence in the wild. In response to these pressures, captive breeding of the MCF has been ongoing since 1999. In 2009, a new, biosecure population of MCFs was established across several European zoos to preserve frogs from the last remaining Montserratian population of the species yet to be extirpated by the fungal pathogen *Batrachochytrium dendrobatidis* (Bd). These MCFs have been managed in captivity for more than ten years, to provide Bd-free frogs for use in reintroductions to the wild. Captive breeding can reduce the genetic diversity and fitness of populations in captivity, as well as wild populations that are supplemented with captive bred individuals. Management of a species across several institutions can also result in differing genetic structure due to drift or varied selection pressures between institutions. Both genetic structure and diversity are important to integrate into MCF conservation management plans, but no genetic assessment has been carried out on the biosecure captive population since 2009. To address this issue, this study used 11 microsatellite markers to assess the neutral genetic diversity and structure of the biosecure MCF captive population and make comparisons with the wild population. It was found that captive breeding to date has been successful in maintaining equivalent levels of heterozygosity and allelic richness to that observed in Montserrat until 2009. In the first decade of captive management, only 0.3 alleles were lost across 11 loci. It was also found that while the genetic variation present in Montserrat was represented across the captive metapopulation, individual zoos each represented only a portion of this diversity. Finally, this study makes several recommendations for breeding and reintroduction management, in order to best preserve diversity in the captive population and ensure viable captive stock for reintroductions – a key aim of the long-term management plan for the MCF.

Introduction

Over the last two decades, the mountain chicken frog (*Leptodactylus fallax*, MCF) has undergone precipitous declines across its home range on the islands of Dominica and Montserrat in the Lesser Antilles (Hudson et al. 2016a). Unsustainable levels of hunting, habitat loss from volcanic eruptions in Montserrat, hurricanes in Dominica, and most notably an outbreak of the disease chytridiomycosis across both islands have culminated to leave fewer than 50 wild individuals remaining (Adams et al. 2014, *Author's unpublished data* 2019). As threats to the survival of the MCF in the wild remain, ex situ captive breeding is vital for the persistence of the species. Captive breeding of the MCF has been ongoing since 1999, before the species was considered Critically Endangered (Gibson and Buley 2004). The first captive population of seven male and six female Montserratian frogs was established at Jersey Zoo (formally Durrell Wildlife Park), UK Channel Islands, in 1999 (Gibson and Buley 2004). Observation of this population led to a better understanding of the unusual breeding ecology of the MCF, which includes foam nests in terrestrial burrows and obligatory oophagy in the tadpoles (Gibson and Buley 2004). The second generation bred from this population founded 18 additional captive populations across Europe and the USA, which have raised awareness and improved our understanding of MCF conservation (Jameson et al. 2019a).

The fungal pathogen *Batrachochytrium dendrobatidis* (Bd) was detected in Dominica in 2002 (McIntyre 2003). Bd infects the skin of amphibians, and can lead to the fatal disease chytridiomycosis in susceptible amphibian species (Berger et al. 1998). At the time of its discovery in Dominica, Bd was associated with mass mortality events and significant amphibian population declines (Berger et al. 1998; McIntyre 2003). In response to this perceived threat, 12 individuals from Dominica were moved into a captive, biosecure population at the Zoological Society of London (ZSL) Zoo in the same year (Jameson et al. 2019a). Preserving the biosecurity of a captive population requires that the population is kept free of pathogens that are non-native to the species' home range and which could be introduced to the home range as invasive pathogens alongside the reintroduced captive hosts (Jameson et al. 2019a). Biosecure populations are managed differently to non-biosecure populations. For example, biosecure MCF populations have more frequent health checks, are located in enclosures separate from other species, and have several more protocols to ensure their protection from novel pathogens (Jameson et al. 2019a). The last animal in the Dominican-bred biosecure population died in 2015, but the biosecure captive breeding programme was expanded in 2009 with the formation of a Montserratian population in response to the detection of Bd in Montserrat (Jameson et al. 2019a).

By 2009 it was evident that the MCF was highly susceptible to chytridiomycosis, with the wild Dominican population having been decimated in the years before (Hudson et al. 2016a). Ahead of the 2009 chytridiomycosis epizootic wave in Montserrat, 50 uninfected mountain chicken frogs were evacuated to three zoos in Europe (ZSL, Jersey/Durrell Zoo, and Parken Zoo, Sweden) to become founders for a new biosecure captive population (Adams et al. 2014). This new biosecure population was subsequently extended to Chester Zoo, Norden's Ark, and Bristol Zoo using descendants of the original founders, or founders themselves (B. Tapley and M. Goetz, *pers. comm*.). While fewer than half of the original founders have produced viable offspring, 205 MCFs were bred in captivity between the years 2009 – 2012 (Jameson et al. 2019a). Offspring from this population have been used for

several experimental releases in Montserrat (Hudson et al. 2016b), most recently in 2019 in a release to a semi-wild enclosure on the island (Jameson et al. 2019a). With no wild individuals detected in Montserrat since 2016 (M. Hudson *pers. comm.*), this biosecure population now represents an essential source of animals for re-establishing the species on the island and could even be used to reinforce the fragile remnant population in Dominica (Adams et al. 2014).

The 2009 biosecure captive population was established with no a priori knowledge of the genetic diversity or structure that existed in wild populations (Jameson et al. 2019a). A lack of genetic data is not uncommon in the establishment of ex situ programmes, especially for endangered species, where founding individuals are scarce and understudied to begin with (Ralls and Ballou 2004; Hedrick and Fredrickson 2008). Simultaneously, a common goal for captive breeding is to maintain genetic diversity at levels similar to wild populations, and genetic data from wild populations provide valuable benchmarks against which captive breeding populations can be assessed (Frankham et al. 2004). In the case of the MCF, the goal for the biosecure population is to "*maintain a demographically and genetically stable and behaviourally competent assurance population with the highest veterinary and health standards for potential future reintroduction*" (Jameson et al. 2019a). Maintaining genetic stability and health can be challenging in captivity, however (Witzenberger and Hochkirch 2011; Tapley et al. 2015). As captive populations are often founded from fewer individuals than the wild source population, their gene pool is limited upon founding and subsequently through successive generations (Frankham 2008). Reduced genetic diversity can be harmful if it leads to inbreeding depression and a lowered resilience of the population in the face of environmental change, disease, or stochastic events such as natural disasters (Keller and Waller 2002). The MCF biosecure population is managed across five institutions. Varied management protocols, outcomes, or selective pressures between institutions create a chance that breeding populations will begin to develop their own distinct genetic signature (Gooley et al. 2020). Genetic structure (or lack of) between institutions may have implications for the management of the population, for example whether it is best managed as a metapopulation, or several reproductively isolated populations (Margan et al. 1998; Gooley et al. 2020). Maintaining genetic diversity is a goal for the biosecure MCF population, but it as of yet has only been studied retrospectively (Hudson et al. 2016a; Jameson et al. 2019a). Hudson et al. (2016a) compared the genetic diversity of eleven founders of the biosecure population to that of the wild source population in Montserrat. It was found that genetic representativeness had, by chance, been captured upon the formation of the ex situ biosecure population in 2009 (Hudson et al. 2016a). However, no further study has been carried out into the impacts of >10 years of captive management on genetic diversity in the biosecure captive population. The captive population is integral to aim 3b of the mountain chicken recovery plan: Establish growing populations at five sites on each island through releases of captive bred frogs (Adams et al. 2014). Understanding the current genetic diversity and structure of this population will allow more fully informed management decisions to be made, to best preserve a viable captive population and successful reintroduction efforts in the future.

This study will aim to address objective 4.1.3 of the long-term recovery strategy set out by Adams et al. (2014) by assessing the level of genetic structure and diversity of the biosecure captive population after a decade of captive management. To do this, the biosecure captive population will be genotyped

at 11 microsatellite markers and its diversity and structure compared to an existing dataset from wild individuals in Dominica and Montserrat. It is hypothesised that some genetic diversity will have been lost given the amount of time spent in captivity and varied breeding successes across the population. The results from this study will help to address objective 4.1.5 from the long-term recovery strategy, by providing recommendations that can be integrated into breeding and institutional targets to best preserve genetic diversity and manage genetic structure between institutions.

Methods

Sample Collection and Study Design

Eighty-three mountain chicken frogs were sampled in 2018 from across the five host zoos of the biosecure captive population (Table 6.1). These five zoo populations represent the captive biosecure metapopulation following almost ten years of captive management. In 2019, some MCFs from the biosecure metapopulation (nine from Durrell and 15 from ZSL) were released to a semi-wild enclosure in Montserrat. This population, named 'released to Montserrat (RTM)', was also assessed to provide specific management recommendations to be made for the semi-wild enclosure (Table 6.1). Following the removal of the RTM population from the biosecure captive population, 33 sampled individuals remained alive in captivity as of November 2021. To enable the most up to date management recommendations to be made for the biosecure metapopulation, this population was assessed as the 2021 biosecure captive population (BCP 2021). BCP 2021 was assessed as a metapopulation, and not as individual zoos like the 2018 populations, due to the small sample sizes remaining for four zoos ($n < 5$). Sample sizes in microsatellite-based population genetics studies should ideally be > 25, and at $n = 5$ are more likely to provide unreliable population genetic inferences (Hale et al. 2012). To provide a benchmark for wild MCF genetic diversity, wild samples from Dominica and Montserrat were included. Dominican samples were taken between the years of 2002 and 2019, capturing the MCF population pre- and post-decline from chytridiomycosis (Table 6.1). Montserratian samples were predominantly from 2009, and two were taken in 2016. Wild individuals were selected from pre-Bd and post-Bd populations, to represent the historic and most recent genetic variation from each island. Captive samples were collected as a buccal swab (Medical Wire & Equipment Co. MWE100). Swab tips were removed and then stored in a sterile 1.5 ml microcentrifuge tube, containing 99% ethanol, and frozen until processing in the lab. Wild samples had previously been collected as tissue or blood (from post mortems) or as a buccal swab in the same manner as the captive samples.

Table 6.1: Study sample information. N = number of individuals.

Population	Captive or Wild	Location	Year Sampled	N
Bristol	Captive	Bristol, UK	2018	6
Norden's Ark		Bohuslän, Sweden	2018	22
Durrell		Jersey, Channel Islands	2018	20
ZSL		London, UK	2018	24
Chester		Chester, UK	2018	11
RTM	Captive	Semi-wild enclosure, Montserrat	2018	24
BCP 2021		Across five zoos listed above	2018	33
Dominica	Wild	Dominica	2002 - 2019	29
Montserrat		Montserrat	2009 - 2016	25

DNA Extraction and Microsatellite Amplification

DNA was extracted from buccal swabs using the QIAGEN DNeasy blood and tissue kit, with modifications to its initial protocol for sample lysis and incubation. Each buccal swab was removed

from its storage ethanol and allowed to dry from residual ethanol at room temperature for ten minutes. Swabs were then placed into 180 µl ATL buffer and 20 µl Proteinase K, before incubation overnight at 56°C. Following this, the usual QIAGEN protocol was followed from step four. Eleven microsatellite markers; eight previously optimised by Hudson et al. (2016a), and three newly optimised for this thesis (Author's *unpublished data* 2018) were used to assess genetic diversity (supplementary Table S6.1). Each 13 µl PCR reaction contained 2.5 µl of 5X GoTaq buffer, 0.5 µl of 0.15 mM BSA, 0.6 µl of 10 mM dNTPs (with each dNTP present at a concentration of 2.5 mM), 0.3 µl each of 10 µM forward and reverse primer, 0.06 µl of GoTaq polymerase, 7.74 µl PCR-grade H_2O, and 1 µl DNA. PCR cycling involved three minutes at 95°C, followed by 35 cycles of 45 seconds at 94°C, 45 seconds at optimal annealing temperature, and 45 seconds at 72°C. A final extension at 72°C was performed for ten minutes. Samples were sent for fragment analysis at DNA sequencing and services, University of Dundee at a 1:10 dilution. Allele calls were made using the microsatellite plugin for Geneious Prime 2021.0.1.

Data Analysis

Unusual mutation steps or allele gaps in initial allele calls were assessed using the error report from Microsatellite Analyser v.4.05 (Dieringer and Schlötterer 2003). Microchecker v.2.2.3 (Van Oosterhout et al. 2004) was used to assess the dataset for null alleles. Samples with missing data for more than two microsatellite markers were removed from the dataset, to minimise the impact of missing data on subsequent analyses (Peel et al. 2013).

Summary Statistic Generation

The cleaned and corrected dataset was used for subsequent analyses. Observed and expected levels of heterozygosity, allele counts per locus, and allele richness (corrected for sample size) were calculated using Microsatellite Analyser v.4.05. Levels of inbreeding, measured as F_{IS}, were assessed using FSTAT v.2.9.4 (Goudet 1995). Genepop v.1.2.6 (Rousset 2008) was used to perform a Hardy-Weinberg exact test of equilibrium and to search for an excess or deficiency of heterozygotes that may explain any deviations from the Hardy-Weinberg equilibrium (HWE). Markov chain parameters were left as default. These analyses were repeated for each of the populations listed in Table 6.1 and once treating all five zoo populations as one metapopulation. To test for the presence of significant associations between loci, a likelihood ratio test between all pairs of loci was run in Arlequin v.3.5 (Excoffier and Lischer 2010), using 10,000 permutations. Fifty-four pairs of loci gave a Bonferroni corrected p-value of 0.00091 to assess the significance of associations.

Genetic Structure

To assess the impact of captive management on genetic differentiation between zoos up until 2018, genetic structure was investigated using Structure v.2.3.4.7 (Pritchard et al. 2000). Wild populations from Dominica and Montserrat were included in the analysis to assess the extent of differentiation in the captive population from potential reintroduction sites. RTM and BCP 2021 populations were not included, as these individuals are already represented in the 2018 captive metapopulation used in the Structure analysis. The degree of admixture (alpha) was set to be inferred from the data, with an initial value of one. The possibility of admixture between populations (which is likely to have occurred due

to the transfer of individuals between zoos) was allowed with the admixture model. The correlated allele frequency model was selected as it can better detect structure when populations have similar allele frequencies, which is likely as all study populations besides Dominica have ancestry in the 2009 founding Montserratian population (Pritchard et al. 2009). Simulated values of K ranged between 1-10, with the first 50,000 steps in the Markov Chain Monte Carlo (MCMC) algorithm discarded as burn in and the following 250,000 MCMC iterations as data collection phase. Each MCMC run was repeated three times to assess the convergence of runs across the same value of K. The optimal value for K was determined using the method of Evanno et al. (2005), taking the highest ΔK as the most likely number of genetic clusters in the dataset. Results were plotted in R (R Development Core Team 2008), using the package pophelper v.2.3.1 (Francis 2017). Genetic divergence between populations was measured as pairwise F_{ST} and calculated between all seven subpopulations and genetic clusters identified by Structure using Microsatellite Analyser. The significance of F_{ST} values was determined using a Bonferroni-corrected alpha level as determined by Microsatellite Analyser. To further assess genetic structure, a discriminant analysis of principal components (DAPC) was carried out using the adegenet package in R (Jombart 2008). DAPC analyses were run twice, once using source populations to divide the dataset and another time using the 'find clusters' method to define groups de novo. The 'find clusters' method uses the lowest Bayesian Information Criterion (BIC) to determine the most probable number of genetic clusters (K). The DAPC with predefined groups was run including all seven populations and then run again excluding Dominica to assess structure between the captive populations and their wild source population in Montserrat. In both cases, the optimal number of principal components (PCs) to retain was chosen based on the minimum number of PCs which explained the largest percentage of cumulative variance – as described in (Jombart and Collins 2015).

Captive Population Resemblance of Wild Populations

The biosecure captive population's genetic representativeness of its wild source population in Montserrat was assessed with a bootstrap resampling method. The expected distribution of wild, Montserratian genetic diversity was calculated and compared to the existing genetic diversity in the biosecure populations as of 2018. Eighty-seven wild, Montserratian individuals previously genotyped at eight microsatellite markers (Hudson et al. 2016a and *Author's unpublished data* 2018) were compared to the 74 individuals that formed the biosecure captive population in 2018 at the same eight microsatellite loci. The wild source population was also compared to the RTM and BCP 2021 populations, at the same eight loci. Bootstrap replicates (100,000 datasets randomly sampled with replacement) were generated, resampling the larger population to be the same size as the smaller population. Distributions of observed and expected heterozygosity and average number of alleles per locus were generated, alongside 2.5% and 97.5% quartiles, and used to compare the expected genetic diversity distribution of the wild population with actual values from the captive populations. These statistics were chosen for their sensitivity to population size change (Hoban et al. 2014). The number of private alleles in each captive population was calculated using Microsatellite Analyser and the frequency of private alleles across populations calculated using Genepop. The proportion of shared alleles between wild and each captive population was calculated using the R package PopGenReport (Adamack and Gruber 2014).

Results

Data Cleaning

Seventy-four samples from the 2018 captive population were retained after removal of individuals with missing data in ≥2 loci. Marker Lepfal_013956 was identified as a potential null allele in the Dominica, Montserrat, and captive populations. Marker Lepfal_011628 was also highlighted as potentially null in Dominican and Montserratian populations. These markers were selected for an experimental removal from the dataset, and analyses were re-run to estimate genetic diversity and structure. Values for observed and expected heterozygosity, as well as $F_{ST,}$ were generated with and without the markers with potential null alleles. A two-tailed pairwise t-test detected no significant difference between either dataset, for any statistic, in any population (supplementary Table S6.2). Therefore, these markers were retained, as they did not significantly alter genetic diversity or divergence across populations. Marker Lepfal_025280 was detected as potentially having null alleles in the captive metapopulation, and marker Lepfal_005205, Lepfal_010673, and Lepfal_017957 in Dominica, but as they were only present in one population each, neither were removed from the dataset.

Genetic Diversity

Wild populations of MCFs showed lower heterozygosity than expected and significant levels of inbreeding (Table 6.2). Despite this, there were still higher allelic richness measures in wild populations compared to individual zoo populations. When zoo populations were combined as a captive metapopulation, allelic richness was higher than in the source population of Montserrat, and ANAPL was only slightly lower (Table 6.2). Allelic richness and ANAPL were lower in the captive metapopulation than in Dominica. The captive metapopulation had slightly higher observed heterozygosity than expected, and observed heterozygosity higher than in either Dominica or Montserrat (Table 6.2). Levels of F_{IS} in the captive metapopulation did not indicate significant in or outbreeding. In individual zoo populations, observed heterozygosity ranged from 0.464 - 0.755 and ANAPL from 2.6 - 3.3 (Table 6.2). Norden's Ark and Chester were the only zoos with lower observed than expected heterozygosity, although their inbreeding coefficients were not significant (Table 6.2). While these populations had relatively low heterozygosity, they had the highest allelic diversity measures of all zoos. Populations at Bristol, Durrell, and ZSL had higher than expected heterozygosity, and negative inbreeding coefficients as a result – ranging from -0.337 to -0.092, indicating a low to moderate level of outbreeding – but these were non-significant values (Wright 1949). Bristol had the lowest ANAPL, but when corrected for sample size, allelic richness was lowest at ZSL (Table 6.2). The RTM population subset had higher than expected heterozygosity and a non-significant signal of outbreeding, but fewer alleles than all other populations (Table 6.2). The remaining biosecure population, BCP 2021, had lower than expected heterozygosity and lower heterozygosity than the captive metapopulation in 2018. Although as with the captive metapopulation in 2018, observed heterozygosity was higher than the source population in Montserrat (Table 6.2). BCP 2021 also maintained relatively high allelic richness, only slightly lower than in 2018, and there was no indication of significant inbreeding (Table 6.2).

Table 6.2: Genetic summary statistics across eleven microsatellite markers, averaged within population groups. N = sample size, Het_{Obs} = Observed Heterozygosity, Het_{Exp} = Expected Heterozygosity, A_R = Allelic Richness, corrected for sample size, ANAPL = Average number of alleles per locus, F_{IS} = inbreeding coefficient, * indicates significantly different from 0.

Population	N	Het_{Obs}	Het_{Exp}	A_R	ANAPL	F_{IS}
Captive Metapopulation	73	0.540	0.538	3.601	3.636	-0.003
Bristol	6	0.755	0.582	2.636	2.636	-0.337
Norden's Ark	21	0.464	0.523	2.782	3.182	0.116
Durrell	19	0.557	0.512	2.618	3.091	-0.092
ZSL	19	0.562	0.487	2.510	2.909	-0.158
Chester	9	0.491	0.507	2.929	3.273	0.033
Dominica	29	0.463	0.613	3.734	5.545	0.248*
Montserrat	25	0.448	0.563	3.018	3.727	0.208*
RTM	24	0.564	0.469	1.941	2.363	-0.207
BCP 2021	33	0.507	0.543	3.545	3.545	0.067

Bristol, ZSL, and Chester zoos were observed to be in HWE, as was their wild source population in Montserrat (Table 6.3). These populations still had heterozygote deficiency or excess detected in some loci (Table 6.3). Norden's Ark and Dominica deviated from HWE due to a deficit of heterozygotes, while Durrell had one locus with a heterozygote deficiency and two loci with a heterozygote excess. Arlequin detected one pair of linked loci in three populations: Norden's Ark, Durrell, and Dominica (p-value < 0.00091). Neither subset of the 2018 captive population, RTM nor BCP 2021, was in HWE (Table 6.3). For RTM, this was due to heterozygote excess while the remaining biosecure population, BCP 2021, had two loci with heterozygote deficiency.

Table 6.3: Results of an exact test of Hardy-Weinberg Equilibrium, and for heterozygote deficiency (Het Def) or excess (Het Excess) across populations.

Pop	HWE	Test Result	Het Def	Het Excess
Bristol	Y	Fisher's $\chi2$ = 14.07, d.f. = 22, prob = 0.8990	0	0
Norden	N	Fisher's $\chi2$ = 49.92 d.f. = 22, prob = 0.0006	3	0
Durrell	N	Fisher's $\chi2$ = 36.01, d.f.= 20, prob = 0.0153	1	2
ZSL	Y	Fisher's $\chi2$ = 27.18, d.f. = 22, prob = 0.2046	1	4
Chester	Y	Fisher's $\chi2$ = 25.41, d.f. = 22, prob = 0.2777	0	1
Dominica	N	Fisher's $\chi2$ = 66.79, d.f. = 22, prob < 0.0001	8	0
Montserrat	Y	Fisher's $\chi2$ = 17.30, d.f. = 22, prob = 0.7464	3	0
RTM	N	Fisher's χ^2 = 59.81, d.f. = 18, prob = 0.000	0	3
BCP 2021	N	Fisher's $\chi2$ = 44.82, d.f. = 22, prob = 0.003	2	0

Genetic Structure

The most likely number of genetic clusters structuring the dataset was five, according to the highest ΔK value (supplementary Figure S6.1). When values of K from 2 - 5 were plotted, the first division of the dataset was evident between Dominica and Montserrat and the captive populations (Figure 6.1). This is expected, as the captive population was founded from Montserratian individuals. Moving to K = 3 and K = 4, it is apparent that the genetic variation present in Montserrat is somewhat unevenly distributed throughout the captive populations (Figure 6.1). One cluster, found at low frequencies in Montserrat, was dominant in Durrell and ZSL. A more common cluster from Montserrat was also dominant in Bristol. Norden's Ark and Chester appeared to more evenly represent the existing genetic variation within Montserrat at K = 3 and 4. At K = 5, Chester and Bristol appeared to be the most admixed zoo populations and better resembled Montserrat than the other zoo populations. Based on the individuals sampled for this study, Durrell and ZSL show a bias towards a particular subset of the genetic variation present in Montserrat (Figure 6.1).

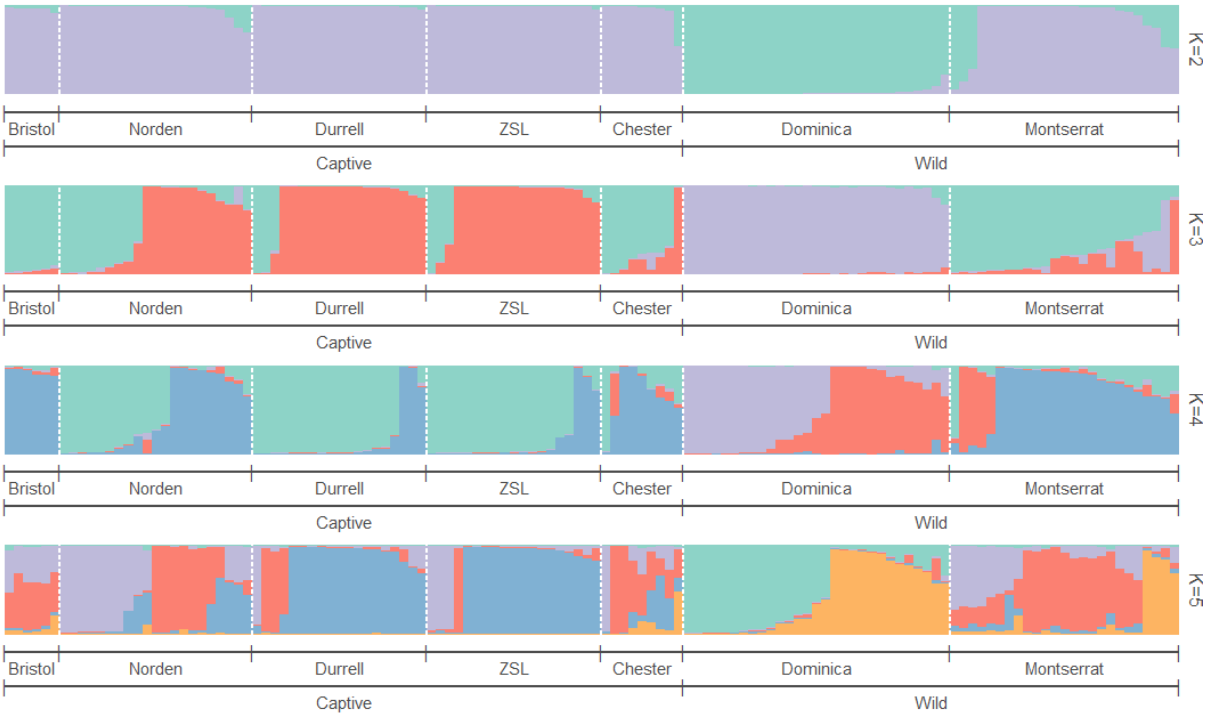

Figure 6.1: Results of STRUCTURE analysis, showing number of genetic clusters (K) from 2 – 5. Each vertical bar represents one individual, and the proportion of that individual's genotype assigned to each genetic cluster.

F_{ST} between populations ranged from 0.008 - 0.225 (Table 6.4). In keeping with the results from STRUCTURE, all F_{ST} values between Dominica and other populations were significant (Table 6.4). Focusing on the wild population of Montserrat and the captive populations, Durrell and ZSL both had a significantly high F_{ST} value when compared with Montserrat. Bristol, Norden's Ark, and Chester did not have significant F_{ST} distances from Montserrat, with Norden's Ark and Chester being the closest genetically. The F_{ST} values between the captive populations ranged from 0.008 (Durrell - ZSL), to 0.122 (Durrell - Bristol). Chester was significantly genetically distinct from Bristol, Durrell, and ZSL (Table 6.4). Bristol was also significantly genetically distinct from Durrell (Table 6.4). No other pairwise comparisons were significant.

Table 6.4: F_{ST} values shown above the diagonal, and Bonferroni-corrected p-values below. *indicates significant.

	Bristol	Norden	Durrell	ZSL	Chester	Dominica	Montserrat
Bristol	-	0.080	0.122*	0.090	0.111*	0.154*	0.064
Norden	*n.s.*	-	0.044	0.037	0.074	0.208*	0.030
Durrell	*0.002*	*n.s.*	-	0.008	0.113*	0.214*	0.066*
ZSL	*n.s.*	*n.s.*	*n.s.*	-	0.092*	0.225*	0.054*
Chester	*0.034*	*n.s.*	*0.002*	*0.002*	-	0.199*	0.030
Dominica	*0.002*	*0.002*	*0.002*	*0.002*	*0.002*	-	0.169*
Montserrat	*n.s*	*n.s.*	*0.002*	*0.002*	*n.s.*	*0.002*	-

DAPC analysis supported STRUCTURE's finding of five as the most likely number of genetic clusters within the dataset (supplementary Figure S6.2 and S6.3). Despite this, three clusters appeared to overlap in the DAPC plot, indicating that three clusters could be a more accurate division of the data (supplementary Figure S6.2). A loading plot revealed two alleles were most influential in driving differences between the five clusters: Lepfal_000867.09 (size 236) and Lepfal_017957.02 (size 191). When using source populations to split the dataset, a clear division between Dominica and other populations was evident (Figure 6.2a). The alleles driving this separation were Lepfal_005205.04 (present in Dominica at 46% and all other populations below 35%), Lepfal_003035.03 (found in Dominica at 62% but absent from all other populations), Lepfal_011628.03 (found in Montserrat at 14% and Dominica at 7%, and not in any captive population), and Lepfal_017957.05 (absent from Dominica and Bristol, but found in all other populations at 4 - 23%). When Dominica was excluded from the DAPC, the 'find clusters' method again indicated that five clusters had the lowest BIC value. The resultant plot showed five clusters, but with clusters 2 and 4 overlapping, indicating that K = 4 is likely a better division for the populations excluding Dominica (supplementary Figure S6.2). Two alleles were driving the division: Lepfal_015759A.03 (size 206 – present in Chester only at 24% though also noted in Dominica), and Lepfal_003035.04 (size 132 – present in Montserrat at frequency of 5%, and absent from any captive population). The DAPC with source populations showed the separation of Montserrat and Bristol from the rest of the captive populations on one axis, with Chester and Bristol also separating along the other (Figure 6.2b). Alleles significantly contributing to differences between populations, in order of loading, matched those detected between clusters.

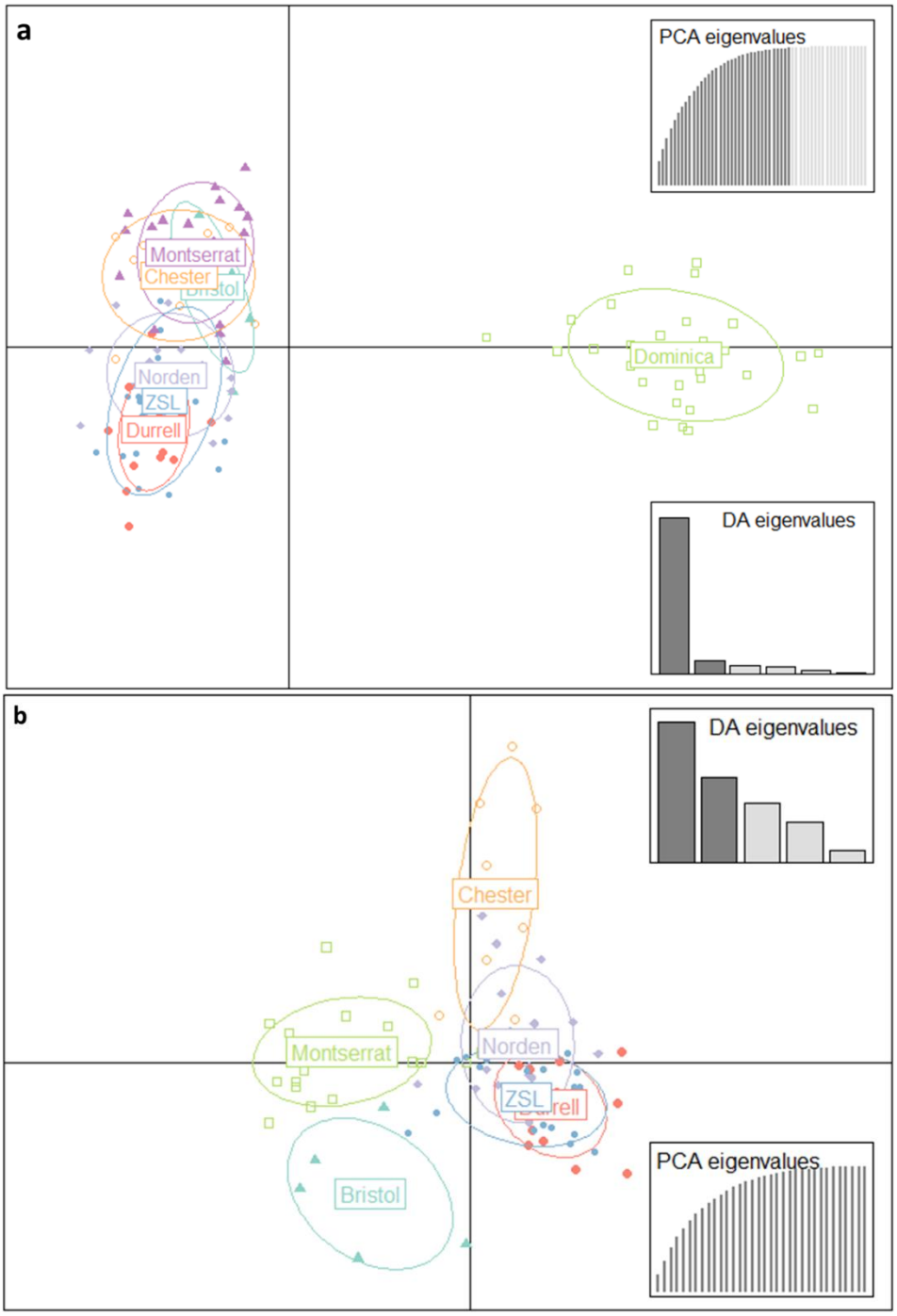

Figure 6.2: a) DAPC analysis including 35 PCAs and six DA Eigenvalues, with source populations used to divide the dataset. b) DAPC analysis of Montserrat and captive populations only, including 35 PCAs and five DA Eigenvalues, with source populations used to divide the dataset.

Representativeness of the Wild Population

Across eight microsatellites, there were 39 alleles in the wild Montserratian population, and the proportion of these alleles shared by the captive metapopulation was 0.7 (Table 6.5), while the average frequency of private alleles was 0.082. After ten years of captive breeding, the captive metapopulation as sampled in 2018 was not genetically representative of the wild Montserratian population, based on the summary statistics produced (Table 6.5). Both expected heterozygosity and the ANAPL in the captive metapopulation were lower than what would be expected in the wild, while observed heterozygosity was higher (supplementary Figure S6.4). From the individual zoo populations as of 2018, only Chester zoo fell within the expected distribution of Montserrat for all three statistics (Table 6.5). Chester and Norden's Ark had representative observed heterozygosity of the wild Montserratian population, while all other zoos had a higher than expected measure (Table 6.5, supplementary Figure S6.4). Expected heterozygosity fell within the range of Montserrat in all zoos except for ZSL, and it was very slightly below the 2.5% quartile at Norden's Ark (Table 6.5, supplementary Figure S6.4). ANAPL was representative of the wild population in Norden's Ark, Durrell, and Chester, but lower than the 2.5% quartile in ZSL and Bristol zoos (Table 6.5, supplementary Figure S6.4). The RTM population in the semi-wild enclosure in Montserrat shared 63% of alleles with its wild source population, but was not representative in heterozygosity or ANAPL (Table 6.5, supplementary Figure S6.4). The biosecure population as of 2021, BCP 2021, was representative of the wild source population in Montserrat, sharing 71% of its alleles (Table 6.5, Figure 6.4). Two alleles are present in BCP 2021 that were not sampled in Montserrat (Table 6.5).

Table 6.5: Assessment of the genetic representativeness of the wild population in Montserrat (n = 87) for each captive population, based on eight microsatellite markers. Each value corresponds to a comparison with the wild population in Montserrat. Higher = higher than the 97.5% quartile of the bootstrap replicate distribution, Lower = lower than the 2.5% quartile, Within = between the 2.5% and 97.5% quartiles.

Population	N	Within 2.5% and 97.5% quartiles?			Proportion of shared alleles	No. private alleles
		Het Obs	***Het Exp***	***ANAPL***		
Captive Metapopulation	74	Higher	Lower	Lower	0.70	3
Bristol	21	Higher	Within	Lower	0.66	0
Norden's Ark	19	Within	Lower	Within	0.68	2
Durrell	19	Higher	Within	Within	0.63	0
ZSL	9	Higher	Lower	Lower	0.67	0
Chester	21	Within	Within	Within	0.69	1
RTM	24	Above	Below	Below	0.63	0
BCP 2021	33	Within	Within	Within	0.71	2

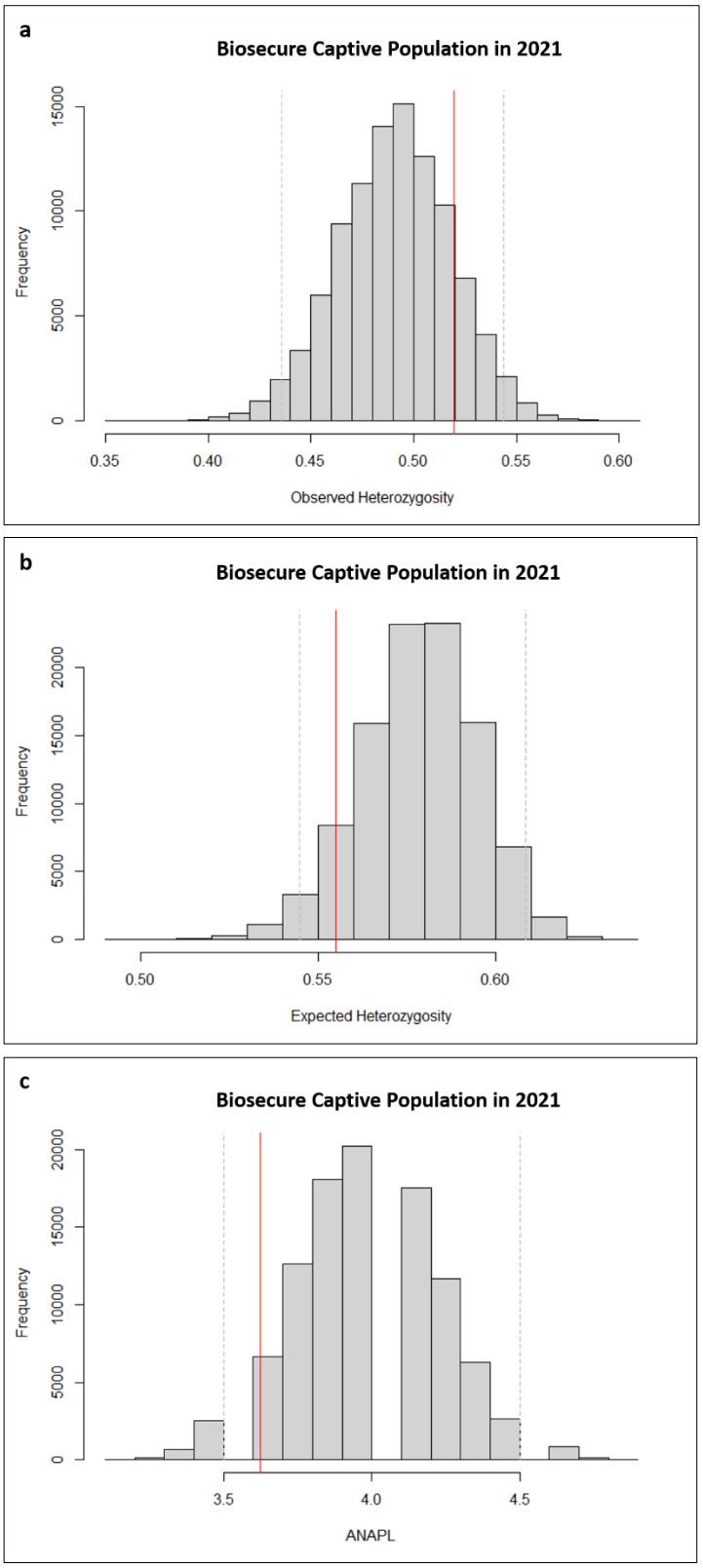

Figure 6.3: The distribution of variation from 100,000 bootstrap replicates of a random sample of 74 wild, Montserratian MCFs. The observed value from the captive population that remains alive as of 2021 is shown as a red line, while 2.5% and 97.5% quartiles of the distribution are shown as grey, dashed lines. a) Observed heterozygosity, b) Expected heterozygosity, c) Average number of alleles per locus.

Discussion

This study aimed to assess the genetic diversity and structure of the biosecure captive population of MCFs after a decade of ex situ management. Reintroductions to the wild will be sourced from this population, so genetic diversity from potential wild release sites in Dominica and Montserrat was assessed to enable a quantification of genetic divergence in the biosecure captive populations.

Genetic Outcome of Captive Management to Date

A decade of captive breeding does not appear to have drastically reduced genetic diversity in relation to the wild source population. Some genetic diversity was still lost, as hypothesised. The captive metapopulation, as of 2018, had maintained observed heterozygosity to expected levels with no sign of in- or outbreeding. Allelic richness and heterozygosity were higher than the source population in Montserrat and ANAPL was only slightly lower. When studied as individual zoos, heterozygosity was maintained at higher levels than Montserrat. There was, however, a loss of allelic diversity in relation to the wild source population, with an average of 0.323 alleles lost across 11 loci from 2009 – 2018. The smaller size of zoo populations in comparison to Montserrat and the captive metapopulation introduces a sampling bias, reducing the likelihood that all alleles will be present in every zoo. This highlights that different inferences can be made depending on whether the biosecure population is treated as one or as separate reproductive units, which could have different consequences for management. The 2018 captive metapopulation was not in HWE due to having loci with heterozygote excess and some with a deficit. Heterozygote deficiency at some loci could have been inherited and perpetuated from the wild founders, which were showing significant levels of inbreeding. It may also be due non-random or consanguineous mating in captivity (Castric et al. 2002). An excess of heterozygotes can be due to small effective population size, sampling bias, or selection favouring heterozygotes within a population (Waples 2015), although it is unclear which would be the case for the captive metapopulation. Both deviations from HWE could be a result of the Wahlund effect or its converse, the isolate breaking effect, through the creation of the captive population from populations in Montserrat with different allele frequencies (Wahlund 1928; Holland 2000; Castric et al. 2002). However, most founders were sourced from one location, Fairy Walk, making this theory less plausible (Adams et al. 2014). The removal of the RTM population left the remaining biosecure population (BCP 2021) with lower-than-expected heterozygosity, but this was still higher than in the source Montserrat population. Comparatively higher allelic richness to Montserrat was maintained in BCP 2021, while ANAPL was only slightly lower – no change from the 2018 captive metapopulation. There was no signal of inbreeding in BCP 2021. In total, the lost allelic richness in BCP 2021 through the Montserrat release was an average of 0.051 alleles across 11 loci. HWE was not present in the BCP 2021 population due to heterozygote deficiency, most likely caused by an inherited deficiency from founders and/or some consanguineous mating (Castric et al. 2002).

As the loss of some genetic diversity in captivity is almost inevitable, captive management of the MCF has been quite successful in maintaining diversity (Frankham 2008). This is especially hard to achieve in the cases of endangered tropical amphibians such as the MCF, where the number of founders is relatively small, and the species has specific environmental requirements for breeding (Tapley et al. 2015; Jameson et al. 2019a). Losses of genetic diversity were relatively small compared with other

published amphibian studies, although the MCF had spent just one or two generations in captivity in 2018. Captive Mallorcan midwife toads (*Alytes muletensis*) suffered a reduction in heterozygosity of 1.2 fold and lost 3.15 alleles over eight generations in captivity, but losses were not significant over fewer generations (Kraaijeveld-Smit et al. 2006). Similarly, reduced allelic richness and heterozygosity were observed in a captive population of *Rana muscosa* when compared with a wild metapopulation, with an average of two alleles lost per locus and heterozygosity reduced by 1.75x over a period of no more than five years – approximately 2.5 generations (Schoville et al. 2011). Like with the MCF captive metapopulation, the Puerto Rican crested toad (*Peltophryne lemur*) did not suffer a significant loss of diversity based on an analysis of two captive populations, though the age of captive populations in that study was unclear (Beauclerc et al. 2010). Despite there being many captive breeding programmes for amphibians, there are far fewer published records of the impact of captivity on genetic diversity compared with wild populations with which to contextualise the MCF breeding programme (Harding et al. 2016). These studies would be very useful for setting taxa-specific benchmarks and guidelines.

Studbooks enabled some maintenance of wild MCF genetic diversity within the biosecure captive population without a priori knowledge of exact levels of diversity. This genetic diversity was not evenly distributed across institutions, which is the unintended outcome of not knowing the genotype of each individual prior to division of samples between zoos. Structure, DAPC, and F_{ST} were consistent in their estimations of Chester and Bristol zoos as the most divergent from other zoos and Durrell and ZSL as most similar to one another. Norden's Ark appeared to be a mid-point in allele frequencies between zoos and was most similar, with Chester zoo, to Montserrat. This has most likely occurred due to the chance distribution of founders in 2009, alongside variation in breeding rates, genetic drift, and pathways/frequency of exchange between institutions. For example, Durrell and ZSL zoos had relatively higher rates of exchange than other zoos, and many of the individuals sampled from Durrell and ZSL were the result of a single, large breeding event (M. Hudson, *pers. comm*.), explaining the high similarity between these institutions.

Based on the bootstrap analysis of expected genetic diversity at eight loci in Montserrat, the captive metapopulation measured in 2018 did not fall within the 2.5% and 97.5% confidence intervals due to high observed heterozygosity but lower expected heterozygosity and ANAPL. Fortunately for future management, the population remaining in captivity as of 2021 (BCP 2021) had levels of heterozygosity and ANAPL equivalent to what might be expected in the wild in Montserrat in a population of the same size. The discrepancy between the populations measured in 2018 and 2021 may be in part due to the difference in the expected wild distribution generated to match the different sample sizes of the captive populations in 2018 (n = 73) and 2021 (n = 33). The 2018 metapopulation's expected heterozygosity and ANAPL would be within the expected distributions of the BCP 2021, for example. Observed heterozygosity could have been higher in the 2018 metapopulation due to the increased number of individuals sampled. The capture of genetic representativeness in the initial founders in 2009 (Hudson et al. 2016a) most likely enabled representativeness in the BCP 2021 population, but it is also testament to the effectiveness of studbook management to date. Pedigrees can be as successful as molecular markers at predicting inbreeding in captive populations and have maintained diversity in

the F1 generation of MCFs (Townsend and Jamieson 2013). As the remaining captive population is still genetically representative of the source population, there is room for optimism that with the same management approaches, diversity close to that which once existed in Montserrat can be maintained. However, samples in this study represent only one or two generations of breeding in the captive population. With each successive future generation, the opportunity for drift and selection to limit the available genetic diversity will increase, especially in a species difficult to breed in captivity such as the MCF, where not all individuals have been contributing to breeding (Kraaijeveld-Smit et al. 2006; Frankham 2008; Tapley et al. 2015). MCFs reach sexual maturity at around three years old (Daltry 2002), which is a longer generation time than characteristic for tropical amphibians but still shorter than some species which have generation times >5 years (Tapley et al. 2015). Longer generation times offer more protection against loss of diversity or adaptation to captivity (Frankham 2008). Difficulties encountered in the management of the population have included declines in fertility, various gastrointestinal issues, and diseases such as adenocarcinoma (Jameson et al. 2019a; Ashpole et al. 2021). While some issues could be diet related, as might occur in captivity where the full wild diet cannot be replicated, any genetic link may be exacerbated if the population tends towards inbreeding, where deleterious mutations can accumulate (Keller and Waller 2002; Jameson et al. 2019a). As two loci from BCP 2021 are already in heterozygote deficiency and the founding source population was already showing signs of genetic diversity loss, captive management must preserve as much genetic diversity as possible into the future.

Implications for Future Management

Breeding

The biosecure captive population was initiated as a rapid response to save MCFs likely to die in the wild due to the approaching wave of chytridiomycosis (Hudson et al. 2016a). The goal for captive management is to maintain the genetic stability and health of the population for potential future reintroductions (Jameson et al. 2019a). A general target against which to assess genetic stability is the maintenance of at least 90% of source population heterozygosity for 100 years (Frankham et al. 2004). The biosecure captive population maintained observed heterozygosity above that of the source population in Montserrat after ten years of captive management. The key goal for future management is to preserve this level over the coming decades.

Frankham (2008) predicted that genetic adaptation to captivity could be reduced by increasing effective population size, preserving genetic diversity, allowing fewer generations in captivity, and reducing the intensity of selection in captivity. The recommended population size for the biosecure population prior to the evaluation with molecular markers was 70 individuals (Garcia and Schad 2015), which so far has proved sufficient to maintain diversity. To assess how well this recommended population size might avoid inbreeding depression in the future, these new genetic data could be incorporated into population viability assessments for the captive population (Zachos et al. 2009; Iwona et al. 2018). New information from these models may allow an improved recommendation to be made for the minimum recommended captive population size. Increasing the population size may be difficult due to constraints on capacity within enclosures, and due to sourcing suitable new stock. There are currently thought to be no wild Montserratian frogs to supplement the captive programme,

which could alleviate the loss of diversity after several generations of captive breeding (Schönhuth et al. 2003). More MCFs do exist in several institutions across Europe and the USA in non-biosecure captive populations, founded from Montserratian MCFs between 1999 and 2006 (Gibson and Buley 2004; Adams et al. 2014). This may not be an attractive option as great efforts have been made to establish the biosecurity of the quarantine population and supplementation with non-biosecure individuals would negate these efforts, as well as fundamentally altering the management plan for both populations (Jameson et al. 2019a). However, given the difficulties encountered with breeding some MCFs in the biosecure population, its relatively small size, and increasing risk of diversity loss through future generations, the addition of non-biosecure individuals at some point in the future should not be ruled out and should at least be explored in population viability assessments.

The biosecure population is managed as one metapopulation (Jameson et al. 2019a), but this study revealed that different zoos had different predominant genetic clusters. Managing an ex situ programme via multiple, reproductively isolated institutions can buffer against genetic adaptation to captivity and the loss of source population diversity more effectively than with a single population (Margan et al. 1998). In this case, continuing to manage the biosecure population as a metapopulation would be recommended on the basis that 1) the source population was sourced from one area at Fairy Walk, and thus unlikely to be highly genetically structured and 2) metapopulation management was successful in preserving diversity to date. However, metapopulation management should now incorporate the new genetic data uncovered in this study, to prevent the loss of the unique or rare genotypes held in some institutions. For example, private alleles in Norden's Ark and Chester represent a portion of Dominican diversity and individuals with these alleles should be prioritised for breeding within or between these institutions to ensure they are not lost. This should also be done for the alleles identified as driving distinction between the biosecure population and Montserrat. One such allele was found in Chester (Lepfal_015759A.03, size 206), alongside Lepfal_003035.04 (size 132) which was lost in the captive population but found in Montserrat. To enable the most relevant breeding recommendations as generations progress, genetic monitoring of the captive population should be continued in order to track rarer alleles, overall diversity levels, and prioritise individuals for breeding (discussed in Schwartz et al. 2007). Regular genetic monitoring will enable the evaluation of management decisions, and if necessary allow breeding management to be amended going forwards.

Reintroductions

Following current management plans, future reintroductions to the wild will be sourced from the remaining biosecure captive population or its future generations (Adams et al. 2014). These individuals will be part of or descended from BCP 2021, which was genetically representative of the wild source population's heterozygosity and number of alleles and shared 70% of its alleles. Despite this, the diversity did not appear evenly distributed between institutions. It is probable that to reintroduce the full suite of alleles back into the wild, individuals should be chosen from all institutions. To enable this, each zoo population requires sufficient numbers of MCFs to allow removal of offspring (M. Hudson, *pers. comm*.). Similar recommendations have been made for the common midwife toad (*Alytes obstetricans*) when selecting individuals to form a captive breeding programme, on the basis that separate wild populations with some evidence of gene flow should all be used to

maximise genetic diversity (Albert et al. 2015). While the observed heterozygosity of the RTM population was higher than Montserrat's, which can be beneficial if it enables greater plasticity in the face of threats (Keller and Waller 2002), the ANAPL was lower, indicating that the higher level of heterozygosity may not be maintained through successive generations unless new alleles are introduced. If individuals were to be chosen to supplement the semi-wild enclosure population, they should ideally come from institutions other than Durrell or ZSL (where the initial RTM population was sourced from), given the high genetic similarity of these populations compared to other zoos.

To date the biosecure captive population has been used for experimental reintroductions to Montserrat (Hudson et al. 2016b). These releases have shown that without mitigating the threat of chytridiomycosis in the wild, MCFs cannot survive without continued intervention such as anti-fungal itraconazole treatment (Hudson et al. 2016b). To be able to fulfil the aim of the recovery plan of having growing populations of mountain chickens at five sites on each island, the negative impacts of *Batrachochytrium dendrobatidis* (Bd) infection on MCF survival must first be mitigated. While there are numerous global efforts to achieve this in the lab, and some in the field (Garner et al. 2016), it may not arise for some time. This is a difficult point to consider in the recovery plan for the MCF, as reintroduction success may decline with generations spent in captivity (Araki et al. 2007; Frankham 2008).

There is potential for released captive bred individuals to lower the fitness of wild populations (Araki et al. 2007), so it is important to consider where releases might be most suitable. In the long-term recovery plan for the MCF, the biosecure captive population is set out as source of individuals for reintroduction to the wild. The home range of the MCF covers Dominica and Montserrat, and is thought to have extended further throughout the Lesser Antilles until a few hundred years ago (King and Ashmore 2014). No distinction is made in the recovery plan between Dominica and Montserrat as potential reintroduction destinations (Adams et al. 2014). Results from this study suggest that Montserrat should be prioritised for reintroductions over Dominica as the BCP 2021 is significantly genetically diverged from Dominica, sharing 54% of its alleles. Reintroductions to Dominica could risk the loss of unique variation of source or destination populations, and any local adaptations of wild Dominican MCFs (Edmands 2007). Besides microsatellite genetic variation, a more specific risk to consider is the fact that the biosecure population is immunologically naïve to Bd, and the current wild population in Dominica has survived the chytridiomycosis outbreak (Hudson et al. 2016a; *Author's unpublished data* 2019). One supposed mechanism for this could be an evolved Bd-tolerance (Adams et al. 2014). Some studies have linked specific major histocompatibility complex (MHC) diversity to Bd response in amphibians (Bataille et al. 2015; Kosch et al. 2019). Understanding the diversity of key immune loci from the MHC would also contribute to a more holistic genetic captive management plan – see Chapter 3 for this study. An additional risk of releasing Montserratian animals in Dominica would be introducing genetic variation linked to Bd-susceptibility into a population which may have evolved tolerance or resistance to Bd. As such, Dominica should be a last resort for reintroductions from the biosecure captive population while a wild population exists there and until the genetic basis for Bd-tolerance can be further studied. The absence of a wild population in Montserrat and the genetic similarity to the captive population makes it a far more suitable location for reintroductions.

Conclusion

This study provides an up-to-date assessment of the genetic structure and diversity held within the biosecure captive population of MCFs up until 2018 and also an assessment of the two populations created after 2019: the RTM and remaining BCP 2021 population. The captive population maintained similar levels of genetic diversity to the source population in Montserrat through the first decade of its management, showing that studbook management was effective at least into the first two generations. Differences in exchange of MCFs and breeding rates between institutions has likely contributed to an uneven distribution of the wild genetic structure across the zoos, but this can be managed through continued metapopulation management with targeted breeding of individuals with rare genotypes. After the removal of some individuals to Montserrat in 2019, the captive population regained its genetic representativeness of the wild source population and breeding recommendations were made to best preserve this diversity. To maintain a genetically diverse biosecure population into the future, non-biosecure sources of genetic variation should be considered in population viability modelling and the incorporation of genetic data into adaptive management should be continued. These recommendations will aid the preservation of diversity until the threat of disease in the wild can be mitigated.

Chapter Seven

General Discussion

Overview

The purpose of this thesis was to further our understanding of the dynamics and determinants of survival in the MCF following a chytridiomycosis epizootic, to aid the conservation of this Critically Endangered species. This objective was approached within the context of the disease triangle theory of infectious disease (McNew 1960). A great deal of research has been carried out into the interaction between other amphibian hosts, the pathogen Bd, and the environmental conditions that mediate the likelihood of chytridiomycosis occurring (reviewed in Fisher and Garner 2020; Brannelly et al. 2021). In the case of the MCF, studies into the dynamics and determinants of Bd infection have been largely environmentally focused (Hudson et al. 2016c) and factors relating to host immunity or the pathogen remained unstudied. To move towards a more holistic overview of the MCF-Bd interaction, this thesis focused on producing new data relating to host and pathogen-associated dynamics and determinants of Bd infection survival or susceptibility.

Dynamics and Determinants of MCF Survival Following a Bd Epizootic

The five data chapters presented in this thesis reveal determinants of MCF susceptibility or survival from Bd that are host-related, rather than pathogen-related. These new data, alongside existing work on the environmental dynamics of Bd infection risk, suggest that susceptibility or survival in the MCF following Bd exposure depends more heavily on the disease triangle corners of host and environment.

Chapter Two provided the first demographic simulation of the origin of modern-day MCF populations on Dominica and Montserrat and provided context for subsequent chapters. Simulations estimated that the MCF had already experienced a large population decline several centuries before the arrival of Bd. This decline is likely to have promoted the genetic divergence of modern day populations in Dominica and Montserrat. Parallels can be drawn between the near-extinction of the MCF in the 21st century and the large population decline estimated around the 17th century in Chapter Two. Recent MCF declines were due to the chytridiomycosis panzootic, which has its roots in anthropogenic activity (O'Hanlon et al. 2018). More ancient population bottlenecks estimated by Chapter Two also coincided with the destruction of biodiversity and societies that resulted from European colonisation of the Caribbean (Wilson 1997; Ricklefs and Bermingham 2008). This observation serves as a reminder of our influence on wildlife and precedes the studies in the thesis which hope to more positively impact the recovery dynamics in the MCF by aiding conservation research and intervention.

More directly addressing the questions of this thesis, Chapter Two provided an explanation as to why, in Chapter Three, the MHC diversity of the MCF is so low compared to other amphibian species. Here we see putative proximal and distal determinants of Bd vulnerability in the MCF. As a proximal determinant, MCF populations were probably overwhelmingly vulnerable to Bd infection in the 2000's

due to their small repertoire of MHC alleles, which were particularly depleted at MHC class II (Bataille et al. 2015). This low MHC diversity is likely to have been at least partly caused by the reduction of the ancestral MCF population size by >90% a few hundred years prior, with this reduction becoming a distal determinant of Bd susceptibility. MHC diversity may also have been reduced as the MCF or its ancestor colonised the Lesser Antilles with a series of founder events in their dispersal from South America (Hedges and Heinicke 2007). A similar phenomenon was observed through the domestication of the guppy *Poecilia reticulata*, where a reduction of MHC class II alleles was induced and subsequently domesticated guppies were more vulnerable to severe infections with the parasite *Gyrodactylus turnbulli* (Smallbone et al. 2021). Chapter Three also provided compelling evidence for a host-related, genetic determinant of Bd-tolerance in the MCF. Within the MCF's low MHC diversity there was evidence of selection and MHC-I variants that were present at significantly high frequencies in groups that survived the Bd epizootic, including a small group which was known to clear detectable Bd infection. The sharp increase in prevalence of three MHC-I alleles, most notably Lepfal-a1*04, but also Lepfal-a1*03 and *05, suggest that some protection from Bd was conferred by MHC-I molecules. This is the first time that MHC-I has been linked to amphibian Bd-tolerance, having previously just been linked to Bd-susceptibility in *P. corroboree* (Kosch et al. 2019).

While Chapter Three covered an important component of the host adaptive immune system, Chapter Four explored a key constitutive innate defence in amphibians: the skin microbiome. The evidence presented by Chapter Four for a determinant of survival from Bd infection or Bd-susceptibility was weaker than that in Chapter Three, though relevant information was still produced. In the first characterisation of the skin-associated bacterial microbiome of the MCF, potential determinants of Bd infection survival were highlighted in Dominican MCFs sampled in 2019. Such determinants included high alpha diversity and increased abundances of particular taxa and metabolic pathways within the skin bacterial community, which have been linked to antifungal defence in other studies (Chaiharn et al. 2009; Ellison et al. 2019; Rojas-Gätjens et al. 2022). Without recorded Bd infection in the sampled wild MCFs, these skin microbiome features cannot yet be confirmed as determinants of Bd-tolerance in the MCF. The low proportions of bacteria listed as Bd-inhibitory in the Dominican MCF's microbiomes may be due to one or a combination of: a lack of selective pressure exerted by Bd in an enzootic state, the evolution of other host defences, irrelevance of microbiome to Bd infection survival, or biases identified in the database of Bd-inhibitory bacteria (Woodhams et al. 2015). Skin microbiome diversity appeared unimportant in preventing Bd infection in a cohort of Bd-naïve MCFs released to Montserrat from captivity. These MCFs regained significant levels of microbiome diversity following their release to the wild, but still suffered a chytridiomycosis outbreak. A persistent reduction in skin microbiome diversity, but not predicted antifungal capacity, was recorded following Bd and itraconazole exposure. Skin microbiome dysbiosis could have been a determinant of lethal chytridiomycosis during the initial Bd epizootic of 2009, via the dysregulation of host physiology or immune function (Jani and Briggs 2014; Walke et al. 2015; Jiménez and Sommer 2017), while antifungal functional redundancy may have protected some individuals (Bletz et al. 2017). Linking this dysbiosis or functional redundancy to Bd-susceptibility was not possible as no MCFs were left to the natural course of Bd infection. Additionally, even if lethal infections were observed, there is no

guarantee that the microbiomes in 2019 would closely resemble those of 2009, during the actual Bd epizootic.

A link between amphibian immunogenes and skin microbiomes has been suggested and could link Chapters Three and Four (Hernández-Gómez et al. 2018; Belasen et al. 2021). In a meta-analysis of plant and animal microbiomes, Woodhams et al. (2020) determined that host immune system complexity (the presence of adaptive immunity) and its regulation of both commensal and pathogenic bacteria may promote microbiome diversity via decreased competition and facilitation of taxa coexistence (Woodhams et al. 2020). *Thoropa taophora* frogs with heterozygous MHC-IIB genotypes had higher skin microbiome alpha diversity, distinct compositions, and negative associations with eukaryotic and fungal parasites compared to MHC-IIB homozygotes (Belasen et al. 2021). Chapter Three found an almost monomorphic MHC-II exon 2 across all MCF groups. Low MHC-II diversity may have rendered the majority of MCFs doubly vulnerable to Bd infection. Firstly, through a reduced immunological capacity to directly respond to Bd (Bataille et al. 2015). Secondly, through a reduced ability to regulate extracellular commensal microorganisms which defend against Bd infection and/or pathogenic microorganisms which exacerbate the stress of Bd infection (Brucker et al. 2008; Johnson and Hoverman 2012). Conversely, higher MHC-I diversity seen in Bd-tolerant groups has the potential to better promote skin microbial diversity as well as respond to active Bd infection. For example, following metamorphosis, significant shifts in amphibian skin microbiome composition and increases in alpha diversity have been observed (Kueneman et al. 2014; Bataille et al. 2018; Jimenez Quiros et al. 2019). These changes coincide with the restructuring of the immune system to include fully functioning MHC-I loci – larval amphibians express MHC-IA loci in their skin at a much lower rate than adults, and MHC-IB loci only appear following metamorphosis (Rollins-Smith 1998; Lau et al. 2020). The MHC-I, therefore, plausibly has some immunoregulatory capacity over skin microorganisms and this has been directly demonstrated in mammals (Linehan et al. 2018). Wild, surviving MCFs in Chapter Four had high microbiome diversity but low predicted antifungal capacity, and Montserratian MCFs the opposite. From the samples which could be matched between Chapters Three and Four (all from Dominica and 17 from the Montserrat release), on average there were 3.3 MHC-I alleles in Dominican MCFs and 2.3 in the Montserratian release cohort. In Dominican MCFs, higher MHC-I diversity could have lessened the need for antifungal bacteria in the corresponding MCF's microbiomes by providing a more effective host immune response to Bd and promoting a diverse, resilient microbiome. Lower MHC diversity in Montserratian MCFs may have increased the need to recruit antifungal bacteria following a Bd-challenge. This in turn may lower alpha diversity, if the recruited bacteria are largely the same or phylogenetically similar taxa with antifungal activity (Kueneman et al. 2014). More research that directly tests the role of the MHC, especially MHC-I, in regulating the amphibian skin microbiome and the ultimate outcomes for defence against Bd infection is required. The MHC-microbiome interaction in the MCF remains only a hypothetical additional determinant of Bd infection survival until this research is available.

With host-related determinants of Bd epizootic survival explored in Chapters Two, Three, and Four, Chapter Five aimed to provide an insight to pathogen-related determinants. Chapter Five re-examined the archive of Bd DNA collected through different years, countries, and amphibian hosts involved in

the chytridiomycosis epizootic that decimated the MCF. Bd samples were assigned to one of six global lineages and the genetic diversity and structure contained within the epizootic was assessed. In the first of such studies from the Caribbean, it was revealed that the hypervirulent BdGPL lineage is solely responsible for the decline of the MCF. No link was found between pathogen genotype, diversity, or genetic structure and differential Bd-infection outcomes in MCFs. Chapter Five extends our understanding of the dynamics of Bd survival in the MCF: it occurred despite the continued presence of a likely clonal and hypervirulent pathogen. This finding is in keeping with other major studies of recovering amphibian populations, where pathogen-related factors such as virulence remain unchanged but hosts exhibit a more robust immune response (Voyles et al. 2018). Taken with the results of Hudson et al. (2019) and Chapters Two, Three and Four in this thesis, we can more readily conclude that surviving Bd-tolerant MCFs likely have evolved defences and/or exist in environmental conditions that limit Bd proliferation.

Chapters Two to Five focused on past and present dynamics and determinants of survival/recovery in the MCF, while Chapter Six looked at a key part of its future recovery: the biosecure assurance population's genetic diversity. In this final data chapter, an up to date assessment of neutral genetic diversity, a common indicator of population fitness, was provided after ten years of captive management. The study revealed positive results: levels of neutral genetic diversity had been maintained close to that of the wild source population in Montserrat, and the population as of 2021 was genetically representative of wild, Montserratian MCFs. The risks of losing this genetic representativeness increase over time, however (Frankham 2008). Given that the population was founded from a declining population showing signs of inbreeding, Chapter Six highlighted that is it crucial to make management choices that maximise genetic diversity and maintain it across all five zoos. Coupled with the findings of Chapter Three, several implications for optimal management of the biosecure population arose – these are discussed in both chapters, as well as the 'implications for MCF conservation' section of this chapter. These findings were incorporated into the European Association of Zoos and Aquaria's (EAZA) breeding strategy for the MCF in 2021 and will hopefully positively impact the future dynamics of recovery in the MCF.

Limitations

The extent to which this thesis could answer the question of determinants of Bd-susceptibility or survival in the MCF was limited by various factors. A potential methodological limitation was that Chapters Two, Three, and Six used microsatellites to estimate neutral genetic diversity and demography. Microsatellites are gradually being replaced with methods such as double digest restriction-site associated DNA sequencing (ddRAD) in population genetic studies as microsatellites are laborious to develop and suggested by some to be inferior for estimating ancestral population structure (Andrews et al. 2016; Sunde et al. 2020)**.** Microsatellites were an appropriate choice for this thesis as they have been shown to perform as well as ddRAD in estimating population structure and differentiation (Sunde et al. 2020) and the primers were pre-existing, enabling the work to fit within the timescale and budget of this thesis.

Sample sizes of Bd-tolerant or wild surviving MCF groups were often smaller than comparison groups (Chapters Three and Four). Hurricane Maria in 2017 prevented MCF surveys until 2019, leaving a data gap in 2018. A field trip to gain genetic samples from Bd-tolerant MCFs in Dominica in 2019 found just seven frogs despite two months of surveys. A second trip to Dominica in 2020 was cancelled due to the COVID-19 pandemic and this reduced the potential number of key Bd-tolerant samples to analyse. Uneven or small sample sizes are undesirable due to the sampling bias or loss of statistical power than can result (Hale et al. 2012). Efforts to address this included using metrics that account for sample size (e.g. allelic richness), using relative allele frequencies, bootstrapping tests, and statistical test adjustments (e.g. Fisher's test in place of chi-squared for small groups). However, some level of sampling bias may still be present. One must also consider that the wild MCF population has numbered < 100 since 2014 (Adams et al. 2014) and probably < 50 since 2017 (*Author's unpublished data* 2019). In this case, the 2019 field trip sampled almost 20% of the entire wild population. Also, as most of the species was Bd-susceptible, the uneven sample sizes in this thesis were somewhat inevitable. Adjusting the number of Bd-susceptible MCFs to match Bd-tolerant sample sizes would have involved ignoring valid data and reducing the sample sizes of the overall datasets much further - e.g. by 50% in the comparison of Bd-tolerant and susceptible MCFs in Chapter Three. Issues of data missingness also impacted Chapter Five. Working with a 20 year old archive enabled important temporal insights, but sometimes limited the quality of the work. Bd DNA had been freeze-thawed over the years and used in other studies. Consequently, samples often had lower quantity and quality than desired. Chapter Five was impacted by levels of locus dropout that required lowering stringency thresholds for phylogenetic analysis below that of published works (Byrne et al. 2019). The number of quality SNPs was also lower than published studies (Basanta et al. 2021), which could limit the resolution of conclusions about population structure and diversity in Chapter Five (Morin et al. 2009).

Endangered species are often quite data-deficient due to their scarcity (Borgelt et al. 2022). For the MCF, very few genetic resources existed prior to starting this thesis. The lack of a MCF reference genome limited Chapter Three's ability to assign variants to loci, which meant that less powerful statistics were used. The protected status of the MCF also meant that genetic sampling of live individuals had to be minimally invasive. Chapter Three's conclusions were limited by the inability to identify expressed MHC variants, which requires amplifying MHC loci from reverse transcribed RNA. As discussed in Chapter Three, obtaining RNA samples was too invasive for MCFs. More pertinent conclusions about the impact of Bd on the microbiome could have been drawn in Chapter Four if MCFs had not been treated with itraconazole. This was not possible because the frogs were needed for an ongoing experiment and it was ethically questionable to not intervene when the MCFs in question represented a significant portion of the entire species. Chapter Four was further limited by the chance lack of Bd infection in the Dominican frogs from 2019, which prevented definite conclusions being drawn on skin microbiome characteristics that were Bd-protective. Equally, microbiome samples from two crucial time points, during and shortly after Bd infection in the semi-wild enclosure, perished due to the shutdown of laboratories during the COVID-19 pandemic in 2020. These limitations were often unavoidable, but they are crucial to note as their cumulative impact is that this thesis has uncovered likely determinants of Bd susceptibility or survival, but further work is required to robustly provide definite determinants. Suggestions for future research are discussed in the following sections.

Implications for Amphibian Chytridiomycosis Research

Knowledge Gaps Addressed

Causes of chytridiomycosis-induced amphibian declines and recoveries have been reviewed several times over recent years (James et al. 2015; Garner et al. 2016; Brannelly et al. 2021; Fisher et al. 2021). A recurring theme has been the call for such research to reconcile host, pathogen, and environmental contributors to population declines or recoveries/persistence. The need for simultaneous assessments of these contributors is especially pressing within highly-endangered amphibians (Brannelly et al. 2021). For example, in a review of 19 species persisting or recovering with endemic Bd, just one Critically Endangered species, *Atelopus varius,* had been tested for a host, environmental, or pathogen factor linked to amphibian population persistence (Voyles et al. 2018; Brannelly et al. 2021). In fact, *A. varius* was just one of two species which had been tested for all three disease triangle sides (Brannelly et al. 2021). This thesis has contributed to filling these knowledge gaps by providing a concurrent assessment of a Critically Endangered amphibian host's innate and adaptive immunity alongside associated Bd genotypes. With existing literature linking environmental factors to Bd infection prevalence and intensity (Hudson et al. 2019), all three disease triangle sides have now been addressed for another highly-endangered amphibian, the MCF. This thesis adds to the body of evidence that amphibian population persistence following Bd epizootics is likely to be host and environmentally mediated, rather than related to pathogen changes (Voyles et al. 2018). This thesis admittedly studies one of hundreds of amphibians species known to harbour Bd infections (Scheele et al. 2019a) but this type of work – addressing multiple determinants of Bd infection survival within a single species – is important to account for the context-dependent nature of chytridiomycosis (Brannelly et al. 2021). The MCF is one of only 23 recovering amphibian species with robust sampling pre- and post-decline (Scheele et al. 2019a). Consequently, this thesis was able provide rare temporal genetic comparisons for host and pathogen either side of a Bd epizootic (Chapters Three and Five). The MCF sampling also encompassed the species' entire geographical range, providing a comprehensive spatial overview of the decline and limited recovery of an amphibian population following chytridiomycosis. Besides addressing what determines an amphibian's Bd-susceptibility or survival, this thesis also extended the known range of the BdGPL lineage into Dominica and has most likely placed BdGPL-2 subclade in the Lesser Antilles for the first time. This provides useful information for researchers and conservationists interested in tracking and planning accordingly with the global spread of Bd.

Areas for Further Research

The amphibian MHC-I is relatively understudied compared to MHC-II in relation to Bd, with just one study published to date (Kosch et al. 2019). Chapter Three makes the important point that with an intracellular pathogen such as Bd, the MHC-I should be considered. This has implications for past and future studies into the amphibian MHC and Bd. Studies into several amphibian species have linked MHC-II conformations to chytridiomycosis resistance (Savage and Zamudio 2011; Bataille et al. 2015; Kosch et al. 2016) and it would be useful if these studies could be revisited to also assess the MHC-I. Future studies should aim to look at both MHC-I and -II, as together these classes can reveal more about the selective pressures exerted by both intra- and extracellular parasites of amphibian hosts

than one class alone. From research for Chapter Five, it became evident that there is a lack of Bd monitoring in the Caribbean relative to South, Central, and North America, Europe, and Australia (Byrne et al. 2019). This is particularly pronounced for the Lesser Antilles, with only a few studies reporting on the presence of Bd on four of 24 islands (Alemu I et al. 2008; Hudson et al. 2019; Hudson et al. 2021). With at least 57 species of amphibian in the Lesser Antilles, of which at least 15 are threatened with extinction, understanding the spatial and temporal distribution of Bd and Bd lineages is crucial for a proper understanding of amphibian chytridiomycosis in the region (IUCN 2021). For example, further genotyping throughout the Lesser Antilles with the method of Byrne et al. (2017) could identify the source of the Bd implicated in the decline of the MCF.

From the 20+ years of research on determinants of amphibian chytridiomycosis across the world and the four years spent exploring a few determinants for this thesis, it is clear that there can be many, interacting determinants of chytridiomycosis. Studies focusing on single or several determinants of chytridiomycosis – including this thesis – have produced meaningful advances in our understanding of the problem, e.g. (Berger et al. 1998; Lips et al. 2003; Harris et al. 2009; Bataille et al. 2015)**.** However, considering the potential breadth of immunogenetic responses and genomic changes within an amphibian host and Bd, the thousands of microorganisms and their respective genomes and metabolomes that exist on one host, and the constantly fluctuating environment within which they all exist, choosing just a few potential determinants to study is probably not enough to capture the full picture. A complex problem is going to require more complex investigations. One way to achieve this, for the MCF and other species, is to move towards using and integrating omics technologies. Such "omics" technologies involve a comprehensive study of a given set of molecules – i.e. genomics refers to the study of an entire genome, rather than single genes (Hasin et al. 2017). Omics expand beyond the fixed genome too: transcriptomics study its expression, proteomics the suite of synthesised proteins, and metabolomics the metabolites produced in subsequent biological reactions. Omics are equally as applicable to commensal microbial communities as they are amphibian hosts and their pathogens. In isolation, omics data can provide insights to associations of genes or biological pathways with disease (Hasin et al. 2017; Crandall et al. 2020). When integrated with one another, termed 'multi-omics', causative agents of disease can begin to be inferred (Hasin et al. 2017).

There are several genomic, transcriptomic, and proteomic studies of Bd (Rosenblum et al. 2008; Fisher et al. 2009a; Farrer et al. 2013; Thekkiniath et al. 2015; O'Hanlon et al. 2018). Whole-genome studies of amphibians in relation to Bd can be conducted as a genome wide association study (GWAS) to search for variants linked to Bd infection survival or susceptibility beyond the MHC. Kosch et al. (2019) linked genome-wide heterozygosity to survival from experimental Bd infection in *P. corroboree* with a GWAS. Gene expression studies have been conducted on amphibians infected with Bd (Ellison et al. 2015; Price et al. 2015; Eskew et al. 2018), as well as concurrently on Bd and an infected host (Ellison et al. 2017). Metabolome studies have been applied to the amphibian skin microbiome (Bates et al. 2022) and would be worth extending to the entire mucosome and AMPs secreted by the host (Jiménez et al. 2022). Ideally, omics should be integrated within the same host-microbiome-Bd system, to provide the fullest view of determinants of chytridiomycosis without being confounded by the context-dependent nature of the disease. Multi-omics research has already been proposed for guiding

probiotic selection to mitigate Bd infection (Rebollar et al. 2016), but has not yet been applied. The advantage of multi-omics studies is in casting a wide net for discovery rather than relying on prior research to guide investigations. There is potential for multi-dimensional studies of host-Bd interactions, from genome to metabolome, to produce answers at a faster rate than the past 20 years (Grogan et al. 2018b). Multi-omics may also facilitate a new frontier of chytridiomycosis mitigation situated in synthetic biology, for example through genetic modification of host immune genes with technologies such as CRISPR/Cas9 (Grogan et al. 2018b; Kosch et al. 2022). The drawback to omics technologies is that they require access to deep freezing facilities (< -80ºC) and expensive reagents for sample preparation and preservation (Koh et al. 2022). This is in addition to specialist laboratory equipment and access to supercomputing clouds and statistical know-how capable of handling the 'big data' produced by these methods (Tarazona et al. 2021). Omics work therefore risks excluding research groups without access to the requisite equipment, staff, and funding. Care should be taken to foster research collaborations that enable the sharing of expertise, equipment, and data to minimise the potential inequalities created by moving to multi-omics research (Abreu et al. 2022).

Implications for Mountain Chicken Frog Research

Assembling an annotated reference genome should be a priority for future MCF research as it would aid several avenues of research into host-related determinants of Bd infection survival. An annotated reference MCF genome would uncover the structure of the MCF MHC, allowing more powerful statistical inferences to be made for the data in Chapter Three. Moving towards an omics approach, a reference genome would make whole-genome level analysis easier by providing a mapping reference and it would aid in the design of genotyping by sequencing studies. Currently available MCF samples exist as DNA extracts or tissues that have been stored at -20ºC. Thus, they are unlikely to be suitable for transcriptomic, proteomic, or metabolomics study (Koh et al. 2022)**.** While this remains the case, there are many other host-related factors which merit investigation for their involvement in determining MCF survival from Bd infection (Grogan et al. 2018b). These could include innate defences such as pathogen recognition receptors (PRRs) (Grogan et al. 2018b). A relatively straightforward study could use an assembled MCF genome to design primers for the PRR, Toll-like receptor 2 (TLR-2), which has been shown to be upregulated in late stages of chytridiomycosis (Ellison et al. 2015; Grogan et al. 2018a). TLR-2 diversity could then be compared between the same groups of MCFs as in Chapter Three. Mitochondrial as well as nuclear genomes should be assembled. In response to the suggestion of Chapter Two to investigate MCF mitochondrial DNA on a whole genome scale, a mitogenome was assembled for the MCF (White et al. 2021). To fully meet the recommendations from Chapter Two, more MCF samples from both islands should have mitogenomes assembled and studied for signatures of selection. This information will further illuminate the demographic past of the species.

This chapter has provided a qualitative discussion of some probable determinants of Bd susceptibility or survival in the MCF. A quantitative synthesis of the environmental, host- and pathogen-related determinants of survival in the MCF is still lacking. With this thesis and that of Hudson et al. (2016c), we now have MCF samples with a large array of metadata related to all three corners of the disease triangle. Without needing to collect new data, there will be a subset of MCFs for which there is associated life history data (sex, body size etc.), microsatellite and MHC genotypes, Bd infection

records, and environmental data such as habitat type and season. A smaller subset of MCFs will also have skin microbiome data available. More data, if collected, would help to expand the subset sizes, and more climate data could be downloaded from the WorldClim website. A similar quantitative analysis has recently been published (Torres-Sánchez and Longo 2022). In this study, season, *E. coqui* genomic diversity, *E. coqui* body condition, skin microbiome diversity, and Bd infection intensity were linked in a series of regression analyses and structural equations to study host-microbiome-pathogen interactions. The ultimate outcome was a direct acyclic graphical overview of these analyses, allowing one to visualise a network of correlations between environment, host, and pathogen (Torres-Sánchez and Longo 2022). Replication of these methods for the MCF would allow simultaneous assessment of Bd infection risk factors or determinants of Bd-tolerance, which would be highly valuable for both general amphibian chytridiomycosis research and MCF conservation.

Some research recommendations from Chapters Three and Four involve experimental challenge to MCFs with Bd. Some assays are possible in vitro, with no need to disturb MCFs, e.g. in vitro Bd growth analyses with MCF skin bacterial isolates (Chapter Four). The experimental challenge of MCFs holding MHC-I variants Lepfal-a1*03 and *05 with Bd (Chapter Three), would require in vivo work. The semi-wild enclosure in Montserrat is already enabling experimental work linking environmental manipulation with Bd infection risk (Jameson et al. 2019a). Additionally, the semi-wild enclosure (or any additional enclosure) should be considered for its potential to facilitate in vivo Bd challenges. With appropriate planning, permits, and population viability assessments, collection of omics-quality samples could be possible from experimental enclosures. These samples could be MCF blood drawn during routine health monitoring, skin mucosome samples, live cultured Bd isolates, or collection of other tissues during any post-mortems that might occur. With prior planning these samples could be stored to preserve DNA and RNA, enabling whole genome, proteome, and transcriptomic studies to be developed for the MCF and its interaction with Bd.

New resources which will aid future MCF conservation research are key outcomes of this thesis. Three new microsatellite primers have been optimised and multiplex PCRs developed to integrate with existing markers for Chapter Six (Hudson et al. 2016a). Multi-locus MHC primers were created for Chapter Three, when previously no resources existed. The MHC primers serve as a foundation for future studies that may seek to explore single loci or neighbouring MHC exons. Together, these new resources will aid in future monitoring of MCF neutral and functional genetic diversity. Improvements to existing protocols were suggested for the routine extraction of Bd DNA. Should future genotyping of Bd DNA be attempted, DNA extraction should increase the volume in which DNA is eluted in order to enable the isopropanol precipitation step advised by Byrne et al. (2017).

Implications for Mountain Chicken Frog Conservation

In a recent review of chytrid-driven amphibian declines, Fisher and Garner (2020) stated that "*There is every possibility that strategies for mitigating chytridiomycosis in nature will involve largely ignoring the pathogen and focusing on mitigating other threats or modifying environments and host communities so that the host responses may operate more effectively".* This certainly does appear to be the case for the MCF. In Dominica, conservation should focus on mitigating threats besides Bd while in Montserrat, host and environmental manipulation will probably be more important for mitigating chytridiomycosis in nature. Fortunately, this recommended differential approach to MCF conservation between Montserrat and Dominica largely aligns with current conservation practices: a conservation and monitoring scheme in Dominica and the establishment of experimental enclosures in Montserrat.

In Dominica, MCFs persist with enzootic Bd, probably due to an evolved immune defence in the MHC and probably other currently unstudied host factors. The Dominican population is vital as a source of Bd-tolerant genotypes and as a self-sustaining MCF population which needs minimal intervention beyond habitat protection and monitoring. If the Dominican population is allowed to dwindle, the chances of establishing a naturally Bd-tolerant population of MCFs elsewhere will be greatly reduced. Priorities for the conservation of Dominican MCFs should be centred on providing optimal conditions for population growth: secure habitat, free from pollution, harvesting, and invasive species (Adams et al. 2014). The larger the population in Dominica becomes, the more feasible it becomes to benefit from their evolved Bd-tolerance through translocation into Bd-susceptible populations.

In Montserrat, the re-establishment of the MCF relies on introductions from captive bred individuals. We now know that these individuals have low frequencies of protective MHC-I genotypes, and insufficient microbiome diversities and compositions to protect from Bd infection. This thesis has also highlighted that the Bd infecting MCFs in the semi-wild enclosure is genetically identical to the causative pathogen of the 2009 epizootic. In this case, conservation must rely more heavily on the environmental side of the disease triangle in order to mitigate Bd. Work is already ongoing to this end in Montserrat, using thermal manipulation to try and lessen Bd infection (Jameson et al. 2019a). Environmental manipulation has been shown as effective in lessening the burden or pathogenicity of chytrid fungi (Berger et al. 2004; Schmeller et al. 2014; Stockwell et al. 2015) but may be unsustainable in terms of cost and labour for re-establishing MCFs across Montserrat (Garner et al. 2016). There is potential for environmental manipulation in enclosures to act as a first, but temporary, stage of reintroduction in Montserrat. If environmental manipulations can lessen the intensity or prevalence of Bd infections, while itraconazole treatment prevents lethal infection, then MCFs may begin to develop their own defences through repeated Bd exposures (McMahon et al. 2014). These defences could include increased quantity or potency of AMP secretions (Voyles et al. 2018), behavioural avoidance or clearing of Bd (McMahon et al. 2014), or increased expression of adaptive and innate immune genes during early stages of Bd infection (Grogan et al. 2018a). Natural recovery of some amphibian populations has been recorded 5-13 years after Bd detection, including a small recovery in the Dominican MCF (Perez et al. 2014; Hudson et al. 2016a; Catenazzi et al. 2017). Natural recoveries may take much longer than this, however (Knapp et al. 2016). To speed up the potential natural development of stronger MCF host defences in the semi-wild enclosure, targeted genetic intervention

could also be applied (Kosch et al. 2022). In this case, artificial selection for, and supplementation of, the protective MHC genotypes identified in Chapter Three could increase the Bd-tolerance of the semi-wild enclosure population. Specific considerations and methods to achieve this are discussed in Chapter Three.

A major takeaway is the importance of genetic monitoring for MCF conservation. With the genetic analyses presented in this thesis, it was possible to add detail to the story of the MCF with historic demographic simulations, to discover new insights to the genetic basis of Bd-tolerance, and assess neutral genetic diversity in the potential founders of a new MCF population in Montserrat. Genetic monitoring is integral to recommended conservation actions in Chapters Three and Six (identify presence of Lepfal-a1*04 in wider captive collection, monitor and breed for Lepfal-a1*03 and *05 in biosecure populations, and monitor and maximise neutral genetic diversity in collections). Going forwards, genetic analysis and monitoring should be a key part of adaptive conservation management of the MCF and mitigating the impact of Bd in the wild.

Conclusion

The research presented in this thesis has built on a body of evidence that the dynamics and determinants of survival from or susceptibility to Bd infection in the MCF are weighted more towards the host and environment sides of the disease triangle than the pathogen side. With these new insights, future research and conservation of the Critically Endangered MCF can be more effectively directed towards mitigating the harmful impacts of Bd in nature and enabling the recovery of the MCF.

References

Abramyan, J. and Stajich, J.E. 2012. Species-specific chitin-binding module 18 expansion in the amphibian pathogen Batrachochytrium dendrobatidis. *mBio* 3(3), pp. e00150-00112. doi: 10.1128/mBio.00150-12.

Abreu, A. et al. 2022. Priorities for ocean microbiome research. *Nature Microbiology* 7(7), pp. 937–947. doi: 10.1038/s41564-022-01145-5.

Acevedo-Whitehouse, K. and Cunningham, A.A. 2006. Is MHC enough for understanding wildlife immunogenetics? *Trends in Ecology and Evolution* 21(8), pp. 433–438. doi: 10.1016/j.tree.2006.05.010.

Adamack, A.T. and Gruber, B. 2014. PopGenReport: simplifying basic population genetic analyses in R. *Methods in Ecology and Evolution* 5(4), pp. 384–387. doi: 10.1111/2041-210X.12158.

Adams, S.L. et al. 2014. Saving the mountain chicken mountain chicken 2014-2034. *Mountain Chicken Recovery Programme* , pp. 1–58.

Aguilar, A., Roemer, G., Debenham, S., Binns, M., Garcelon, D. and Wayne, R.K. 2004. High MHC diversity maintained by balancing selection in an otherwise genetically monomorphic mammal. *Proceedings of the National Academy of Sciences* 101(10), pp. 3490–3494. doi: 10.1073/PNAS.0306582101.

Aislabie, J., Deslippe, J.R., and Dymond, J. R. 2013. Soil microbes and their contribution to soil services. In: *Ecosystem Services in New Zealand - conditions and trends.* Lincoln, New Zealand: Manaaki Whenua Press, pp. 143–161.

Albert, E.M., Fernández-Beaskoetxea, S., Godoy, J.A., Tobler, U., Schmidt, B.R. and Bosch, J. 2015. Genetic management of an amphibian population after a chytridiomycosis outbreak. *Conservation Genetics* 16(1), pp. 103–111. doi: 10.1007/s10592-014-0644-6.

Alemu I, J.B. et al. 2008. Presence of the chytrid fungus Batrachochytrium dendrobatidis in populations of the critically endangered frog Mannophryne olmonae in Tobago, West Indies. *EcoHealth* 5(1), pp. 34–39. doi: 10.1007/s10393-008-0154-4.

Alexander, D.H. and Lange, K. 2011. Enhancements to the ADMIXTURE algorithm for individual ancestry estimation. *BMC Bioinformatics* 12(1), p. 246. doi: 10.1186/1471-2105-12-246.

Alho, J.S., Herczeg, G. and Merilä, J. 2008. Female-biased sex ratios in subarctic common frogs. *Journal of Zoology* 275(1), pp. 57–63. doi: 10.1111/j.1469-7998.2007.00409.x.

Allio, R., Donega, S., Galtier, N. and Nabholz, B. 2017. Large variation in the ratio of mitochondrial to nuclear mutation rate across animals: Implications for genetic diversity and the use of mitochondrial DNA as a molecular marker. *Molecular Biology and Evolution* 34(11), pp. 2762–2772. doi: 10.1093/molbev/msx197.

Almathen, F. et al. 2016. Ancient and modern DNA reveal dynamics of domestication and cross-continental dispersal of the dromedary. *Proceedings of the National Academy of Sciences of the United States of America* 113(24), pp. 6707–6712. doi: 10.1073/pnas.1519508113.

Amills, M. et al. 2004. Low diversity in the major histocompatibility complex class II DRB1 gene of the Spanish ibex, Capra pyrenaica. *Heredity* 93(3), pp. 266–272. doi: 10.1038/sj.hdy.6800499.

Anderson, M.J. and Walsh, D.C.I. 2013. PERMANOVA, ANOSIM, and the Mantel test in the face of heterogeneous dispersions: What null hypothesis are you testing? *Ecological Monographs* 83(4), pp. 557–574. doi: 10.1890/12-2010.1.

Andrews, K.R., Good, J.M., Miller, M.R., Luikart, G. and Hohenlohe, P.A. 2016. Harnessing the power of RADseq for ecological and evolutionary genomics. *Nature reviews. Genetics* 17(2), pp. 81–92. doi: 10.1038/nrg.2015.28.

Araki, H., Cooper, B. and Blouin, M.S. 2007. Genetic effects of captive breeding cause a rapid, cumulative fitness decline in the wild. *Science* 318(5847), pp. 100–103. doi: 10.1126/science.1145621.

Argüello, H. et al. 2018. Early Salmonella Typhimurium infection in pigs disrupts Microbiome composition and functionality principally at the ileum mucosa. *Scientific Reports* 8(1), p. 7788. doi: 10.1038/s41598-018-26083-3.

Ashpole, I.P. et al. 2021. A retrospective review of post-metamorphic mountain chicken frog (leptodactylus fallax) necropsy findings from european zoological collections, 1998 to 2018. *Journal of Zoo and Wildlife Medicine* 52(1), pp. 133–144. doi: 10.1638/2019-0158.

Auwera, G.A. et al. 2013. From FastQ Data to High-Confidence Variant Calls: The Genome Analysis Toolkit Best Practices Pipeline. *Current Protocols in Bioinformatics* 43(1), p. 11.10.1-11.10.33. doi: 10.1002/0471250953.bi1110s43.

Baayen, R.H., Davidson, D.J. and Bates, D.M. 2008. Mixed-effects modeling with crossed random effects for subjects and items. *Journal of Memory and Language* 59(4), pp. 390–412. doi: 10.1016/J.JML.2007.12.005.

Babik, W. 2010. Methods for MHC genotyping in non-model vertebrates. *Molecular Ecology Resources* 10(2), pp. 237–251. doi: 10.1111/j.1755-0998.2009.02788.x.

Bahrndorff, S., Alemu, T., Alemneh, T. and Lund Nielsen, J. 2016. The Microbiome of Animals: Implications for Conservation Biology. *International Journal of Genomics* 2016, p. e5304028. doi: 10.1155/2016/5304028.

Balloux, F., Lehmann, L. and De Meeûs, T. 2003. The population genetics of clonal and partially clonal diploids. *Genetics* 164(4), pp. 1635–1644. doi: 10.2135/cropsci1967.0011183X000700040005x.

Bancroft, B.A. et al. 2011. Species-level correlates of susceptibility to the pathogenic amphibian fungus Batrachochytrium dendrobatidis in the United States. *Biodiversity and Conservation* 20(9), pp. 1911–1920. doi: 10.1007/s10531-011-0066-4.

Barnosky, A.D. et al. 2011. Has the Earth's sixth mass extinction already arrived? *Nature* 471(7336), pp. 51–57. doi: 10.1038/nature09678.

Barragán-Barrera, D.C., May-Collado, L.J., Tezanos-Pinto, G., Islas-Villanueva, V., Correa-Cárdenas, C.A. and Caballero, S. 2017. High genetic structure and low mitochondrial diversity in bottlenose dolphins of the Archipelago of Bocas del Toro, Panama: A population at risk? Chiang, T.-Y. ed. *PLOS ONE* 12(12), p. e0189370. doi: 10.1371/journal.pone.0189370.

Basanta, M.D., Byrne, A.Q., Rosenblum, E.B., Piovia-Scott, J. and Parra-Olea, G. 2021. Early presence of Batrachochytrium dendrobatidis in Mexico with a contemporary dominance of the global panzootic lineage. *Molecular Ecology* 30(2), pp. 424–437. doi: 10.1111/mec.15733.

Basanta, M.D., Rebollar, E.A., García-Castillo, M.G., Rosenblum, E.B., Byrne, A.Q., Piovia-Scott, J. and Parra-Olea, G. 2022. Genetic variation of Batrachochytrium dendrobatidis is linked to skin bacterial diversity in the Pacific treefrog Hyliola regilla (hypochondriaca). *Environmental Microbiology* 24(1), pp. 494–506. doi: 10.1111/1462-2920.15861.

Bataille, A. et al. 2015. Susceptibility of amphibians to chytridiomycosis is associated with MHC class II conformation. *Proceedings of the Royal Society B: Biological Sciences* 282(1805). Available at: http://dx.doi.org/10.1098/rspb.2014.3127orviahttp://rspb.royalsocietypublishing.org. [Accessed: 8 January 2019].

Bataille, A., Lee-Cruz, L., Tripathi, B. and Waldman, B. 2018. Skin Bacterial Community Reorganization Following Metamorphosis of the Fire-Bellied Toad (Bombina orientalis). *Microbial Ecology* 75(2), pp. 505–514. doi: 10.1007/s00248-017-1034-7.

Bates, D., Mächler, M., Bolker, B.M. and Walker, S.C. 2015. Fitting Linear Mixed-Effects Models Using lme4. *Journal of Statistical Software* 67(1), pp. 1–48. doi: 10.18637/JSS.V067.I01.

Bates, K.A. et al. 2022. Microbiome function predicts amphibian chytridiomycosis disease dynamics. *Microbiome 2022 10:1* 10(1), pp. 1–16. doi: 10.1186/S40168-021-01215-6.

Battaglia, T. 2019. btools: A suite of R function for all types of microbial diversity analyses.

Bazin, E., Glémin, S. and Galtier, N. 2006. Population size does not influence mitochondrial genetic diversity in animals. *Science* 312(5773), pp. 570–572. doi: 10.1126/science.1122033.

Beauclerc, K.B., Johnson, B. and White, B.N. 2010. Genetic rescue of an inbred captive population of the critically endangered Puerto Rican crested toad (Peltophryne lemur) by mixing lineages. *Conservation Genetics* 11(1), pp. 21–32. doi: 10.1007/s10592-008-9782-z.

Beaumont, M.A. 1999. Detecting population expansion and decline using microsatellites. *Genetics* 153(4), pp. 2013–2029.

Becker, C.G. et al. 2017a. Variation in phenotype and virulence among enzootic and panzootic amphibian chytrid lineages. *Fungal Ecology* 26, pp. 45–50. doi: 10.1016/j.funeco.2016.11.007.

Becker, C.G., Longo, A.V., Haddad, C.F.B. and Zamudio, K.R. 2017b. Land cover and forest connectivity alter the interactions among host, pathogen and skin microbiome. *Proceedings of the Royal Society B: Biological Sciences* . doi: 10.1098/rspb.2017.0582.

Becker, M.H. et al. 2011. Towards a better understanding of the use of probiotics for preventing chytridiomycosis in Panamanian golden frogs. *EcoHealth* 8(4), pp. 501–506. doi: 10.1007/s10393-012-0743-0.

Becker, M.H. et al. 2015. Composition of symbiotic bacteria predicts survival in Panamanian golden frogs infected with a lethal fungus. *Proceedings of the Royal Society B: Biological Sciences* 282(1805), pp. 20142881–20142881. doi: 10.1098/rspb.2014.2881.

Belasen, A.M., Bletz, M.C., Leite, D. da S., Toledo, L.F. and James, T.Y. 2019. Long-Term Habitat Fragmentation Is Associated With Reduced MHC IIB Diversity and Increased Infections in Amphibian Hosts. *Frontiers in Ecology and Evolution* 6(JAN), p. 236. doi: 10.3389/fevo.2018.00236.

Belasen, A.M., Riolo, M.A., Bletz, M.C., Lyra, M.L., Toledo, L.F. and James, T.Y. 2021. Geography, Host Genetics, and Cross-Domain Microbial Networks Structure the Skin Microbiota of Fragmented Brazilian Atlantic Forest Frog Populations. *Ecology and Evolution* 11(14), pp. 9293–9307. doi: 10.1002/ECE3.7594.

Bell, S.C., Garland, S. and Alford, R.A. 2018. Increased Numbers of Culturable Inhibitory Bacterial Taxa May Mitigate the Effects of Batrachochytrium dendrobatidis in Australian Wet Tropics Frogs. *Frontiers in Microbiology* 9, p. 1604. doi: 10.3389/fmicb.2018.01604.

Benjamini, Y. and Yekutieli, D. 2001. The control of the false discovery rate in multiple testing under dependency. *The Annals of Statistics* 29(4), pp. 1165–1188. doi: 10.1214/AOS/1013699998.

Berg, G. et al. 2020. Microbiome definition re-visited: old concepts and new challenges. *Microbiome* 8(1), pp. 1–22. doi: 10.1186/s40168-020-00875-0.

Berger, L. et al. 1998. Chytridiomycosis causes amphibian mortality associated with population declines in the rain forests of Australia and Central America. *Proceedings of the National Academy of Sciences* 95(15), pp. 9031–9036.

Berger, L. et al. 2004. Effect of season and temperature on mortality in amphibians due to chytridiomycosis. *Australian Veterinary Journal* 82(7), pp. 434–439. doi: 10.1111/j.1751-0813.2004.tb11137.x.

Berger, L., Hyatt, A., Speare, R. and Longcore, J. 2005. Life cycle stages of the amphibian chytrid Batrachochytrium dendrobatidis. *Diseases of Aquatic Organisms* 68(1), pp. 51–63. doi: 10.3354/dao068051.

Bernardo-Cravo, A.P., Schmeller, D.S., Chatzinotas, A., Vredenburg, V.T. and Loyau, A. 2020. Environmental Factors and Host Microbiomes Shape Host–Pathogen Dynamics. *Trends in Parasitology* 36(7), pp. 616–633. doi: 10.1016/j.pt.2020.04.010.

Bertorelle, G., Benazzo, A. and Mona, S. 2010. ABC as a flexible framework to estimate demography over space and time: Some cons, many pros. *Molecular Ecology* 19(13), pp. 2609–2625. doi: 10.1111/j.1365-294X.2010.04690.x.

Biedrzycka, A., Sebastian, A., Migalska, M., Westerdahl, H. and Radwan, J. 2017. Testing genotyping strategies for ultra-deep sequencing of a co-amplifying gene family: MHC class I in a passerine bird. *Molecular Ecology Resources* 17(4), pp. 642–655. doi: 10.1111/1755-0998.12612.

Bielby, J., Cooper, N., Cunningham, A. a., Garner, T. w. j. and Purvis, A. 2008. Predicting susceptibility to future declines in the world's frogs. *Conservation Letters* 1(2), pp. 82–90. doi: 10.1111/j.1755-263X.2008.00015.x.

Binladen, J., Gilbert, M.T.P., Bollback, J.P., Panitz, F., Bendixen, C., Nielsen, R. and Willerslev, E. 2007. The Use of Coded PCR Primers Enables High-Throughput Sequencing of Multiple Homolog Amplification Products by 454 Parallel Sequencing. *PLOS ONE* 2(2), p. e197. doi: 10.1371/JOURNAL.PONE.0000197.

Bletz, M.C. et al. 2016. Amphibian gut microbiota shifts differentially in community structure but converges on habitat-specific predicted functions. *Nature Communications 2016 7:1* 7(1), pp. 1–12. doi: 10.1038/ncomms13699.

Bletz, M.C. et al. 2017. Amphibian skin microbiota exhibits temporal variation in community structure but stability of predicted Bd-inhibitory function. *The ISME Journal 2017 11:7* 11(7), pp. 1521–1534. doi: 10.1038/ismej.2017.41.

Bletz, M.C., Rebollar, E.A. and Harris, R.N. 2015. Differential efficiency among DNA extraction methods influences detection of the amphibian pathogen Batrachochytrium dendrobatidis. *Diseases of Aquatic Organisms* 113(1), pp. 1–8. doi: 10.3354/dao02822.

Bohenek, J.R. and Resetarits Jr, W.J. 2017. An optimized method to quantify large numbers of amphibian eggs. *Herpetology Notes* 10, pp. 573–578.

Bolger, A.M., Lohse, M. and Usadel, B. 2014. Trimmomatic: a flexible trimmer for Illumina sequence data. *Bioinformatics* 30(15), pp. 2114–2120. doi: 10.1093/bioinformatics/btu170.

Borgelt, J., Dorber, M., Høiberg, M.A. and Verones, F. 2022. More than half of data deficient species predicted to be threatened by extinction. *Communications Biology* 5(1), p. 679. doi: 10.1038/s42003-022-03638-9.

Boyle, D.G., Boyle, D.B., Olsen, V., Morgan, J.A.T. and Hyatt, A.D. 2004. Rapid quantitative detection of chytridiomycosis (Batrachochytrium dendrobatidis) in amphibian samples using real-time Taqman PCR assay. *Diseases of Aquatic Organisms* 60(2), pp. 141–148. doi: 10.3354/dao060141.

Brace, S., Turvey, S.T., Weksler, M., Hoogland, M.L.P.P. and Barnes, I. 2015. Unexpected evolutionary diversity in a recently extinct caribbean mammal radiation. *Proceedings of the Royal Society B: Biological Sciences* 282(1807), pp. 20142371–20142371. doi: 10.1098/rspb.2014.2371.

Bradley, P.W., 1¤, I.D., Snyder, P.W. and Blaustein, A.R. 2019. Host age alters amphibian susceptibility to Batrachochytrium dendrobatidis, an emerging infectious fungal pathogen. *PLOS ONE* 14(9), p. e0222181. doi: 10.1371/journal.pone.0222181.

Brannelly, L., McMahon, T., Hinton, M., Lenger, D. and Richards-Zawacki, C. 2015. Batrachochytrium dendrobatidis in natural and farmed Louisiana crayfish populations: prevalence and implications. *Diseases of Aquatic Organisms* 112(3), pp. 229–235. doi: 10.3354/dao02817.

Brannelly, L.A. et al. 2021. Mechanisms underlying host persistence following amphibian disease emergence determine appropriate management strategies. Drake, J. ed. *Ecology Letters* 24(1), pp. 130–148. doi: 10.1111/ELE.13621.

Brannelly, L.A., Webb, R., Skerratt, L.F. and Berger, L. 2016. Amphibians with infectious disease increase their reproductive effort: evidence for the terminal investment hypothesis. *Open Biology* 6(6), p. 150251. doi: 10.1098/rsob.150251.

Briggs, C.J., Knapp, R.A. and Vredenburg, V.T. 2010. Enzootic and epizootic dynamics of the chytrid fungal pathogen of amphibians. *Proceedings of the National Academy of Sciences of the United States of America* 107(21), pp. 9695–9700.

Brooks, M.E. et al. 2019. Statistical modeling of patterns in annual reproductive rates. *Ecology* 100(7), p. e02706. doi: 10.1002/ECY.2706.

Brooks, S.P. and Gelman, A. 1998. General Methods for Monitoring Convergence of Iterative Simulations. *Journal of Computational and Graphical Statistics* 7(4), pp. 434–455. doi: 10.1080/10618600.1998.10474787.

Brucker, R.M., Harris, R.N., Schwantes, C.R., Gallaher, T.N., Flaherty, D.C., Lam, B.A. and Minbiole, K.P.C. 2008. Amphibian chemical defense: antifungal metabolites of the microsymbiont Janthinobacterium lividum on the salamander Plethodon cinereus. *Journal of Chemical Ecology* 34(11), pp. 1422–1429. doi: 10.1007/s10886-008-9555-7.

Bulut, Z., McCormick, C.R., Gopurenko, D., Williams, R.N., Bos, D.H. and Dewoody, J.A. 2009. Microsatellite mutation rates in the eastern tiger salamander (Ambystoma tigrinum tigrinum) differ 10-fold across loci. *Genetica* 136(3), pp. 501–504. doi: 10.1007/s10709-008-9341-z.

van den Burg, M.P., Brisbane, J.L.K. and Knapp, C.R. 2020. Post-hurricane relief facilitates invasion and establishment of two invasive alien vertebrate species in the Commonwealth of Dominica, West Indies. *Biological Invasions* 22(2), pp. 195–203. doi: 10.1007/s10530-019-02107-5.

Bushley, K.E., Ripoll, D.R. and Turgeon, B.G. 2008. Module evolution and substrate specificity of fungal nonribosomal peptide synthetases involved in siderophore biosynthesis. *BMC Evolutionary Biology* 8(1), p. 328. doi: 10.1186/1471-2148-8-328.

Byrne, A.Q. et al. 2019. Cryptic diversity of a widespread global pathogen reveals expanded threats to amphibian conservation. *Proceedings of the National Academy of Sciences* 116(41), pp. 20382–20387. doi: 10.1073/PNAS.1908289116.

Byrne, A.Q. et al. 2022. Host species is linked to pathogen genotype for the amphibian chytrid fungus (Batrachochytrium dendrobatidis). *PLOS ONE* 17(3), p. e0261047. doi: 10.1371/journal.pone.0261047.

Byrne, A.Q., Rothstein, A.P., Poorten, T.J., Erens, J., Settles, M.L. and Rosenblum, E.B. 2017. Unlocking the story in the swab: A new genotyping assay for the amphibian chytrid fungus *Batrachochytrium dendrobatidis*. *Molecular Ecology Resources* 17(6), pp. 1283–1292. doi: 10.1111/1755-0998.12675.

Byrne, A.Q., Voyles, J., Rios-Sotelo, G. and Rosenblum, E.B. 2016. Insights From Genomics Into Spatial and Temporal Variation in Batrachochytrium dendrobatidis. In: *Progress in Molecular Biology and Translational Science*. Elsevier B.V., pp. 269–290. doi: 10.1016/bs.pmbts.2016.05.009.

Cabaj, A. and Kosakowska, A. 2009. Iron-dependent growth of and siderophore production by two heterotrophic bacteria isolated from brackish water of the southern Baltic Sea. *Microbiological Research* 164(5), pp. 570–577. doi: 10.1016/j.micres.2007.07.001.

Callahan, B.J., McMurdie, P.J., Rosen, M.J., Han, A.W., Johnson, A.J.A. and Holmes, S.P. 2016. DADA2: High-resolution sample inference from Illumina amplicon data. *Nature Methods* 13(7), pp. 581–583. doi: 10.1038/nmeth.3869.

Calsbeek, R. and Smith, T.B. 2003. Ocean currents mediate evolution in island lizards. *Nature* 426(6966), pp. 552–555. doi: 10.1038/nature02143.

Camargo, A., Ronald Heyer, W. and De Sá, R.O. 2009. Phylogeography of the frog Leptodactylus validus (Amphibia: Anura): Patterns and timing of colonization events in the Lesser Antilles. *Molecular Phylogenetics and Evolution* 53(2), pp. 571–579. doi: 10.1016/j.ympev.2009.07.004.

Caporaso, J.G. et al. 2011. Global patterns of 16S rRNA diversity at a depth of millions of sequences per sample. *Proceedings of the National Academy of Sciences of the United States of America* 108(SUPPL. 1), pp. 4516–4522. doi: 10.1073/pnas.1000080107.

Caspi, R. et al. 2016. The MetaCyc database of metabolic pathways and enzymes and the BioCyc collection of pathway/genome databases. *Nucleic Acids Research* 44(D1), pp. D471–D480. doi: 10.1093/NAR/GKV1164.

Castric, V., Bernatchez, L., Belkhir, K. and Bonhomme, F. 2002. Heterozygote deficiencies in small lacustrine populations of brook charr Salvelinus Fontinalis Mitchill (Pisces, Salmonidae): a test of alternative hypotheses. *Heredity 2002 89:1* 89(1), pp. 27–35. doi: 10.1038/sj.hdy.6800089.

Catenazzi, A., Swei, A., Finkle, J., Foreyt, E., Wyman, L. and Vredenburg, V.T. 2017. Epizootic to enzootic transition of a fungal disease in tropical Andean frogs: Are surviving species still susceptible? *PLoS ONE* 12(10). doi: 10.1371/journal.pone.0186478.

Chaiharn, M., Chunhaleuchanon, S. and Lumyong, S. 2009. Screening siderophore producing bacteria as potential biological control agent for fungal rice pathogens in Thailand. *World Journal of Microbiology and Biotechnology* 25(11), pp. 1919–1928. doi: 10.1007/S11274-009-0090-7/FIGURES/1.

Chao, A. and Chiu, C.-H. 2016. Nonparametric Estimation and Comparison of Species Richness. In: *eLS*. Chichester: John Wiley & Sons, Ltd., pp. 1–11. doi: 10.1002/9780470015902.a0026329.

Charif, D. and Lobry, J.R. 2007. SeqinR 1.0-2: A Contributed Package to the R Project for Statistical Computing Devoted to Biological Sequences Retrieval and Analysis. In: *Structural Approaches to Sequence Evolution*. Biological and Medical Physics, Biomedical Engineering. Berlin, Heidelberg: Springer, pp. 207–232. doi: 10.1007/978-3-540-35306-5_10.

Chow, N.A. et al. 2020. Tracing the evolutionary history and global expansion of candida auris using population genomic analyses. *mBio* 11(2). doi: 10.1128/mBio.03364-19.

Christie, M.R. and Searle, C.L. 2018. Evolutionary rescue in a host–pathogen system results in coexistence not clearance. *Evolutionary Applications* 11(5), pp. 681–693. doi: 10.1111/eva.12568.

Ciofi, C., Beaumontf, M.A., Swingland, I.R. and Bruford, M.W. 1999. Genetic divergence and units for conservation in the Komodo dragon Varanus komodoensis. *Proceedings of the Royal Society of London. Series B: Biological Sciences* 266(1435), pp. 2269–2274. doi: 10.1098/rspb.1999.0918.

Couto, A., Da Silveira, R., Soares, A. and Menin, M. 2018. Diet of the Smoky Jungle Frog, Leptodactylus pentadactylus, (Anura, Leptodactylidae) in an urban forest fragment and in a preserved forest in Central Amazonia, Brazil. *Herpetology Notes* 11, pp. 519–525.

Cowie, R.H., Bouchet, P. and Fontaine, B. 2022. The Sixth Mass Extinction: fact, fiction or speculation? *Biological Reviews* 97(2), pp. 640–663. doi: 10.1111/brv.12816.

Crandall, S.G., Gold, K.M., Jiménez-Gasco, M. del M., Filgueiras, C.C. and Willett, D.S. 2020. A multi-omics approach to solving problems in plant disease ecology. *PLOS ONE* 15(9), p. e0237975. doi: 10.1371/journal.pone.0237975.

Crawford, A.J. 2003. Relative Rates of Nucleotide Substitution in Frogs. *Journal of Molecular Evolution* 57(6), pp. 636–641. doi: 10.1007/s00239-003-2513-7.

Criscuolo, N.G. and Angelini, C. 2020. StructuRly: A novel shiny app to produce comprehensive, detailed and interactive plots for population genetic analysis. Gilestro, G. F. ed. *PLOS ONE* 15(2), p. e0229330. doi: 10.1371/journal.pone.0229330.

Crutzen, P.J. 2006. The "Anthropocene". *Earth System Science in the Anthropocene* , pp. 13–18. doi: 10.1007/3-540-26590-2_3.

Culp, C.E., Falkinham, J. and Belden, L.K. 2007. Identification of the natural bacterial microflora on the skin of eastern newts, bullfrog tadpoles and redback salamanders. *Herpetologica* 63(1), pp. 66–71. doi: 10.1655/0018-0831(2007)63[66:IOTNBM]2.0.CO;2.

Daltry, J. and Gray, G. 1999. Effects of Volcanic Activity on the Endangered Mountain Chicken Frog (Leptodactylus fallax). *Frog Log* 32(1), pp. 1–2.

Daltry, J.C. 1999. *Unpublished report to Montserrat Forestry and Environment Division on 1995 survey of reptiles and amphibians on Montserrat.* Fauna and Flora International.

Daltry, J.C. 2002. *Mountain Chicken Monitoring Manual*. Cambridge: Fauna and Flora International., pp. 1–54.

Dang, T., Searle, C. and Blaustein, A. 2017. Virulence variation among strains of the emerging infectious fungus Batrachochytrium dendrobatidis (Bd) in multiple amphibian host species. *Diseases of Aquatic Organisms* 124(3), pp. 233–239. doi: 10.3354/dao03125.

Daszak, P., Cunningham, A.A. and Hyatt, A.D. 2000. Emerging Infectious Diseases of Wildlife-- Threats to Biodiversity and Human Health. *Science* 287(5452), pp. 443–449. doi: 10.1126/science.287.5452.443.

Davis, N.M., Proctor, Di.M., Holmes, S.P., Relman, D.A. and Callahan, B.J. 2018. Simple statistical identification and removal of contaminant sequences in marker-gene and metagenomics data. *Microbiome* 6(1), pp. 1–14. doi: 10.1186/S40168-018-0605-2/FIGURES/6.

De Castro, F. and Bolker, B. 2005. Mechanisms of disease-induced extinction. *Ecology Letters* 8(1), pp. 117–126. doi: 10.1111/j.1461-0248.2004.00693.x.

Dieringer, D. and Schlötterer, C. 2003. microsatellite analyser (MSA): a platform independent analysis tool for large microsatellite data sets. *Molecular Ecology Notes* 3(1), pp. 167–169. doi: 10.1046/j.1471-8286.2003.00351.x.

Dirzo, R., Young, H.S., Galetti, M., Ceballos, G., Isaac, N.J.B. and Collen, B. 2014. Defaunation in the Anthropocene. *Science* 345(6195), pp. 401–406.

D'Onofrio, A. et al. 2010. Siderophores from Neighboring Organisms Promote the Growth of Uncultured Bacteria. *Chemistry & biology* 17(3), pp. 254–264. doi: 10.1016/j.chembiol.2010.02.010.

Douglas, G.M. et al. 2020. PICRUSt2 for prediction of metagenome functions. *Nature Biotechnology 2020 38:6* 38(6), pp. 685–688. doi: 10.1038/s41587-020-0548-6.

Dudek, K., Gaczorek, T.S., Zieliński, P. and Babik, W. 2019. Massive introgression of major histocompatibility complex (MHC) genes in newt hybrid zones. *Molecular Ecology* 28(21), pp. 4798–4810.

Duryea, M.C., Zamudio, K.R. and Brasileiro, C.A. 2015. Vicariance and marine migration in continental island populations of a frog endemic to the Atlantic Coastal forest. *Heredity* 115(3), pp. 225–234. doi: 10.1038/hdy.2015.31.

Edmands, S. 2007. Between a rock and a hard place: evaluating the relative risks of inbreeding and outbreeding for conservation and management. *Molecular Ecology* 16(3), pp. 463–475. doi: 10.1111/J.1365-294X.2006.03148.X.

Edwards, R.J. et al. 2018. Draft genome assembly of the invasive cane toad, Rhinella marina. *GigaScience* 7(9), pp. 1–13. doi: 10.1093/GIGASCIENCE/GIY095.

Eisenhofer, R., Minich, J.J., Marotz, C., Cooper, A., Knight, R. and Weyrich, L.S. 2019. Contamination in Low Microbial Biomass Microbiome Studies: Issues and Recommendations. *Trends in Microbiology* 27(2), pp. 105–117. doi: 10.1016/j.tim.2018.11.003.

Ejsmond, M.J. and Radwan, J. 2011. MHC diversity in bottlenecked populations: A simulation model. *Conservation Genetics* 12(1), pp. 129–137. doi: 10.1007/s10592-009-9998-6.

Ellison, A.R. et al. 2015. More than Skin Deep: Functional Genomic Basis for Resistance to Amphibian Chytridiomycosis. *Genome Biology and Evolution* 7(1), pp. 286–298. doi: 10.1093/gbe/evu285.

Ellison, A.R., DiRenzo, G.V., McDonald, C.A., Lips, K.R. and Zamudio, K.R. 2017. First in Vivo Batrachochytrium dendrobatidis Transcriptomes Reveal Mechanisms of Host Exploitation, Host-Specific Gene Expression, and Expressed Genotype Shifts. *G3 Genes|Genomes|Genetics* 7(1), pp. 269–278. doi: 10.1534/g3.116.035873.

Ellison, A.R., Savage, A.E., DiRenzo, G.V., Langhammer, P., Lips, K.R. and Zamudio, K.R. 2014. Fighting a losing battle: Vigorous immune response countered by pathogen suppression of host defenses in the chytridiomycosis-susceptible frog Atelopus zeteki. *G3: Genes, Genomes, Genetics* 4(7), pp. 1275–1289. doi: 10.1534/g3.114.010744.

Ellison, S., Knapp, R. and Vredenburg, V. 2021. Longitudinal patterns in the skin microbiome of wild, individually marked frogs from the Sierra Nevada, California. *ISME Communications 2021 1:1* 1(1), pp. 1–11. doi: 10.1038/s43705-021-00047-7.

Ellison, S., Knapp, R.A., Sparagon, W., Swei, A. and Vredenburg, V.T. 2019. Reduced skin bacterial diversity correlates with increased pathogen infection intensity in an endangered amphibian host. *Molecular Ecology* 28(1), pp. 127–140. doi: 10.1111/mec.14964.

Eskew, E.A., Shock, B.C., Ladouceur, E.E.B., Keel, K., Miller, M.R., Foley, J.E. and Todd, B.D. 2018. Gene expression differs in susceptible and resistant amphibians exposed to batrachochytrium dendrobatidis. *Royal Society Open Science* 5(2), p. 170910. doi: 10.1098/rsos.170910.

Estrada, A., Medina, D., Gratwicke, B., Ibáñez, R. and Belden, L.K. 2022. Body condition, skin bacterial communities and disease status: insights from the first release trial of the limosa harlequin frog, Atelopus limosus. *Proceedings of the Royal Society B: Biological Sciences* 289(1978), p. 20220586. doi: 10.1098/rspb.2022.0586.

Evanno, G., Regnaut, S. and Goudet, J. 2005. Detecting the number of clusters of individuals using the software STRUCTURE: A simulation study. *Molecular Ecology* 14(8), pp. 2611–2620. doi: 10.1111/j.1365-294X.2005.02553.x.

Evans, M.L., Neff, B.D. and Heath, D.D. 2010. MHC genetic structure and divergence across populations of Chinook salmon (Oncorhynchus tshawytscha). *Heredity* 104(5), pp. 449–459. doi: 10.1038/HDY.2009.121.

Excoffier, L., Dupanloup, I., Huerta-Sánchez, E., Sousa, V.C. and Foll, M. 2013. Robust Demographic Inference from Genomic and SNP Data. Akey, J. M. ed. *PLoS Genetics* 9(10), p. e1003905. doi: 10.1371/journal.pgen.1003905.

Excoffier, L. and Lischer, H.E.L. 2010. Arlequin suite ver 3.5: A new series of programs to perform population genetics analyses under Linux and Windows. *Molecular Ecology Resources* 10(3), pp. 564–567. doi: 10.1111/j.1755-0998.2010.02847.x.

Fa, J., Hedges, B., Ibéné, B., Breuil, M., Powell, R. and Magin, C. 2008. IUCN Red List of Threatened Species: Leptodactylus fallax. *IUCN Red List of Threatened Species* . Available at: https://www.iucnredlist.org/en [Accessed: 7 September 2022].

Falush, D., Stephens, M. and Pritchard, J.K. 2003. Inference of Population Structure Using Multilocus Genotype Data: Linked Loci and Correlated Allele Frequencies. *Genetics* 164(4), pp. 1567–1587. doi: 10.1093/GENETICS/164.4.1567.

Farrer, R.A. et al. 2011. Multiple emergences of genetically diverse amphibian-infecting chytrids include a globalized hypervirulent recombinant lineage. *Proceedings of the National Academy of Sciences of the United States of America* 108(46), pp. 18732–18736. doi: 10.1073/pnas.1111915108.

Farrer, R.A. et al. 2017. Genomic innovations linked to infection strategies across emerging pathogenic chytrid fungi. *Nature Communications* 8(14742). doi: 10.1038/ncomms14742.

Farrer, R.A., Henk, D.A., Garner, T.W.J., Balloux, F., Woodhams, D.C. and Fisher, M.C. 2013. Chromosomal Copy Number Variation, Selection and Uneven Rates of Recombination Reveal Cryptic Genome Diversity Linked to Pathogenicity. *PLoS Genetics* 9(8), p. 1003703. doi: 10.1371/journal.pgen.1003703.

Ferreira, R., Dantas, R. and Teixeira, R. 2007. Reproduction and ontogenetic diet shifts in Leptodactylus natalensis (Anura, Leptodactylidae) from southeastern Brazil. *Boletim do Museu de Biologia Mello Leitão* 22(22), pp. 45–55.

Fierer, N., Hamady, M., Lauber, C.L. and Knight, R. 2008. The influence of sex, handedness, and washing on the diversity of hand surface bacteria. *Proceedings of the National Academy of Sciences of the United States of America* 105(46), pp. 17994–17999. doi: 10.1073/pnas.0807920105.

Fisher, M.C. et al. 2009a. Proteomic and phenotypic profiling of the amphibian pathogen Batrachochytrium dendrobatidis shows that genotype is linked to virulence. *Molecular Ecology* 18(3), pp. 415–429. doi: 10.1111/j.1365-294X.2008.04041.x.

Fisher, M.C. and Garner, T.W.J. 2007. The relationship between the emergence of Batrachochytrium dendrobatidis, the international trade in amphibians and introduced amphibian species. *Fungal Biology Reviews* 21(1), pp. 2–9. doi: 10.1016/j.fbr.2007.02.002.

Fisher, M.C. and Garner, T.W.J. 2020. Chytrid fungi and global amphibian declines. *Nature Reviews Microbiology* 18(6), pp. 332–343. doi: 10.1038/s41579-020-0335-x.

Fisher, M.C., Garner, T.W.J. and Walker, S.F. 2009b. Global Emergence of *Batrachochytrium dendrobatidis* and Amphibian Chytridiomycosis in Space, Time, and Host. *Annual Review of Microbiology* 63(1), pp. 291–310. doi: 10.1146/annurev.micro.091208.073435.

Fisher, M.C., Pasmans, F. and Martel, A. 2021. Virulence and pathogenicity of chytrid fungi causing amphibian extinctions. *Annual Review of Microbiology* 75, pp. 673–693. doi: 10.1146/annurev-micro-052621-124212.

Fitzpatrick, S.M. 2013. Seafaring Capabilities in the Pre-Columbian Caribbean. *Journal of Maritime Archaeology* 8(1), pp. 101–138. doi: 10.1007/s11457-013-9110-8.

Flajnik, M.F. 2018. A cold-blooded view of adaptive immunity. *Nature Reviews Immunology* 18(7), pp. 438–453. doi: 10.1038/s41577-018-0003-9.

Flajnik, M.F. and Du Pasquier, L. 2004. Evolution of innate and adaptive immunity: can we draw a line? *Trends in Immunology* 25(12), pp. 640–644. doi: 10.1016/j.it.2004.10.001.

Flechas, S.V. et al. 2018. Microbiota and skin defense peptides may facilitate coexistence of two sympatric Andean frog species with a lethal pathogen. *ISME Journal* 25 September, p. 1.

Foster, D.R. 2000. Conservation: lessons and challenges. *Forest History Today* (Fall), pp. 2–11.

Fouladi, F. et al. 2020. Air pollution exposure is associated with the gut microbiome as revealed by shotgun metagenomic sequencing. *Environment International* 138, p. 105604. doi: 10.1016/j.envint.2020.105604.

Francis, R.M. 2017. pophelper: an R package and web app to analyse and visualize population structure. In: *Molecular Ecology Resources*. Blackwell Publishing Ltd, pp. 27–32. doi: 10.1111/1755-0998.12509.

Frankham, R. 2008. Genetic adaptation to captivity in species conservation programs. *Molecular Ecology* 17(1), pp. 325–333. doi: 10.1111/j.1365-294X.2007.03399.x.

Frankham, R., Ballou, J.D. and Briscoe, D.A. 2004. Captive breeding and reintroduction. In: *A Primer of Conservation Genetics*. Cambridge: Cambridge University Press, pp. 145–167. Available at: https://books.google.co.uk/books?hl=en&lr=&id=Q7Jts0zy_DgC&oi=fnd&pg=PA13&dq=Introduction+to+Conservation+Genetics+90%25+source+population+heterozygosity&ots=x7E--SxfPP&sig=ubkgZTw-unJ1BLVKkvyUxTwJf_U#v=onepage&q&f=false.

Frost, D.R., Hammerson, G.A. and Santos-Barrera, G. 2021. Amphibian Species of the World: an Online Reference. Available at: https://amphibiansoftheworld.amnh.org/ [Accessed: 27 March 2023].

Fu, M. and Waldman, B. 2017. Major histocompatibility complex variation and the evolution of resistance to amphibian chytridiomycosis. *Immunogenetics* 69(8–9), pp. 529–536. doi: 10.1007/S00251-017-1008-4.

Garcia, G. et al. 2007. Mountain chickens Leptodactylus fallax and sympatric amphibians appear to be disease free on Montserrat. *ORYX* 41(3), pp. 398–401. doi: 10.1017/S0030605307001012.

Garcia, G. and Schad, K. 2015. *Long-term management plan for the mountain chicken frog (Leptodactylus fallax) European Studbook (ESB)*. Chester Zoo, Chester, England.

García-Dorado, A. and Caballero, A. 2021. Neutral genetic diversity as a useful tool for conservation biology. *Conservation Genetics 2021 22:4* 22(4), pp. 541–545. doi: 10.1007/S10592-021-01384-9.

Garmyn, A., Van Rooij, P., Pasmans, F., Hellebuyck, T., Van Den Broeck, W., Haesebrouck, F. and Martel, A. 2012. Waterfowl: Potential Environmental Reservoirs of the Chytrid Fungus Batrachochytrium dendrobatidis. Fisher, M. (Mat) C. ed. *PLoS ONE* 7(4), p. e35038. doi: 10.1371/journal.pone.0035038.

Garner, T.W.J. et al. 2016. Mitigating amphibian chytridiomycoses in nature. *Philosophical Transactions of the Royal Society B: Biological Sciences* 371(1709). doi: 10.1098/rstb.2016.0207.

Garrison, E. and Marth, G. 2012. Haplotype-based variant detection from short-read sequencing. *arXiv:1207.3907* . Available at: http://arxiv.org/abs/1207.3907 [Accessed: 29 April 2021].

Gaur, L.K. and Nepom, G.T. 1996. Ancestral major histocompatibility complex DRB genes beget conserved patterns of localized polymorphisms. *Proceedings of the National Academy of Sciences of the United States of America* 93(11), pp. 5380–5383.

Gazoni, T., Haddad, C.F.B., Narimatsu, H., Cabral-de-Mello, D.C., Lyra, M.L. and Parise-Maltempi, P.P. 2018. More sex chromosomes than autosomes in the Amazonian frog Leptodactylus pentadactylus. *Chromosoma* 127(2), pp. 269–278. doi: 10.1007/s00412-018-0663-z.

Gervasi, S.S. et al. 2017. Linking Ecology and Epidemiology to Understand Predictors of Multi-Host Responses to an Emerging Pathogen, the Amphibian Chytrid Fungus. *PLOS ONE* 12(1), p. e0167882. doi: 10.1371/journal.pone.0167882.

Gervasi, S.S., Urbina, J., Hua, J., Chestnut, T., A. Relyea, R. and R. Blaustein, A. 2013. Experimental Evidence for American Bullfrog (Lithobates catesbeianus) Susceptibility to Chytrid Fungus (Batrachochytrium dendrobatidis). *EcoHealth* 10(2), pp. 166–171. doi: 10.1007/s10393-013-0832-8.

Ghosh, P.N. et al. 2020. Discriminating lineages of *Batrachochytrium dendrobatidis* using quantitative PCR. *Molecular Ecology Resources* , pp. 1755–0998.13299. doi: 10.1111/1755-0998.13299.

Gibson, R.C. and Buley, K.R. 2004. Maternal Care and Obligatory Oophagy in Leptodactylus fallax: A New Reproductive Mode in Frogs. Douglas, M. E. ed. *Copeia* 2004(1), pp. 128–135.

Gillingham, M.A.F., Montero, B.K., Wihelm, K., Grudzus, K., Sommer, S. and Santos, P.S.C. 2021. A novel workflow to improve genotyping of multigene families in wildlife species: An experimental set-up with a known model system. *Molecular Ecology Resources* 21(3), pp. 982–998. doi: 10.1111/1755-0998.13290.

Girod, C., Vitalis, R., Leblois, R. and Fréville, H. 2011. Inferring population decline and expansion from microsatellite data: A simulation-based evaluation of the msvar method. *Genetics* 188(1), pp. 165–179. doi: 10.1534/genetics.110.121764.

Gloor, G.B., Macklaim, J.M., Pawlowsky-Glahn, V. and Egozcue, J.J. 2017. Microbiome datasets are compositional: And this is not optional. *Frontiers in Microbiology* 8(NOV), p. 2224. doi: 10.3389/FMICB.2017.02224/BIBTEX.

Gooley, R.M. et al. 2020. Comparison of genomic diversity and structure of sable antelope (Hippotragus niger) in zoos, conservation centers, and private ranches in North America. *Evolutionary Applications* 13(8), pp. 2143–2154. doi: 10.1111/EVA.12976.

Goudet, J. 1995. FSTAT (Version 1.2): A Computer Program to Calculate F-statistics. *Journal of Heredity* 86(6), pp. 485–486. doi: 10.1093/oxfordjournals.jhered.a111627.

Goudet, J. 2005. HIERFSTAT, a package for R to compute and test hierarchical F-statistics. *Molecular Ecology Notes* 5(1), pp. 184–186. doi: 10.1111/j.1471-8286.2004.00828.x.

Grantham, R. 1974. Amino acid difference formula to help explain protein evolution. *Science* 185(4154), pp. 862–864. doi: 10.1126/science.185.4154.862.

Grayson, K.L., De Lisle, S.P., Jackson, J.E., Black, S.J. and Crespi, E.J. 2012. Behavioral and physiological female responses to male sex ratio bias in a pond-breeding amphibian. *Frontiers in Zoology* 9(1), p. 24. doi: 10.1186/1742-9994-9-24.

Greener, M.S. et al. 2020. Presence of low virulence chytrid fungi could protect European amphibians from more deadly strains. *Nature Communications* 11(1), p. 5393. doi: 10.1038/s41467-020-19241-7.

Greenspan, S.E., Lambertini, C., Carvalho, T., James, T.Y., Toledo, L.F., Haddad, C.F.B. and Becker, C.G. 2018. Hybrids of amphibian chytrid show high virulence in native hosts. *Scientific Reports* 8(1), pp. 1–10. doi: 10.1038/s41598-018-27828-w.

Grogan, L.F. et al. 2018a. Evolution of resistance to chytridiomycosis is associated with a robust early immune response. *Molecular Ecology* 27(4), pp. 919–934. doi: 10.1111/mec.14493.

Grogan, L.F. et al. 2018b. Review of the amphibian immune response to chytridiomycosis, and future directions. *Frontiers in Immunology* 9(NOV), p. 2536. doi: 10.3389/fimmu.2018.02536.

Grogan, L.F., Humphries, J.E., Robert, J., Lanctôt, C.M., Nock, C.J., Newell, D.A. and McCallum, H.I. 2020. Immunological aspects of chytridiomycosis. *Journal of Fungi* 6(4), pp. 1–24. doi: 10.3390/jof6040234.

Guarino, F., Garcia, G. and Andreone, F. 2014. Huge but moderately long-lived: Age structure in the mountain chicken, Leptodactylus fallax, from Montserrat, West Indies. *The Herpetological Journal* 24(3), pp. 167–173.

Haas, H., Eisendle, M. and Turgeon, B.G. 2008. Siderophores in fungal physiology and virulence. *Annual Review of Phytopathology* 46, pp. 149–187. doi: 10.1146/ANNUREV.PHYTO.45.062806.094338.

Hale, M.L., Burg, T.M. and Steeves, T.E. 2012. Sampling for Microsatellite-Based Population Genetic Studies: 25 to 30 Individuals per Population Is Enough to Accurately Estimate Allele Frequencies. Poon, A. F. Y. ed. *PLoS ONE* 7(9), p. e45170. doi: 10.1371/journal.pone.0045170.

Halekoh, U. and Højsgaard, S. 2014. A Kenward-Roger Approximation and Parametric Bootstrap Methods for Tests in Linear Mixed Models – The R Package pbkrtest. *Journal of Statistical Software* 59(9), pp. 1–32. doi: 10.18637/JSS.V059.I09.

Haller, B.C. and Messer, P.W. 2019. SLiM 3: Forward Genetic Simulations Beyond the Wright–Fisher Model. *Molecular Biology and Evolution* 36(3), pp. 632–637. doi: 10.1093/molbev/msy228.

Hammer, T.J., Sanders, J.G. and Fierer, N. 2019. Not all animals need a microbiome. *FEMS Microbiology Letters* 366(10), p. fnz117. doi: 10.1093/femsle/fnz117.

Harding, G., Griffiths, R.A. and Pavajeau, L. 2016. Developments in amphibian captive breeding and reintroduction programs. *Conservation Biology* 30(2), pp. 340–349. doi: 10.1111/cobi.12612.

Harper, G.L., Maclean, N. and Goulson, D. 2008. Molecular evidence for a recent founder event in the UK populations of the Adonis blue butterfly (Polyommatus bellargus). *Journal of Insect Conservation* 12(2), pp. 147–153. doi: 10.1007/s10841-007-9072-y.

Harris, K. and Nielsen, R. 2016. The genetic cost of neanderthal introgression. *Genetics* 203(2), pp. 881–891. doi: 10.1534/genetics.116.186890.

Harris, R.N. et al. 2009. Skin microbes on frogs prevent morbidity and mortality caused by a lethal skin fungus. *ISME Journal* 3(7), pp. 818–824. doi: 10.1038/ismej.2009.27.

Harris, R.N., James, T.Y., Lauer, A., Simon, M.A. and Patel, A. 2006. Amphibian pathogen Batrachochytrium dendrobatidis is inhibited by the cutaneous bacteria of amphibian species. *EcoHealth* 3(1), pp. 53–56. doi: 10.1007/s10393-005-0009-1.

Hart, E. 2016. From field to plate: The colonial livestock trade and the development of an American economic culture. *William and Mary Quarterly* 73(1), pp. 107–140. doi: 10.5309/willmaryquar.73.1.0107.

Hasin, Y., Seldin, M. and Lusis, A. 2017. Multi-omics approaches to disease. *Genome Biology* 18(1), p. 83. doi: 10.1186/s13059-017-1215-1.

Hawley, D.M., Briggs, J., Dhondt, A.A. and Lovette, I.J. 2008. Reconciling molecular signatures across markers: Mitochondrial DNA confirms founder effect in invasive North American house finches (Carpodacus mexicanus). *Conservation Genetics* 9(3), pp. 637–643. doi: 10.1007/s10592-007-9381-4.

He, K., Minias, P. and Dunn, P.O. 2021. Long-Read Genome Assemblies Reveal Extraordinary Variation in the Number and Structure of MHC Loci in Birds. *Genome Biology and Evolution* 13(2). Available at: https://academic.oup.com/gbe/article/13/2/evaa270/6050824 [Accessed: 16 February 2022].

Hedges, S.B. and Heinicke, M.P. 2007. Molecular phylogeny and biogeography of West Indian frogs of the genus Leptodactylus (Anura, Leptodactylidae). *Molecular Phylogenetics and Evolution* 44(1), pp. 308–314. doi: 10.1016/j.ympev.2006.11.011.

Hedrick, P.W. and Fredrickson, R.J. 2008. Captive breeding and the reintroduction of Mexican and red wolves. *Molecular ecology* 17(1), pp. 344–350. doi: 10.1111/J.1365-294X.2007.03400.X.

Heinsohn, T.E. 2006. Spread of the cane toad Bufo marinus to San Cristobal (Makira) Island, Solomon Islands. *Australian Zoologist* 33(4), pp. 474–475. doi: 10.7882/AZ.2006.019.

Heitman, J. 2010. Evolution of eukaryotic microbial pathogens via covert sexual reproduction. *Cell Host and Microbe* 8(1), pp. 86–99. doi: 10.1016/j.chom.2010.06.011.

Hernández-Gómez, O., Briggler, J.T. and Williams, R.N. 2018. Influence of immunogenetics, sex and body condition on the cutaneous microbial communities of two giant salamanders. *Molecular Ecology* 27(8), pp. 1915–1929. doi: 10.1111/mec.14500.

Hoban, S. et al. 2014. Comparative evaluation of potential indicators and temporal sampling protocols for monitoring genetic erosion. *Evolutionary Applications* 7(9), pp. 984–998. doi: 10.1111/EVA.12197.

Hofman, C., Mol, A., Hoogland, M. and Rojas, R.V. 2014. Stage of encounters: migration, mobility and interaction in the pre-colonial and early colonial Caribbean. *World Archaeology* 46(4), pp. 590–609. doi: 10.1080/00438243.2014.925820.

Hofman, C.L., Bright, A.J. and Ramos, R.R. 2010. Crossing The Caribbean Sea: Towards A Holistic View Of Pre-Colonial Mobility And Exchange. *Journal of Caribbean Archaeology* 3, pp. 1–18.

Holderegger, R., Kamm, U. and Gugerli, F. 2006. Adaptive vs. neutral genetic diversity: implications for landscape genetics. *Landscape Ecology* 21(6), pp. 797–807. doi: 10.1007/s10980-005-5245-9.

Holland, B.S. 2000. Genetics of marine bioinvasions. *Hydrobiologia* 420(1), pp. 63–71. doi: 10.1023/A:1003929519809.

Honeychurch, L. 2003. Inter-Island Migration and Cultural Change: The Impact of Montserratians on Dominica. University of the West Indies. Available at: https://www.open.uwi.edu/sites/default/files/bnccde/montserrat/conference/papers/honychurch.html [Accessed: 16 July 2020].

Horner, A.A., Hoffman, E.A., Tye, M.R., Hether, T.D. and Savage, A.E. 2017. Cryptic chytridiomycosis linked to climate and genetic variation in amphibian populations of the southeastern United States. *PLOS ONE* 12(4), p. e0175843. doi: 10.1371/journal.pone.0175843.

Huang, H. and Knowles, L.L. 2016. Unforeseen Consequences of Excluding Missing Data from Next-Generation Sequences: Simulation Study of RAD Sequences. *Systematic Biology* 65(3), pp. 357–365. doi: 10.1093/sysbio/syu046.

Hudson, M.A. et al. 2016a. Dynamics and genetics of a disease-driven species decline to near extinction: Lessons for conservation. *Scientific Reports* 6(1), p. 30772. doi: 10.1038/srep30772.

Hudson, M.A. et al. 2016b. In-situ itraconazole treatment improves survival rate during an amphibian chytridiomycosis epidemic. *Biological Conservation* 195, pp. 37–45. doi: 10.1016/j.biocon.2015.12.041.

Hudson, M.A. et al. 2019. Reservoir frogs: Seasonality of Batrachochytrium dendrobatidis infection in robber frogs in Dominica and Montserrat. *PeerJ* (6), p. e7021. doi: 10.7717/peerj.7021.

Hudson, M.A., Garcia, G., Chaulet, A., Gitton, D., Perkins, M.W., White, N.F.D. and Cunningham, A.A. 2021. First Detection of the Amphibian Chytrid Fungus Batrachochytrium dendrobatidis in Guadeloupe: Implications for Conservation. *Herpetological Rev.* 52(4), pp. 765–768.

Hudson, M.A., Griffiths, R.A., Cunningham, A.A. and Young, R.P. 2016c. *Conservation Management of the Mountain Chicken Frog*. PhD, University of Kent.

Hughey, M.C. et al. 2016. Short-Term Exposure to Coal Combustion Waste Has Little Impact on the Skin Microbiome of Adult Spring Peepers (Pseudacris crucifer). *Applied and Environmental Microbiology* 82(12), pp. 3493–3502. doi: 10.1128/AEM.00045-16.

Hyatt, A.D. et al. 2007. Diagnostic assays and sampling protocols for the detection of Batrachochytrium dendrobatidis. *Diseases of Aquatic Organisms* 73(3), pp. 175–192. doi: 10.3354/dao073175.

IUCN 2021. *The IUCN Red List of Threatened Species. Version 2021-3*.

IUCN SSC Amphibian Specialist Group 2017. *Leptodactylus fallax. The IUCN Red List of Threatened Species 2017.* International Union for Conservation of Nature - IUCN. Available at: https://www.iucnredlist.org/species/57125/3055585 [Accessed: 18 January 2019].

Iwona, M., Marek, P., Katarzyna, W., Edward, B. and Julia, S. 2018. Use of a genetically informed population viability analysis to evaluate management options for Polish populations of endangered beetle Cerambyx cerdo L. (1758) (Coleoptera, Cerambycidae). *Journal of Insect Conservation* 22(1), pp. 69–83. doi: 10.1007/S10841-017-0039-3/FIGURES/5.

James, T.Y. et al. 2006. A molecular phylogeny of the flagellated fungi (Chytridiomycota) and description of a new phylum (Blastocladiomycota). *Mycologia* 98(6), pp. 860–871. doi: 10.3852/mycologia.98.6.860.

James, T.Y. et al. 2009. Rapid Global Expansion of the Fungal Disease Chytridiomycosis into Declining and Healthy Amphibian Populations. May, R. C. ed. *PLoS Pathogens* 5(5), p. e1000458. doi: 10.1371/journal.ppat.1000458.

James, T.Y. et al. 2015. Disentangling host, pathogen, and environmental determinants of a recently emerged wildlife disease: Lessons from the first 15 years of amphibian chytridiomycosis research. *Ecology and Evolution* 5(18), pp. 4079–4097. doi: 10.1002/ece3.1672.

Jameson, T.J.M. et al. 2019a. *Best Practice Guidelines for the Mountain Chicken (Leptodactylus fallax).* Amsterdam, The Netherlands: European Association of Zoos and Aquaria.

Jameson, T.J.M., Blankenship, J., Christensen, T., Lopez, J. and Garcia, G. 2019b. Wild diet of the critically endangered mountain chicken (Leptodactylus fallax). *Herpetological Journal* 29(4), pp. 299–303. doi: 10.33256/hj29.4.299303.

Janeway, C.A.J., Travers, P., Walport, M. and Shlomchik, M.J. 2001. The major histocompatibility complex and its functions. In: *Immunobiology: The Immune System in Health and Disease*. New York: Garland Science

Jani, A.J. and Briggs, C.J. 2014. The pathogen Batrachochytrium dendrobatidis disturbs the frog skin microbiome during a natural epidemic and experimental infection. *Proceedings of the National Academy of Sciences* 111(47), pp. E5049–E5058. doi: 10.1073/pnas.1412752111.

Jani, A.J. and Briggs, C.J. 2018. Host and aquatic environment shape the amphibian skin microbiome but effects on downstream resistance to the pathogen Batrachochytrium dendrobatidis are variable. *Frontiers in Microbiology* 9, p. 487. doi: 10.3389/fmicb.2018.00487.

Jani, A.J., Bushell, J., Arisdakessian, C.G., Belcaid, M., Boiano, D.M., Brown, C. and Knapp, R.A. 2021. The amphibian microbiome exhibits poor resilience following pathogen-induced disturbance. *The ISME Journal 2021 15:6* 15(6), pp. 1628–1640. doi: 10.1038/s41396-020-00875-w.

Jenkinson, T.S. et al. 2016. Amphibian-killing chytrid in Brazil comprises both locally endemic and globally expanding populations. *Molecular Ecology* 25(13), pp. 2978–2996. doi: 10.1111/mec.13599.

Jimenez Quiros, R.R., Alvarado, G., Estrella, J. and Sommer, S. 2019. Moving Beyond the Host: Unravelling the Skin Microbiome of Endangered Costa Rican Amphibians. *Frontiers in Microbiology* 10, p. 2060. doi: 10.3389/FMICB.2019.02060.

Jiménez, R.R. et al. 2022. Inhibitory Bacterial Diversity and Mucosome Function Differentiate Susceptibility of Appalachian Salamanders to Chytrid Fungal Infection. *Applied and Environmental Microbiology* 88(8), pp. e01818-21. doi: 10.1128/aem.01818-21.

Jiménez, R.R. and Sommer, S. 2017. The amphibian microbiome: natural range of variation, pathogenic dysbiosis, and role in conservation. *Biodiversity and Conservation* 26(4), pp. 763–786. doi: 10.1007/s10531-016-1272-x.

Johnson, M., Berger, L., Philips, L. and Speare, R. 2003. Fungicidal effects of chemical disinfectants, UV light, desiccation and heat on the amphibian chytrid Batrachochytrium dendrobatidis. *Diseases of Aquatic Organisms* 57(3), pp. 255–260. doi: 10.3354/dao057255.

Johnson, P.J., Hargreaves, L.L., Zobrist, C.N. and Ericsson, A.C. 2018. Utility of a portable desiccant system for preservation of fecal samples for downstream 16S rRNA amplicon sequencing. *Journal of Microbiological Methods* 146, pp. 1–6. doi: 10.1016/j.mimet.2018.01.007.

Johnson, P.T.J. and Hoverman, J.T. 2012. Parasite diversity and coinfection determine pathogen infection success and host fitness. *Proceedings of the National Academy of Sciences of the United States of America* 109(23), pp. 9006–9011. doi: 10.1073/pnas.1201790109.

Jombart, T. 2008. Adegenet: A R package for the multivariate analysis of genetic markers. *Bioinformatics* 24(11), pp. 1403–1405. doi: 10.1093/bioinformatics/btn129.

Jombart, T. and Collins, C. 2015. A tutorial for Discriminant Analysis of Principal Components (DAPC) using adegenet 2.0.0. Available at: https://adegenet.r-forge.r-project.org/files/tutorial-dapc.pdf.

Jost, L. 2008. GST and its relatives do not measure differentiation. *Molecular Ecology* 17(18), pp. 4015–4026. doi: 10.1111/j.1365-294X.2008.03887.x.

Ju, K.-S. and Parales, R.E. 2010. Nitroaromatic Compounds, from Synthesis to Biodegradation. *Microbiology and Molecular Biology Reviews : MMBR* 74(2), pp. 250–272. doi: 10.1128/MMBR.00006-10.

Jullien, M., Navascués, M., Ronfort, J., Loridon, K. and Gay, L. 2019. Structure of multilocus genetic diversity in predominantly selfing populations. *Heredity* 123(2), pp. 176–191. doi: 10.1038/s41437-019-0182-6.

Kaiser, H. 1997. Origins and introductions of the Caribbean frog, Eleutherodactylus johnstonei (Leptodactylidae): Management and conservation concerns. *Biodiversity and Conservation* 6(10), pp. 1391–1407. doi: 10.1023/A:1018341814510.

Kearse, M. et al. 2012. Geneious Basic: An integrated and extendable desktop software platform for the organization and analysis of sequence data. *Bioinformatics* 28(12), pp. 1647–1649. doi: 10.1093/bioinformatics/bts199.

Keller, L.F. and Waller, D.M. 2002. Inbreeding effects in wild populations. *Trends in Ecology and Evolution* 17(5), pp. 230–241. doi: 10.1016/S0169-5347(02)02489-8.

Kemp, M.E., Mychajliw, A.M., Wadman, J. and Goldberg, A. 2020. 7000 years of turnover: historical contingency and human niche construction shape the Caribbean's Anthropocene biota. *Proceedings of the Royal Society B: Biological Sciences* 287(1927), p. 20200447. doi: 10.1098/rspb.2020.0447.

Kiemnec-Tyburczy, K.M., Richmond, J.Q., Savage, A.E., Lips, K.R. and Zamudio, K.R. 2012. Genetic diversity of MHC class I loci in six non-model frogs is shaped by positive selection and gene duplication. *Heredity 2012 109:3* 109(3), pp. 146–155. doi: 10.1038/hdy.2012.22.

Kiemnec-Tyburczy, K.M. and Zamudio, K.R. 2013. Novel locus-specific primers for major histocompatibility complex class II alleles from glass frogs developed via genome walking. *Conservation Genetics Resources* 5(1), pp. 109–111. doi: 10.1007/S12686-012-9744-0.

Kim, S.B., Nedashkovskaya, O.I., Mikhailov, V.V., Han, S.K., Kim, K.-O., Rhee, M.-S. and Bae, K.S. 2004. Kocuria marina sp. nov., a novel actinobacterium isolated from marine sediment. *International Journal of Systematic and Evolutionary Microbiology* 54(5), pp. 1617–1620. doi: 10.1099/ijs.0.02742-0.

King, J.D. and Ashmore, P.C. 2014. Conservation and historical biogeography: How did the mountain chicken frog get to the Caribbean? *International Journal of Biodiversity and Conservation* 6(11), pp. 754–764. doi: 10.5897/IJBC2011.075.

Kingman, J.F.C. 1982. The coalescent. *Stochastic Processes and their Applications* 13(3), pp. 235–248. doi: 10.1016/0304-4149(82)90011-4.

Kirshtein, J.D., Anderson, C.W., Wood, J.S., Longcore, J.E. and Voytek, M.A. 2007. Quantitative PCR detection of Batrachochytrium dendrobatidis DNA from sediments and water. *Diseases of Aquatic Organisms* 77(1), pp. 11–15. doi: 10.3354/dao01831.

Klein, J. et al. 1990. Nomenclature for the major histocompatibility complexes of different species: a proposal. *Immunogenetics* 31(4), pp. 217–219. doi: 10.1007/BF00204890.

Knapp, R.A., Fellers, G.M., Kleeman, P.M., Miller, D.A.W., Vredenburg, V.T., Rosenblum, E.B. and Briggs, C.J. 2016. Large-scale recovery of an endangered amphibian despite ongoing exposure to multiple stressors. *Proceedings of the National Academy of Sciences* 113(42), pp. 11889–11894. doi: 10.1073/pnas.1600983113.

Koh, E.J., Kim, S.H. and Hwang, S.Y. 2022. Sample management: a primary critical starting point for successful omics studies. *Molecular & Cellular Toxicology* 18(2), pp. 141–148. doi: 10.1007/s13273-021-00213-x.

Kolby, J.E., Ramirez, S.D., Berger, L., Richards-Hrdlicka, K.L., Jocque, M. and Skerratt, L.F. 2015. Terrestrial dispersal and potential environmental transmission of the amphibian chytrid fungus (Batrachochytrium dendrobatidis). *PLoS ONE* 10(4), p. e0125386. doi: 10.1371/journal.pone.0125386.

Korner-Nievergelt, F., Roth, T., von Felten, S., Guélat, J., Almasi, B. and Korner-Nievergelt, P. 2015. *Bayesian Data Analysis in Ecology using Linear Models with R, BUGS and Stan*. Elsevier. doi: 10.1016/B978-0-12-801370-0.00001-0.

Kosakovsky Pond, S.L. et al. 2020. HyPhy 2.5—A Customizable Platform for Evolutionary Hypothesis Testing Using Phylogenies. *Molecular Biology and Evolution* 37(1), pp. 295–299. doi: 10.1093/MOLBEV/MSZ197.

Kosakovsky Pond, S.L. and Kosakovsky, S.L. 2016. Quantifying Natural Selection in Coding Sequences.

Kosch, T.A. et al. 2019. Genetic potential for disease resistance in critically endangered amphibians decimated by chytridiomycosis. *Animal Conservation* 22(3), pp. 238–250. doi: 10.1111/acv.12459.

Kosch, T.A., Bataille, A., Didinger, C., Eimes, J.A., Rodríguez-Brenes, S., Ryan, M.J. and Waldman, B. 2016. Major histocompatibility complex selection dynamics in pathogen-infected túngara frog (Physalaemus pustulosus) populations. *Biology Letters* 12(8), p. 20160345. doi: 10.1098/rsbl.2016.0345.

Kosch, T.A., Eimes, J.A., Didinger, C., Brannelly, L.A., Waldman, B., Berger, L. and Skerratt, L.F. 2017. Characterization of MHC class IA in the endangered southern corroboree frog. *Immunogenetics* 69(3), pp. 165–174. doi: 10.1007/s00251-016-0965-3.

Kosch, T.A., Waddle, A.W., Cooper, C.A., Zenger, K.R., Garrick, D.J., Berger, L. and Skerratt, L.F. 2022. Genetic approaches for increasing fitness in endangered species. *Trends in Ecology & Evolution* 37(4), pp. 332–345. doi: 10.1016/j.tree.2021.12.003.

Kozich, J.J., Westcott, S.L., Baxter, N.T., Highlander, S.K. and Schloss, P.D. 2013. Development of a Dual-Index Sequencing Strategy and Curation Pipeline for Analyzing Amplicon Sequence Data on the MiSeq Illumina Sequencing Platform. *Applied and Environmental Microbiology* 79(17), pp. 5112–5120. doi: 10.1128/AEM.01043-13.

Kraaijeveld-Smit, F.J.L., Griffiths, R.A., Moore, R.D. and Beebee, T.J.C. 2006. Captive breeding and the fitness of reintroduced species: A test of the responses to predators in a threatened amphibian. *Journal of Applied Ecology* 43(2), pp. 360–365. doi: 10.1111/j.1365-2664.2006.01137.x.

Kramer, J., Özkaya, Ö. and Kümmerli, R. 2020. Bacterial siderophores in community and host interactions. *Nature Reviews Microbiology* 18(3), pp. 152–163. doi: 10.1038/s41579-019-0284-4.

Kueneman, J.G. et al. 2022. Effects of captivity and rewilding on amphibian skin microbiomes. *Biological Conservation* 271, p. 109576. doi: 10.1016/j.biocon.2022.109576.

Kueneman, J.G., Parfrey, L.W., Woodhams, D.C., Archer, H.M., Knight, R. and McKenzie, V.J. 2014. The amphibian skin-associated microbiome across species, space and life history stages. *Molecular Ecology* 23(6), pp. 1238–1250. doi: 10.1111/mec.12510.

Kueneman, J.G., Woodhams, D.C., Harris, R., Archer, H.M., Knight, R. and McKenzie, V.J. 2016. Probiotic treatment restores protection against lethal fungal infection lost during amphibian captivity. *Proceedings of the Royal Society B: Biological Sciences* 283(1839), p. 20161553. doi: 10.1098/rspb.2016.1553.

Kumar, S., Stecher, G., Li, M., Knyaz, C. and Tamura, K. 2018. MEGA X: Molecular Evolutionary Genetics Analysis across Computing Platforms. *Molecular Biology and Evolution* 35(6), p. 1547. doi: 10.1093/MOLBEV/MSY096.

Kvarnemo, C. and Ahnesjö, I. 1996. The dynamics of operational sex ratios and competition for mates. *Trends in Ecology and Evolution* 11(10), pp. 404–408. doi: 10.1016/0169-5347(96)10056-2.

Kwiecinski, G.G. et al. 2018. *Bats of Saint Vincent, Lesser Antilles*. Lubbock, Texas: Museum of Texas Tech University. Available at: https://www.biodiversitylibrary.org/bibliography/156880 [Accessed: 15 July 2020].

Lampo, M., Señaris, C. and García, C.Z. 2017. Population dynamics of the critically endangered toad Atelopus cruciger and the fungal disease chytridiomycosis. *PLOS ONE* 12(6), p. e0179007. doi: 10.1371/JOURNAL.PONE.0179007.

Langille, M.G.I. et al. 2013. Predictive functional profiling of microbial communities using 16S rRNA marker gene sequences. *Nature biotechnology* 31(9), pp. 814–821. doi: 10.1038/nbt.2676.

Lau, Q., Igawa, T., Komaki, S. and Satta, Y. 2020. Expression Changes of MHC and Other Immune Genes in Frog Skin during Ontogeny. *Animals : an Open Access Journal from MDPI* 10(1), p. 91. doi: 10.3390/ani10010091.

Laurens, V., Chapusot, C., Ordonez, M.D.R., Bentrari, F., Padros, M.R. and Tournefier, A. 2001. Axolotl MHC class II β chain: Predominance of one allele and alternative splicing of the β1 domain. *European Journal of Immunology* 31(2), pp. 506–515. doi: 10.1002/1521-4141(200102)31:2<506::AID-IMMU506>3.0.CO;2-P.

Le Sage, E.H., LaBumbard, B.C., Reinert, L.K., Miller, B.T., Richards-Zawacki, C.L., Woodhams, D.C. and Rollins-Smith, L.A. 2021. Preparatory immunity: Seasonality of mucosal skin defences and Batrachochytrium infections in Southern leopard frogs. *Journal of Animal Ecology* 90(2), pp. 542–554. doi: 10.1111/1365-2656.13386.

Lenth, R.V. et al. 2022. emmeans: Estimated Marginal Means, aka Least-Squares Means. Available at: https://CRAN.R-project.org/package=emmeans [Accessed: 1 November 2022].

Li, H. et al. 2009. The Sequence Alignment/Map format and SAMtools. *Bioinformatics* 25(16), pp. 2078–2079. doi: 10.1093/bioinformatics/btp352.

Li, H. 2013. Aligning sequence reads, clone sequences and assembly contigs with BWA-MEM. *arXiv* 1303.3997v2, pp. 1–3.

Liew, N. et al. 2017. Chytrid fungus infection in zebrafish demonstrates that the pathogen can parasitize non-amphibian vertebrate hosts. *Nature Communications* 8(1), p. 15048. doi: 10.1038/ncomms15048.

Lillie, M., Shine, R. and Belov, K. 2014. Characterisation of Major Histocompatibility Complex Class I in the Australian Cane Toad, Rhinella marina. *PLOS ONE* 9(8), p. e102824. doi: 10.1371/JOURNAL.PONE.0102824.

Lin, H. and Peddada, S.D. 2020. Analysis of compositions of microbiomes with bias correction. *Nature Communications 2020 11:1* 11(1), pp. 1–11. doi: 10.1038/s41467-020-17041-7.

Linehan, J.L. et al. 2018. Non-classical Immunity Controls Microbiota Impact on Skin Immunity and Tissue Repair. *Cell* 172(4), pp. 784-796.e18. doi: 10.1016/j.cell.2017.12.033.

Lips, K.R., Reeve, J.D. and Witters, L.R. 2003. Ecological Traits Predicting Amphibian Population Declines in Central America. *Conservation Biology* 17(4), pp. 1078–1088. doi: 10.1046/j.1523-1739.2003.01623.x.

Liu, Y., Athanasiadis, G. and Weale, M.E. 2008. A survey of genetic simulation software for population and epidemiological studies. *Human genomics* 3(1), pp. 79–86. doi: 10.1186/1479-7364-3-1-79.

Lloyd-Smith, J.O. et al. 2005. Should we expect population thresholds for wildlife disease? *Trends in Ecology & Evolution* 20(9), pp. 511–519. doi: 10.1016/j.tree.2005.07.004.

Lomolino, M.V. 1985. Body Size of Mammals on Islands: The Island Rule Reexamined. *The American Naturalist* 125(2), pp. 310–316. doi: 10.1086/284343.

Longcore, J.E., Pessier, A.P. and Nichols, D.K. 1999. Batrachochytrium dendrobatidis gen. et sp. nov., a chytrid pathogenic to amphibians. *Mycologia* 91(2), pp. 219–227. doi: 10.2307/3761366.

Longo, A.V. 2022. Metabarcoding Approaches in Amphibian Disease Ecology: Disentangling the Functional Contributions of Skin Bacteria on Disease Outcome. *Integrative and Comparative Biology* 00(0), pp. 1–10. doi: 10.1093/ICB/ICAC062.

Longo, A.V., Savage, A.E., Hewson, I. and Zamudio, K.R. 2015. Seasonal and ontogenetic variation of skin microbial communities and relationships to natural disease dynamics in declining amphibians. *Royal Society Open Science* 2(7). doi: 10.1098/rsos.140377.

Longo, A.V. and Zamudio, K.R. 2017. Temperature variation, bacterial diversity and fungal infection dynamics in the amphibian skin. *Molecular Ecology* 26(18), pp. 4787–4797. doi: 10.1111/mec.14220.

Loudon, A.H., Woodhams, D.C., Parfrey, L.W., Archer, H., Knight, R., McKenzie, V. and Harris, R.N. 2014. Microbial community dynamics and effect of environmental microbial reservoirs on red-backed salamanders (plethodon cinereus). *ISME Journal* 8(4), pp. 830–840. doi: 10.1038/ismej.2013.200.

Lucas, E.M., Brasileiro, C.A., Oyamaguchi, H.M. and Martins, M. 2008. The reproductive ecology of Leptodactylus fuscus (Anura, Leptodactylidae): New data from natural temporary ponds in the Brazilian Cerrado and a review throughout its distribution. *Journal of Natural History* 42(35–36), pp. 2305–2320. doi: 10.1080/00222930802254698.

Luke, S.G. 2017. Evaluating significance in linear mixed-effects models in R. *Behavior Research Methods* 49(4), pp. 1494–1502. doi: 10.3758/S13428-016-0809-Y/TABLES/1.

MacArthur, R.H. and Wilson, E.O. 1967. *The Theory of Island Biogeography*. Princeton, N. J.: Princeton University Press. Available at: https://books.google.co.uk/books?hl=en&lr=&id=a10cdkywhVgC&oi=fnd&pg=PR7&dq=theory+of+island+biogeography&ots=Rhc_xHWfDD&sig=RyjLhjdUqzVQgeh7L4KRk6oGkMk#v=onepage&q=theory of island biogeography&f=false [Accessed: 23 July 2020].

Magoc, T. and Salzberg, S.L. 2011. FLASH: fast length adjustment of short reads to improve genome assemblies. *Bioinformatics* 27(21), pp. 2957–2963. doi: 10.1093/bioinformatics/btr507.

Marchesi, J.R. et al. 2016. The gut microbiota and host health: a new clinical frontier. *Gut* 65(2), pp. 330–339. doi: 10.1136/gutjnl-2015-309990.

Margan, S.H., Nurthen, R.K., Montgomery, M.E., Woodworth, L.M., Lowe, E.H., Briscoe, D.A. and Frankham, R. 1998. Single large or several small? Population fragmentation in the captive management of endangered species. *Zoo Biology* 17(6), pp. 467–480. doi: 10.1002/(sici)1098-2361(1998)17:6<467::aid-zoo1>3.3.co;2-v.

Marr, S.R., Mautz, W.J. and Hara, A.H. 2008. Parasite loss and introduced species: A comparison of the parasites of the Puerto Rican tree frog, (Eleutherodactylus coqui), in its native and introduced ranges. *Biological Invasions* 10(8), pp. 1289–1298. doi: 10.1007/s10530-007-9203-0.

Marshall, T.L., Baca, C.R., Correa, D.T., Forstner, M.R.J., Hahn, D. and Rodriguez, D. 2018. Genetic characterization of chytrids isolated from larval amphibians collected in central and east Texas. *bioRxiv* . Available at: https://doi.org/10.1101/451385 [Accessed: 8 May 2021].

Martel, A. et al. 2013. Batrachochytrium salamandrivorans sp. nov. causes lethal chytridiomycosis in amphibians. *Proceedings of the National Academy of Sciences of the United States of America* 110(38), pp. 15325–15329. doi: 10.1073/PNAS.1307356110/SUPPL_FILE/PNAS.201307356SI.PDF.

Martel, A. et al. 2014. Recent introduction of a chytrid fungus endangers Western Palearctic salamanders. *Science (New York, N.Y.)* 346(6209), pp. 630–631. doi: 10.1126/science.1258268.

Martin, M. 2011. Cutadapt removes adapter sequences from high-throughput sequencing reads. *EMBnet.journal* 17(1), p. 10. doi: 10.14806/ej.17.1.200.

May, S. and Beebee, T.J.C. 2009. Characterisation of major histocompatibility complex class II alleles in the natterjack toad, Bufo calamita. *Conservation Genetics Resources* 1(1), pp. 415–417. doi: 10.1007/s12686-009-9096-6.

McIntyre, S. 2003. *The current status of the mountain chicken Leptodactylus fallax on Dominica, Eastern Caribbean; an amphibian in decline.* University of East Anglia.

McLaren, M.R. and Callahan, B.J. 2020. Pathogen resistance may be the principal evolutionary advantage provided by the microbiome. *Philosophical Transactions of the Royal Society B: Biological Sciences* 375(1808), p. 20190592. doi: 10.1098/rstb.2019.0592.

McMahon, T.A. et al. 2014. Amphibians acquire resistance to live and dead fungus overcoming fungal immunosuppression. *Nature* 511(7508), pp. 224–227. doi: 10.1038/nature13491.

McMurdie, P.J. and Holmes, S. 2013. phyloseq: An R Package for Reproducible Interactive Analysis and Graphics of Microbiome Census Data. *PLOS ONE* 8(4), p. e61217. doi: 10.1371/JOURNAL.PONE.0061217.

McMurdie, P.J. and Holmes, S. 2014. Waste Not, Want Not: Why Rarefying Microbiome Data Is Inadmissible. *PLOS Computational Biology* 10(4), p. e1003531. doi: 10.1371/JOURNAL.PCBI.1003531.

McNew, G.L. 1960. The nature, origin, and evolution of parasitism. In: Horsfall, J. G. and Dimond, A. E. eds. *Plant pathology: An advanced treatise*. New York: Academic Press, pp. 19–69.

Meredith, M. and Kruschke, J. 2018. HDInterval: Highest (Posterior) Density Intervals. Available at: https://cran.r-project.org/package=HDInterval.

Miller, H.C., Bowker-Wright, G., Kharkrang, M. and Ramstad, K. 2011. Characterisation of class II B MHC genes from a ratite bird, the little spotted kiwi (Apteryx owenii). *Immunogenetics* 63(4), pp. 223–233. doi: 10.1007/S00251-010-0503-7/FIGURES/4.

Milne, I., Bayer, M., Cardle, L., Shaw, P., Stephen, G., Wright, F. and Marshall, D. 2010. Tablet-next generation sequence assembly visualization. *Bioinformatics Applications Note* 26(3), pp. 401–402. doi: 10.1093/bioinformatics/btp666.

Minatel, I.O., Borges, C.V., Ferreira, M.I., Gomez, H.A.G. and Lima, C.-Y.O.C. and G.P.P. 2017. Phenolic Compounds: Functional Properties, Impact of Processing and Bioavailability. In: *Phenolic Compounds - Biological Activity*. London: IntechOpen. doi: 10.5772/66368.

Minias, P., Bateson, Z.W., Whittingham, L.A., Johnson, J.A., Oyler-McCance, S. and Dunn, P.O. 2016. Contrasting evolutionary histories of MHC class I and class II loci in grouse—effects of selection and gene conversion. *Heredity* 116(5), pp. 466–476. doi: 10.1038/hdy.2016.6.

Minias, P., Pikus, E. and Anderwald, D. 2019a. Allelic diversity and selection at the MHC class i and class II in a bottlenecked bird of prey, the White-tailed Eagle. *BMC Evolutionary Biology* 19(1), pp. 1–13. doi: 10.1186/s12862-018-1338-3.

Minias, P., Pikus, E., Whittingham, L.A. and Dunn, P.O. 2018. A global analysis of selection at the avian MHC. *Evolution* 72(6), pp. 1278–1293. doi: 10.1111/EVO.13490.

Minias, P., Pikus, E., Whittingham, L.A. and Dunn, P.O. 2019b. Evolution of Copy Number at the MHC Varies across the Avian Tree of Life. *Genome Biology and Evolution* 11(1), p. 17. doi: 10.1093/GBE/EVY253.

Mirarab, S., Bayzid, M.S. and Warnow, T. 2016. Evaluating Summary Methods for Multilocus Species Tree Estimation in the Presence of Incomplete Lineage Sorting. *Systematic Biology* 65(3), pp. 366–380. doi: 10.1093/sysbio/syu063.

Misslinger, M., Hortschansky, P., Brakhage, A.A. and Haas, H. 2021. Fungal iron homeostasis with a focus on Aspergillus fumigatus. *Biochimica et Biophysica Acta (BBA) - Molecular Cell Research* 1868(1), p. 118885. doi: 10.1016/J.BBAMCR.2020.118885.

Molloy, E.K. and Warnow, T. 2018. To Include or Not to Include: The Impact of Gene Filtering on Species Tree Estimation Methods. *Systematic Biology* 67(2), pp. 285–303. doi: 10.1093/sysbio/syx077.

Moragues, M., Comadran, · J, Waugh, · R, Milne, · I, Flavell, · A J and Russell, J.R. 2010. Effects of ascertainment bias and marker number on estimations of barley diversity from high-throughput SNP genotype data. *Theoretical and Applied Genetics* 120, pp. 1525–1534. doi: 10.1007/s00122-010-1273-1.

Morehouse, E.A., James, T.Y., Ganley, A.R.D., Vilgalys, R., Berger, L., Murphy, P.J. and Longcore, J.E. 2003. Multilocus sequence typing suggests the chytrid pathogen of amphibians is a recently emerged clone. *Molecular Ecology* 12(2), pp. 395–403. doi: 10.1046/j.1365-294X.2003.01732.x.

Morin, P.A., Martien, K.K. and Taylor, B.L. 2009. Assessing statistical power of SNPs for population structure and conservation studies. *Molecular Ecology Resources* 9(1), pp. 66–73. doi: 10.1111/j.1755-0998.2008.02392.x.

Moro, D., Byrne, M., Kennedy, M., Campbell, S. and Tizard, M. 2018. Identifying knowledge gaps for gene drive research to control invasive animal species: The next CRISPR step. *Global Ecology and Conservation* 13, p. e00363. doi: 10.1016/j.gecco.2017.e00363.

Muletz-Wolz, C.R., DiRenzo, G.V., Yarwood, S.A., Grant, E.H.C., Fleischer, R.C. and Lips, K.R. 2017. Antifungal bacteria on woodland salamander skin exhibit high taxonomic diversity and geographic variability. *Applied and Environmental Microbiology* 83(9), pp. e00186-17.

Nater, A. et al. 2015. Reconstructing the demographic history of orang-utans using Approximate Bayesian Computation. *Molecular Ecology* 24(2), pp. 310–327. doi: 10.1111/mec.13027.

Nei, M. and Gojobori, T. 1986. Simple methods for estimating the numbers of synonymous and nonsynonymous nucleotide substitutions. *Molecular Biology and Evolution* 3(5), pp. 418–426. doi: 10.1093/oxfordjournals.molbev.a040410.

Newsom, L. A. and Wing, E.S. 2013. On land and sea: Native American uses of biological resources in the West Indies. *Choice Reviews Online* 42(06), pp. 42-3514-42–3514. doi: 10.5860/choice.42-3514.

Nguyen, T.T., Nguyen, T.V., Ziegler, T., Pasmans, F. and Martel, A. 2017. Trade in wild anurans vectors the urodelan pathogen Batrachochytrium salamandrivorans into Europe. *Amphibia-Reptilia* 38(4), pp. 554–556. doi: 10.1163/15685381-00003125.

O'Hanlon, S.J. et al. 2018. Recent Asian origin of chytrid fungi causing global amphibian declines. *Science (New York, N.Y.)* 360(6389), pp. 621–627. doi: 10.1126/science.aar1965.

Ohta, T. and Kimura, M. 1973. A model of mutation appropriate to estimate the number of electrophoretically detectable alleles in a finite population. *Genetical Research* 22(2), pp. 201–204. doi: 10.1017/S0016672300012994.

Oksanen, J., Kindt, R., O', B. and Maintainer, H. 2005. Vegan: Community Ecology Package. Available at: http://cc.oulu.fi/~jarioksa/ [Accessed: 16 May 2022].

Van Oosterhout, C., Hutchinson, W.F., Wills, D.P.M. and Shipley, P. 2004. MICRO-CHECKER: Software for identifying and correcting genotyping errors in microsatellite data. *Molecular Ecology Notes* 4(3), pp. 535–538. doi: 10.1111/j.1471-8286.2004.00684.x.

Orozco-terWengel, P., Andreone, F., Louis, E. and Vences, M. 2013. Mitochondrial introgressive hybridization following a demographic expansion in the tomato frogs of Madagascar, genus D yscophus. *Molecular Ecology* 22(24), pp. 6074–6090. doi: 10.1111/mec.12558.

Ortega, N., Price, W., Campbell, T. and Rohr, J. 2015. Acquired and introduced macroparasites of the invasive Cuban treefrog, Osteopilus septentrionalis. *International Journal for Parasitology: Parasites and Wildlife* 4(3), pp. 379–384. doi: 10.1016/J.IJPPAW.2015.10.002.

Osorio, D., Rondón-Villarreal, P. and Torres, R. 2015. Peptides: A package for data mining of antimicrobial peptides. *R Journal* 7(1), pp. 4–14. doi: 10.32614/RJ-2015-001.

Papadopoulou, A. and Knowles, L.L. 2015. Genomic tests of the species-pump hypothesis: Recent island connectivity cycles drive population divergence but not speciation in Caribbean crickets across the Virgin Islands. *Evolution* 69(6), pp. 1501–1517. doi: 10.1111/evo.12667.

Peel, D., Waples, R.S., Macbeth, G.M., Do, C. and Ovenden, J.R. 2013. Accounting for missing data in the estimation of contemporary genetic effective population size (Ne). *Molecular Ecology Resources* 13(2), pp. 243–253. doi: 10.1111/1755-0998.12049.

Peng, B., Amos, C.I. and Kimmel, M. 2007. Forward-Time Simulations of Human Populations with Complex Diseases. Allison, D. B. ed. *PLoS Genetics* 3(3), p. e47. doi: 10.1371/journal.pgen.0030047.

Perez, R. et al. 2014. Field surveys in Western Panama indicate populations of Atelopus varius frogs are persisting in regions where Batrachochytrium dendrobatidis is now enzootic. *Amphibian and Reptile Conservation* 8(2), pp. 30–35.

Perlman, S.J., Hodson, C.N., Hamilton, P.T., Opit, G.P. and Gowen, B.E. 2015. Maternal transmission, sex ratio distortion, and mitochondria. *Proceedings of the National Academy of Sciences of the United States of America* 112(33), pp. 10162–10168. doi: 10.1073/pnas.1421391112.

Pessier, A.P. 2008. Chapter 17 - Amphibian Chytridiomycosis. In: Fowler, M. E. and Miller, R. E. eds. *Zoo and Wild Animal Medicine (Sixth Edition)*. Saint Louis: W.B. Saunders, pp. 137-cp1. Available at: https://www.sciencedirect.com/science/article/pii/B9781416040477500208 [Accessed: 5 August 2022].

Piertney, S.B. and Oliver, M.K. 2006. The evolutionary ecology of the major histocompatibility complex. *Heredity* 96, pp. 7–21. doi: 10.1038/sj.hdy.6800724.

Piotrowski, J.S., Annis, S.L. and Longcore, J.E. 2004. Physiology of Batrachochytrium dendrobatidis, a Chytrid Pathogen of Amphibians. *Mycologia* 96(1), p. 9. doi: 10.2307/3761981.

Piovia-Scott, J. et al. 2017. Greater Species Richness of Bacterial Skin Symbionts Better Suppresses the Amphibian Fungal Pathogen Batrachochytrium Dendrobatidis. *Microbial Ecology* 74(1), pp. 217–226. doi: 10.1007/s00248-016-0916-4.

Pitt, D. et al. 2019. Domestication of cattle: Two or three events? *Evolutionary Applications* 12(1), pp. 123–136. doi: 10.1111/eva.12674.

Ploner, A. 2012. Heatplus: Heatmaps with row and/or column covariates and colored clusters. Available at: https://github.com/alexploner/Heatplus/issues [Accessed: 16 May 2022].

Plummer, M. and Murrell, P. 2006. CODA: Convergence Diagnosis and Output Analysis for MCMC. *R News* 6(1), pp. 7–11.

Pond, S.K. and Muse, S.V. 2005. Site-to-Site Variation of Synonymous Substitution Rates. *Molecular Biology and Evolution* 22(12), pp. 2375–2385. doi: 10.1093/MOLBEV/MSI232.

Price, S.J., Garner, T.W.J., Balloux, F., Ruis, C., Paszkiewicz, K.H., Moore, K. and Griffiths, A.G.F. 2015. A de novo Assembly of the Common Frog (Rana temporaria) Transcriptome and Comparison of Transcription Following Exposure to Ranavirus and Batrachochytrium dendrobatidis. *PLOS ONE* 10(6), p. e0130500. doi: 10.1371/journal.pone.0130500.

Pritchard, J.K., Stephens, M. and Donnelly, P. 2000. Inference of population structure using multilocus genotype data. *Genetics* 155, pp. 945–959. doi: 10.1111/j.1471-8286.2007.01758.x.

Pritchard, J.K., Wen, X. and Falush, D. 2009. Documentation for structure software: Version 2.3.

Purcell, S. et al. 2007. PLINK: A tool set for whole-genome association and population-based linkage analyses. *American Journal of Human Genetics* 81(3), pp. 559–575. doi: 10.1086/519795.

R Development Core Team 2008. R: A language and environment for statistical computing. Available at: http://www.r-project.org. [Accessed: 5 March 2019].

Radwan, J., Babik, W., Kaufman, J., Lenz, T.L. and Winternitz, J. 2020. Advances in the Evolutionary Understanding of MHC Polymorphism. *Trends in Genetics* 36(4), pp. 298–311. doi: 10.1016/j.tig.2020.01.008.

Radwan, J., Biedrzycka, A. and Babik, W. 2010. Does reduced MHC diversity decrease viability of vertebrate populations? *Biological Conservation* 143(3), pp. 537–544. doi: 10.1016/j.biocon.2009.07.026.

Rakus, K., Ronsmans, M. and Vanderplasschen, A. 2017. Behavioral fever in ectothermic vertebrates. *Developmental and Comparative Immunology* 66, pp. 84–91. doi: 10.1016/j.dci.2016.06.027.

Ralls, K. and Ballou, J.D. 2004. Genetic Status and Management of California Condors. *The Condor* 106(2), pp. 215–228. doi: 10.1093/CONDOR/106.2.215.

Razali, H., O'Connor, E., Drews, A., Burke, T. and Westerdahl, H. 2017. A quantitative and qualitative comparison of illumina MiSeq and 454 amplicon sequencing for genotyping the highly polymorphic major histocompatibility complex (MHC) in a non-model species. *BMC Research Notes* 10(1), p. 346. doi: 10.1186/s13104-017-2654-1.

Reading, C.J. and Jofre, G.M. 2003. Reproduction in the nest building vizcacheras frog Leptodactylus bufonis in central Argentina. *Amphibia-Reptilia* 24, pp. 415–427.

Rebollar, E.A. et al. 2016. Using "Omics" and Integrated Multi-Omics Approaches to Guide Probiotic Selection to Mitigate Chytridiomycosis and Other Emerging Infectious Diseases. *Frontiers in Microbiology* 7(68), p. 26870025.

Rebollar, E.A. et al. 2018. The skin microbiome of the neotropical frog Craugastor fitzingeri: Inferring potential bacterial-host-pathogen interactions from metagenomic data. *Frontiers in Microbiology* 9(MAR), p. 466. doi: 10.3389/FMICB.2018.00466/BIBTEX.

Rebollar, E.A., Martínez-Ugalde, E. and Orta, A.H. 2020. The amphibian skin microbiome and its protective role against chytridiomycosis. *Herpetologica* 76(2), pp. 167–177. doi: 10.1655/0018-0831-76.2.167.

Rebouças, R., da Silva, H.R. and Solé, M. 2018. Frog size on continental islands of the coast of Rio de Janeiro and the generality of the Island Rule. Navas, C. A. ed. *PLOS ONE* 13(1), p. e0190153. doi: 10.1371/journal.pone.0190153.

Reeder, N.M.M., Pessier, A.P. and Vredenburg, V.T. 2012. A Reservoir Species for the Emerging Amphibian Pathogen Batrachochytrium dendrobatidis Thrives in a Landscape Decimated by Disease. *PLOS ONE* 7(3), p. e33567. doi: 10.1371/journal.pone.0033567.

Ricklefs, R. and Bermingham, E. 2008. The West Indies as a laboratory of biogeography and evolution. *Philosophical Transactions of the Royal Society B: Biological Sciences* 363(1502), pp. 2393–2413. doi: 10.1098/rstb.2007.2068.

Ritchie, M.D. and Bush, W.S. 2010. Genome simulation approaches for synthesizing in silico datasets for human genomics. *Advances in Genetics* 72(C), pp. 1–24. doi: 10.1016/B978-0-12-380862-2.00001-1.

Robinson, K.A., Prostak, S.M., Campbell Grant, E.H. and Fritz-Laylin, L.K. 2022. Amphibian mucus triggers a developmental transition in the frog-killing chytrid fungus. *Current Biology* 32(12), pp. 2765-2771.e4. doi: 10.1016/j.cub.2022.04.006.

Robinson, N.M. et al. 2020. Be nimble with threat mitigation: lessons learned from the reintroduction of an endangered species. *Restoration Ecology* 28(1), pp. 29–38. doi: 10.1111/rec.13028.

Roelants, K. et al. 2007. Global patterns of diversification in the history of modern amphibians. *Proceedings of the National Academy of Sciences* 104(3), pp. 887–892. doi: 10.1073/PNAS.0608378104.

Rojas-Gätjens, D., Valverde-Madrigal, K.S., Rojas-Jimenez, K., Pereira, R., Avey-Arroyo, J. and Chavarría, M. 2022. Antibiotic-producing Micrococcales govern the microbiome that inhabits the fur of two- and three-toed sloths. *Environmental Microbiology* 24(7), pp. 3148–3163. doi: 10.1111/1462-2920.16082.

Rollins-Smith, L.A. 1998. Metamorphosis and the amphibian immune system. *Immunological Reviews* 166(1), pp. 221–230. doi: 10.1111/j.1600-065X.1998.tb01265.x.

Rollins-Smith, L.A. 2009. The role of amphibian antimicrobial peptides in protection of amphibians from pathogens linked to global amphibian declines. *Biochimica et Biophysica Acta (BBA) - Biomembranes* 1788(8), pp. 1593–1599. doi: 10.1016/j.bbamem.2009.03.008.

Rollins-Smith, L.A. and Conlon, J.M. 2005. Antimicrobial peptide defenses against chytridiomycosis, an emerging infectious disease of amphibian populations. 29(7), pp. 589–598.

Rollins-Smith, L.A., King, J.D., Nielsen, P.F., Sonnevend, A. and Conlon, J.M. 2005. An antimicrobial peptide from the skin secretions of the mountain chicken frog Leptodactylus fallax (Anura:Leptodactylidae). *Regulatory Peptides* 124(1–3), pp. 173–178.

Rollins-Smith, L.A., Ramsey, J.P., Pask, J.D., Reinert, L.K. and Woodhams, D.C. 2011. Amphibian immune defenses against chytridiomycosis: Impacts of changing environments. In: *Integrative and Comparative Biology*., pp. 552–562. doi: 10.1093/icb/icr095.

Rosa, G.M., Bradfield, K., Fernández-Loras, A., Garcia, G. and Tapley, B. 2012. Two remarkable prey items for a chicken: Leptodactylus fallax Müller, 1926 predation upon the theraphosid spider Cyrtopholis femoralis Pocock, 1903 and the colubrid snake Liophis juliae (Cope, 1879). *Tropical Zoology* 25(3), pp. 135–140. doi: 10.1080/03946975.2012.717795.

Rosa, G.M. and Fernandez Loras, A. 2014. Emergency procedures in the field: A report of wound treatment and fast healing in the giant ditch frog (Leptodactylus fallax). *Animal Welfare* 21(4), pp. 559–562. doi: 10.7120/09627286.21.4.559.

Rosenblum, E.B. et al. 2013. Complex history of the amphibian-killing chytrid fungus revealed with genome resequencing data. *Proceedings of the National Academy of Sciences of the United States of America* 110(23), pp. 9385–9390. doi: 10.1073/pnas.1300130110.

Rosenblum, E.B., Poorten, T.J., Settles, M. and Murdoch, G.K. 2012. Only skin deep: Shared genetic response to the deadly chytrid fungus in susceptible frog species. *Molecular Ecology* 21(13), pp. 3110–3120. doi: 10.1111/j.1365-294X.2012.05481.x.

Rosenblum, E.B., Poorten, T.J., Settles, M., Murdoch, G.K., Robert, J., Maddox, N. and Eisen, M.B. 2009. Genome-wide transcriptional response of Silurana (Xenopus) tropicalis to infection with the deadly chytrid fungus. *PLoS ONE* 4(8). doi: 10.1371/journal.pone.0006494.

Rosenblum, E.B., Stajich, J.E., Maddox, N. and Eisen, M.B. 2008. Global gene expression profiles for life stages of the deadly amphibian pathogen Batrachochytrium dendrobatidis. *Proceedings of the National Academy of Sciences* 105(44), pp. 17034–17039. doi: 10.1073/pnas.0804173105.

Rosenblum, E.B., Voyles, J., Poorten, T.J. and Stajich, J.E. 2010. The Deadly Chytrid Fungus: A Story of an Emerging Pathogen. Madhani, H. D. ed. *PLoS Pathogens* 6(1), p. e1000550. doi: 10.1371/journal.ppat.1000550.

Rothstein, A.P., Byrne, A.Q., Knapp, R.A., Briggs, C.J., Voyles, J., Richards-Zawacki, C.L. and Rosenblum, E.B. 2021. Divergent regional evolutionary histories of a devastating global amphibian pathogen. *Proceedings of the Royal Society B* 288(1953). Available at: https://royalsocietypublishing.org/doi/abs/10.1098/rspb.2021.0782 [Accessed: 10 February 2022].

Rousset, F. 2008. GENEPOP'007: A complete re-implementation of the GENEPOP software for Windows and Linux. *Molecular Ecology Resources* 8(1), pp. 103–106. doi: 10.1111/j.1471-8286.2007.01931.x.

Rozas, J., Ferrer-Mata, A., Sánchez-DelBarrio, J.C., Guirao-Rico, S., Librado, P., Ramos-Onsins, S.E. and Sánchez-Gracia, A. 2017. DnaSP 6: DNA Sequence Polymorphism Analysis of Large Data Sets. *Molecular Biology and Evolution* 34(12), pp. 3299–3302. doi: 10.1093/molbev/msx248.

Rumschlag, S.L. and Boone, M.D. 2020. Amphibian Infection Risk Changes with Host Life Stage and across a Landscape Gradient. *Journal of Herpetology* 54(3), pp. 347–354. doi: 10.1670/19-107.

Ruthsatz, K. et al. 2020. Skin microbiome correlates with bioclimate and Batrachochytrium dendrobatidis infection intensity in Brazil's Atlantic Forest treefrogs. *Scientific Reports 2020 10:1* 10(1), pp. 1–15. doi: 10.1038/s41598-020-79130-3.

Sallaberry-Pincheira, N. et al. 2016. Contrasting patterns of selection between MHC I and II across populations of Humboldt and Magellanic penguins. *Ecology and Evolution* 6(20), pp. 7498–7510. doi: 10.1002/ECE3.2502.

Salter, S.J. et al. 2014. Reagent and laboratory contamination can critically impact sequence-based microbiome analyses. *BMC Biology* 12(1), p. 87. doi: 10.1186/s12915-014-0087-z.

Sam, Q.H., Chang, M.W. and Chai, L.Y.A. 2017. The Fungal Mycobiome and Its Interaction with Gut Bacteria in the Host. *International Journal of Molecular Sciences* 18(2), p. 330. doi: 10.3390/ijms18020330.

Sauer, E.L., Fuller, R.C., Richards-Zawacki, C.L., Sonn, J., Sperry, J.H. and Rohr, J.R. 2018. Variation in individual temperature preferences, not behavioural fever, affects susceptibility to chytridiomycosis in amphibians. *Proceedings. Biological Sciences* 285(1885), p. 20181111. doi: 10.1098/rspb.2018.1111.

Sauer, E.L., Trejo, N., Hoverman, J.T. and Rohr, J.R. 2019. Behavioural fever reduces ranaviral infection in toads. *Functional Ecology* 33(11), pp. 2172–2179. doi: 10.1111/1365-2435.13427.

Savage, A.E., Becker, C.G. and Zamudio, K.R. 2015. Linking genetic and environmental factors in amphibian disease risk. *Evolutionary Applications* 8(6), pp. 560–572. doi: 10.1111/eva.12264.

Savage, A.E. and Zamudio, K.R. 2011. MHC genotypes associate with resistance to a frog-killing fungus. *Proceedings of the National Academy of Sciences* 108(40), pp. 16705–16710. doi: 10.1073/pnas.1106893108.

Savage, A.E. and Zamudio, K.R. 2016. Adaptive tolerance to a pathogenic fungus drives major histocompatibility complex evolution in natural amphibian populations. *Proceedings of the Royal Society B: Biological Sciences* 283(1827), p. 20153115. doi: 10.1098/rspb.2015.3115.

Scharschmidt, T.C. et al. 2015. A Wave of Regulatory T Cells into Neonatal Skin Mediates Tolerance to Commensal Microbes. *Immunity* 43(5), pp. 1011–1021. doi: 10.1016/j.immuni.2015.10.016.

Scheele, B.C. et al. 2017. After the epidemic: Ongoing declines, stabilizations and recoveries in amphibians afflicted by chytridiomycosis. *Biological Conservation* 206, pp. 37–46.

Scheele, B.C. et al. 2019a. Amphibian fungal panzootic causes catastrophic and ongoing loss of biodiversity. *Science (New York, N.Y.)* 363(6434), pp. 1459–1463. doi: 10.1126/science.aav0379.

Scheele, B.C., Foster, C.N., Hunter, D.A., Lindenmayer, D.B., Schmidt, B.R. and Heard, G.W. 2019b. Living with the enemy: Facilitating amphibian coexistence with disease. *Biological Conservation* 236, pp. 52–59. doi: 10.1016/j.biocon.2019.05.032.

Schliep, K.P. 2011. phangorn: phylogenetic analysis in R. *Bioinformatics* 27(4), pp. 592–593. doi: 10.1093/BIOINFORMATICS/BTQ706.

Schloegel, L.M. et al. 2012. Novel, panzootic and hybrid genotypes of amphibian chytridiomycosis associated with the bullfrog trade. *Molecular Ecology* 21(21), pp. 5162–5177. doi: 10.1111/j.1365-294X.2012.05710.x.

Schloegel, L.M., Daszak, P., Cunningham, A.A., Speare, R. and Hill, B. 2010. Two amphibian diseases, chytridiomycosis and ranaviral disease, are now globally notifiable to the World Organization for Animal Health (OIE): An assessment. *Diseases of Aquatic Organisms* 92(2–3), pp. 101–108. doi: 10.3354/dao02140.

Schmeller, D.S. et al. 2014. Microscopic Aquatic Predators Strongly Affect Infection Dynamics of a Globally Emerged Pathogen. *Current Biology* 24(2), pp. 176–180. doi: 10.1016/j.cub.2013.11.032.

Schoch, C.L. et al. 2012. Nuclear ribosomal internal transcribed spacer (ITS) region as a universal DNA barcode marker for Fungi. *Proceedings of the National Academy of Sciences* 109(16), pp. 6241–6246. doi: 10.1073/pnas.1117018109.

Scholthof, K.B.G. 2006. The disease triangle: pathogens, the environment and society. *Nature Reviews Microbiology 2007 5:2* 5(2), pp. 152–156. doi: 10.1038/nrmicro1596.

Schönhuth, S., Luikart, G. and Doadrio, I. 2003. Effects of a founder event and supplementary introductions on genetic variation in a captive breeding population of the endangered Spanish killifish. *Journal of Fish Biology* 63(6), pp. 1538–1551. doi: 10.1111/J.1095-8649.2003.00265.X.

Schoville, S.D., Tustall, T.S., Vredenburg, V.T., Backlin, A.R., Gallegos, E., Wood, D.A. and Fisher, R.N. 2011. Conservation genetics of evolutionary lineages of the endangered mountain yellow-legged frog, Rana muscosa (Amphibia: Ranidae), in southern California. *Biological Conservation* 144(7), pp. 2031–2040. doi: 10.1016/J.BIOCON.2011.04.025.

Schwartz, M.K., Luikart, G. and Waples, R.S. 2007. Genetic monitoring as a promising tool for conservation and management. *Trends in Ecology & Evolution* 22(1), pp. 25–33. doi: 10.1016/J.TREE.2006.08.009.

Seppä, P. and Laurila, A. 1999. Genetic structure of island populations of the anurans Rana temporaria and Bufo bufo. *Heredity* 82(3), pp. 309–317. doi: 10.1038/sj.hdy.6884900.

Seyedsayamdost, M.R. 2019. Toward a global picture of bacterial secondary metabolism. *Journal of Industrial Microbiology and Biotechnology* 46(3–4), pp. 301–311. doi: 10.1007/s10295-019-02136-y.

Shapard, E.J., Moss, A.S. and San Francisco, M.J. 2012. Batrachochytrium dendrobatidis Can Infect and Cause Mortality in the Nematode Caenorhabditis elegans. *Mycopathologia* 173(2–3), pp. 121–126. doi: 10.1007/s11046-011-9470-2.

Shapiro, B. 2015. Cartographers in the Caribbean: Economics and Mapping in the Colonial New World. *Elements* 11(2), pp. 1–8. doi: 10.6017/eurj.v11i2.9065.

Shaw, S.D. et al. 2014. Baseline Cutaneous Bacteria Of Free-Living New Zealand Native Frogs (Leiopelma Archeyi And Leiopelma Hochstetteri) And Implications For Their Role In Defense Against The Amphibian Chytrid (Batrachochytrium dendrobatidis). *Journal of Wildlife Diseases* 50(4), pp. 723–732. doi: 10.7589/2013-07-186.

Shu, Y.L., Hong, P., Yang, Y.W. and Wu, H.L. 2013. An endemic frog harbors multiple expression loci with different patterns of variation in the MHC class II B gene. *Journal of Experimental Zoology Part B: Molecular and Developmental Evolution* 320(8), pp. 501–510. doi: 10.1002/JEZ.B.22525.

Shum, B.P., D, A., Du Pasquier, L., Kasahara, M. and Flajnik, M.F. 1993. Isolation of a classical MHC class I cDNA from an amphibian. Evidence for only one class I locus in the Xenopus MHC. *The Journal of Immunology* 151(10), pp. 5376–5386.

Siegel, P.E. et al. 2015. Paleoenvironmental evidence for first human colonization of the eastern Caribbean. *Quaternary Science Reviews* 129, pp. 275–295. doi: 10.1016/J.QUASCIREV.2015.10.014.

Silverman, J.D., Washburne, A.D., Mukherjee, S. and David, L.A. 2017. A phylogenetic transform enhances analysis of compositional microbiota data. *eLife* 6. doi: 10.7554/ELIFE.21887.

Slatkin, M. 1985. Gene Flow in Natural Populations. *Annual Review of Ecology and Systematics* 16(1), pp. 393–430. doi: 10.1146/annurev.es.16.110185.002141.

Smallbone, W., Ellison, A., Poulton, S., van Oosterhout, C. and Cable, J. 2021. Depletion of MHC supertype during domestication can compromise immunocompetence. *Molecular Ecology* 30(3), pp. 736–746. doi: 10.1111/mec.15763.

Smith, D. et al. 2022. Challenging a host–pathogen paradigm: Susceptibility to chytridiomycosis is decoupled from genetic erosion. *Journal of Evolutionary Biology* 35(4), pp. 589–598. doi: 10.1111/JEB.13987.

Song, S.J., Amir, A., Metcalf, J.L., Amato, K.R., Xu, Z.Z., Humphrey, G. and Knight, R. 2016. Preservation Methods Differ in Fecal Microbiome Stability, Affecting Suitability for Field Studies. *mSystems* 1(3), pp. e00021-16.

Spurgin, L.G. and Richardson, D.S. 2010. How pathogens drive genetic diversity: MHC, mechanisms and misunderstandings. *Proceedings. Biological sciences* 277(1684), pp. 979–988. doi: 10.1098/RSPB.2009.2084.

Steadman, D.W., Norton, R.L., Browning, M.R. and Arendt, W.J. 1997. The birds of St. Kitts, Lesser Antilles. *Caribbean Journal of Science* 33(1–2), pp. 1–20.

Stegen, G. et al. 2017. Drivers of salamander extirpation mediated by Batrachochytrium salamandrivorans. *Nature* 544(7650), pp. 353–356. doi: 10.1038/nature22059.

Stockwell, M.P., Storrie, L.J., Pollard, C.J., Clulow, J. and Mahony, M.J. 2015. Effects of pond salinization on survival rate of amphibian hosts infected with the chytrid fungus. *Conservation Biology: The Journal of the Society for Conservation Biology* 29(2), pp. 391–399. doi: 10.1111/cobi.12402.

Streicher, J.W., Schulte Ii, J.A. and Wiens, J.J. 2016. How Should Genes and Taxa be Sampled for Phylogenomic Analyses with Missing Data? An Empirical Study in Iguanian Lizards. *Rosenberg and Kumar* 65(1), pp. 128–145. doi: 10.1093/sysbio/syv058.

Sumpter, N.A. 2018. *Hybrid Assembly of the Chytrid Genome-Insights into the Evolution and Outbreak of a Major Amphibian Pathogen*. M.Sc., Dunedin, New Zealand: University of Otago.

Sunde, J., Yıldırım, Y., Tibblin, P. and Forsman, A. 2020. Comparing the Performance of Microsatellites and RADseq in Population Genetic Studies: Analysis of Data for Pike (Esox lucius) and a Synthesis of Previous Studies. *Frontiers in Genetics* 11, p. 218. doi: 10.3389/FGENE.2020.00218/BIBTEX.

Symington, L.S., Rothstein, R. and Lisby, M. 2014. Mechanisms and regulation of mitotic recombination in saccharomyces cerevisiae. *Genetics* 198(3), pp. 795–835. doi: 10.1534/genetics.114.166140.

Tajima, F. 1989. Statistical method for testing the neutral mutation hypothesis by DNA polymorphism. *Genetics* 123(3), pp. 585–595.

Tapley, B., Bradfield, K.S., Michaels, C. and Bungard, M. 2015. Amphibians and conservation breeding programmes: do all threatened amphibians belong on the ark? *Biodiversity and Conservation* 24(11), pp. 2625–2646. doi: 10.1007/s10531-015-0966-9.

Tarazona, S., Arzalluz-Luque, A. and Conesa, A. 2021. Undisclosed, unmet and neglected challenges in multi-omics studies. *Nature Computational Science* 1(6), pp. 395–402. doi: 10.1038/s43588-021-00086-z.

Thekkiniath, J., Zabet-Moghaddam, M., Kottapalli, K.R., Pasham, M.R., Francisco, S.S. and Francisco, M.S. 2015. Quantitative Proteomics of an Amphibian Pathogen, Batrachochytrium dendrobatidis, following Exposure to Thyroid Hormone. *PLOS ONE* 10(6), p. e0123637. doi: 10.1371/journal.pone.0123637.

Thorvaldsdóttir, H., Robinson, J.T. and Mesirov, J.P. 2013. Integrative Genomics Viewer (IGV): High-performance genomics data visualization and exploration. *Briefings in Bioinformatics* 14(2), pp. 178–192. doi: 10.1093/bib/bbs017.

Tian, F., Ding, Y., Zhu, H., Yao, L. and Du, B. 2009. Genetic diversity of siderophore-producing bacteria of tobacco rhizosphere. *Brazilian Journal of Microbiology* 40(2), pp. 276–284. doi: 10.1590/S1517-838220090002000013.

Tibayrenc, M. 2010. *Genetics and Evolution of Infectious Diseases*. London: Elsevier. Available at: www.elsevierdirect.com [Accessed: 9 May 2021].

Torres-Sánchez, M. and Longo, A.V. 2022. Linking pathogen–microbiome–host interactions to explain amphibian population dynamics. *Molecular Ecology* 31(22), pp. 5784–5794. doi: 10.1111/mec.16701.

Townsend, S.M. and Jamieson, I.G. 2013. Molecular and pedigree measures of relatedness provide similar estimates of inbreeding depression in a bottlenecked population. *Journal of evolutionary biology* 26(4), pp. 889–899. doi: 10.1111/JEB.12109.

Trujillo, A.L., Hoffman, E.A., Becker, C.G. and Savage, A.E. 2021. Spatiotemporal adaptive evolution of an MHC immune gene in a frog-fungus disease system. *Heredity* 126(4), pp. 640–655. doi: 10.1038/s41437-020-00402-9.

Tyc, Olaf, Song, C., Dickschat, J.S., Vos, M. and Garbeva, P. 2017. The Ecological Role of Volatile and Soluble Secondary Metabolites Produced by Soil Bacteria. *Trends in Microbiology* 25(4), pp. 280–292. doi: 10.1016/j.tim.2016.12.002.

Van Rooij, P., Martel, A., Haesebrouck, F. and Pasmans, F. 2015. Amphibian chytridiomycosis: A review with focus on fungus-host interactions. *Veterinary Research* 46(1), p. 137. doi: 10.1186/s13567-015-0266-0.

Van Sluys, M., Kriger, K.M., Phillott, A.D., Campbell, R., Skerratt, L.F. and Hero, J.M. 2008. Storage of samples at high temperatures reduces the amount of amphibian chytrid fungus Batrachochytrium dendrobatidis DNA detectable by PCR assay. *Diseases of Aquatic Organisms* 81(2), pp. 93–97. doi: 10.3354/dao01953.

Viggers, K.L., Lindenmayer, D.B. and Spratt, D.M. 1993. The importance of disease in Reintroduction programmes. *Wildlife Research* 20(5), pp. 687–698. doi: 10.1071/WR9930687.

Voyles, J. et al. 2007. Electrolyte depletion and osmotic imbalance in amphibians with chytridiomycosis. *Diseases of Aquatic Organisms* 77, pp. 113–118. doi: 10.3354/dao01838.

Voyles, J. et al. 2009. Pathogenesis of chytridiomycosis, a cause of catastrophic amphibian declines. *Science* 326(5952), pp. 582–585. doi: 10.1126/science.1176765.

Voyles, J. et al. 2014. Experimental evolution alters the rate and temporal pattern of population growth in Batrachochytrium dendrobatidis, a lethal fungal pathogen of amphibians. *Ecology and Evolution* 4(18), pp. 3633–3641. doi: 10.1002/ece3.1199.

Voyles, J. et al. 2018. Shifts in disease dynamics in a tropical amphibian assemblage are not due to pathogen attenuation. *Science* 359(6383), pp. 1517–1519. doi: 10.1126/science.aao4806.

Vredenburg, V.T., Knapp, R.A., Tunstall, T.S. and Briggs, C.J. 2010. Dynamics of an emerging disease drive large-scale amphibian population extinctions. *Proceedings of the National Academy of Sciences of the United States of America* 107(21), pp. 9689–94. doi: 10.1073/pnas.0914111107.

Vuong, H.E., Yano, J.M., Fung, T.C. and Hsiao, E.Y. 2017. The Microbiome and Host Behavior. *Annual Review of Neuroscience* 40(1), pp. 21–49. doi: 10.1146/annurev-neuro-072116-031347.

Wahlund, S. 1928. Zusammensetzung Von Populationen Und Korrelationserscheinungen Vom Standpunkt Der Vererbungslehre Aus Betrachtet. *Hereditas* 11(1), pp. 65–106. doi: 10.1111/J.1601-5223.1928.TB02483.X.

Wake, D.B. and Vredenburg, V.T. 2008. Are we in the midst of the sixth mass extinction? A view from the world of amphibians. *Proceedings of the National Academy of Sciences of the United States of America* 105(SUPPL. 1), pp. 11466–11473. doi: 10.1073/PNAS.0801921105.

Walke, J.B., Becker, M.H., Loftus, S.C., House, L.L., Teotonio, T.L., Minbiole, K.P.C. and Belden, L.K. 2015. Community structure and function of amphibian skin microbes: An experiment with bullfrogs exposed to a chytrid fungus. *PLoS ONE* 10(10), p. e0139848. doi: 10.1371/journal.pone.0139848.

Wallman, D. 2018. Histories and Trajectories of Socio-Ecological Landscapes in the Lesser Antilles: Implications of Colonial Period Zooarchaeological Research. *Environmental Archaeology* 23(1), pp. 13–22. doi: 10.1080/14614103.2017.1345086.

Wang, J. 2004. Application of the one-migrant-per-generation rule to conservation and management. *Conservation Biology* 18(2), pp. 332–343. doi: 10.1111/j.1523-1739.2004.00440.x.

Wang, Q., Garrity, G.M., Tiedje, J.M. and Cole, J.R. 2007. Naive Bayesian classifier for rapid assignment of rRNA sequences into the new bacterial taxonomy. *Applied and environmental microbiology* 73(16), pp. 5261–5267. doi: 10.1128/AEM.00062-07.

Waples, R.S. 2015. Testing for Hardy–Weinberg Proportions: Have We Lost the Plot? *Journal of Heredity* 106(1), pp. 1–19. doi: 10.1093/jhered/esu062.

Warnes, G., Bolker, B., Huber, W., Lumley, T., Maechler, M., Magnusson, A. and Moeller, S. 2019. gplots: Various R Programming Tools for Plotting Data. Available at: https://www.researchgate.net/publication/303186599_gplots_Various_R_programming_tools_for_plotting_data [Accessed: 16 May 2022].

Weaver, S., Shank, S.D., Spielman, S.J., Li, M., Muse, S.V. and Kosakovsky Pond, S.L. 2018. Datamonkey 2.0: A Modern Web Application for Characterizing Selective and Other Evolutionary Processes. *Molecular Biology and Evolution* 35(3), pp. 773–777. doi: 10.1093/MOLBEV/MSX335.

Wegmann, D., Leuenberger, C. and Excoffier, L. 2009. Efficient approximate Bayesian computation coupled with Markov chain Monte Carlo without likelihood. *Genetics* 182(4), pp. 1207–18. doi: 10.1534/genetics.109.102509.

Wegmann, D., Leuenberger, C., Neuenschwander, S. and Excoffier, L. 2010. ABCtoolbox: a versatile toolkit for approximate Bayesian computations. *BMC Bioinformatics* 11(1), p. 116. doi: 10.1186/1471-2105-11-116.

Weiss, S. et al. 2017. Normalization and microbial differential abundance strategies depend upon data characteristics. *Microbiome* 5(1), pp. 1–18. doi: 10.1186/S40168-017-0237-Y/FIGURES/8.

White, A.W. and Shine, R. 2009. The extra-limital spread of an invasive species via 'stowaway' dispersal: toad to nowhere? *Animal Conservation* 12(1), pp. 38–45. doi: 10.1111/j.1469-1795.2008.00218.x.

White, N.F.D., Cunningham, A.A., Hudson, M.A. and Orozco-terWengel, P. 2021. The complete mitogenome of the Mountain chicken frog, Leptodactylus fallax. *Mitochondrial DNA B Resources* 6(4), pp. 1372–1373. doi: 10.1080/23802359.2021.1907809.

Wieczorek, M., Abualrous, E.T., Sticht, J., Álvaro-Benito, M., Stolzenberg, S., Noé, F. and Freund, C. 2017. Major histocompatibility complex (MHC) class I and MHC class II proteins: Conformational plasticity in antigen presentation. *Frontiers in Immunology* 8(MAR). doi: 10.3389/fimmu.2017.00292.

Wilson, S.M. 1997. Surviving European Conquest in the Caribbean. *Revista de Arqueología Americana* 12(12), pp. 141–160.

Witzenberger, K.A. and Hochkirch, A. 2011. Ex situ conservation genetics: A review of molecular studies on the genetic consequences of captive breeding programmes for endangered animal species. *Biodiversity and Conservation* 20(9), pp. 1843–1861. doi: 10.1007/s10531-011-0074-4.

Woodhams, D.C. et al. 2007. Symbiotic bacteria contribute to innate immune defenses of the threatened mountain yellow-legged frog, Rana muscosa. *Biological Conservation* 138(3–4), pp. 390–398. doi: 10.1016/j.biocon.2007.05.004.

Woodhams, D.C. et al. 2008. Chytridiomycosis and amphibian population declines continue to spread eastward in panama. *EcoHealth* 5(3), pp. 268–274. doi: 10.1007/S10393-008-0190-0/TABLES/2.

Woodhams, D.C. et al. 2015. Antifungal isolates database of amphibian skin-associated bacteria and function against emerging fungal pathogens. *Ecology* 96(2), pp. 595–595. doi: 10.1890/14-1837.1.

Woodhams, D.C. et al. 2018. Prodigiosin, Violacein, and Volatile Organic Compounds Produced by Widespread Cutaneous Bacteria of Amphibians Can Inhibit Two Batrachochytrium Fungal Pathogens. *Microbial Ecology* 75(4), pp. 1049–1062. doi: 10.1007/s00248-017-1095-7.

Woodhams, D.C. et al. 2020. Host-associated microbiomes are predicted by immune system complexity and climate. *Genome biology* 21(1), p. 23. doi: 10.1186/s13059-019-1908-8.

Woodhams, D.C. and Alford, R.A. 2005. Ecology of Chytridiomycosis in Rainforest Stream Frog Assemblages of Tropical Queensland. *Conservation Biology* 19(5), pp. 1449–1459. doi: 10.1111/J.1523-1739.2005.004403.X.

Wright, E. 2013. Using DECIPHER v2. 0 to Analyze Big Biological Sequence Data in R. *The R Journal* 8(1), pp. 352–359.

Wright, S. 1931. Evolution in Mendelian Populations. *Genetics* 16(2), pp. 97–159.

Wright, S. 1949. The Genetical Structure of Populations. *Annals of Eugenics* 15(1), pp. 323–354. doi: 10.1111/j.1469-1809.1949.tb02451.x.

Xi, Z., Liu, L. and Davis, C.C. 2016. The Impact of Missing Data on Species Tree Estimation. *Molecular Biology and Evolution* 33(3), pp. 838–860. doi: 10.1093/molbev/msv266.

Yang, Z. and Nielsen, R. 2000. Estimating Synonymous and Nonsynonymous Substitution Rates Under Realistic Evolutionary Models. *Molecular Biology and Evolution* 17(1), pp. 32–43. doi: 10.1093/oxfordjournals.molbev.a026236.

Yilmaz, P. et al. 2014. The SILVA and "All-species Living Tree Project (LTP)" taxonomic frameworks. *Nucleic Acids Research* 42(Database issue), p. D643. doi: 10.1093/NAR/GKT1209.

Yuan, X., Miller, D.J., Zhang, J., Herrington, D. and Wang, Y. 2012. An overview of population genetic data simulation. *Journal of Computational Biology* 19(1), pp. 42–54. doi: 10.1089/cmb.2010.0188.

Zachos, F.E., Hajji, G.M., Hmwe, S.S., Hartl, G.B., Lorenzini, R. and Mattioli, S. 2009. Population Viability Analysis and Genetic Diversity of the Endangered Red Deer Cervus elaphus Population from Mesola, Italy. *Wildlife Biology* 15(2), pp. 175–186. doi: 10.2981/07-075.

Zhang, C., Rabiee, M., Sayyari, E. and Mirarab, S. 2018. ASTRAL-III: Polynomial time species tree reconstruction from partially resolved gene trees. *BMC Bioinformatics* 19(S6), p. 153. doi: 10.1186/s12859-018-2129-y.

Zhao, M., Wang, Y., Shen, H., Li, C., Chen, C., Luo, Z. and Wu, H. 2013. Evolution by selection, recombination, and gene duplication in MHC class I genes of two Rhacophoridae species. *BMC evolutionary biology* 13(1). Available at: https://pubmed.ncbi.nlm.nih.gov/23734729/ [Accessed: 2 December 2021].

Zhbannikov, I.Y., Hunter, S.S., Foster, J.A. and Settles, M.L. 2017. Seqyclean: A pipeline for high-throughput sequence data preprocessing. In: *ACM-BCB 2017 - Proceedings of the 8th ACM International Conference on Bioinformatics, Computational Biology, and Health Informatics*. Association for Computing Machinery, Inc, pp. 407–416. doi: 10.1145/3107411.3107446.

Supplementary Information

Chapter Two Supplementary Information

Scenario 1: Divergence from Anc then no migration

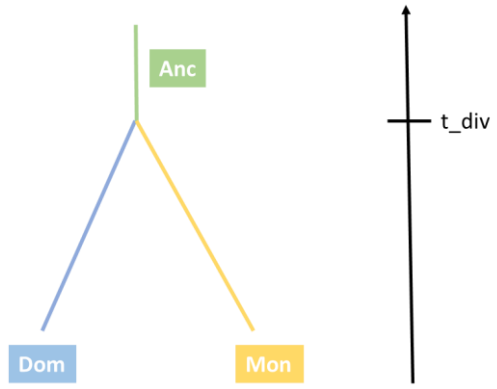

Scenario 2: Divergence from Anc then single migration Mon to Dom

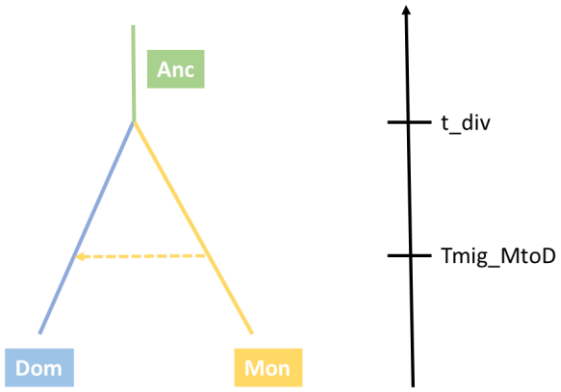

Scenario 3: Divergence from Anc then single migration Dom to Mon

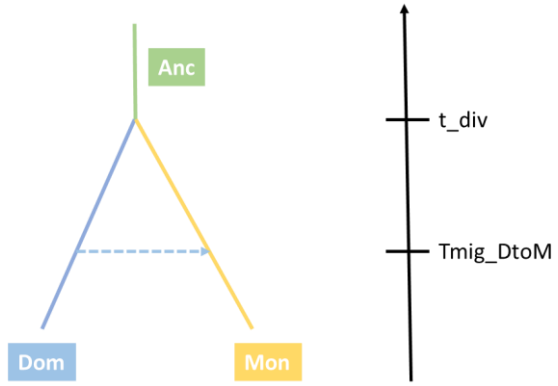

Scenario 4: Divergence from Anc then single bidirectional migration

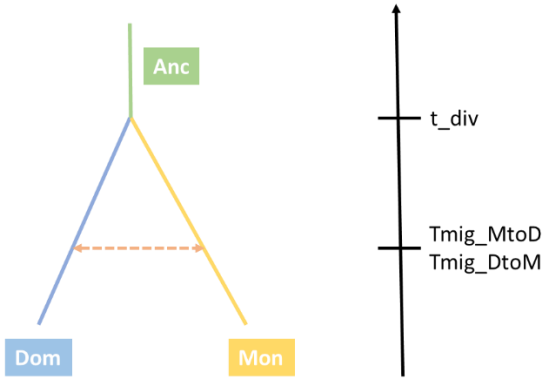

Scenario 5: Divergence from Anc then single, modern bidirectional migration

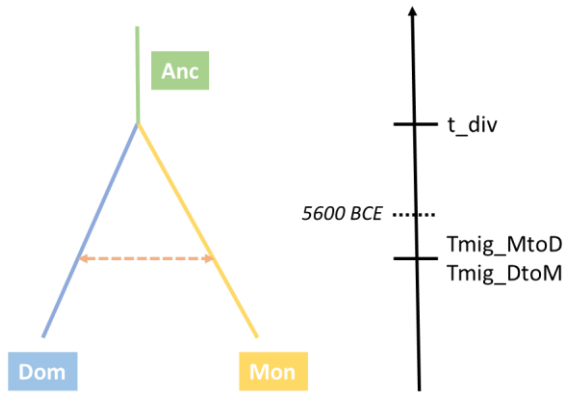

Scenario 6: Divergence from Anc then single, ancient bidirectional migration

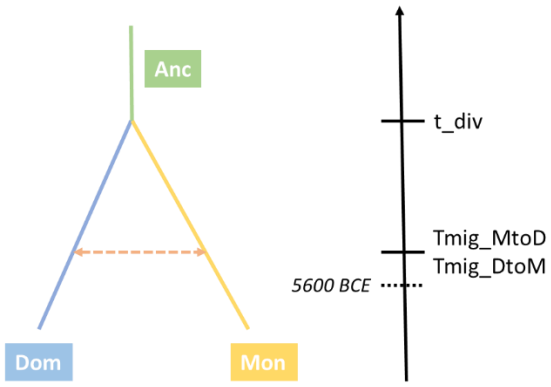

Scenario 7: Divergence from Anc then a Dom to Mon migration before Mon to Dom

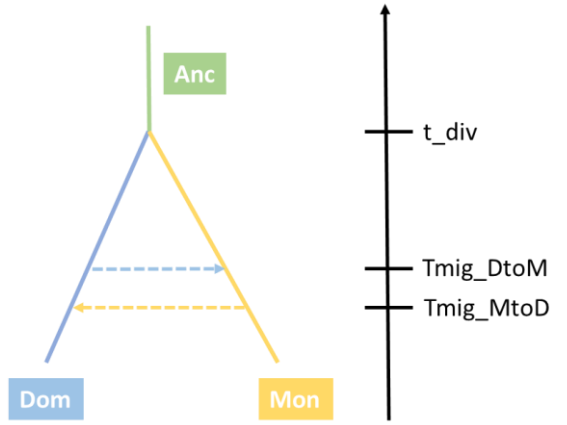

Scenario 8: Divergence from Anc then a Mon to Dom migration before Dom to Mon

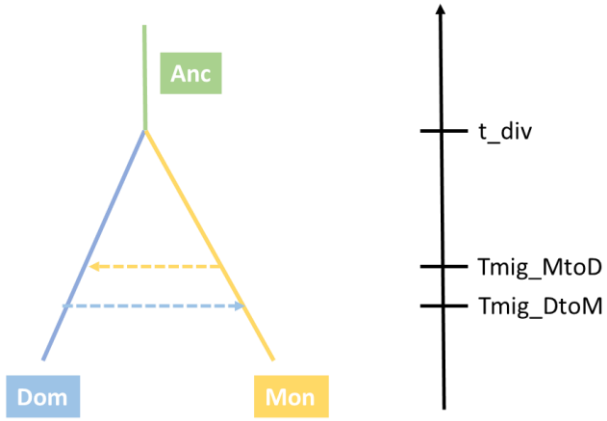

Scenario 9: Divergence from Anc then an equal migration matrix

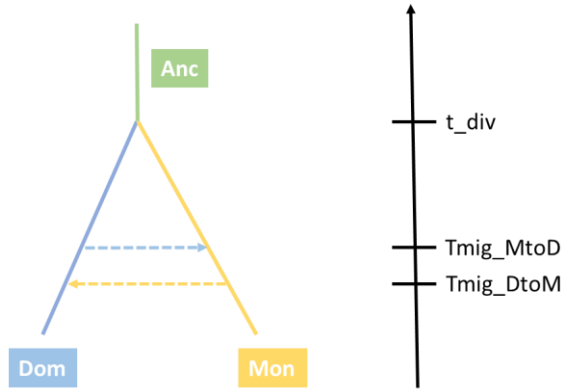

Scenario 10: Divergence from Anc then a migration matrix – < 10% from Mon, < 5% from Dom

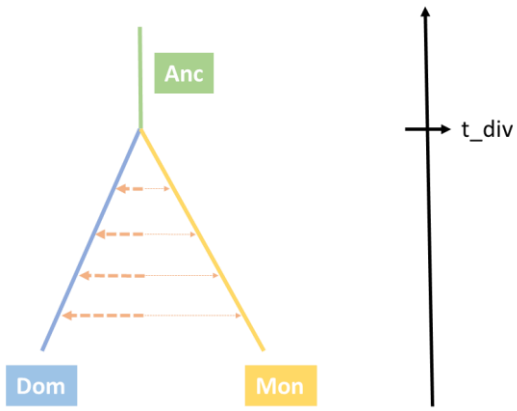

Scenario 11: Divergence from Anc then a migration matrix – < 10% from Dom, < 5% from Mon

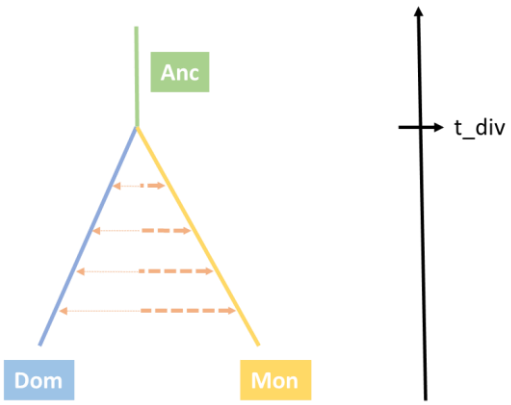

Scenario 12: Divergence from Anc then 1 ancient & 1 modern migration event

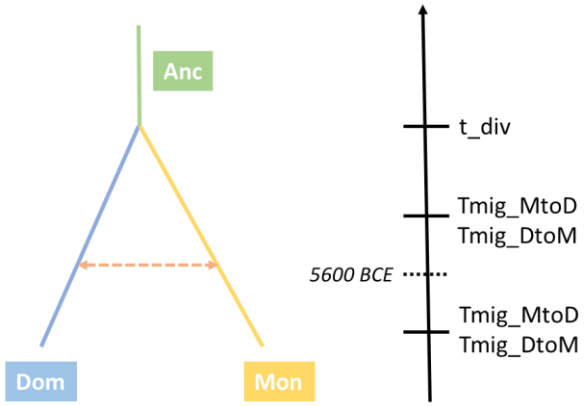

Scenario 13: Mon founded by Dom (no ancestral pop)

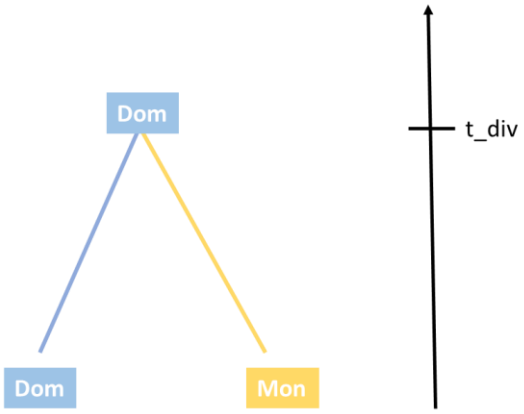

Scenario 14: Mon founded by Dom (ancestral pop)

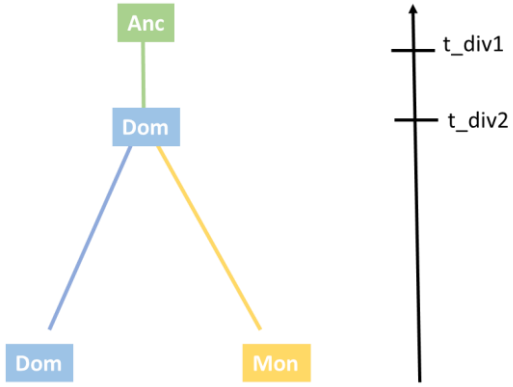

Scenario 15: Mon founded by Dom, then one, equal bidirectional migration event

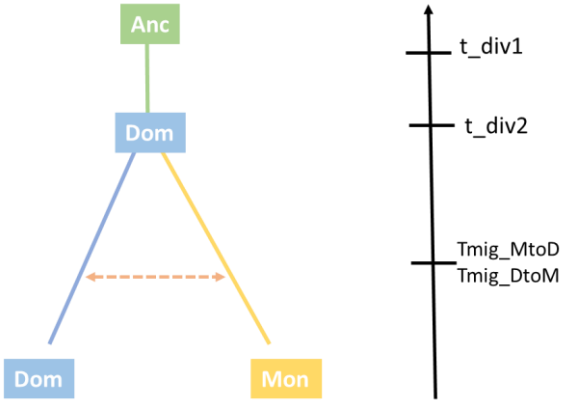

Scenario 16: Dom founded by Mon (ancestral pop)

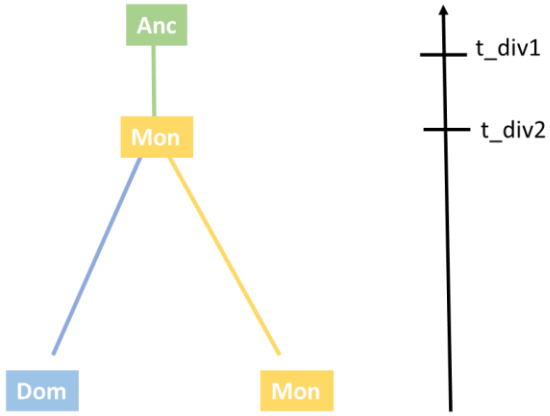

Scenario 17: Divergence from Anc to Dom + intermediate pop. Admixture of Dom and intermediate forms Mon

Scenario 18: Divergence from Anc then three birdirectional migration events

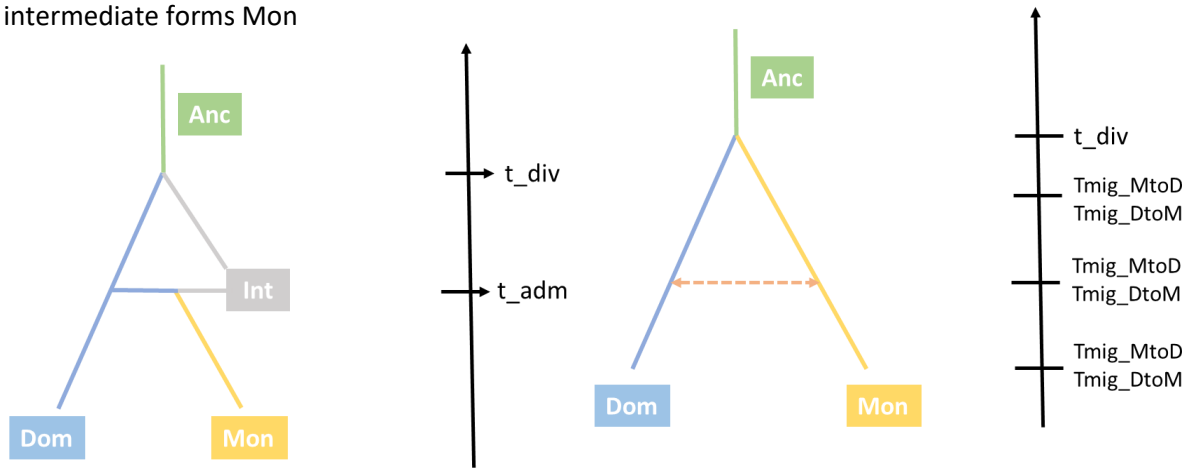

Figure S2.1: Illustration of demographic scenarios modelled in ABCtoolbox. Anc = Ancestral Population. Mon = Montserrat. Dom = Dominica.

Table S2.1: Priors used in ABC modelling

Prior	Corresponding Factor	Range (* = Log10)	Scenario
Log_Ne_Anc	Ancestral effective population size	1 – 6 *	Both
Log_Ne_Dom	Dominican effective population size	1 – 5.5 *	Both
Log_Ne_Mon	Montserratian population size	1 – 5.5 *	Both
Log_Ne_Int	Intermediate population size	1 – 5.5 *	17
MSAT_MUT	Microsatellite mutation rate	0.00001 – 0.01	Both
t_div	Time of divergence	1 – 7.5 *	Both
t_adm	Time of admixture		17
GAMMA	Gamma distribution of mutation rate	1 – 15	Both
Mig_MtoD	Migration rate into Dominica	0 – 0.1	10
Mig_DtoM	Migration rate into Montserrat	0 – 0.05	10

Table S2.2: Mode Posterior Density values for each parameter gained from ABCtoolbox simulations and used to build SLiM models

Parameter	Scenario 10	Scenario 17
Ne_Anc	78425	227
Ne_Dom	295	1644
Ne_Mon	52	315
Ne_Int		327
T_div	500	20993
T_adm		63
Migrants		0.9
Mig_MtoD	0.07	
Mig_DtoM	0.005	

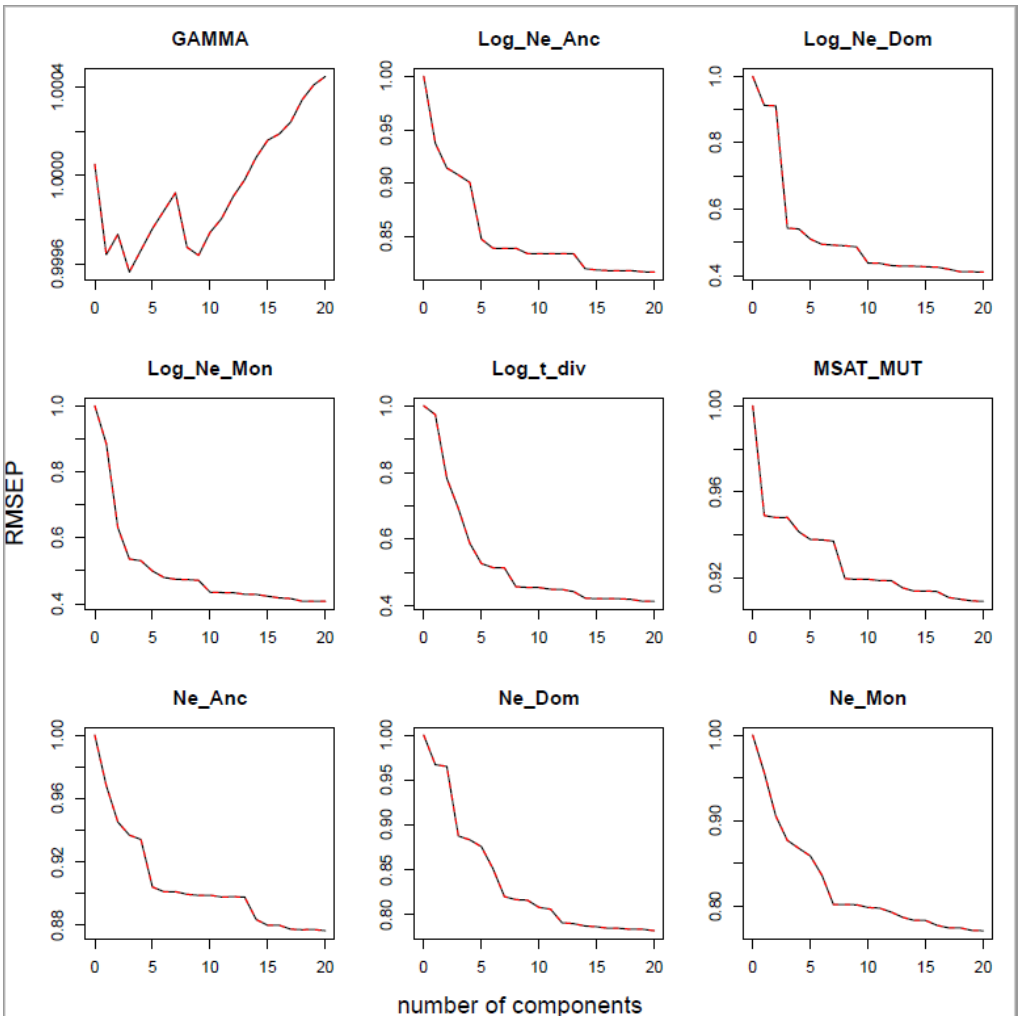

Figure S2.2: Partial least squares regression analysis results, used to determine the best number of summary statistics to use in ABCtoolbox analysis. Y axis = prediction error rate. RMSEP = (root mean squared error plot).

Scenario 10

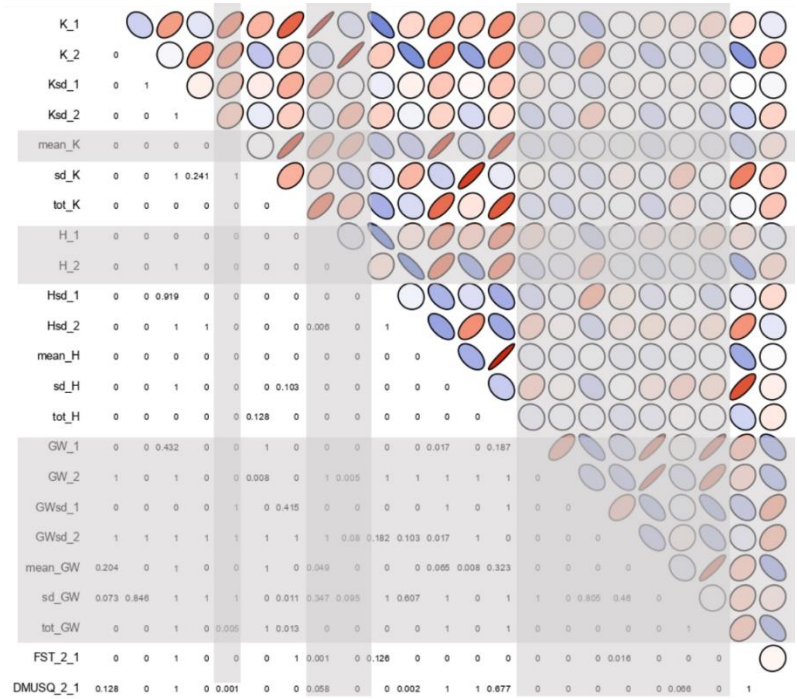

Scenario 17

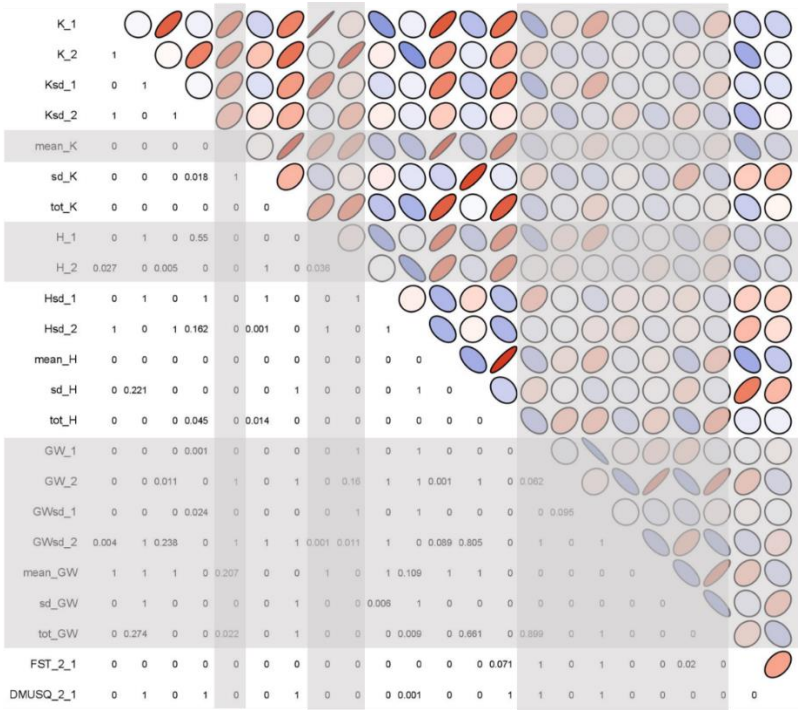

Figure S2.3: Spearman's rank correlation results to identify highly correlated summary statistics. Ellipses represent the Spearman's coefficient, with the blue to red scale indicating the direction of the correlation. Bonferroni corrected p-values are shown in the lower half of the matrix. Those removed from final ABCtoolbox analysis are shaded grey.

Scenario 10

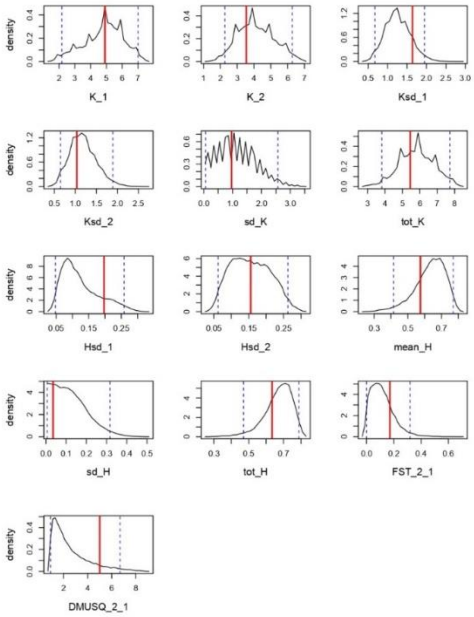

Scenario 17

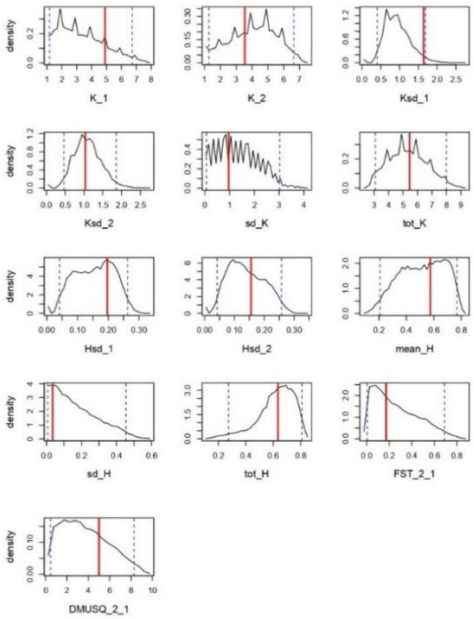

Figure S2.4: Relative distributions of simulated summary statistics (black line) in relation to the observed value for summary statistics (red line), 2.5% and 97.5% confidence intervals are denoted by dashed lines.

Table S2.3: Pairwise comparison of scenarios tested in ABCtoolbox. Values correspond to Bayes factors calculated as the quotient of the marginal density of the scenarios being compared. Above diagonal = **bold** vs. *italic*, below diagonal = *italic* vs. **bold**. BF > 3 indicated by green highlighted cell.

Scenario	**1**	**2**	**3**	**4**	**5**	**6**	**7**	**8**	**9**	**10**	**11**	**12**	**13**	**14**	**15**	**16**	**17**	**18**
1		4.1	3.6	22.5	0.7	0.0	22.7	23.7	108.7	388.8	91.9	0.0	1.0	110.2	0.5	16.8	180.5	0.0
2	0.2		0.9	5.5	0.2	0.0	5.6	5.8	26.6	95.2	22.5	0.0	0.2	27.0	0.1	4.1	44.2	0.0
3	0.3	1.1		6.3	0.2	0.0	6.3	6.6	30.3	108.2	25.6	0.0	0.3	30.7	0.1	4.7	50.3	0.0
4	0.0	0.2	0.2		0.0	0.0	1.0	1.1	4.8	17.3	4.1	0.0	0.0	4.9	0.0	0.7	8.0	0.0
5	1.4	5.9	5.2	32.4		0.0	32.7	34.1	156.5	560.0	132.3	0.0	1.4	158.8	0.7	24.1	259.9	0.0
6	3.27E+25	1.33E+26	1.17E+26	7.35E+26	2.27E+25		7.42E+26	7.74E+26	3.55E+27	1.27E+28	3.00E+27	1.04E+16	3.13E+25	3.60E+27	1.66E+25	5.47E+26	5.90E+27	6.39E+05
7	0.0	0.2	0.2	1.0	0.0	0.0		1.0	4.8	17.1	4.0	0.0	0.0	4.9	0.0	0.7	7.9	0.0
8	0.0	0.2	0.2	0.9	0.0	0.0	1.0		4.6	16.4	3.9	0.0	0.0	4.7	0.0	0.7	7.6	0.0
9	0.0	0.0	0.0	0.2	0.0	0.0	0.2	0.2		3.6	0.8	0.0	0.0	1.0	0.0	0.2	1.7	0.0
10	0.0	0.0	0.0	0.1	0.0	0.0	0.1	0.1	0.3		0.2	0.0	0.0	0.3	0.0	0.0	0.5	0.0
11	0.0	0.0	0.0	0.2	0.0	0.0	0.2	0.3	1.2	4.2		0.0	0.0	1.2	0.0	0.2	2.0	0.0
12	3.13E+09	1.28E+10	1.12E+10	7.04E+10	2.17E+09	9.57E-17	7.10E+10	7.41E+10	3.40E+11	1.22E+12	2.87E+11		2.99E+09	3.45E+11	1.59E+09	5.24E+10	5.64E+11	6.12E-11
13	1.0	4.3	3.8	23.5	0.7	0.0	23.7	24.8	113.5	406.1	96.0	0.0		115.1	0.5	17.5	188.5	0.0
14	0.0	0.0	0.0	0.2	0.0	0.0	0.2	0.2	1.0	3.5	0.8	0.0	0.0		0.0	0.2	1.6	0.0
15	2.0	8.0	7.1	44.3	1.4	0.0	44.7	46.6	213.8	764.9	180.8	0.0	1.9	216.9		33.0	355.1	0.0
16	0.1	0.2	0.2	1.3	0.0	0.0	1.4	1.4	6.5	23.2	8.2	0.0	0.1	6.6	0.0		10.8	0.0
17	0.0	0.0	0.0	0.1	0.0	0.0	0.1	0.1	0.6	2.2	0.5	0.0	0.0	0.6	0.0	0.1		0.0
18	5.11E+19	2.09E+20	1.84E+20	1.15E+21	3.55E+19	1.57E-06	1.16E+21	1.21E+21	5.56E+21	1.99E+22	4.70E+21	1.63E+10	4.89E+19	5.64E+21	2.60E+19	8.57E+20	9.23E+21	

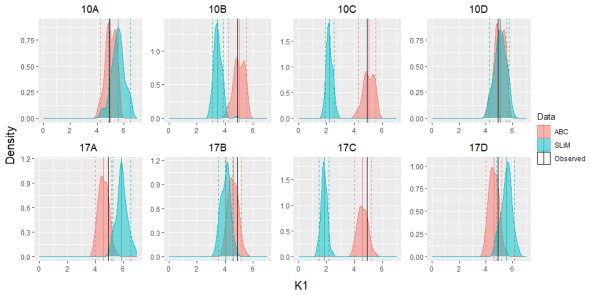
10A
10B
10C
10D
17A
17B
17C
17D
Density
Data
ABC
SLIM
Observed
K1

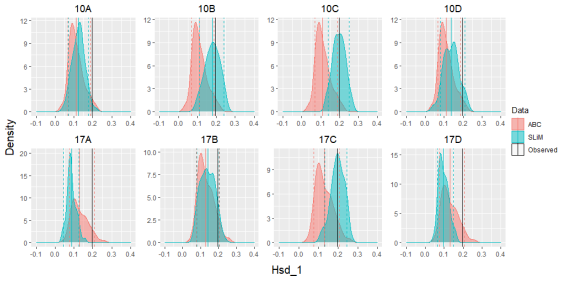
10A
10B
10C
10D
17A
17B
17C
17D
Density
Data
ABC
SLIM
Observed
Hsd_1

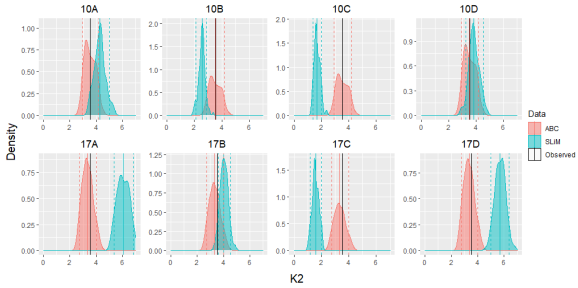
10A
10B
10C
10D
17A
17B
17C
17D
Density
Data
ABC
SLIM
Observed
K2

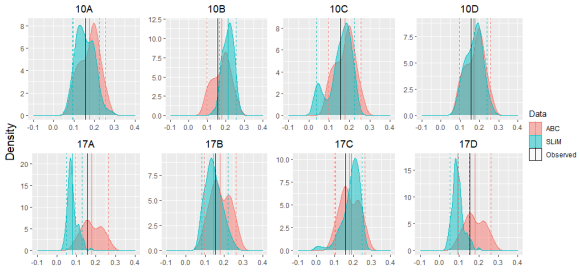
10A
10B
10C
10D
17A
17B
17C
17D
Density
Data
ABC
SLIM
Observed
Hsd_2

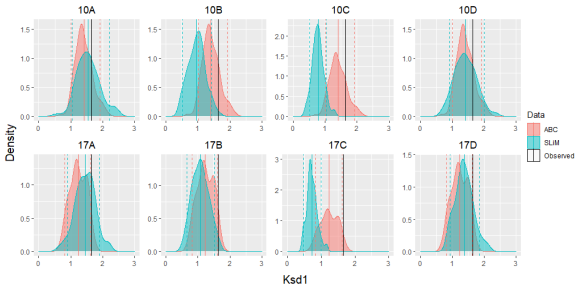
10A
10B
10C
10D
17A
17B
17C
17D
Density
Data
ABC
SLIM
Observed
Ksd1

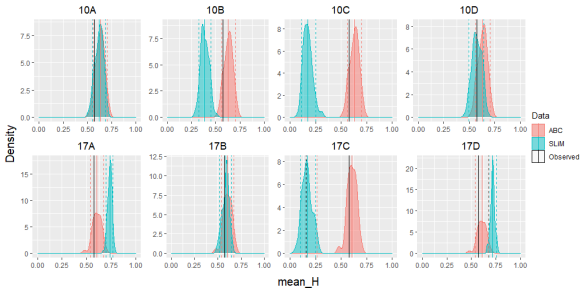
10A
10B
10C
10D
17A
17B
17C
17D
Density
Data
ABC
SLIM
Observed
mean_H

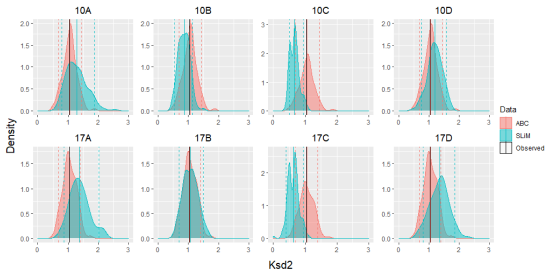
10A
10B
10C
10D
17A
17B
17C
17D
Density
Data
ABC
SLIM
Observed
Ksd2

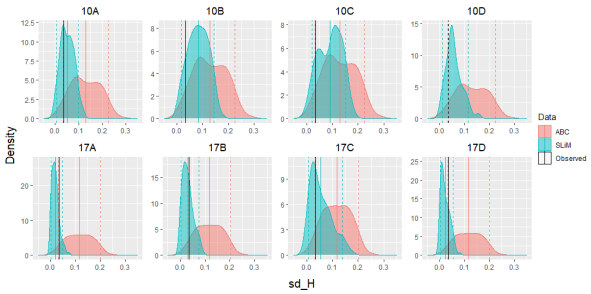
10A
10B
10C
10D
17A
17B
17C
17D
Density
Data
ABC
SLIM
Observed
sd_H

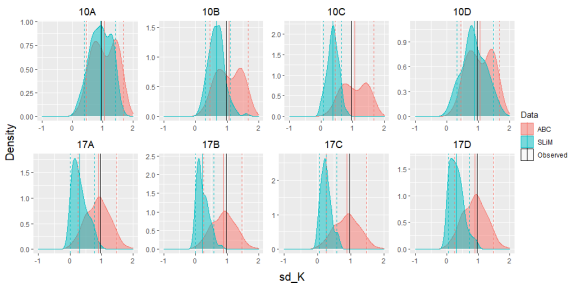
10A
10B
10C
10D
17A
17B
17C
17D
Density
Data
ABC
SLIM
Observed
sd_K

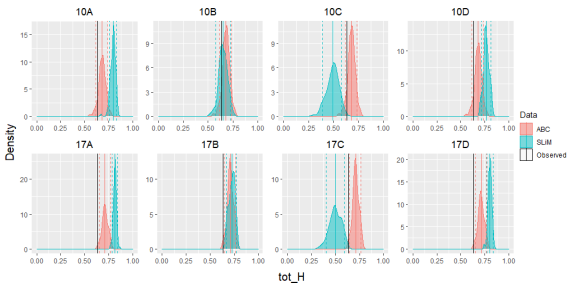
10A
10B
10C
10D
17A
17B
17C
17D
Density
Data
ABC
SLIM
Observed
tot_H

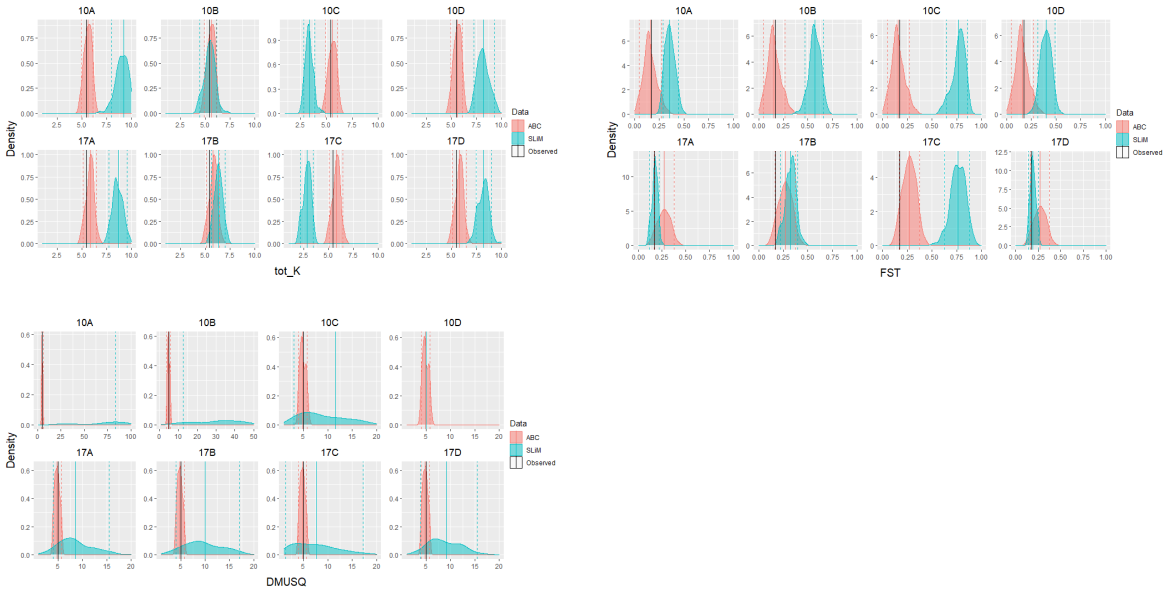

Figure S2.5: Relative distributions and their means (solid line) of summary statistics from the 100 ABCtoolbox and SLiM simulations closest to the observed values (black solid line). 5% and 95% confidence intervals are denoted by dashed lines.

Chapter Three Supplementary Information

Table S3.1: List of newly designed and published primers used to amplify the MHC Class I alpha-1 domain in *Leptodactylus fallax.* Final primers chosen for amplification are highlighted in bold.

Primer ID	Direction	Sequence (5' – 3')	Length	Reference	GC%	Tm
LfMhcIEx2F1	F	CTCTCAGACAGTCACTCTCTGC	22	This study	54.5	61
LfMhcIEx2F2	F	TCTCTCTCAGACAGTCACTCTCT	23	This study	47.8	59
LfMhcIEx2F3	**F**	**ACAGTCACTCTCTGCVTTATT**	**21**	**This study**	**38.1**	**60.9**
LfMhcIEx2R2	R	YGCTGTCCTCACATYATGTCT	21	This study	42.9	50.1
LfMhcIEx2R3	R	TCTGGTTGAAYCKGCTCATC	20	This study	45	62.8
LfMhcIEx2R4	R	TCTGGTTGAAGCGKCTCATC	20	This study	50	60.5
LfMhcIEx2R5	R	TCTGSTTGAAGCGKCTCATC	20	This study	45	62
PclAex2-2F1	F	TCTGGTTGAAGCGGCTCATC	20	Kosch *et al.* 2017	55	67.7
PclAex2-2R1	R	GCTGRGAGATGACGGCAGCA	20	Kosch *et al.* 2017	60	70
ClassI_Alpha1domF	F	ACAGTCACTCTCTGCGTTATT	21	Lillie *et al*. 2014	42.9	58.1
ClassI_Alpha1domR	**R**	**GTTGAAGCGGCTCATC**	**16**	**Lillie *et al*. 2014**	**56.2**	**57.8**

Table S3.2: List of newly designed and published primers used to amplify the MHC Class II beta domain in *Leptodactylus fallax.* Final primers chosen for amplification are highlighted in bold.

Primer ID	Direction	Sequence (5' – 3')	Length	Reference	GC%	Tm
LfMhcIIEx2F1	F	TGTGAGCCCCATGTAACTCTC	21	This study	52	60
BCFDEG	F	TTSTACAATCMGGAGGAGCAG	21	This study	42.9	63.2
LfMhcIIEx2F2	**F**	**CTGCCGTGGATTACATGTTAGAA**	**23**	**This study**	**43.5**	**64.7**
LfMhcIIEx2R1	R	TGGCTGTTCCAGTAATCTGCA	21	This study	48	59
LfMhcIIEx2R2	R	ACACTCCATAGTTGTGTWTACAGW	24	This study	-	55-56
BobomMCF1	R	CCATAGTTGTGTATACAGTATCTCTCCAC	29	This study	41	58
BobomDEG	**R**	**CCATAGTTGTGTWTACAGWMTSTYTCCAC**	**29**	**This study**	**-**	**57-61**
BCF6	F	CATTGTACAATCAGGAGGAG	20	May & BeeBee 2009	45	57.7
BobomSR	R	CCATAGTTGTGTTTACAGACTGTTTCCAC	29	May & BeeBee 2009	41.4	67.3

Table S3.3: Final parameters selected for the ACACIA allele calling pipeline and justifications

Step	Selection	Justification
1. FastQC	Yes	To generate quality reports
2. Trimming low quality ends	No	Reads good quality from FastQC report
3. Merging paired reads	Pair (default)	Paired end data requires merging and default overlap lengths suitable for my read lengths
4. Trim Primers	Yes	Do not want primers in final allele calls
5. Quality Control	Yes – default q 30 and p 90	Sequence quality sufficient for default filters
6. Remove Singletons	Yes	Likely to be artefacts
7. Remove Chimeras	Yes	Likely to be artefacts
8. Remove Unrelated sequences	Yes	Likely to be artefacts
9. Align	No setting to choose	
10. Call candidate alleles	Automated parameter value selection by ACACIA	
11. Allele calling		
Removal of unique variants?	Yes	Removes all alleles identified in a single amplicon (most conservative estimate)
Abs_nor (0 – 1000)	15 (class I and II)	*Generated highest repeatability between replicates*
Low_por (0 – 1)	0.03 (class I) 0.025 (class II)	*Generated highest repeatability between replicates*

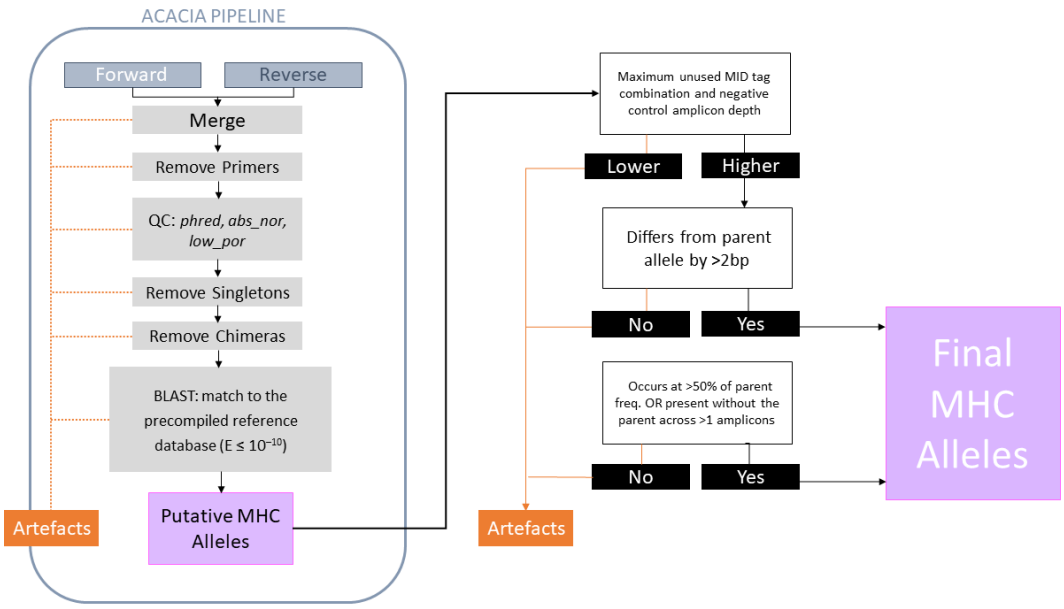

Figure S3.1: Overview of data filtering steps to produce final MHC alleles.

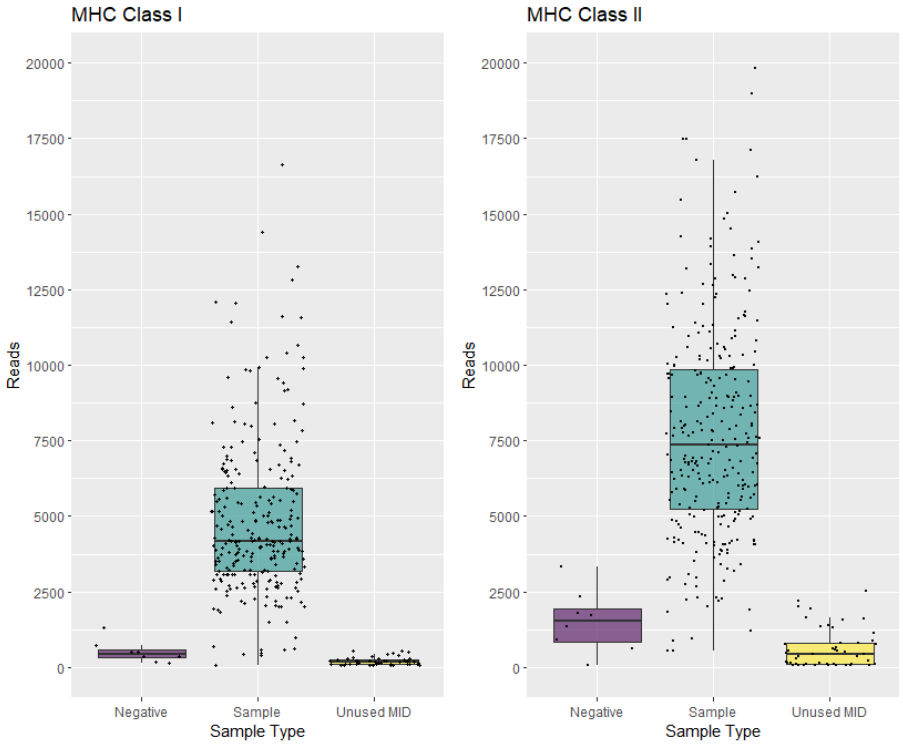

Figure S3.2: Read depths generated for PCR negatives, unused MID-tag combinations, and real samples during sequencing.

Table S3.4: Significant results of site-specific tests for selection run on MHC class I data. MEME = test for episodic positive selection. FEL = test for pervasive positive or purifying selection. LRT = likelihood ratio test statistic result. Values significant at an alpha level of 0.05 are shown in bold and values significant at 0.1 are in regular font.

	POSITIVE		PURIFYING
Codon #	**MEME (LRT, p-value)**	**FEL (dN/dS, p-value)**	**FEL (dN/dS, p-value)**
2			**(0, 0.019)**
15			(0, 0.09)
26			**(0, 0.027)**
32			**(0, 0.013)**
36	(3.49, 0.08)	(10, 0.063)	
39			**(0, 0.003)**
44			**(0, 0.021)**
48			**(0, 0.023)**
50			**(0, 0.045)**
55	**(5.29, 0.03)**		
60		(10, 0.078)	
69			**(0, 0.018)**
70			**(0, 0.015)**
71			(0, 0.071)

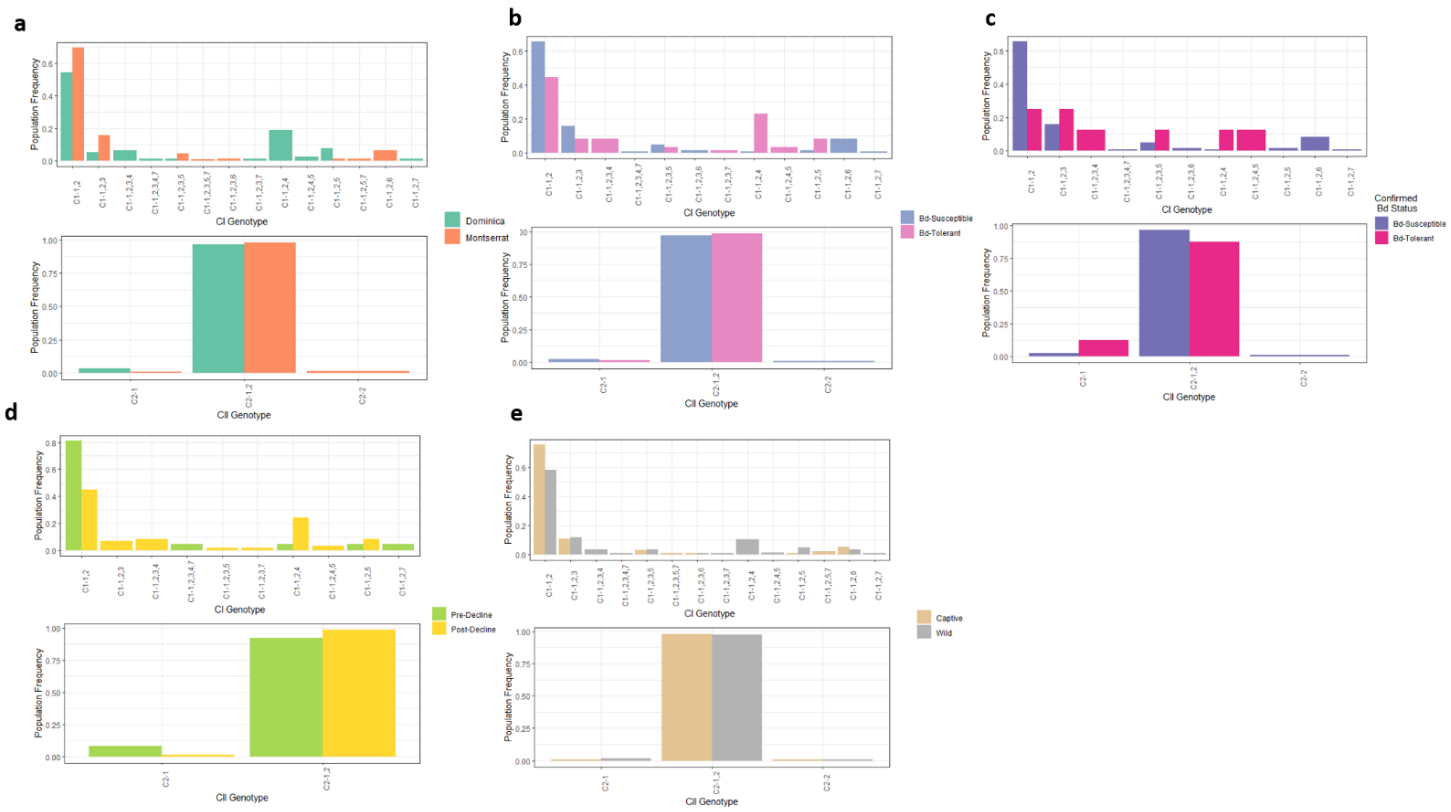

Figure S3.3: MHC class I and II genotype frequencies in four different population groupings of the mountain chicken frog dataset. A) Dominica and Montserrat, B) Bd-susceptible or Bd-tolerant, C) Bd-susceptible or CONFIRMED Bd-tolerant, D) Pre-decline or Post-decline, E) captive or wild. Genotypes are denoted as the MHC class (C1 = I or C2 = II) and then the alleles present are numbered following this. E.g. C1-1-2-3 = Lepfal-I-a1*01,02,03.

Table S3.5: Pairwise Chi-squared or Fisher's Exact Test Results for pairwise MHC Class I Allele Comparisons. Group comparisons are labelled per table section. Below diagonal: P = chi-squared p-value, F = Fisher's test p-value. Above diagonal: chi-squared test statistic where applicable. P-values are corrected for multiple comparisons using a false discovery rate correction of Benjamini and Yekutieli. Significant results are shown in bold.

Dominica : Montserrat

	1	2	3	4	5	6	7
1		$\chi^2 = 0$	$\chi^2 = 0.70708$	$\chi^2 = 36.785$	$\chi^2 = 0.4485$		
2	P = 1		$\chi^2 = 0.70708$	$\chi^2 = 36.785$	$\chi^2 = 0.4485$		
3	P = 1	P = 1		$\chi^2 = 31.341$	$\chi^2 = 1.3101$		
4	**P < 0.00001**	**P < 0.00001**	**P < 0.00001**		$\chi^2 = 15.305$		
5	P = 1	P = 1	P = 1	**P = 0.0014**			
6	F = 0.1751	F = 0.1751	F = 0.7043	**F < 0.00001**	F = 0.1335		
7	F = 1	F = 1	F = 1	F = 0.07	F = 1	F = 0.1876	

Bd-susceptible : Bd-tolerant

	1	2	3	4	5	6	7
1		$\chi^2 = 0$	$\chi^2 = 0.015$	$\chi^2 = 26.056$	$\chi^2 = 1.7914$		
2	P = 1		$\chi^2 = 0.015$	$\chi^2 = 26.056$	$\chi^2 = 1.7914$		
3	P = 1	P = 1		$\chi^2 = 18.69$	$\chi^2 = 1.4879$		
4	**P < 0.00001**	**P < 0.00001**	**P = 0.0002**				
5	P = 1	P = 1	P = 1	F = 0.11			
6	F = 0.188	F = 0.188	F = 0.218	**F < 0.00001**	F = 0.051		
7	F = 1	F = 1	F = 1	F = 0.4	F = 1	F = 1	

Bd-susceptible : Bd-tolerant (CONFIRMED)

	1	2	3	4	5	6	7
1		$\chi^2 = 0$					
2	P = 1						
3	F = 1	F = 1					
4	F = 0.147	F = 0.147	F = 0.716				
5	F = 1	F = 1	F = 1	F = 1			
6	F = 1	F = 1	F = 1	F = 0.375	F = 1		
7	F = 1	F = 1	F = 1	F = 1	F = 1	F = 1	

Pre-decline : Post-decline

	1	2	3	4	5	7
1		$\chi^2 = 0$		$\chi^2 = 2.3195$		
2	P = 1			$\chi^2 = 2.3195$		
3	F = 1	P = 1				
4	P = 1	P = 1	F = 1			
5	F = 1	F = 1	F = 1	F = 1		
7	F = 1	F = 1	F = 1	F = 1	F = 1	

Captive : Wild

	1	2	3	4	5	6	7
1		$\chi^2 = 0$	$\chi^2 = 0.3604$	$\chi^2 = 12.481$	$\chi^2 = 0.098$		
2	P = 1		$\chi^2 = 0.3604$	$\chi^2 = 12.481$	$\chi^2 = 0.098$		
3	P = 1	P = 1		$\chi^2 = 7.993$	$\chi^2 = 0$		
4	**P = 0.0145**	**P = 0.0145**	P = 0.07				
5	P = 1	P = 1	P = 1	F = 0.06			
6	F = 1	F = 1	F = 1	**F = 0.0145**	F = 1		
7	F = 1	F = 1	F = 1	F = 0.07	F = 1	F = 1	

Table S3.6: Results of bootstrap resampling analysis to assess whether MHC-I allele frequency ratios between groups with different Bd survival were significantly different. Only alleles with an observed change between groups were tested. Smaller = observed allele frequency ratio falls below the 2.5% confidence interval of the bootstrap replicate distribution. Larger = observed allele frequency ratio falls above the 97.5% confidence interval of the bootstrap replicate distribution. Within = observed value falls within the 2% and 97.5% confidence intervals. Na = allele not in dataset. AVG = the average across all alleles. A1 = Lepfal-I-a1*01, etc.

Bd-tolerant / Bd-susceptible		**COMPARISON ALLELE**						
		A1	**A2**	**A3**	**A4**	**A5**	**A7**	**AVG**
FOCAL ALLELE	**A3**	larger	larger	na	within	within	within	within
	A4	larger	larger	larger	na	larger	larger	larger
	A5	larger	larger	within	within	na	within	larger
	A7	within	within	within	within	within	na	within

Bd-tolerant (CONFIRMED) / Bd-susceptible		**COMPARISON ALLELE**						
		A1	**A2**	**A3**	**A4**	**A5**	**A7**	**AVG**
FOCAL ALLELE	**A3**	within	within	na	smaller	within	na	within
	A4	larger	larger	larger	na	larger	na	larger
	A5	larger	larger	within	within	na	na	within

Pre-decline / Post-decline		**COMPARISON ALLELE**						
		A1	**A2**	**A3**	**A4**	**A5**	**A7**	**AVG**
FOCAL ALLELE	**A3**	larger	larger	na	within	larger	larger	larger
	A4	larger	larger	larger	na	larger	larger	larger
	A5	larger	larger	larger	within	na	larger	larger
	A7	smaller	smaller	within	within	within	na	smaller

Table S3.7: Population diversity statistics for the subset of samples with data for MHC class I, class II, and microsatellites. N = number of individuals, Ap = total number of unique alleles within population, Ai = average number of alleles per individual, Pa = private alleles, DNUC = Average of the square root pairwise distance between nucleotides of alleles within individuals, DAA = Average of the square root pairwise distance between amino acids of alleles within individuals. Jost's D value given is the pairwise differentiation between the two populations. * indicates significantly different means between the population pair as determined by a Two-sample Wilcoxon Test (p-value < 0.05).

MHC Class I Subset

Population	N	Ap	Ai	Pa	DNUC	DAA	Jost's D
Dominica	35	6	2.63	1	0.261	0.308	0.012
Montserrat	148	6	2.38	1	0.258	0.301	
Bd-Tolerant	19	6	2.84*	0	0.264	0.313	0.020
Bd-Susceptible	112	7	2.46*	1	0.259	0.302	
Bd-Tolerant (CONFIRMED)	6	5	3.00	0	0.272	0.322	0.009
Bd-Susceptible	112	7	2.46	2	0.259	0.302	
Pre-decline	17	6	2.35*	0	0.256	0.301	0
Post-decline	18	6	2.89*	0	0.265	0.315	
Wild Bred	94	7	2.26*	0	0.253	0.296	0
Captive Bred	86	6	2.72*	1	0.266	0.309	

MHC Class II Subset

Population	N	Ap	Ai	Pa	DNUC	DAA	Jost's D
Dominica	35	2	1.94	0	0.068	0.102	0
Montserrat	148	2	1.98	0	0.071	0.106	
Bd-Tolerant	19	2	1.95	0	0.068	0.102	0
Bd-Susceptible	112	2	1.97	0	0.070	0.105	
Bd-Tolerant (CONFIRMED)	6	2	1.83	0	0.060	0.090	0
Bd-Susceptible	112	2	1.97	0	0.070	0.105	
Pre-decline	17	2	1.94	0	0.068	0.101	0
Post-decline	18	2	1.94	0	0.068	0.102	
Wild Bred	94	2	1.99	0	0.071	0.106	0
Captive Bred	86	2	1.99	0	0.071	0.107	

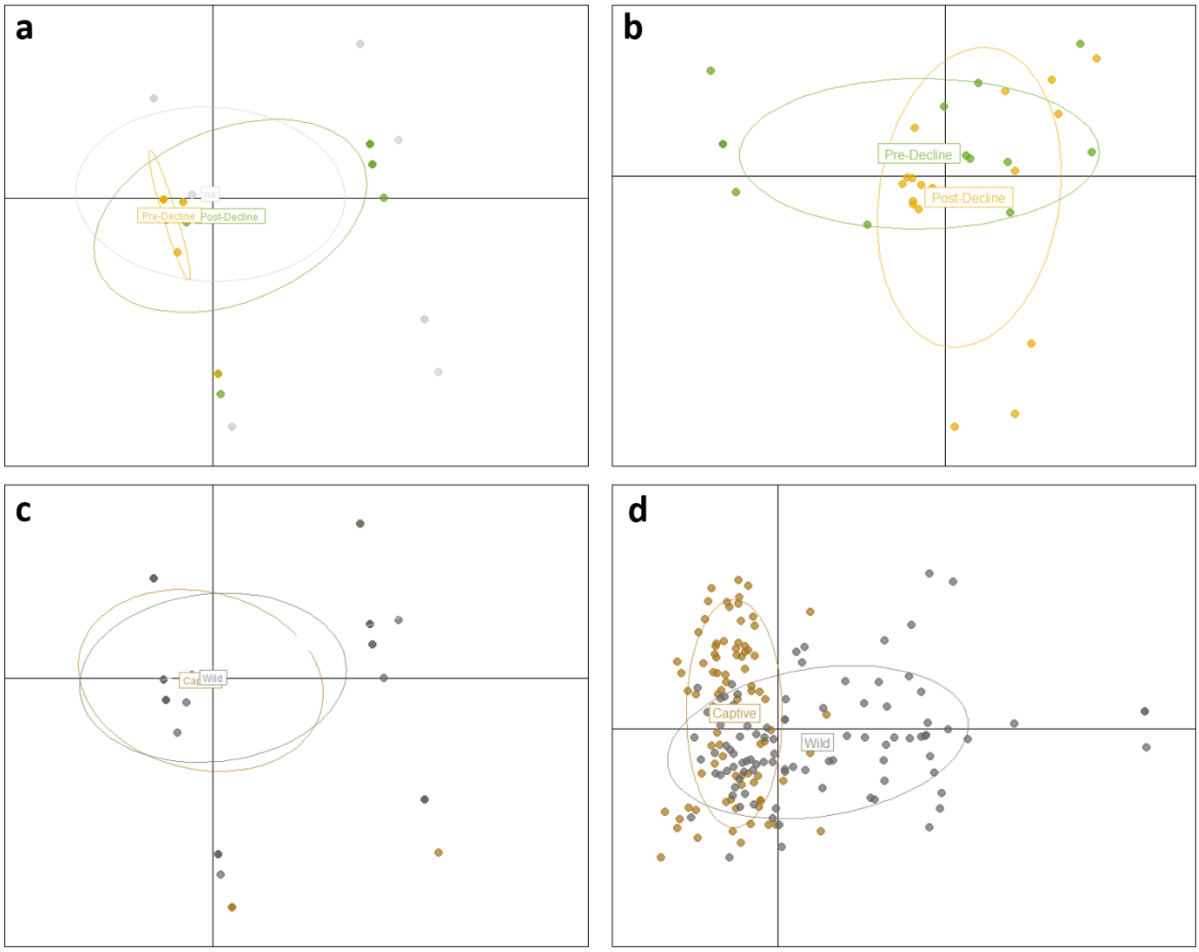

Figure S3.4: Principal components analysis (PCA) comparing collated MHC class I and II allele occurrence with microsatellite allele frequencies across a subset of 183 samples with data for all three marker types. a) MHC: Pre- and Post-decline, b) Microsatellite: Pre- and Post-decline, c) MHC: Captive or Wild, d) Microsatellite: Captive or Wild.

Chapter Four Supplementary Information

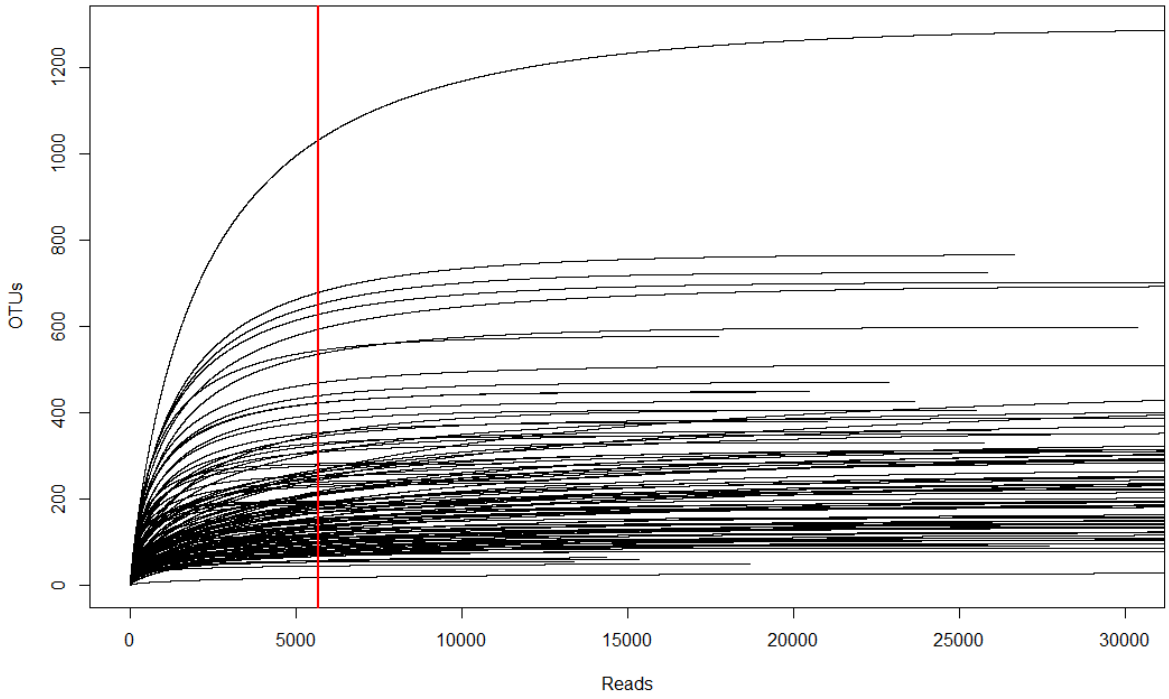

Figure S4.1: Rarefaction curves showing the number of exact sequence variants, ASVs (OTUs) captured at different read depths for each sample. Red line indicates the read depth chosen for rarefaction (5694) where most ASVs can be captured for the majority of samples.

CLR-based

A

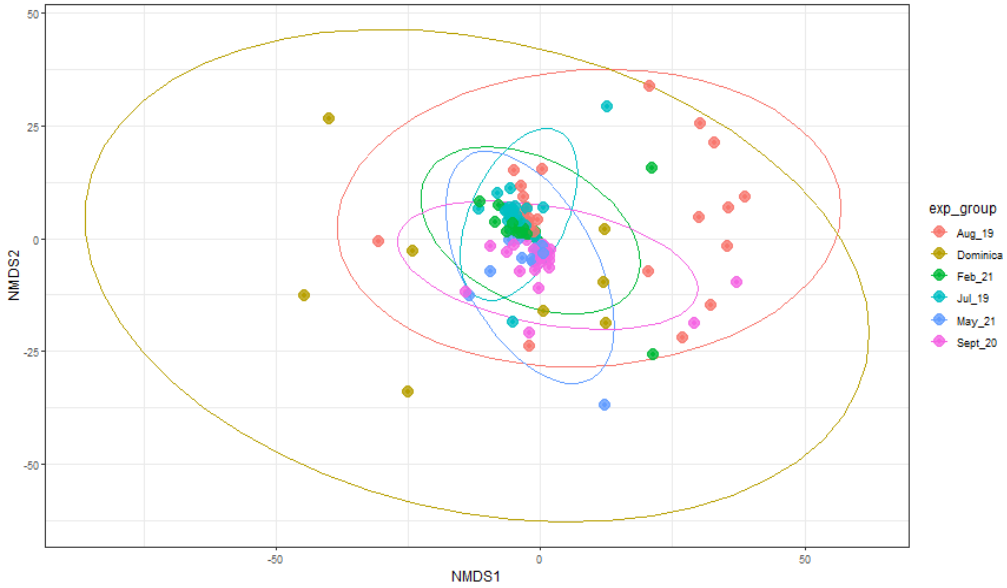

PHILR-based

B

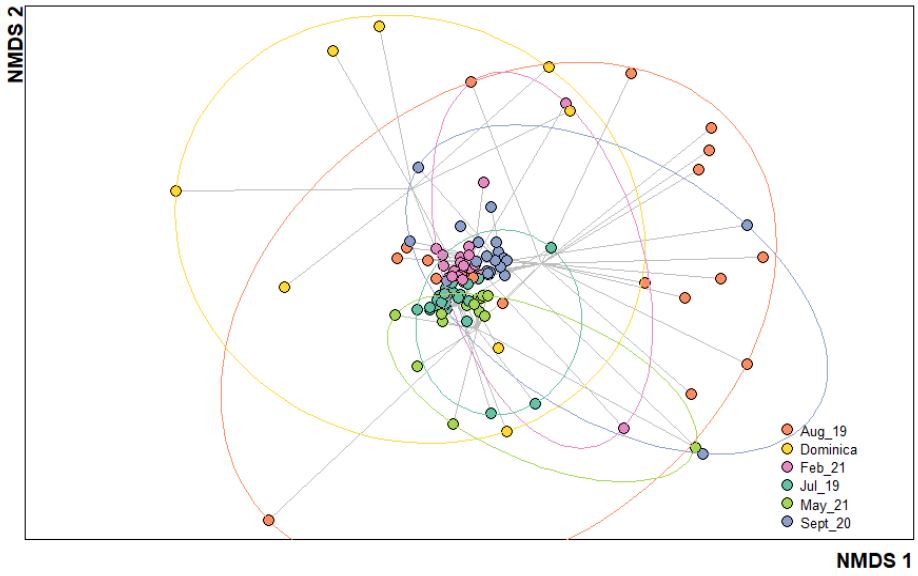

Figure S4.2: Non-metric Multidimensional Scaling (NMDS) plots illustrating the dispersion between sample groups for CLR-transformed data (A) and PhILR-transformed data (B).

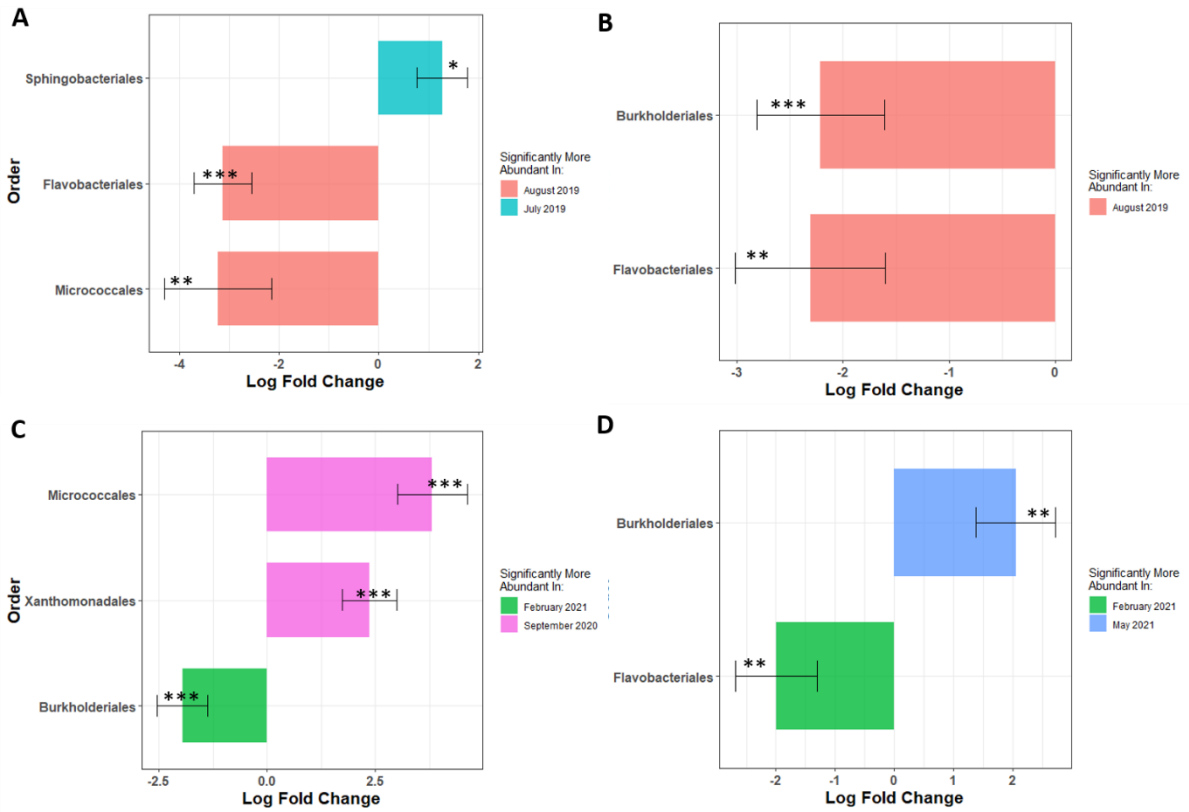

Figure S4.3: Significantly differentially abundant taxa between months of the Montserrat release from ANCOM-BC analysis. Values represent log fold change in abundance between A) July 2019 and August 2019, B) August 2019 and September 2020, C) September 2020 and February 2021, D) February 2021 and May 2021. P-values: *p < .05, **p < .01, ***p < .001. The orders not presented in a given figure were not statistically different between the months in that figure.

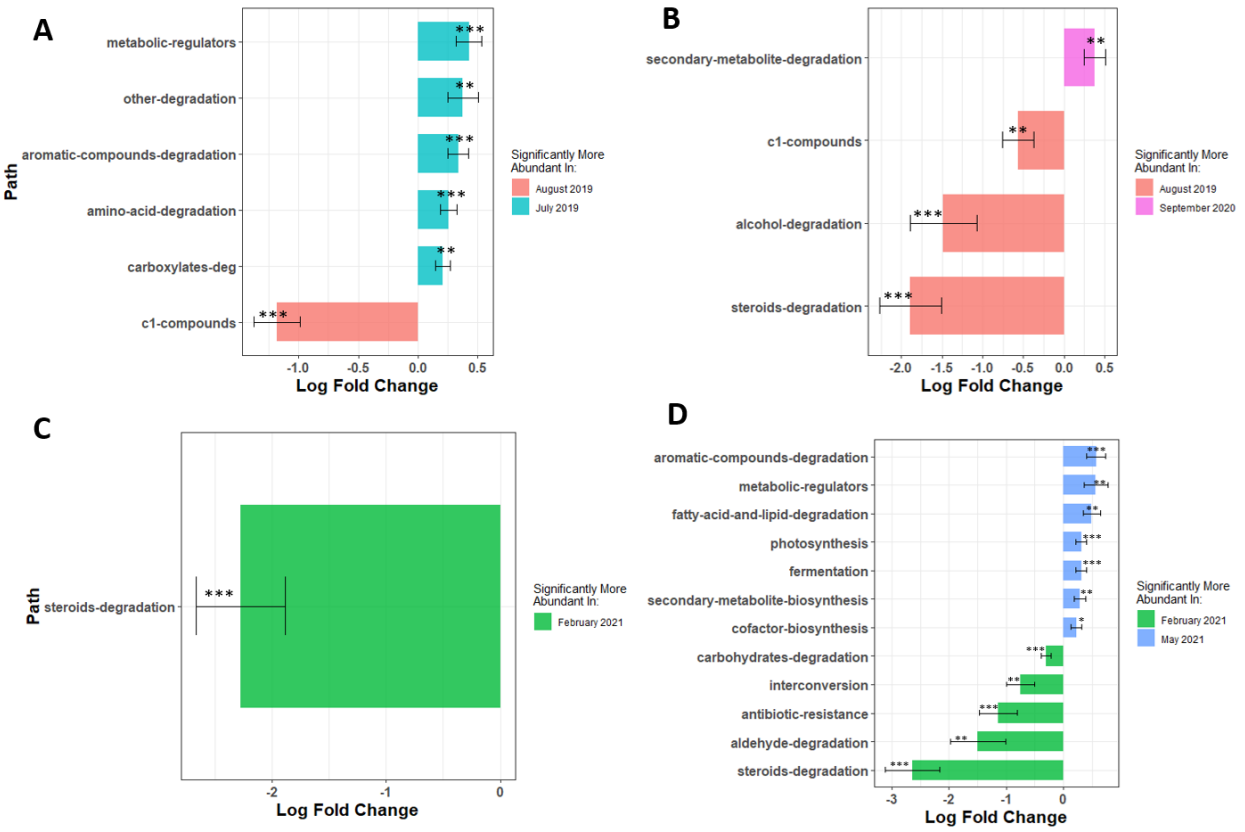

Figure S4.4: Significantly differentially abundant MetaCyc metabolic pathway classes between months of the Montserrat release from ANCOM-BC analysis. A) July 2019 and August 2019, B) August 2019 and September 2020, C) September 2020 and February 2021, D) February 2021 and May 2021. Pathway abundances are predictions from Picrust2. Values represent log fold change in abundances (false discovery rate corrected p-values: *p < .05, **p < .01, ***p < .001).

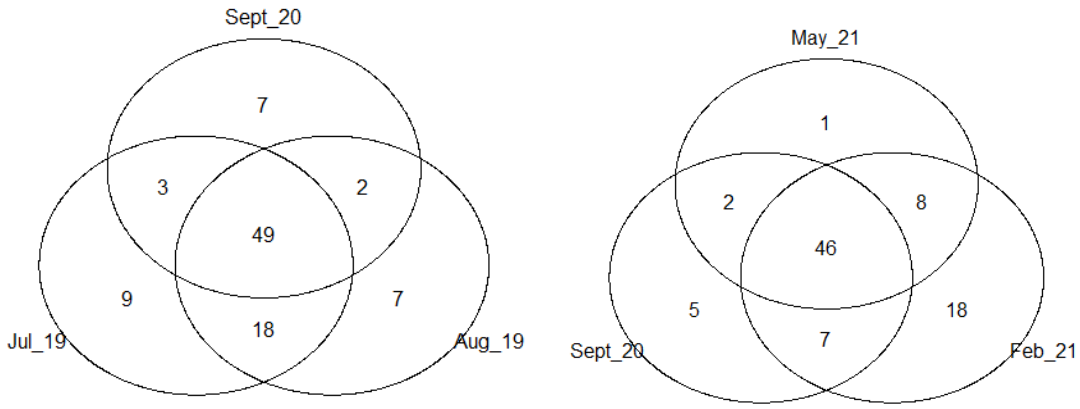

Figure S4.5: Number of shared ASVs with predicted Bd-inhibitory function between successive months of the Montserrat release.

Chapter Five Supplementary Information

Table S5.1: Sample Details. Bd GE = *Batrachochytrium dendrobatidis* genomic equivalents as measured from qPCR.

Sample ID	Year	Host Species	Country	Bd GE	WGS or Fluidigm	SRA
D03-244	2003	*Leptodactylus fallax*	Dominica	NA	Fluidigm	
D03-249	2003	*Leptodactylus fallax*	Dominica	NA	Fluidigm	
D03-252	2003	*Leptodactylus fallax*	Dominica	NA	Fluidigm	
D03-253	2003	*Leptodactylus fallax*	Dominica	NA	Fluidigm	
D14-0061	2014	*Leptodactylus fallax*	Dominica	19630.56	Fluidigm	
D14-0062	2014	*Leptodactylus fallax*	Dominica	22774.8	Fluidigm	
D14-0069	2014	*Leptodactylus fallax*	Dominica	103.9764	Fluidigm	
D14-0070	2014	*Leptodactylus fallax*	Dominica	216.9624	Fluidigm	
D14-0707	2014	*Leptodactylus fallax*	Dominica	632.04	Fluidigm	
D14-0743	2014	*Leptodactylus fallax*	Dominica	552.24	Fluidigm	
D15-0364a	2015	*Leptodactylus fallax*	Dominica	2052.6	Fluidigm	
D15-0372	2015	*Leptodactylus fallax*	Dominica	16425	Fluidigm	
D15-0373	2015	*Leptodactylus fallax*	Dominica	14236.08	Fluidigm	
D15-0386	2015	*Leptodactylus fallax*	Dominica	379.56	Fluidigm	
D15-0387	2015	*Leptodactylus fallax*	Dominica	2201.04	Fluidigm	
D15-0411	2015	*Leptodactylus fallax*	Dominica	19223.76	Fluidigm	
M09-115	2009	*Leptodactylus fallax*	Montserrat	1617600	Fluidigm	
M09-129	2009	*Rhinella marina*	Montserrat	871.5804	Fluidigm	
M09-131	2009	*Rhinella marina*	Montserrat	313.0032	Fluidigm	
M09-140	2009	*Rhinella marina*	Montserrat	11247.948	Fluidigm	
M09-154	2009	*Rhinella marina*	Montserrat	283.9188	Fluidigm	
M09-208	2009	*Eleutherodactylus johnstonei*	Montserrat	505.3332	Fluidigm	
M09-261	2009	*Eleutherodactylus johnstonei*	Montserrat	677910	Fluidigm	
M09-262	2009	*Eleutherodactylus johnstonei*	Montserrat	794770.8	Fluidigm	
M09-263	2009	*Eleutherodactylus johnstonei*	Montserrat	303794.4	Fluidigm	
M09-380	2009	*Leptodactylus fallax*	Montserrat	3804000	Fluidigm	
M09-395	2009	*Leptodactylus fallax*	Montserrat	41978400	Fluidigm	
M09-400	2009	*Leptodactylus fallax*	Montserrat	2984340	Fluidigm	
M09-906	2009	*Leptodactylus fallax*	Montserrat	466614	Fluidigm	
M09-994	2009	*Leptodactylus fallax*	Montserrat	2.964564	Fluidigm	
M09-997	2009	*Leptodactylus fallax*	Montserrat	763083.6	Fluidigm	
M11-0010	2011	*Eleutherodactylus johnstonei*	Montserrat	756.258	Fluidigm	
M11-0050	2011	*Eleutherodactylus johnstonei*	Montserrat	868.9332	Fluidigm	
M11-0072	2011	*Eleutherodactylus johnstonei*	Montserrat	1292.976	Fluidigm	
M11-0158	2011	*Eleutherodactylus johnstonei*	Montserrat	2478.876	Fluidigm	

M12-0867	2012	*Leptodactylus fallax*	Montserrat	293935.2	Fluidigm
M12-0883	2012	*Leptodactylus fallax*	Montserrat	28768.56	Fluidigm
M12-0967	2012	*Leptodactylus fallax*	Montserrat	127898.4	Fluidigm
M12-0976	2012	*Leptodactylus fallax*	Montserrat	81085.08	Fluidigm
M12-0982	2012	*Leptodactylus fallax*	Montserrat	97428.84	Fluidigm
M12-0986	2012	*Leptodactylus fallax*	Montserrat	67860.96	Fluidigm
M12-0992	2012	*Leptodactylus fallax*	Montserrat	177120	Fluidigm
M12-1139	2012	*Eleutherodactylus johnstonei*	Montserrat	1635.048	Fluidigm
M12-1141	2012	*Eleutherodactylus johnstonei*	Montserrat	3093.348	Fluidigm
M12-1212	2012	*Leptodactylus fallax*	Montserrat	283.7184	Fluidigm
M12-1312	2012	*Eleutherodactylus johnstonei*	Montserrat	514.776	Fluidigm
M12-1369	2012	*Leptodactylus fallax*	Montserrat	81851.04	Fluidigm
M12-1387	2012	*Leptodactylus fallax*	Montserrat	125.8332	Fluidigm
M12-1422	2012	*Leptodactylus fallax*	Montserrat	5621.28	Fluidigm
M12-1423	2012	*Leptodactylus fallax*	Montserrat	299.3172	Fluidigm
M12-1457	2012	*Eleutherodactylus johnstonei*	Montserrat	919.2336	Fluidigm
M12-1527	2012	*Leptodactylus fallax*	Montserrat	68075.64	Fluidigm
M13-0342	2013	*Eleutherodactylus johnstonei*	Montserrat	44781.24	Fluidigm
M13-0352	2013	*Eleutherodactylus johnstonei*	Montserrat	46928.52	Fluidigm
M13-0357	2013	*Eleutherodactylus johnstonei*	Montserrat	3222.6	Fluidigm
M13-1481	2013	*Leptodactylus fallax*	Montserrat	80125.5602	Fluidigm
M13-1533	2013	*Leptodactylus fallax*	Montserrat	47299.92	Fluidigm
M13-1652	2013	*Eleutherodactylus johnstonei*	Montserrat	699.12	Fluidigm
M13-1674	2013	*Eleutherodactylus johnstonei*	Montserrat	4472.04	Fluidigm
M13-1689	2013	*Eleutherodactylus johnstonei*	Montserrat	704.76	Fluidigm
M14-0365	2014	*Leptodactylus fallax*	Montserrat	10.354512	Fluidigm
M14-0374	2014	*Leptodactylus fallax*	Montserrat	20459.04	Fluidigm
M14-0379	2014	*Leptodactylus fallax*	Montserrat	6826.26	Fluidigm
M14-0395	2014	*Leptodactylus fallax*	Montserrat	84145.68	Fluidigm
M14-0405	2014	*Leptodactylus fallax*	Montserrat	22217.52	Fluidigm
M14-0406	2014	*Leptodactylus fallax*	Montserrat	64785.96	Fluidigm
M14-0431	2014	*Leptodactylus fallax*	Montserrat	76502.28	Fluidigm
M14-0432	2014	*Leptodactylus fallax*	Montserrat	4435632	Fluidigm
M14-0435	2014	*Leptodactylus fallax*	Montserrat	27269.88	Fluidigm
M14-0436	2014	*Leptodactylus fallax*	Montserrat	10628196	Fluidigm
M14-0464	2014	*Leptodactylus fallax*	Montserrat	99015.12	Fluidigm
M14-0469	2014	*Leptodactylus fallax*	Montserrat	54021.36	Fluidigm
M14-0484	2014	*Leptodactylus fallax*	Montserrat	100226.28	Fluidigm
M14-1612	2014	*Eleutherodactylus johnstonei*	Montserrat	1565.52	Fluidigm

M14-1621	2014	*Eleutherodactylus johnstonei*	Montserrat	3048	Fluidigm	
M14-2008	2014	*Leptodactylus fallax*	Montserrat	159488.4	Fluidigm	
M15-0537	2015	*Leptodactylus fallax*	Montserrat	238730.4	Fluidigm	
M15-0744	2015	*Eleutherodactylus johnstonei*	Montserrat	250.9404	Fluidigm	
M15-0772	2015	*Eleutherodactylus johnstonei*	Montserrat	558.402	Fluidigm	
M15-0971	2015	*Leptodactylus fallax*	Montserrat	6.81510396 2	Fluidigm	
M15-0977	2015	*Leptodactylus fallax*	Montserrat	574.873732 9	Fluidigm	
M20-207	2020	*Leptodactylus fallax*	Montserrat	1155.24	Fluidigm	
M20-216	2020	*Leptodactylus fallax*	Montserrat	220525.8	Fluidigm	
M20-218	2020	*Leptodactylus fallax*	Montserrat	4402.92	Fluidigm	
M20-219	2020	*Leptodactylus fallax*	Montserrat	4799.64	Fluidigm	
M20-220	2020	*Leptodactylus fallax*	Montserrat	182379.36	Fluidigm	
M20-221	2020	*Leptodactylus fallax*	Montserrat	837.96	Fluidigm	
M20-231	2020	*Leptodactylus fallax*	Montserrat	6173.28	Fluidigm	
M20-253	2020	*Leptodactylus fallax*	Montserrat	927.24	Fluidigm	
M20-279	2020	*Leptodactylus fallax*	Montserrat	390.24	Fluidigm	
M20-283	2020	*Leptodactylus fallax*	Montserrat	1183.56	Fluidigm	
M20-285	2020	*Leptodactylus fallax*	Montserrat	502.32	Fluidigm	
KB347	2014	*Bombina orientalis*	South Korea	NA	WGS	SRS2757075
KRBOOR_323	2014	*Bombina orientalis*	South Korea	NA	WGS	SRS2757080
KRBOOR_331	2014	*Bombina orientalis*	South Korea	NA	WGS	SRS2757081
CLFT061	2013	*Hylodes meridionalis*	Brazil	NA	WGS	SRS2757098
CLFT136	2014	*Bokermannohyla hylax*	Brazil	NA	WGS	SRS2757087
KB108	2014	*Rana catesbeianus*	South Korea	NA	WGS	SRS2757135
CCB1	2007	*Alytes muletensis*	Spain	NA	WGS	SRS2757205
MC58	2008	*Hadromophryne natalensis*	South Africa	NA	WGS	SRS2757116
SA5c	2010	*Amietia angolensis*	South Africa	NA	WGS	SRS2757117
0739	2007	*Alytes obstetricans*	Switzerland	NA	WGS	SRS2757206
L2203	2009	*Leptodactylus fallax*	Montserrat	NA	WGS	SRS2757145
Hung_2039	2014	*Bombina variegata*	Hungary	NA	WGS	SRS2757169
MexMkt	2009	*Ambystoma*	Mexico	NA	WGS	SRS380118
JEL270	1999	*Rana catesbeianus*	USA	NA	WGS	SRS2757312
JEL423	2004	*Agalychnis lemur*	Panama	NA	WGS	SRS2757141
JEL427	2004	*Eleutherodactylus coqui*	Puerto Rico	NA	WGS	SRS380111
SA-EC3	2015	*NA*	South Africa	NA	WGS	SRS2757071

Table S5.2: Fluidigm primer details. Chr = chromosome.

Primer Name	Pool	Forward	Reverse	Target Size	Chr
AB1	A	GCATCGGGTGCATTATCTCT	TTGCAGAATTCCAACGTGTC	185	1
AB2	B	TTCCTGGTGTTGGGCTATTT	GATATGCTACCGTCGGCATT	172	1
AB3	B	GAAGACTCGAAGCCTTCTTCTG	TCAACCCTAGGTCAAAGAATCG	190	1
AB4	A	GTCAAATATCTGGCATCAATGG	GATGCGAGCAACACTCAAGA	152	1
AB5	A	ATGGTGTGCAAGTTCTGTCG	TCAGATGAGTTGCAGCGTCT	200	1
AB6	B	AGCGTGTGTGTCCTTTCTGA	GAAACAGGTTATGCGCGATT	177	1
AB7	A	TGCTGCTGCTGCTCTTATTG	AGAAATTGCAGGAAGGCAAG	196	1
AB8	B	TCCAAAGTCTACCGTCTGAGG	TGTGTGCGAGTCGAATTTCT	158	1
AB9	A	CTCGGTACTTGATCCCGAAA	CGGTGGTTGTCGTAGTGGTA	197	1
AB10	B	GCCGACCGAACTATCTGTTG	GGGCAGAGGCAGGTAAGAAT	161	1
AB11	A	CGGAAAGCCAATACCAACAA	CATTGCGCATTCTAATTGTCA	181	1
AB12	B	AAAGAATGGCGAGTTGATGG	TCGATGTGGACGACTGTGTT	154	1
AB13	A	ATGTGCACCTATGCGAGATG	GGCGCTTCAAATGAGGTTT	152	1
AB14	B	AAACGACGTGACTTGAAATGC	CGTGCTGGTAAGTCCAATCA	192	1
AB15	A	ATCTTGGCCATCAACAGTCC	CTTGGCCATCAACGACAAC	191	1
AB16	B	TTACCAAGCCTGTCGAGGAT	TGATAGGATGCTAGTGATTTCAGG	195	1
AB17	A	CGTTTCGATGGTTGTTCCTT	GTCTAGCGTATTTCTCAAGGGTTT	176	1
AB18	B	AATCGTATGTGTCATGTCAGGAA	TTTGATCGTATGCTGGCAGT	181	1
AB19	A	TCTGTTGCTGCCAACTCAAC	TGGATTTGAATGGAGGGTAAA	179	1
AB20	A	GATGCTTTACCCACATCAAGC	CGTCCAACTACAGGCGTAGG	161	1
AB22	B	TGACAAGTAGGTCTTTATGGTCTAGC	GGCTCCAGCTTTGTTGATTT	197	1
AB23	A	GAAGTGGTACTGATGGGCTGA	AAAGAACCACGGCAATCAAC	150	1
AB24	B	GCAAATGTATGATTTGGGTCAG	TTTATGGGTGGTTATTATTAATGCAA	187	1
AB26	B	AATAAACCAAGATGGTGTGC	CGAAACTTTCTACCAGTTCAA	194	1
AB28	B	TGCTACCTTGATTGTTTGG	AAACAAGATGGCATAGAACC	197	1
AB29	A	CGTGGTGTCAGTTTGCTAGG	GGATGAATTTGATGATGACGAA	189	1
AB30	A	CTTCCCATCTTCAGCATCGT	AGAGCGCTTATTTCCGAAGA	152	1
AB31	B	GGGTTTAAAGTCTCTAGTCAAGTCGT	CACTCAACTTTGTCAAACACACAC	159	1
AB32	A	GAGATGAAGCATTAGTATCCGCTAA	TGAAAGAATTAATAGCCATGATAAGC	200	1
AB33	B	TCACCAATATCTAGCCCTTC	AGGAGCAATTGGAGGTAATA	188	1
AB34	A	TTGCATCCTTGTGGTTATCG	ACACGGATCGTTGATGCTTT	154	1
AB35	B	GCGTCTCTGACTTGGTGGTT	TGGCATTCATCAGGTACCAA	184	1
AB36	A	CTCGCATCTTGACGGAAGTT	TGGTACACTGCCAATACTAAGCA	190	1
AB37	B	CCGAGTGTTTCACAGATGGA	GTTTATGCACTTACCATTCACGA	152	1
AB38	A	TCCATCCATGAGAACTGCTG	ACGGAGTTGTTCCTGCTTTG	169	1
AB39	B	ATTACTCTTGGTTCTTAATGCATCC	CGCTTCTTCCATTCGACATT	184	1
AB40	B	AACTGATGGAGACGTGACGA	CTGATCATGCCAACTGGATTT	177	1
AB41	A	GTGGTGAGCAAGGTGATGTG	CTCGAGAGCTCTGCTGATCC	181	1
AB42	B	TGTATGGCAATGCTGTTCAGT	ACCAAAGCACAATTTCTGCAC	150	1
AB43	A	AGTGCGTCACCAGGTTTAGC	CAAACTGTTGCAGCATCGAC	157	1
AB44	B	CGCCAACGTCTACTCATCTTT	ACAAGAGCTCCAATGCTTATGTT	191	1
AB45	A	CAGACGATGCTGATGACGAT	AAGGCAGATGCATTTGAAGC	163	1
AB46	B	GGATCGCATCAACCCTCTAA	GATGGAGGTGCATCTCGTG	155	1
AB47	A	CGTCGTGCTGATCTCTACTAGG	GTCTATCCTACGGTGATGGCTTA	198	1
AB48	B	TGATTGATATTGAGCAGGCTGT	TCGGCTTGAGCATCTACAAA	151	1
AB49	B	ACACATGGCAATCACCAAGA	TCACTCACCAATATGCTTGACA	170	2
AB50	A	GTTGCATCAAGGGTTTCGAT	GTCGTGGACCACTTTCTCCT	182	2
AB51	B	CCATTATGCACGACTGTTGC	TCGGAATAAACCAAGTGCAAA	199	2
AB52	A	TTGTAGGGTCGAGCAGTAGGA	CAAATCTTCCTGGCATGCTT	181	2
AB53	B	ACCGCACTAAACAAATGAGT	CCGCATAGCAATCACTTTA	195	2
AB54	A	CCGTACTTGGACACATGCAA	GCAACTGTCTTGAGCAAACG	151	2
AB55	B	GCAGATGGCTTGGTTGATTT	GCCGCTCAATTGTCTGGTA	186	2
AB56	A	AGCGCACTCCACAACTCTG	TGCGACTGTTTGAAATCGAG	187	2
AB57	B	CATTCCGCTTTGTTCGACTT	TCGGCCAATATCTGGTGAAT	174	2
AB58	A	GCTTGATCCGCTTCTGATGT	TCTGCTGTCCTTGATGCTTG	158	2
AB59	B	ACGATCACCGAGTTCAAGAGA	GGTGTGAATGCATTACGACTGT	197	2
AB60	A	TGTCCATGTTCTAATTCCCTTACA	AGCGACGAGGAAGAAGATTG	158	2
AB61	B	GCCAGACTCCGCTTAGCTC	AATAGCGGGTGTTGGTTCAC	161	2
AB62	A	CGCGTTCTAACCCAAGAAAG	CAGCTGTACTCGCCAATGAA	190	2
AB63	B	GTGCCGATTACAAACCACCT	CTCCCGGTTTGACTAGCACT	196	2

AB64	A	TCCAAACGCATTACCATCAA	GCGACACATGGACTGAGCTA	164	2
AB65	A	CAAACAATATCGAGCCCAATAAA	TCATTGTTTGAATGATTTGCATTA	191	3
AB66	B	ACAGCATTCATCAAGCCTAGC	AGAAGGAATGGATGGCAAGTT	183	3
AB67	A	ATTGCCAAGCGATGTTCAA	TAGCATCGCCTAACCCAAAC	199	3
AB68	B	CGTACATTCTTTGATGATTATATTGCT	CTTGAGTACCAGCGCAATCA	178	3
AB69	A	ATCGATCGTCCAAGAAATGG	GCAAGTGTAGCTCTGGGATGA	196	3
AB70	B	CAACTGTCGCATTCCTGAAA	AAAGCAATGGAAGCAAATGG	162	3
AB71	A	GCTGCACGCTGATACTCTTG	GCTTTGGGCCATGTCAAATA	176	3
AB72	B	ACAATGTCGAGGCAGGAAAT	GGCTCGAAACTCGTCAACTT	185	3
AB73	A	GCGCCAGCTATTTCTAATGC	AACTGGAGCTGCGATTGTCT	174	3
AB74	B	GGTTGCTCAGGATGCACAA	CAAACCCAAGACGGTACAGAA	200	3
AB75	A	TGGACACGATTCGTCGTATT	TTGGGTTCAAATGCTGTCAA	166	3
AB76	B	ATTCCTCCAATGCATCCAAC	AGCTGCAGACACGTCAAAGA	200	3
AB77	A	TACATCACCACCCTGGGTTT	GGCTGTTGCATATCGTCAAA	181	3
AB78	B	TGACTGGACCCATTTCTCAA	CGTAAGAGACGAGTTTGTCGTG	197	3
AB79	A	GGTGCACTTTCGATCCACTC	CAACACTTCATGTCGGGAAA	167	4
AB80	B	CTGATTGCTCTAGCCCAGTTG	CGATTCAGCTAGGCTTTGGA	150	4
AB81	A	TTTGGATTGGATGGAAAGAGA	ACAGGGAAACCAAAGTGCAT	194	4
AB82	B	ACTCTTCCAAGCGACCAATC	ACAGTTCGCGGAACATTTG	196	4
AB83	A	CCCAATTGTTTCATTCCTTCA	GGGTAAGTTGATCAATACGTCTAGC	195	4
AB84	B	GATGCGGTTGCTGCTCTAA	TGTTGACGGTGATGACATGAT	193	4
AB85	A	GCCAAAGGCATTCCAGAGTA	TAGTCCAAACGGCAGGAATC	152	4
AB86	B	ATTGCCTTCTTGTTGGTTGC	TTTGGTTTCCTCAACAACACTATC	199	4
AB87	A	CTGATGCTGGATTGCAGAAA	GCTGAAACACACCAACTTTGAA	167	4
AB88	B	TCAACTGGCTTTGAGCACAC	CTTCAACTCCGTCACAACGA	191	4
AB89	A	AGGCAAATGTGGAATGGAAG	TTCTTGTTGCCATATCTTCAGC	184	4
AB90	B	ATGCTGCTGCAAATGTCATC	GGTCGTTCAGAGGTGGGTAA	161	5
AB91	A	CAGTTGGCATAGTGCATACGA	CATCATGGTGAAACCAACCA	185	5
AB92	B	TTGATTGTGCGAGCAAGATG	TGGAAGAACTCTCTCGCCATA	176	5
AB93	A	TGTTGATGGAGCACCAAGTC	AGCGTCATTCAACCGAGAAT	186	5
AB94	B	GAGTGCTATTTGCCGACGA	TCGACGCCATTTGACAATAA	178	5
AB95	A	ACCTCGTCCAAACCAACAAG	CGCGCTGATTAACCAAACTT	179	5
AB96	B	ACATCAACGTGCCAGACACT	GCAGTTGGAAGATGTGGTGA	160	5
AB97	A	TCTCAAGATACGAGCGAATGC	TCGAGCAGATCATTGTCGAT	193	5
AB98	B	GCATTCATCTTGGCTGCATA	GGCGAATGCATTGTTGACTA	169	5
AB99	A	TGGACACCGTTACGTTGAAA	TTCAAAGAAACCCAAACAACAA	186	5
AB100	A	CGGCACGATTGTATTTGGAT	CATTCATGGCTGGAACATTG	185	5
AB101	B	TTCAGAATGGTTTAGAGTGTGGAA	AGGGCTGCAACAACTGGAT	172	5
AB102	A	GGTGTCGAGGATGGTATGAAA	GTCCAGCCACCTATGCAAGT	175	5
AB103	B	CTGCGCAAGAACGACTACAC	TGGTTGACGATGCTCAAGTC	179	5
AB104	A	CTTGGCTGTCGATGCAGTTA	ATCATACCAGGCCATCAAGG	162	5
AB105	B	CCAGAAACTATTCGCCAACC	GAAACTCTCGGCACTCTTGC	195	5
AB106	A	CGCGTTCAAGACAACAAGAA	GCCAGTCTTGTGAATGATGG	192	5
AB107	B	ATGTTTGGAACGCCAATCTC	CAATGTCTTGGCCAGTTTGA	190	5
AB108	A	CGATGCAAATCATGACCATT	TGCTCTGCTTTCCATGAGTC	199	5
AB109	B	GGTCCACGATTGAGTTGTAT	AAAGGCACAATGTTCAGTAAA	196	5
AB110	B	AGAGAGGGCAGACAAACGAA	CGCCTATGGTGGCATTATTC	153	6
AB111	A	CTTGCAGTGTACTCCTGTTCAAA	CACGTAAAGTGGAGCACTGAAT	200	6
AB112	B	ATGACCAGACCATCAAAGC	GATGGCTCTCATCCAAGAC	200	6
AB113	A	ATTGTTGGGCCAATTGTGTT	TCGATTGAGTGAAGGCATGA	189	6
AB114	B	TTGATTGGCAGCACCATCT	CTCCCGAGTTCTATGGTGGA	192	6
AB115	A	AATGACCAAACACGATTAAAGATG	TGTGCAAATTCACTAAACCTCGT	182	6
AB116	B	CACCTCTGCTCTTGTGTCCA	CAGCCAATTCAGGACGATAAT	155	6
AB117	A	TTGCATTGTTCCACATGGTT	GCCAACGACTCCAATGTAAGA	190	6
AB118	B	ACGACGCTCAAATCGAGTCT	TTCGGGTAAACCAGCCAGT	189	6
AB119	A	GATCTCGGATACCTGCATCG	TTCGCTGATTTCTTCAAACG	174	6
AB120	B	TTTCTGGAGTGGCAAATGGT	AATGTGTACTCGATCCATCTCTGA	194	6
AB121	A	GAAGCACTGCCAGATTTCATT	TCAAGTGTGCTTGTGATCCTG	157	6
AB122	B	CATCATGGGTGTTCTCAACG	TGTGACTCGTTCAAGCTCGT	190	6
AB123	A	AGATGTGGGTGTTGTTGTCG	ACAAACTAGATGCACTGGAGGAT	196	6
AB124	B	TCCCAATTCCATTTACTGCTATC	TTCAATCAAGGCTCACGTTG	179	6
AB125	A	CTGCACAACAGGTCAGCCTA	GAGCTTGAGGTTTGATTGCTG	163	6
AB126	B	ATGCTGCTGCAGTCTCGTT	TTGATGTCGATGTCGATGCT	165	6

AB127	A	GCACCACCATAAGTATTTCC	GAAGGCTGCAATCAATATGT	169	6
AB128	B	AGTGATGCGGTTCAGGAAAT	CGTTTGGAGTGGCAGCTT	163	6
AB129	B	TCAAACAAACGTCCAAACAAA	CGAAACAGACAAAGGTCAGTACA	198	7
AB130	A	ACATATCCCAATTGCGAAGC	CGTTTAGGCGATCTTGGTGT	187	7
AB131	B	TCCTGTTCCACTTGCTCCTT	CCAAATCTACCAACACGCTATTC	163	7
AB132	A	GACGGTCTTGTAGTCCTCTCAAA	CAATCACTTACACGCCTTCG	169	7
AB133	B	GAGCGGGTTCTTTAATGTATCG	GGACAAATCTGGCCAATGTAA	152	8
AB134	A	CACAGCACTGGCAGTTGAAT	CTCAACACCAAAGCCTCGAC	157	8
AB135	B	AACTCGTGTCAAGCGTGTCTT	CACACCGGTTGAGGGTTTAG	178	8
AB136	A	GGATTCCTCCGTATTTCTTGG	TTAAAGCCAAGCATGTGCAA	160	8
AB137	B	CTGCGATTGGATGTGGTTTA	CAAGTGATCCACACGACACC	165	8
AB138	A	GACAAAGTGCCGAGTGTTTG	ACGTTGGCGATATCCCTTG	200	8
AB139	B	CAGGATCTGCCAGTTTCGAT	GGTGCTCCATAAAGTGACAGG	199	9
AB140	A	TTTCGTCAGTGGTCCAAACA	CTAACATGCCGATTGTGTCG	187	9
AB141	B	TAGTGCTCCATCTTGCGTGA	TGGAGCTTGTTCATCATACTGTG	185	9
AB142	A	TTCAATCGCTTCTGCAGTCTT	TGAGCAAGTCTGTTCAAGGTG	200	9
AB143	B	TTGCTTTGCTTTACAATCTTGC	GCAGCTGCAAGAGCTTTGTT	173	9
AB145	B	TTCCTGCTGGAATTGAAAGC	TCGTCCTTCAGCAGTGACTTT	186	9
AB146	A	CAAGTGCCCACACATGGTAA	CCAGTTCCACACTCCGAAAT	167	10
AB147	B	CCAATCGGTGTCAAATAACTCA	GCAGTCCGTAACACCAAACA	197	10
AB148	A	GCAATTGTCTCGCGATAAGG	TGATAGCTCTCTTGAAACATCCAC	198	10
AB149	B	GCAGGTAGAAGGCAAGCAAT	CGGGAGCTATATATTTCCAGCA	184	10
AB150	A	GCTGAATTCCAACGTCCTGT	AGCCTTGTTGCCATCTTCAT	197	10
AB151	A	GTCTCGAACACAAGGGCATT	TTACCAACGAACCCAAATCC	180	11
AB152	B	ATGGAAACAGGTGGAGCAAG	TTCTGAACTGCAGCATCCAC	194	11
AB153	A	AACCAAGTTGTATGGGTCACG	CGTAATACCGATCAAACATGACA	176	11
AB154	B	ATGATGATGGGAGCAAGTCC	TTTGTTACATCAGGAGCAGCA	161	11
AB155	A	GACAAAATGGAAATCATTACATCG	TTTTGTTCCAAACACAATATCCA	150	11
AB156	B	TGACGGAACCAAAGACATGA	GCAGCTTGAAGTGCCTTGAT	193	11
AB157	A	CCCTTTCTATTGCATTTCACAA	TGTGACATTGTTGCTTGCTG	159	12
AB158	B	TGATGACAACCCATGGAACA	TCCAACATACTCCAGTCCAACA	180	12
AB159	A	ATCGAGCGTGAAATGACAAA	TCGAACCGATATGCAAGAAA	188	12
AB160	B	CCTCCCTTGTATGGCATTTG	GGATGCAGCCAAGTATCTCC	150	12
AB161	A	GCCAGCAAACTCAAACCACT	TGAGAATATTTGCTGGGCTGA	198	12
AB162	B	CGCATTCAGACACCACAGAT	GCATCAAATTGGCGAGAGTT	191	12
AB163	A	GACGTAAATCGTTCCACTTTCC	AGTCCATTTGGGATCGTCAC	158	12
AB164	B	AGAGCCTGAGCAGTGCAAAT	TTTCCTGCAAGGATGCTCTT	160	12
AB165	A	CGTCATGAGAAAGACCGAGAA	GACATCTCTGCCAAGGCTTC	169	12
AB166	B	AACCTGATTGATCATGGATGG	GCAACAATCCCTTTACCACTG	182	12
AB167	A	GCTGACCATATTTGCGGACT	TGTTGACGTTGCTTGTGGTT	172	12
AB168	A	ACAGTTGAACATGAAGCAGCA	GCAGCCTGTTGACAAGGAAT	193	13
AB169	B	CTTCCGACTCCAAGTACTACACC	TCAGTGGAGAATGCAGACTCTT	195	13
AB170	A	CCTGACTCCATCTCCGTCAT	AAACGCAGGCGATAGATTTG	183	14
AB171	B	TGACATTGCTTTATAGATGGCTTC	TTCTGAACCTCGCCATTCTT	171	14
AB172	A	TTTATTGTCGAAGTGTTGGTGAA	TTGAACCATTCTGTGGCCTA	195	14
AB173	B	AAAGCAGTTCCAGCCTTCAA	TACGAGAAGAGCCAGCCATT	195	14
AB174	A	TTGGAATGCACCATCTCTTG	TAGTCATGCCAGCCACTACG	163	14
AB175	B	CAGCTGTAAGCCAACACAGG	TCAAGGACTTTAGACAGTGCTCA	192	15
AB176	A	GTGCGCCAACAGAATGGTAT	AGACCAACAGGACCGAGAGA	171	15
AB177	B	GTCAATCGTGTTGGATGGTTT	AATACGCCTGGTCCTGACAT	165	15
AB178	A	GCAAGCATGAGTGGTTGAAA	TGATATGGTTGGGCGTAACA	182	15
AB180	A	GCAAACACGCTCCGTTAAA	GCAGCTATGGACCACATTGA	195	15
AB181	B	ATAAGCCGCTGAAACAATGC	CGACTCGACAATCAGCAGAA	168	15
AB182	B	TGGCTTGCAAGATGATGGTA	CCAATGCCAAGATTCCTGTT	163	16
AB183	A	CAGCAGTATTGATACTCGAGGTATTTC	AGATGATGCGCGGTGTATTT	171	16
AB184	B	AATGGGACGAGTGACATATCG	TTGAGCATTGCACGCTTATC	165	16
AB185	A	TCACGGAATAGTTCATCGGTAA	ACAGTGCTGGTGCAGTCTTG	173	16
AB186	B	CATCCAGTTGATCCAAGCAA	GCGTTGACTCCAGCTACAGA	185	16
AB187	A	AGCAATGAGCAGACAATCTTACC	GAATCCCAAGGAACCCGTAT	172	16
AB188	A	CCCATATGACCTTCGGATTC	TTGATGAATATCTCCACCCTATCA	163	Mt
AB189	B	AATTTCTGAGTTAACCTATCCATC	CCCAGAGGTCCTCATAGAAT	200	Mt
AB190	A	GATTCGCTTTAGCATAACCT	CTTGCTGCTCCAGGTAGTAT	155	Mt
AB191	B	TGAACGCACATTGCACTCTAC	CACTCATTATCTGCTCCATCTCC	172	BsaI

PANA18	A	TCAGCCGGTGGATCTGACTA	TCCTGCAACTCATCAACCACT	194	6
PANA36	B	ATGAACGTTGTCGAGTGCCT	CACGGACACCAAAGCAGAGA	200	6
PANA39	A	TGTGGTGGTAGTAGTCCTCGT	AGTCAAGGCTGCCAAGTTCA	199	7
PANA47	A	AGGTAGTTGATAGCTCATACTGCA	ATGTATCCCTCTTGCTACGCTT	177	Mt
PANA48	B	TCACTCTAGACCAGCTCACCA	ATCTAGGTAGCTCGACCCGT	185	Mt
PANA57	B	CTCTGCCCAAAGAAGCGAGA	CTGTCTTCTCACATCCTCTCGT	199	12

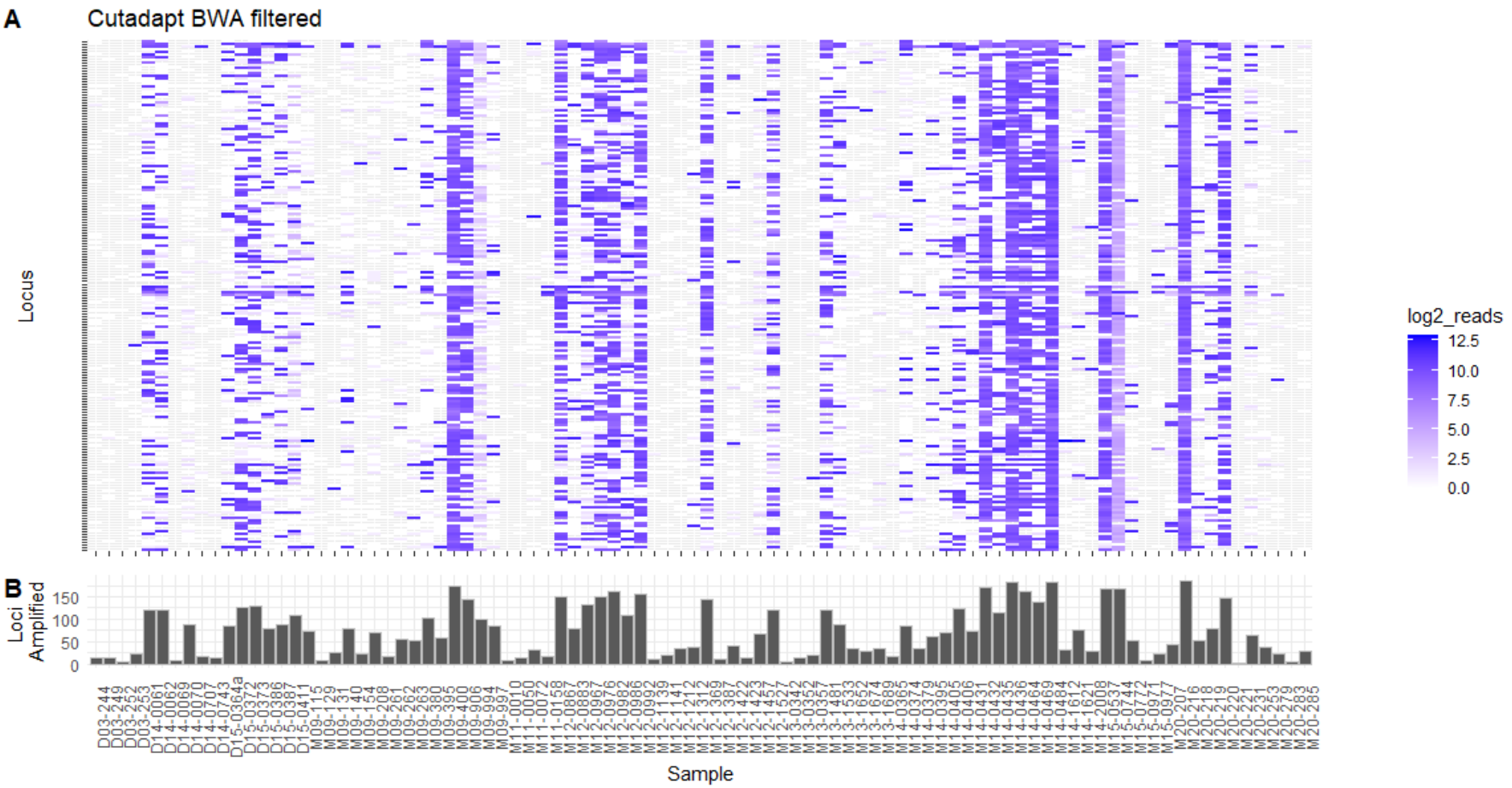

Figure S5.1: A) Illustration of read coverage across all samples and loci – read depth on a log2 scale indicated by intensity of colour. B) Number of loci (out of 192) successfully amplified.

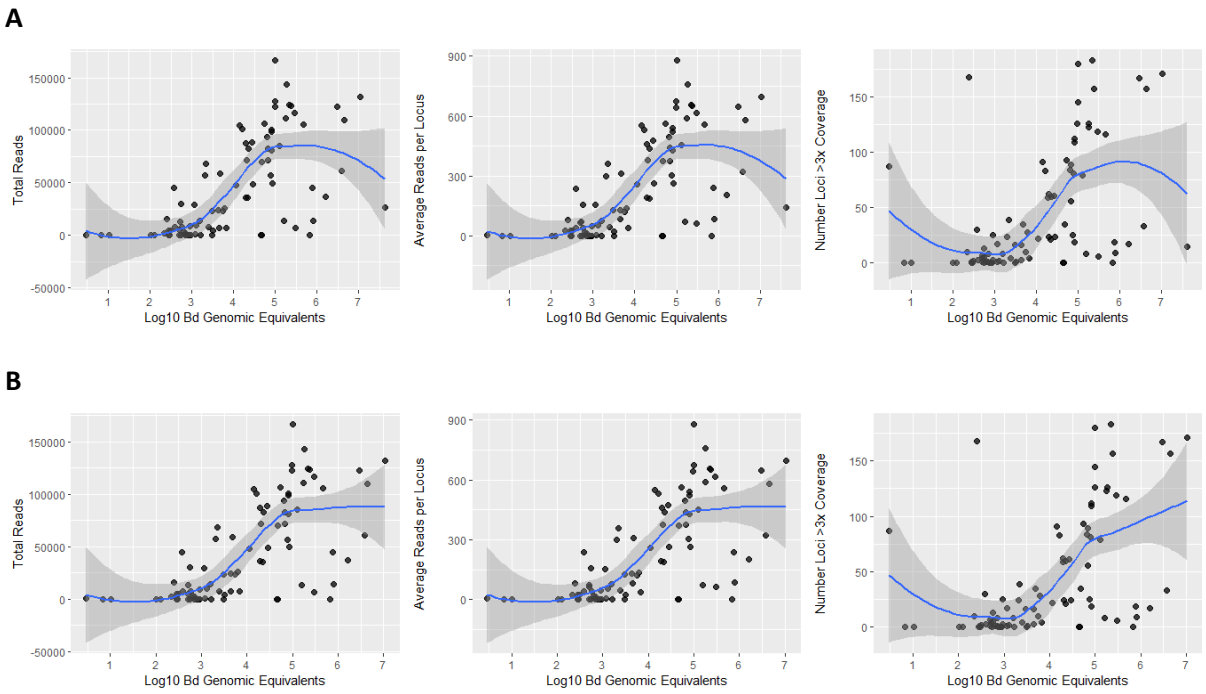

Figure S5.2: Relationship between assay success - measured as the total number of reads passing filters, the average number of reads per locus, or the number of loci with coverage >3 – and Bd load, measured as Log_{10}(Genomic Equivalents). A LOESS smoothing curve is fitted using a span of 0.75 and degree of polynomial fit = 2. A) Raw data, B) data with outliers as identified in model diagnostic plots removed.

A

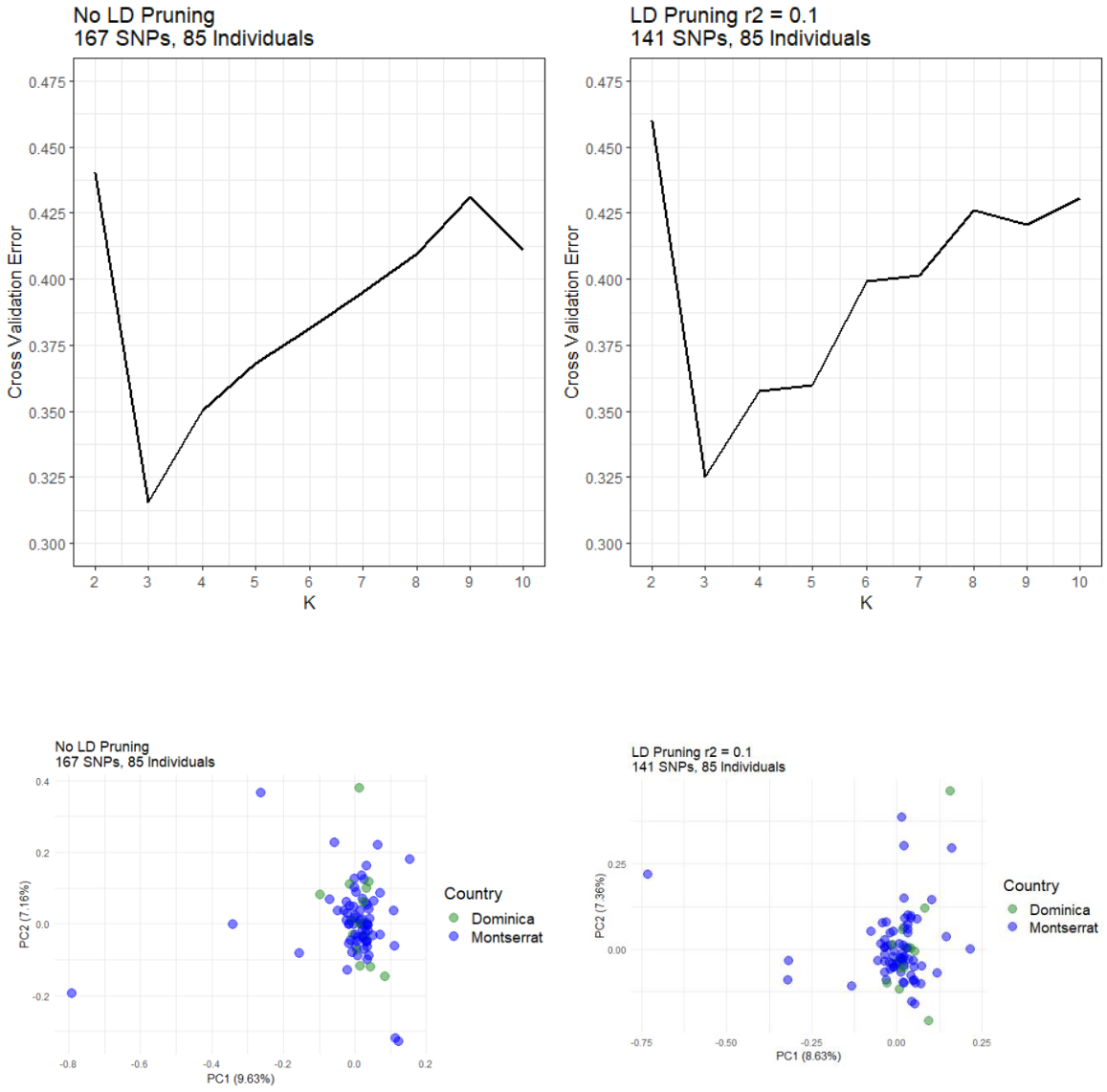

B

Figure S5.3: A) Cross validation error from ADMIXTURE, comparing unpruned SNPs and SNPs pruned at r^2 = 0.1 and not pruned. LD = linkage disequilibrium. B) PCA between Dominica and Montserrat generated from unpruned and pruned SNPs.

Chapter Six Supplementary Information

Table S6.1: Microsatellite loci used in this study. Newly optimised loci are marked with an asterisk (*)

Marker	Tm (°C)	Primer sequence (5'-3')	Direction	Motif	Range
Lepfal_010673	64	AGCAATTCTTGTTGCCTCCC	Fwd	(TAGA)	217-241
		AGCCTAAGTTCTTGCAGGGC	Rev		
Lepfal_015759A	64	AAGATCAGCCAGGGACAGAC	Fwd	(TTTC)	189-234
		CACTGTGATATTTAGGGGTGC	Rev		
Lepfal_000867	64	CGTGAGAAAGACTAGGGCAC	Fwd	(TAGA)	200-244
		AAAAGGGAGCACTCCACAGG	Rev		
Lepfal_002969	64	AGCATCACAGGGAACCAGTC	Fwd	(AC)	169-191
		GCTCCTGAAGTACAAACGCC	Rev		
Lepfal_003035	64	ACATACAGAACTGCTTACATGTCC	Fwd	(TG)	126-134
		GCTTTGTCACTGGCTCCAAG	Rev		
Lepfal_011628	64	ATGATTGGCCCCAGTGTATG	Fwd	(CA)	207-234
		GATCGCAGAACCTGGACCTC	Rev		
Lepfal_013956	64	AGCGTTCGATTAGTAGCTGTG	Fwd	(AC)	134-162
		AGTTCACCCCAACGTAGGAC	Rev		
Lepfal_017957	64	TGTATGATGTGGGCCTTCCC	Fwd	(TG)	189-242
		CACCACTGAAATAACCTATCATTTGTC	Rev		
Lepfal_025280*	60	GGCTATGGAGCTCAGTGGTG	Fwd	(GT)	180-200
		AGAGAGCATAATCTAGTCCTGGG	Rev		
Lepfal_021800*	60	ACACAAGAAGGACATGCCAC	Fwd	(CA)	200-240
		GGCAAGGATGCCTCGTAAAG	Rev		
Lepfal_005205*	60	AGAGGACAAACAGATAGATAGGGG	Fwd	(AGAT)	100-120
		TTCCTTCAGGTCCCATTTGC	Rev		

Table S6.2: P-values from t-test with null allele removal

Population	Observed Heterozygosity	Expected Heterozygosity	F_{ST}
Total	0.430	0.724	NA
Wild	0.292	0.928	0.89
Captive	0.596	0.561	
Bristol	0.860	0.995	
Norden's Ark	0.702	0.598	
Durrell	0.612	0.532	
ZSL	0.526	0.611	0.69
Chester	0.739	0.832	
Dominica	0.334	0.670	
Montserrat	0.300	0.839	

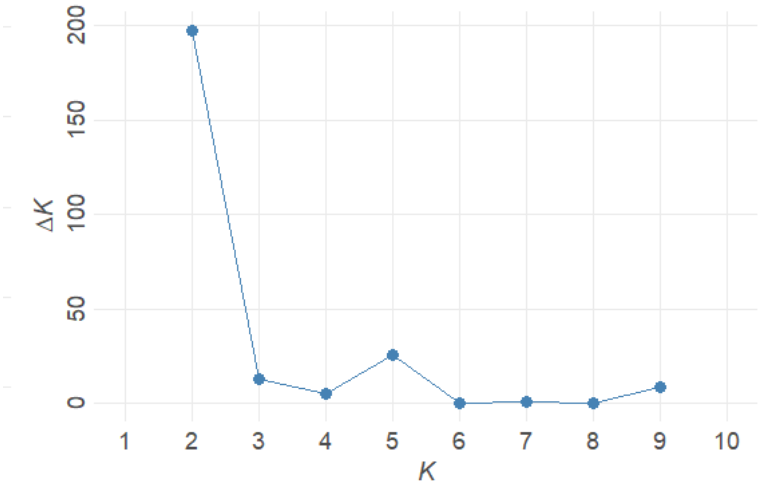

Figure S6.1: Delta K plot produced from the Evanno et al. (2005) method assessment of STRUCTURE runs. Most likely number of clusters = peak of delta K.

A

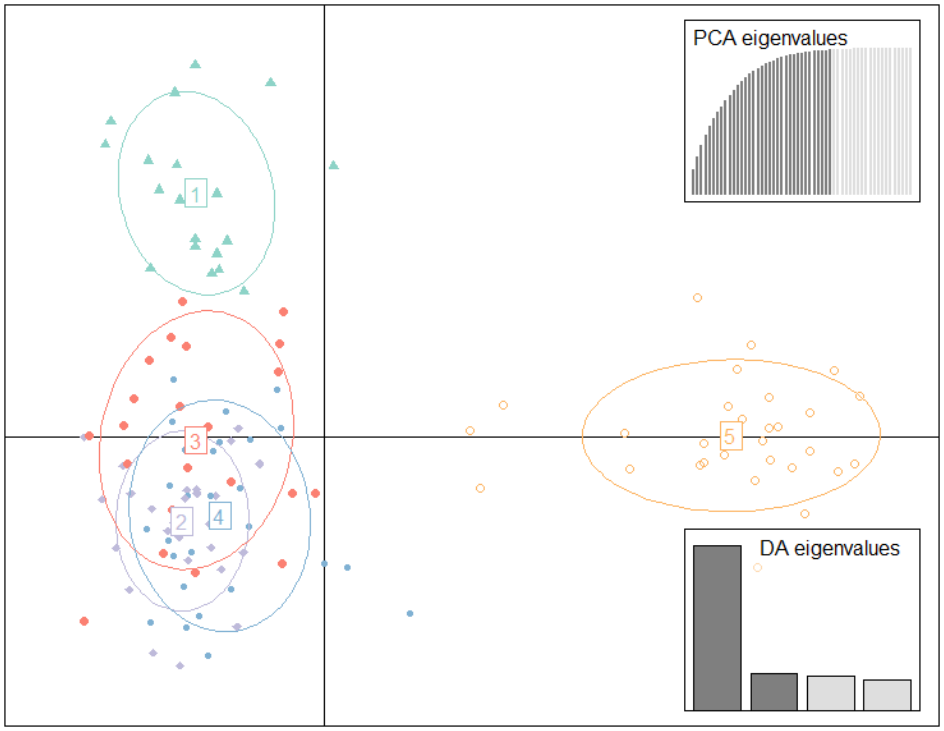

B

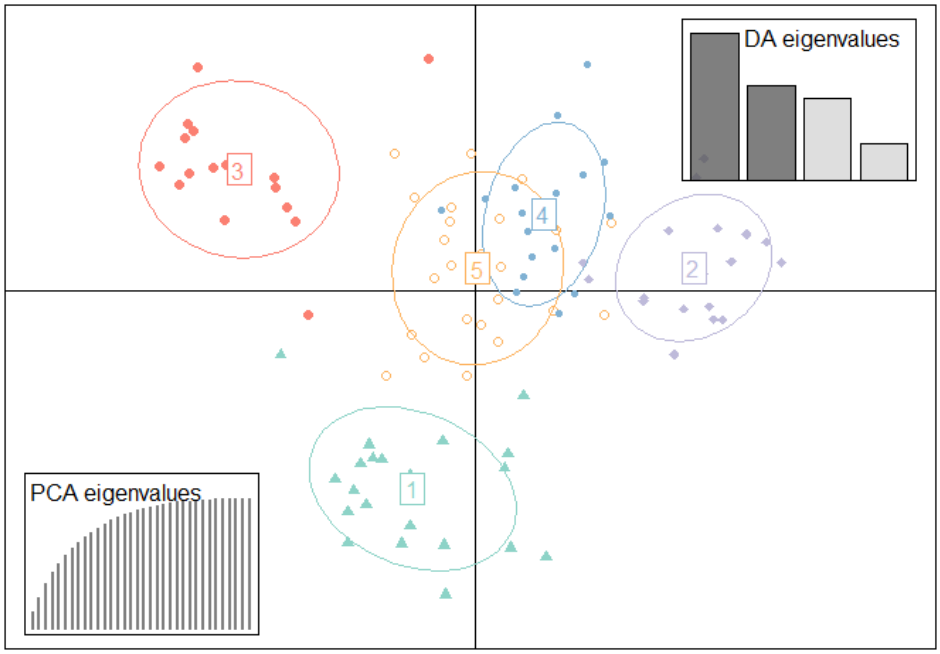

Figure S6.2: DAPC analysis using 'find clusters' and representing the dataset structured according to the most probable number of clusters. A) DAPC based on 35 PCAs and 4 DA eigenvalues, showing the division of the dataset into 5 clusters. B) DAPC, excluding Dominica, based on 35 PCAs and 4 DA eigenvalues, showing the division of the dataset into 5 clusters.

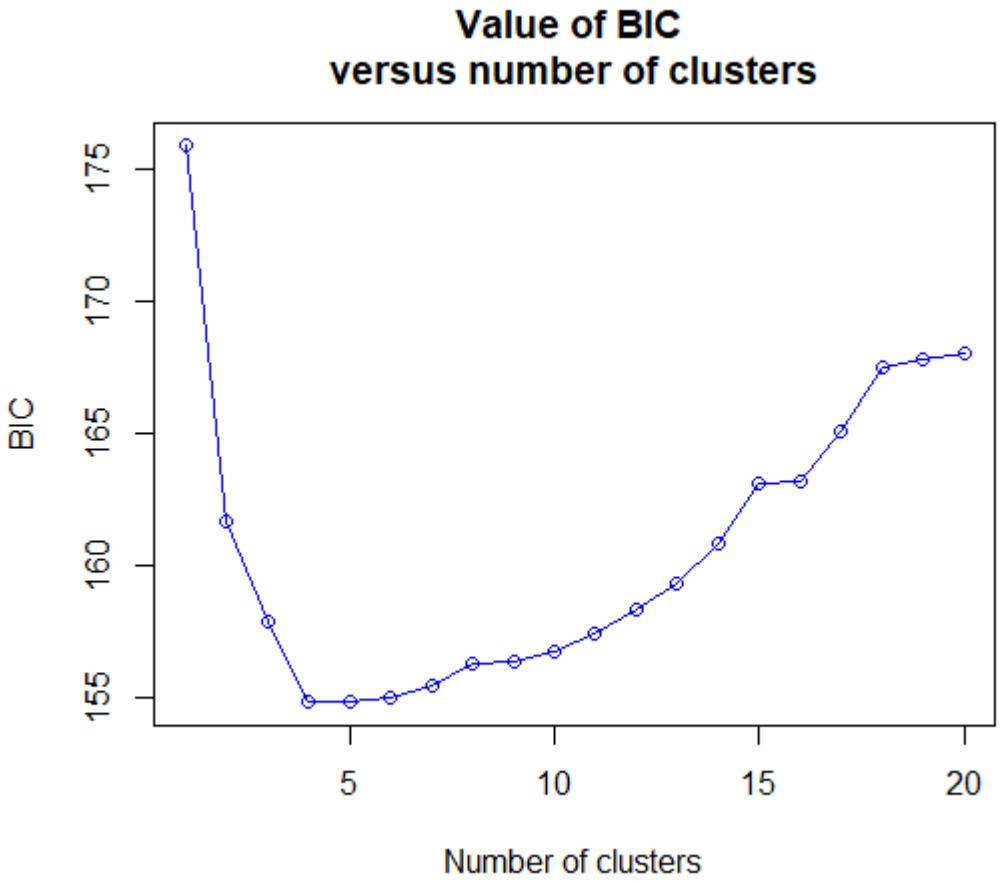

Figure S6.3: Bayesian Information Criterion (BIC) plot used to determine the optimal number of genetic clusters (K) when using the 'find clusters' DAPC method. The optimal K was determined to be five, based on this having the lowest BIC value.

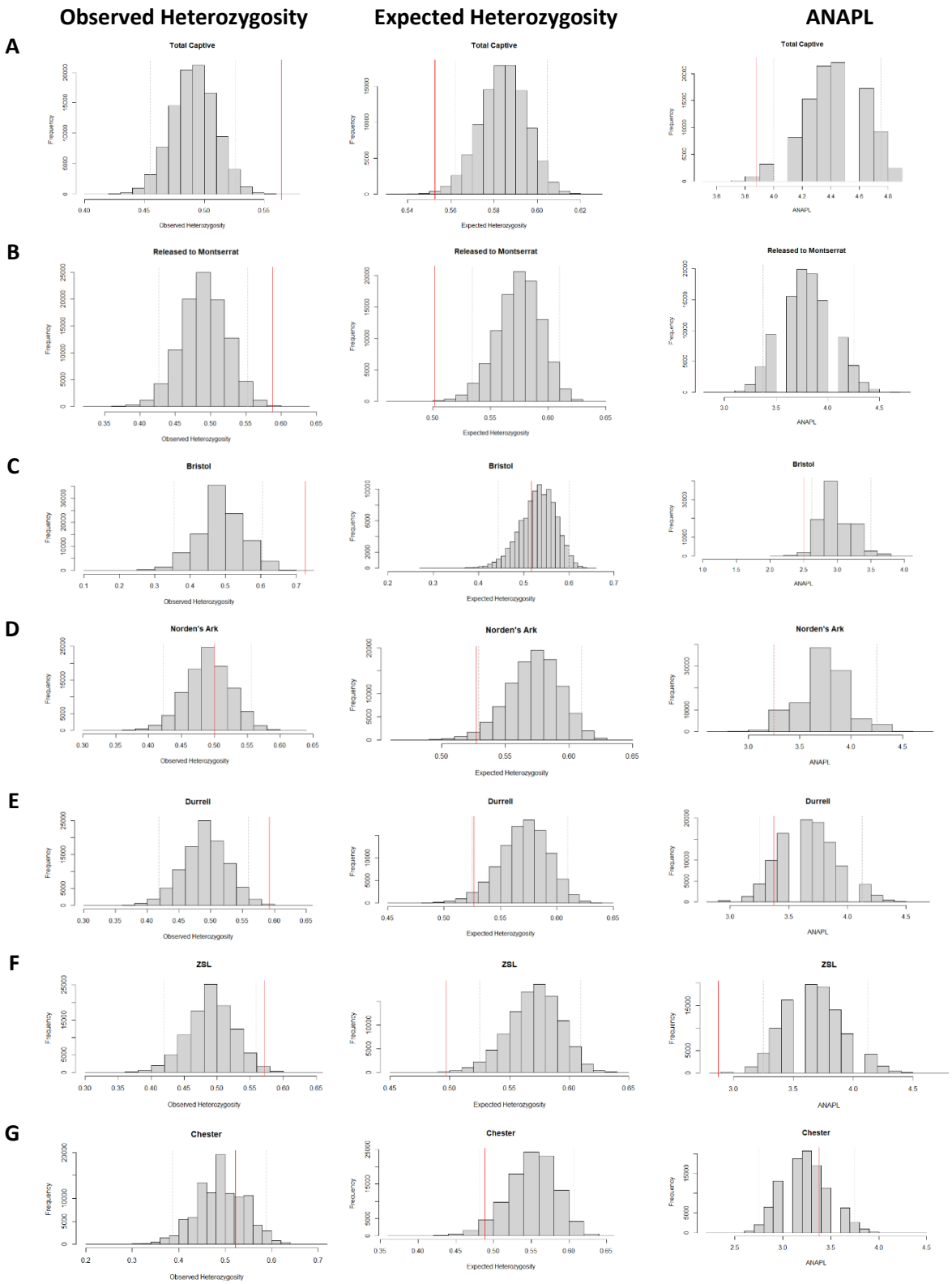

Figure S6.4: The distribution of variation from 100,000 bootstrap replicates of a random sample of wild, Montserratian MCFs, resampled to a number matching that of the population to be compared. The observed value from each captive population is shown as a red line, while 2.5% and 97.5% quartiles of the distribution are shown as grey, dashed lines. A = Total, initial captive population (n = 74), B = Population released to semi-wild enclosure in Montserrat (n = 24), C – G = individual zoos: Bristol (n = 6), Norden's Ark (n = 21), Durrell (n = 19), ZSL (n = 19), and Chester (n = 9). ANAPL = Average number of alleles per locus.